Into the wild: Deploying Brain and Physiological Sensing in Natural Environments to Enhance Wake and Sleep Cognitive Behavioral Studies

by

Guillermo Román Bernal Cubias

B.Arch, Pratt Institute (2010)
S.M., Massachusetts Institute of Technology (2014)

Submitted to the Program in Media Arts and Sciences,
School of Architecture and Planning,
in partial fulfillment of the requirements for the degree of

Doctor of Philosophy

at the

MASSACHUSETTS INSTITUTE OF TECHNOLOGY

June 2023

Author_____

Guillermo Bernal
Program in Media Arts and Sciences
April 1, 2023

Certified by_____

Pattie Maes
Professor of Media Arts and Sciences, MIT
Director of Fluid Interfaces Research Group
Thesis Supervisor

Accepted by_____

Tod Machover
Academic Head, Program in Media Arts and Sciences, MIT

Into the wild: Deploying Brain and Physiological Sensing in Natural Environments to Enhance Wake and Sleep Cognitive Behavioral Studies

by

Guillermo Román Bernal Cubias

Submitted to the Program in Media Arts and Sciences,
School of Architecture and Planning,
on April 1, 2023, in partial fulfillment of the
requirements for the degree of
Doctor of Philosophy

Abstract

This thesis presents two experimental platforms for performing cognitive behavioral studies in natural settings: one for wake time and one for sleep. The equipment utilized today in behavioral and sleep labs is not very accessible, comfortable, portable, or simple to operate. The systems documented in this dissertation demanded the creation of novel wearables, sensors, signal processing, communications, and machine learning solutions that vastly outperformed current systems.

The first platform introduced here is Entwine, a toolkit for behavioral researchers to create VR experiments. The first half of this toolkit includes Unity modules to help create a VR behavioral experiment. These modules are meant to lower the barrier of entry rather than replace Unity development, and they can be built on or modified by the user. I present a study that is able to identify the spatiotemporal dynamics between the autonomic nervous system (HR, EDA) and the central nervous system (Frontal and Parietal cortices) during a high cognitive demand task. I also explored how such a system can help measure and test the field of vision to evaluate retinal and early afferent visual pathways.

The second contribution of this dissertation is the Fascia Ecosystem, which reinvents sleep studies using three key technologies. First, the Fascia Sleep Mask uses fabric-based sensing to collect polysomnogram-like data in a soft sleep mask. Second, the Fascia Hub lets a researcher or scientist give the patient audio and visual feedback and stimulation. This helps with sleep and dream research by allowing for interventions to be made. Finally, the machine learning API provides real-time sleep staging, spindles, and slow-wave saliency maps in the Fascia Portal, where sleep researchers can view patient signals and store experiment data. The presented work streamlines cognitive study procedures by introducing two novel solutions that will be shared with the scientific community. I have shown through user studies that these prototypes are easy to use and have the ability to significantly enhance cognitive research, diagnosis, and understanding of sleep structure.

Thesis Supervisor: Pattie Maes
Title: Professor of Media Arts and Sciences, MIT, Director of Fluid Interfaces Research Group

Into the wild: Deploying Brain and Physiological Sensing in Natural Environments to Enhance Wake and Sleep Cognitive Behavioral Studies

by

Guillermo Román Bernal Cubias

This doctoral thesis has been reviewed and approved by the following committee members:

Thesis Supervisor_____

Pattie Maes
Professor of Media Arts and Sciences, MIT
Director of Fluid Interfaces Research Group

Thesis Reader_____

Pawan Sinha
Professor at the department of Brain and Cognitive Sciences, MIT
Director of the Sinha Laboratory for Vision Research

Thesis Reader_____

Joseph Paradiso
Alexander W. Dreyfoos Professor of Media Arts and Sciences, MIT
Director of Responsive Environments Research Group

Acknowledgments

It's truly surreal to be penning the acknowledgements for my PhD dissertation. As a young immigrant from El Salvador, I arrived in this country with a dream to pursue an education, never imagining that I would one day join the ranks of esteemed scholars at one of the world's most prestigious universities. This incredible journey would not have been possible without the love, support, and guidance of my family, Tio Oscar and Tia Daisy, who welcomed me with open arms. Their generosity and kindness have profoundly impacted my life, and I am eternally grateful for the opportunity to have thrived within their nurturing embrace.

I would also like to express my heartfelt gratitude to Ted and Hilda Cockram, who provided invaluable assistance during my early days in this country. Despite language barriers and seemingly insurmountable challenges, they encouraged me to persevere and enroll in the Middlesex Community College in New Jersey. Their support during my ESL program was instrumental in overcoming those initial hurdles, and I am forever indebted to them for their faith in my abilities.

I would like to acknowledge the immeasurable impact of the Medina and Soliven families. They instilled in me the belief that I could achieve far more than I ever dared to dream. Their steadfast encouragement and support have been truly transformative, and I am deeply grateful for their presence in my life.

Next, I must express my profound gratitude to my advisor, Professor Dr. Pattie Maes. In short, without Pattie, this dissertation would not have been possible. Pattie's mentorship has not only molded me into the scientist I am today but has also shaped the person I have become. Accepting me into the Master's program and subsequently, the Ph.D. program, you turned my dreams into reality. Your influence has catalyzed remarkable growth in both my professional and personal life, and for that, I will be eternally grateful.

Additionally, I extend my sincerest appreciation to my committee members, Professor Dr. Pawan Sinha and Professor Dr. Joseph A. Paradiso, for their invaluable guidance and support throughout this journey. Their expertise, encouragement, and commitment to excellence have been

instrumental in the realization of this project. I am truly honored to have had the opportunity to work with such distinguished and dedicated scholars.

I feel incredibly fortunate to have collaborated with numerous talented and passionate individuals over the years. I would like to extend my heartfelt thanks to all my collaborators for their significant contributions to my research. Your insights, expertise, and dedication have been essential to the success of our projects, and I am profoundly grateful for the opportunity to have worked alongside such extraordinary colleagues. Thank you for everything

I must convey my heartfelt appreciation to my wife, Caitlin Bernal. Your steadfast love and support have served as a wellspring of strength and motivation throughout this journey. I am truly grateful for your patience and understanding as I pursued this PhD degree. Your unwavering belief in me and your presence during every challenge have been instrumental in my success. I could not have accomplished any of this without you by my side. Thank you for being my rock, my confidante, and my inspiration in all aspects of life.

Finalmente, quiero expresar mi más sincera gratitud a mis padres, Ramón Bernal, Alicia de Bernal Cubias y mi hermana Jacqueline Bernal por todo su apoyo y suporte incondicional. Su amor y su dedicación han sido una constante fuente de fuerza y motivación para mí. No podría haber logrado nada de esto sin ellos. Este logro es suyos tambien.

Sincerely,
Guillermo Bernal

A roadmap for this thesis

Chapter 1 introduces this dissertation, provides some background on the differences between data collection and running experiments in the lab vs. in the wild, and highlights the benefits of collecting data in more naturalistic settings. It also describes the primary contributions of this thesis. This thesis is divided into two major sections: Into the Day and Into the Night.

The "Into the Day" section begins with Chapter 2, where the *PhysioHMD* project is introduced. This project becomes the core technology that is later used in other devices. It describes the technology and presents validation analyses and examples using machine learning to recognize facial expressions. Chapter 3 presents the *Galea* headset, a headset that takes the physioHMD design and expands the number of brain sensing capabilities. The device was created in collaboration with an open-source company with the goal of making devices available to a wider audience outside of research labs. This chapter delves into signal validation in depth and serves as an introduction for those new to the field of physiological computing. Two Brain-Computer Interfaces (BCI) paradigms are presented in this chapter: one for Steady State Visual Evoked Potential (SSVEP) and another for electrooculographic (EOG) visual attention.

Chapter 4 is where the Entwine toolkit is introduced as a way to support developers using the Galea headset. We assume that not everyone in the field of cognitive-behavioral neuroscience would have the skills to make virtual reality apps, so we made a series of VR experiments and put them in a Github repository under the name "Entwine." Chapter 5 and Chapter 6 document two in-depth studies for which the code is available in the Entwine repository. Chapter 5 is a study conducted to evaluate the health of the visual pathway. This is done by exploring the effect of different stimulus configurations on the Visual Evoked Potentials (VEP) in VR. VEPs provide a more accurate measurement of optic circuit functional integrity than MRIs because VEP is used to examine the retina, optic nerves, and visual cortex in the brain. The study presents VEP 56 recordings from 8 subjects, showing differences in the visual field for participants with and without eye correction. Chapter 6 explores

the relationship between the Central Nervous System (CNS) and the Autonomic Nervous System (ANS). This chapter describes a study in which 32 people played a modified version of the popular game Tetris while wearing the Galea headset in order to learn how the CNS and ANS respond during a high-spatial and mental workload task. A model is then presented based on these findings.

The "Into the Night" section begins with the introduction of the Fascia ecosystem in Chapter 7. This chapter provides a background on sleep research and the types of sleep tests, according to the American Association for Sleep Medicine. Background on sleep architecture and the physiology of sleep is also provided in this chapter, all with the goal of providing the reader with enough contextual information for the latest chapters. This chapter concludes with an introduction to the main components of the Fascia ecosystem. Chapter 8 describes the Fascia sleep mask. This chapter goes through the design process of developing the Fascia sleep mask. A detailed description is provided for the hardware components that make up the sleep mask. A section on the different signals and modalities provided by the device is presented.
Chapter 9 provides an overview of the Fascia hub. The Fascia hub is a companion to the Fascia sleep mask for stimulation and communication with the person sleeping in a remote location. The Fascia hub is designed to be placed on a nightstand near the person sleeping in order to receive stimulation or monitoring via an infrared camera. In this chapter, background on different types of sleep interventions and descriptions of the modalities available via the hub are presented. Chapter 10 provides an overview of the Fascia portal and its different parts. The Fascia Portal is where sleep researchers can inspect the patient's signals in real-time and store experiment information that is analyzed by the machine learning API that provides sleep staging, spindles, and slow-wave recognition in real-time. Fascia's pilot study and signal validation from 12 sleep nights recording at home are presented in Chapter 11. The findings of ten interviews with sleep experts, dubbed "super users," are presented. The interviews sought to learn from the super users how useful and viable the Fascia Ecosystem is in comparison to the current systems available to these researchers. A comparison to existing gold standard polysomnography data is also presented. The comparison data for Fascia comes from the 12-night recording, and for the polysomnographam data, we used datasets available via the PhysioNet database. Finally, Chapter

12 provides the conclusion to this thesis.

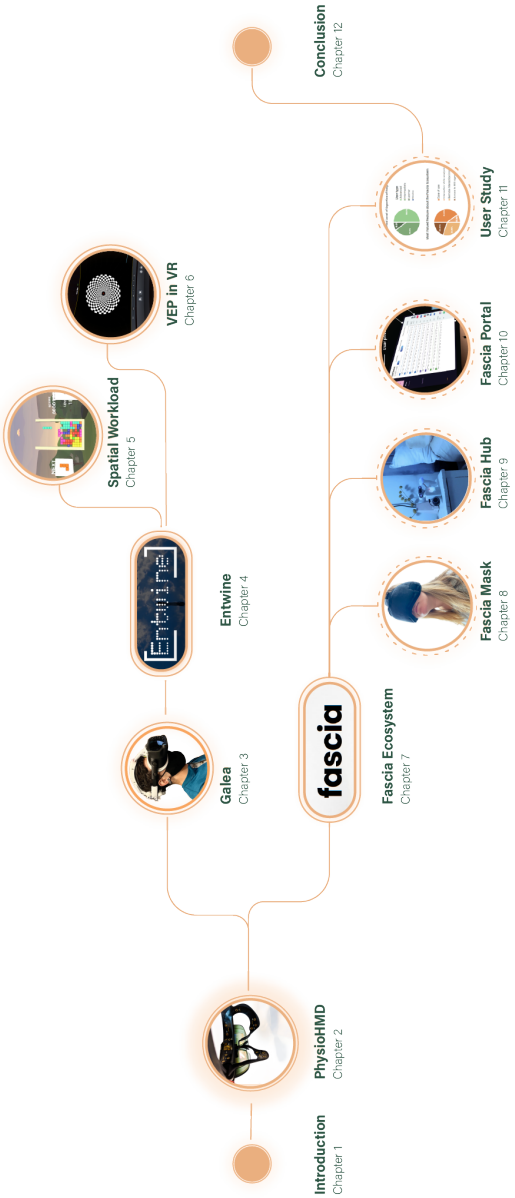

Figure 0-1: A roadmap diagram for this thesis

Table of Contents

List of Figures

List of Tables

Introduction 1

1.1 What Does Data In The Wild Tell Us, That Lab Data Doesn't

Data collected from users in the "wild" (i.e., outside of a controlled laboratory environment) can provide insights into the true behavior, mental state, and emotions of subjects. This is because the data reflects the users' natural behavior and interactions in their everyday environment, rather than being influenced by the artificial constraints of a lab setting.
For example, data collected from users interacting with a product or service in the wild might include:

- The frequency and duration of use
- The specific features or tasks the user engages with
- The user's location and context of use
- The user's actions and interactions with other people or devices
- More accurate physiological data during use, as the context is more natural

Naturalistic observation can be used to understand how users are actually using a product or service, and can provide insights into their needs, motivations, and emotions. It can give us insight into complex behaviors and interactions that we may not see in the controlled setting of a lab, or under the limited guise of an experimental research question. It can also help identify areas for improvement or opportunities for innovation.
The main advantage of naturalistic observation approaches are that they allow us to see everyday behavior. When we bring people into a lab, they know they are being observed and may act differently, which is called the Hawthorne effect. The Hawthorne effect is a type of reactivity in which individuals modify a behavior trait in response to their awareness of being observed [1][2]. The effect was discovered in the context of research conducted at the Hawthorne Western Electric plant; however, one of the later interpretations by Landsberger suggested that the novelty of being research subjects and the increased attention received could lead to temporary increases in workers' productivity[3]. This interpretation was dubbed "the Hawthorne effect."

When conducting sleep studies, a similar effect is observed. The first night effect, also known as the first night phenomenon, is a phenomenon that occurs during sleep studies in which data collected on the first night of a study is frequently disrupted as a result of unfamiliarity with the environment and the study. This disruption may cause the data collected on the first night to differ significantly from those collected on subsequent nights. The first night effect is believed to be caused by the body's natural reaction to a new environment and the stress of participating in a sleep study. This can result in a decrease in the quality of sleep as well as the amount of time spent in each sleep stage. This may cause inaccuracies in the data collected from the first night, as it may not accurately reflect the user's natural sleep patterns.

The first night effect can have a significant impact on the results of sleep studies, particularly those conducted over multiple nights[4]. It is essential that researchers are aware of this phenomenon and take measures to mitigate its effects. For instance, researchers can ensure that the environment is as comfortable and familiar as possible, and that participants are adequately prepared for the experiment. In addition, researchers can use techniques such as data averaging to mitigate the impact of the first-night effect on data collected over multiple nights. By taking measures to mitigate the effects of the first-night effect, researchers can ensure that the collected data is more accurate and representative of the user's true sleep patterns.

In general, data collected for behavioral studies in a lab setting might be more limited and may not accurately reflect the full range of user behavior and experience. Lab studies can be useful for controlled experimentation and testing specific hypotheses, but they may not always provide a complete picture of user behavior in the real world. For example, in a lab setting, participants may be more self-conscious or aware of being observed, which could affect their behavior and physiological responses. Similarly, the lab environment itself may be unfamiliar or artificial, which could also influence the participants' behavior and responses.

An experiment conducted in a natural setting allows the participant to feel at ease with his or her surroundings. Plus, the outcome of such an experiment may be more valid because the participant may open up more in reference to thoughts and feelings. A downside is that such experiments require obtaining permission to complete the experiment at any chosen location. If permission is not granted, then there will be a halt

to the experimental process. A controlled setting allows the researcher to have complete control over other factors that may affect the study. He or she will be able to manipulate the environment to allow for a more concise experiment.

In summary, by collecting user physiological data in the wild, we can gain more accurate insights into user behavior without introducing any external factors that may skew the results. This can provide a better understanding of user experience and response than what can be obtained from a lab setting.

Data in the wild can give us insight into the user's true emotional states and motivations which may not be present in a lab setting. For example, data collected in the wild can show us how users interact with an application when they are in a hurry, or in a different social setting. Additionally, data in the wild can provide evidence of how users feel about an application or feature, as opposed to the response they may provide in a lab setting, where they may be more inclined to give a socially acceptable reaction. By collecting physiological data in the wild, we can gain a more accurate understanding of user behavior that can inform product and design decisions.

1.2 Problem Statement And Goals

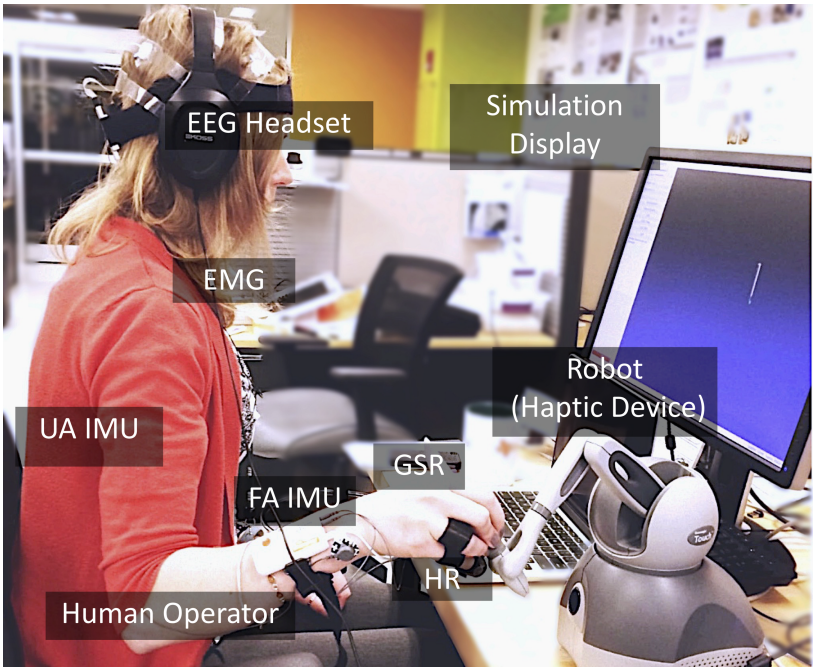

Figure 1-1: Subjects interacted with the virtual task by controlling a robotic interface (i.e., haptic device). Physiological response (e.g., EEG, GSR, EMG) and user kinematic movements were recorded from wireless inertial measurement units (IMUs) on the upper-arm and forearm, as well as encoder readings from the haptic device. Image by Wang et al.

Typically, immersive environment-based therapy requires that the user

not just wear a Head-Mounted Display, but also an array of other sensors and devices that enable real-time monitoring of the user's physiological and cognitive state[5]. For instance, Electrocardiogram (ECG) and Electrodermal Activity (EDA) are used to understand emotional arousal and identify the magnitude of the emotional response[6]. Electrooculography (EOG) and Electroencephalography (EEG) provide data relevant to attention and valence[7]. These sensing technologies are not just cumbersome to set up and wear, but they are also very costly, not standardized, and often prone to errors. The lack of standardization contributes to a growing body of datasets that are not cross-compatible since different devices sample data at different frequencies. Some datasets share data that has already been preprocessed through some proprietary algorithm, and in some cases, there is no documentation at all of the processes used for the data collection.

To better understand this problem, we can look at how closed-source/closed-data ecosystems limit research in the scope of possible questions. When examining EEG data, if only power-band statistics (alpha, beta, gamma, etc.) are made available (the case for the standard Emotiv license), much of the information about synchrony in the brain is lost. Specifically, it is impossible to investigate whether two brain regions exhibit coherence or phase-lock with one another. There is a widespread consensus among neuroscientists [8] that synchrony is important in determining the efficacy of neuronal communication, plasticity, learning, and possibly even for governing aspects of consciousness [9]. For example, the phase-locking of EEG oscillations has been shown to increase between different medial temporal lobe regions during successful memory formation[10], suggesting an essential role in memory encoding or selective attention[11].

Timing and synchrony in the brain are important for researching some of the most interesting cognitive functions including memory encoding and retrieval, associative learning, attention, and likely others. When EEG data is reduced to power-band statistics, the phase relationships and cycle-by-cycle timing information is inherently lost and in doing so, some of the most important information about the operation of the brain and how it relates to cognition may be irreversibly irretrievable. Similarly, if only power-band data or other potentially impoverished derivative metrics are used as inputs when gathering EEG data, this may fundamentally limit the effectiveness of the resulting machine learning

models. In some cases, the resulting models may lack statistical power to make reliable predictions. In other cases, the models may overfit the power-band data and cannot adequately generalize and replicate the results. As neuroscience and computer science fields continue to work together to understand the most important parameters of brain function and derive cognitive processes, using large and powerful neural networks in addition to having access to the raw EEG data will likely be critical to unlocking discoveries. My goal is to make devices available to researchers that provide state-of-the-art signal quality, while at the same time providing the base for creating a standardized approach to sharing data from behavioral experiments. Apart from making EEG data openly available, and facilitating integration with machine learning models for feature extraction, our devices also collect additional physiological data including Electrooculography, Electromyography, Electrodermal Activity, Heart Rate, and Skin Temperature to provide a more comprehensive view of the subjects' cognitive and affective state.

In the past number of years, research in Human-Computer Interaction has explored how to best integrate Physiological Computing into our everyday life. A large portion of design decisions made in this dissertation are based on the theory of behavior settings, which states that the behavior of individuals is strongly influenced by the physical and social environment in which they function[12]. One example in which the setting of an experiment can heavily influence the results is with sleep studies, where researchers often struggle to create a natural setting since these studies are conducted in sleep labs where the patient has to sleep overnight while wearing a minimum of 22 wires attached to their body to track physiological signals. While they do so, a sleep technician or "scorer" observes in real-time their biometric signals and interprets the data to diagnose sleep disorders and quality of sleep. This environment is far from the natural setting in which the patient lives, and the data likely reflects inaccuracies and variations due to this unfamiliar setting.

The limitations of conventional lab-based experiments often result in the use of a narrow set of participants, typically university students, with similar cognitive abilities, low variance in age, education, income, etc. A natural concern is whether results obtained in this specific population represent behavior in a more diverse population. Henrich, Heine, and Norenzayan (2010) argue that participants in laboratory experiments are typically drawn from Western, Educated, Industrialized, Rich, and

Democratic (WEIRD) societies, and results obtained from such studies may not generalize to other populations and settings[13]. One of the goals of this research is to make technology that can translate from the lab into the wild while preserving signal integrity and quality, thereby making these devices easy to access for a broader demographic population, while at the same time being conformable to the user and their natural environment. The first contribution of this dissertation is that of hardware and software platforms that support (1) standardized data collection and feature extraction from a wide range of physiological sensors, and (2) system for real-time adaptation of the stimuli based on the user's current mental and affective state as inferred from the sensor data. We believe that these platforms will be scalable and adaptable to a broad range of applications and are poised to impact cognitive-behavior research significantly. A second contribution of this work involves potential variations that can be achieved, one of which is Fascia, a smart sleep mask that aims to gather all relevant polysomnography (PSG) data without disturbing sleep quality, the other being Galea and Entwine, designed for VR based physiological experiments. A third and final contribution consists of the design and evaluation of 2-3 use cases that demonstrate the utility of the proposed platforms.

1.3 Vision And Framework Questions

The work presented in this thesis aims to address several important questions related to the development and validation of platforms for conducting cognitive experiments and collecting physiological data during wake and sleep time. These questions encompass various aspects of the systems, ranging from technical feasibility to user experience and privacy concerns.

How can we develop hardware and software platforms that enable closed-loop cognitive experiments in more naturalistic settings, both during wake and sleep time? This question pertains to the design and implementation of the core technology, such as the physioHMD, Galea headset, and Fascia ecosystem, as well as the integration of these devices with virtual reality and other experimental paradigms.

What are the key technical challenges in designing, validating, and deploying these platforms? This question explores the technical aspects of the systems, including signal quality, hardware performance, and

integration with existing experimental setups.

How can we ensure that the platforms are accessible and useful to researchers with varying levels of expertise in cognitive-behavioral neuroscience and virtual reality? This question highlights the importance of creating user-friendly tools and frameworks, such as the Entwine toolkit, to support the wider adoption of these platforms by the research community.

What are the potential applications and implications of using these platforms for studying various cognitive and physiological processes during wake and sleep time? This question delves into the potential benefits and challenges of conducting experiments in more naturalistic settings and the insights that can be gained from studying the relationship between the central nervous system (CNS) and the autonomic nervous system (ANS), as well as sleep research.

How can we address the privacy and ethical concerns associated with collecting and sharing sensitive physiological data? This question emphasizes the importance of incorporating privacy safeguards and data protection measures into the design and implementation of these platforms, as well as fostering transparency and trust among users and researchers.

By addressing these questions, the thesis aims to provide a comprehensive and in-depth understanding of the development and validation of platforms for cognitive experiments and physiological data collection, as well as their potential applications and implications in the field of cognitive-behavioral neuroscience and beyond.

1.4 Neurofeedback Research

In recent years, neurofeedback research has emerged as an increasingly significant area of study due to its potential applications in various domains such as cognitive enhancement, mental health, and rehabilitation [14, 15] Neurofeedback, a form of biofeedback, enables individuals to modulate their brain activity by providing real-time feedback about their neural signals [16]. Understanding and contextualizing neurofeedback research is crucial as it sheds light on the underlying neural mechanisms and offers insights into how individuals can learn to self-regulate their brain activity [17]. This, in turn, can lead to the development of targeted interventions and personalized therapies for a range of neurological and

psychiatric disorders, as well as optimizing cognitive performance in healthy individuals [14, 18]. Furthermore, advancements in neurofeedback research have the potential to transform not only clinical practice but also educational and occupational settings, thereby enhancing overall human performance and well-being [19].

Early neuroanatomy studies relied on a lesion approach to study principles of cognition. In contrast, neurofeedback studies cognition with a perturbative approach. There are two types of neurofeedback approaches: direct and indirect. Traditionally, direct neurofeedback allows for scientific inquiry by directly eliciting the subject's brain dynamics based on a stimulus that perturbs their current brain state.[20]. Indirect feedback elicits brain dynamics by engaging the subject in a mental task and comparing "healthy subjects with patients to better diagnose individuals with disabilities and mental illness." The ability to elicit the behavioral state based on underlying brain dynamics has extensive benefits in exposing functional mechanisms underlying changes in behavior[21].

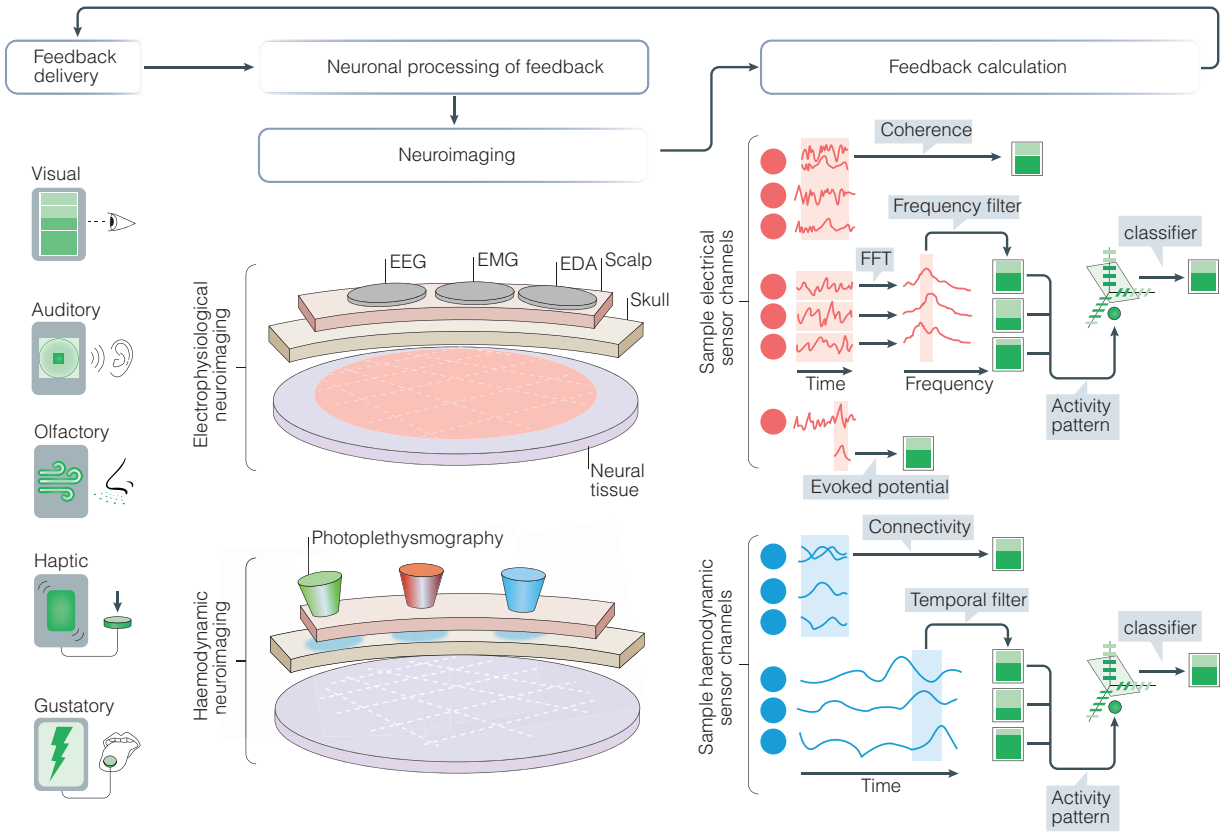

Figure 1-2: Overview of the procedure of neurofeedback.

Neurofeedback begins with the observation of physiological activity. Electrophysiological methods to detect such activity include electroencephalography (EEG), Electromyography (EMG), and Electrodermal Activity (EDA). Haemodynamic imaging methods for detecting blood flow activity include Photoplethysmography (PPG). Sample signals that are extracted from both types of these sensor channels provide a qualitative representation of the difference in temporal resolution. Electrophysiological and haemodynamic signals can be processed in similar ways. Univariate approaches extract a signal from a single channel or region of interest, for example, an evoked potential. Features from a set of sensors, such as the power at a frequency window or the level of activation, can be classified as multivariate patterns of activity (MVPAs). The calculated signal is then presented to the individual via visual, auditory, haptic or electrical stimulation feedback, allowing the user to alter the neural function and complete the loop with neural processing of feedback[22, -60pt].

To test whether a subject's capacity to modulate the target brain region directly increases task performance, researchers can present sensory feedback that scales with the amplitude of brain activity.

The use of neurofeedback has revealed that subjects can learn to regulate the activity of subcortical areas, for example, the amygdala[23, -80pt], and extended areas of the limbic systems[24, pp. –30]. Prior work has shown that subjects who learned to modulate regional activity demonstrated improved performance on various cognitive tasks, including processes critical for memory[25, pp. –15], mood[26], motor imagery[27], and perception of pain[28].

1.5 Physiological Computing Research In HCI

In the past number of years, research in Human-Computer Interaction has explored how to best integrate Physiological Computing into everyday products and services. Early work explored adding sensing actuators to eye-wear to collect facial deformation[29] and more recently Bernal et al.[30] developed EmotionalBeasts, a system to track and visualize emotions using avatars in a virtual environment. This was done by adding a sensor to a virtual reality headset that would record the user's Electrodermal Activity (EDA) and Heart Rate (HR), and then train a neural network to estimate four emotions from the raw EDA and HR data.

The PhysioHMD project demonstrated that multi-sensory physiological recordings can be integrated into a Head-Mounted Display (HMD) in a way that provides better fit and comfort[31].

The wearable EOG goggles are designed to meet certain requirements, including being lightweight and low-power for long-term use, providing real-time signal processing capabilities and compensating for EOG signal artifacts through the use of a light sensor and accelerometer [32]. The hardware is made up of two components, the goggles and a wearable processing unit, and has a weight of 188g and can last for 7.2 hours of use. The EOG signals are processed in real-time and can be transmitted via Bluetooth or stored on an Memory card. Eye gesture recognition involves detecting and removing blinks, detecting saccades, mapping them to basic directions, combining diagonal saccades into a string sequence, and recognizing eye gestures through string matching with templates. A case study showed that EOG signals can be efficiently processed for eye gesture recognition, with eye gestures quickly learned by subjects, although 30% reported difficulties staying focused during use.

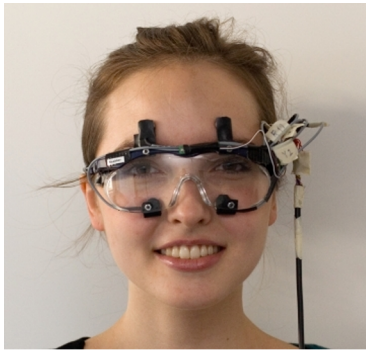

Figure 1-3: Goggles worn by a person with the small board for EOG signal amplification attached to the left side of the frame. Image from Bulling 2009

The implementation of PhysioHMD consists of a flexible printed circuit board with a wide range of electrodes (heart rate, electrodermal activity, facial expression from muscle activity, eye movement, and brain signal from the prefrontal cortex region). Shaped as an eye mask, it takes advantage of the close contact of an HMD to the face to collect the physiological signals. These signals allow for Affective Computing integration (such as recognition of emotions and facial expressions) into Virtual Reality Environment applications. The work described here goes beyond PhysioHMD by creating an open platform for the community to utilize Physiological Computing in VR.

PsychicVR, developed by Amores, is a VR system that integrates the Muse, a consumer BCI headband, with a VR headset to teach mindfulness while enjoying a playful, immersive experience[33]. The setup can be seen in Figure 1-4. Another relevant study is by Casanova et. al. who demonstrated that VR can be used to understand a patient's cognitive state in the operating room during awake brain surgery. Typically awake brain surgery makes use of language mapping to avoid critical brain regions, however cognitive functions such as visuo-spatial cognition and non-verbal language, including facial expressions and eye gaze, are

rarely used during brain surgery even though they are equally important. Casanova's work uses physiological computing and VR to make these tasks compatible with the restrictive environment of an operating room and awake brain surgery procedures[34].

These research projects share a common need for the sensing and feedback system to be more integrated. Amores' and Casanova's research makes valuable contributions, but the replicability and scaling of these works are very limited due to their ad-hoc nature. With the platforms presented in this dissertation, we hope to remove these limitations.

The MindFlex® game is one of the few BCI technologies that has gone on to become a commercial entertainment product. In a study conducted by O'Hara et. al. participants were asked to play the game at home with others and videotape their sessions. The collected video data (about 4 hours) was analyzed to understand the embodied nature of interactions and collaborations during the game play. The study showed the importance of considering the social organization of bodily and mindful behavior in BCI gaming and how it affects the application of BCI design in social contexts. The study also highlighted the role of actions, gestures, expressions, and utterances in making internal brain states and intentions visible to others, which is important for creating social meaning and forming social relationships between players and audiences [35].

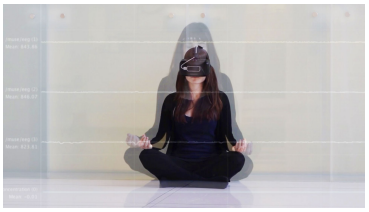

Figure 1-4: Image from psychicVR publication

1.6 The Need For A Standard Platform

All of the projects mentioned before are tackling similar challenges, namely how to monitor and gain insights from the user's physiology into virtual environments. More recently, Looxid Labs, Neurable, and EmteqVR have taken a similar approach to Bernal et. al. and commercialized a sensing add-on for VR headsets. In the case of Looxid Labs, their product reads brain signals from the prefrontal cortex region in order to assess the user's attention and relaxation[36]. Neurable released a limited number of units as a proof of concept that collected signals from the occipital region of the brain, enabling it to collect signals related to the stimulus presented to the participant's visual field[37]. The EmteqVR add-on uses the facial muscle signals generated by the person wearing the device to understand the user's affective state[38]. Each of these products looks at one specific physiological signal which provides insight into one domain, but they do not result in a novel research tool that allows researchers

to examine how these individual signals may work together or impact one another. In order to understand more complex human behavioral processes, it is important to be able to monitor and assess multiple signals, as is possible with the platforms proposed in this dissertation.

The development of sensing devices that are comfortable to wear and maintain signal fidelity is essential for realizing the full potential of Physiological Computing. Despite the research developed to date, the Physiological Computing community still lacks adequate hardware platforms for collecting large multi-sensory datasets and facilitating collaborative sharing of experimental protocols and data aggregation, which is especially important for creating the large datasets needed for machine learning.

Part I: Open source physiological sensing add-on for Head-Mounted Displays

2 PhysioHMD

To bridge the gap between the current limitations of Physiological Computing and realizing its full potential, a new solution was needed. This solution presented itself in the form of virtual and augmented reality headsets. With their unique access to the facial area, these headsets provide a prime opportunity for collecting bio-signals and facial expressions for insight into the user's state. To take advantage of this opportunity, the PhysioHMD platform was developed. This software and hardware modular interface allows for the collection of affect and physiological data from a user wearing a head-mounted display. With its flexible architecture, PhysioHMD enables real-time aggregation and interpretation of signals, leading to the development of novel, personalized interactions and evaluation of virtual experiences. Additionally, PhysioHMD offers a user-friendly interface that is easily extendable and accompanied by a suite of tools for testing and analysis.

PhysioHMD Publications

The research presented in this chapter has resulted in the following peer-reviewed publications to date.

Bernal, Guillermo, Tao Yang, Abhinandan Jain, and Pattie Maes. ***PhysioHMD: a conformable, modular toolkit for collecting physiological data from head-mounted displays.*** *In Proceedings of the 2018 ACM International Symposium on Wearable Computers, pp. 160-167. 2018.*

Bernal, Guillermo, and Pattie Maes. ***Emotional beasts: visually expressing emotions through avatars in VR.*** *In Proceedings of the 2017 CHI*

conference extended abstracts on human factors in computing systems, pp. 2395-2402. 2017.

2.1 Background

Augmented Reality (AR) and Virtual Reality (VR) technologies, hereafter referred to jointly as extended reality (XR) technologies, have enjoyed increasing popularity in the last few years thanks to the emergence of inexpensive and easy to deploy headsets. While XR technologies primarily support applications in the entertainment and gaming industry, they are also increasingly used in health care and human behavior research to treat anxiety, phobias, psychosis, and post-traumatic stress disorder (PTSD). In both entertainment and health care applications, it is essential to understand the behavior, performance, and engagement of the user [39–41]. In clinical settings, XR technology has recently gained much interest because it enables novel, promising methods for treating anxiety and other mental disorders [42]. XR-based therapy is also opening up new and exciting opportunities for pain management and personalized physical and sports therapy [43, 44].

Typically, XR based therapies require that the user not just wear a head-mounted display but also an array of other sensors and devices that enable real-time monitoring of the user's physiological and cognitive state. For instance, Electrocardiogram (ECG) and Electrodermal Activity (EDA) are used to understand emotional arousal and are used to identify the magnitude of the emotional response. Electrooculography (EOG) and Electroencephalography (EEG) provide data relevant to information about attention as well as valence, and Electromyography (EMG) provides data on facial expressions linked to positive or negative valence. This sensing technology is not just cumbersome to set up and wear, but it is also very costly, not standardized, and often error-prone. To overcome these problems, this chapter introduces a new platform called PhysioHMD that consists of both hardware and software, and that makes collecting and using information about the internal state of the user cheap and easy. This platform offers a standard for obtaining and comparing data across different users, sessions, and study settings across multiple disciplines.

XR technologies offer the potential to develop human testing and training environments that allow for the precise control of elaborate stimulus presentations in which human cognitive and functional performance can be carefully evaluated and rehabilitated. In the case of AR, measuring

focus and attention in learning/training scenarios is a novel application which is gaining traction in industry.

Emotions are multifaceted events with corresponding physiological signs as well as human expressions [45]. Even though the majority of existing methods for automatic emotion recognition are based on audio-visual analysis [46], there is an increasing body of research on emotion recognition from peripheral and central nervous system physiological responses [47, 48]. There are multiple advantages to using physiological signals for emotion recognition as opposed to using only audio-visual signals: they cannot easily be faked, they do not require a front-facing camera, and they can be used in any degree of illumination/noise. Moreover, they can be combined with audio-visual modalities to construct a more robust and accurate multi-modal emotion recognizer [46]. A system like BIOPAC [49] is now being employed in a variety of applications [50, 51] for measuring facial movements using standardized tools such as Ekman and Friesen's Facial Action Coding System (FACS) and facial electromyography (sEMG). There are some startup companies like Emteq Labs [52] and MindMaze [53] that are working on toolkits focused on bringing affective data into VR. However these setups focus only on EMG, and not much it is known about their setup and high price tag.

Filmmakers, entertainers and other storytellers are trying to figure out what XR as a medium might mean for their respective fields. Some interesting experiments that make use of physiological or affect data include PsychicVR [54], a VR system that integrates a brain-computer interface device with a VR headset to improve mindfulness while enjoying a playful, immersive experience. The interactive storytelling platform PINTER [55] uses physiological data to drive the unfolding of a plot. PINTER features an underlying narrative that consists of a medical drama which combines aspects of medical practice with the evolution of personal relationships between lead characters. Entertainment works like those mentioned above can leverage a system like PhysioHMD to drive the immersive experience with the audience's data, thereby exploring new ways of telling a story.

2.2 System Description

PhysioHMD is a sensor and computing platform developed to support the analysis of multi-modal data related to the behavior and responses of

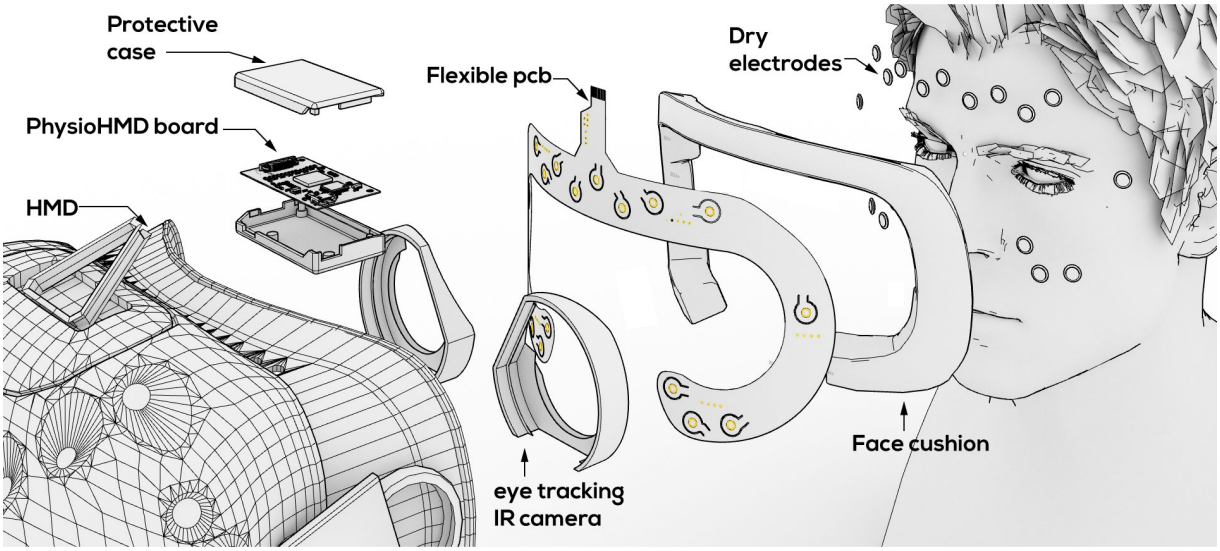

Figure 2-1: Exploded view of PhysioHMD hardware setup for a VR experience. Electrodes are embedded into a foam face cushion in order for the flexible PCB to record data through contact with the user's skin. The assembly for AR headsets is similar, with the addition of a rigid face plate that allows for electrode contact with the skin.

a user, with the goal of enabling evaluation and customization of virtual experiences.

Although hardware costs have come down for XR devices, researchers still do not have access to simple interfaces for deploying Virtual Environments (VEs), interfaces that require little knowledge of game engine content creation, sensor data, data logging, or data visualization. Given these constraints, the following list of requirements was developed for the PhysioHMD platform:

1. A plug and play pipeline that can be deployed with minimal development effort.
2. Physical form factor must be comfortable to the user and easy to use.
3. System supports standard implementations of existing algorithms, feature extraction, and classification.
4. Offers a publicly available open-source code base for use and further improvement by the community interested in this body of work.
5. Includes a game engine interface with sample scenes and relevant tools.

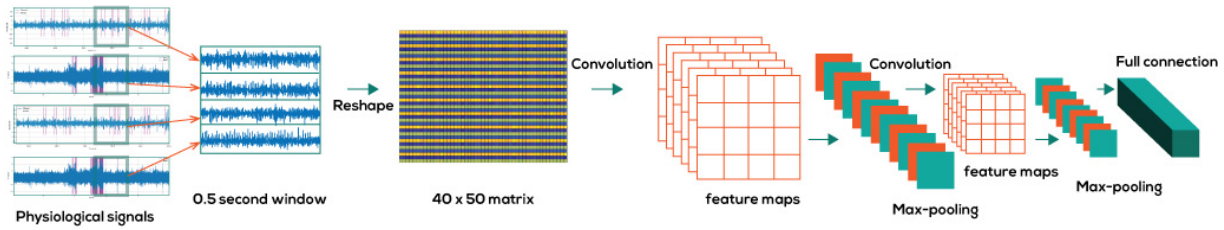

Figure 2-2: The process of our classification system and the CNN architecture used.

2.2.1 Hardware

There are two main components to the PhysioHMD hardware: first there is the main PCB, an analog front end that collects bio-potential signals from muscle movements, eye movements, skin response and brain signals. The second component is an ergo-electronics face-pad; a flexible PCB with gold-plated pickup electrodes that can connect to electrodes like Ag/AgCl (silver/silver chloride), hydro-gels or can be used by themselves as depicted in Figure 2-4. The PhysioHMD system collects sEMG, EEG, EDA, ECG and eye-tracking data.

Electronics

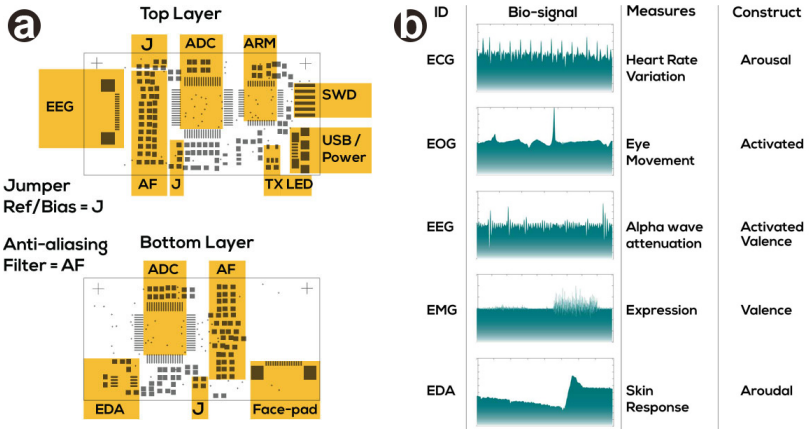

Figure 2-3: a) PCB configuration is depicting locations of main components on top and bottom planes. b) A sample of signals gathered from PhysioHMD and their relevance in gathering affect data.

The PhysioHMD hardware was built to capture bio-signals coherently and to avoid the inconvenience caused during the setup of multiple signal acquisition devices as shown in Figure 2-3 a. A pair of TI ADS1299 (ADS) were used as the front-end for the Analog-to-digital converter (ADC) operations: one ADS is used for sEMG and the possibility for EOG data acquisition, while the other ADS acquires the frontal EEG data. Both the ADS's are controlled by an ARM Cortex M0+ processor using SPI communication standard. This PCB design provides flexibility on the board configuration by exposing multiple jumpers of both ADC's

Reference and Bias. Communication with the PC is done by using the inbuilt USB interface. Anti-aliasing filters are used before both ADC's and sample at 500Hz. EDA measurement is integrated by using a voltage divider and a bandpass filter of 1.5 Hz to 15 Hz to remove artifacts. The signal is then buffered with an amplifier of gain 2 V/V and use ARM's ADC to sample the data.

Electrodes

The sensing face pad that integrates the bio-signal sensors for detecting affect of users (Figure 2-4) was built into and tested on two HMD platforms: into the face cushion of an HTC VIVE VR headset and into the Meta 2 AR headset. To fit into an HMD face-pad, it was quickly determined that a flexible PCB that connects directly into the PhysioHMD's face pad would be the best solution for integration. The flexible PCB has gold plated pads which can either be used as standalone electrodes or as a connector compatible with external electrodes.

The EDA electrodes were placed on the forehead region because it is one of the regions most dense with sweat glands to provide arousal information. The sEMG electrodes were placed above the eyebrows on the *frontalis* muscle and on the cheeks on the *zygomaticus* muscle, providing insight into facial muscle activation. Eye movement is measured by setting EOG Vertical (EOGV) and EOG Horizontal (EOGH) electrodes in a standard placement. Furthermore, EEG electrodes were set according to the 10-20 international electrode system on the user's frontal lobe.

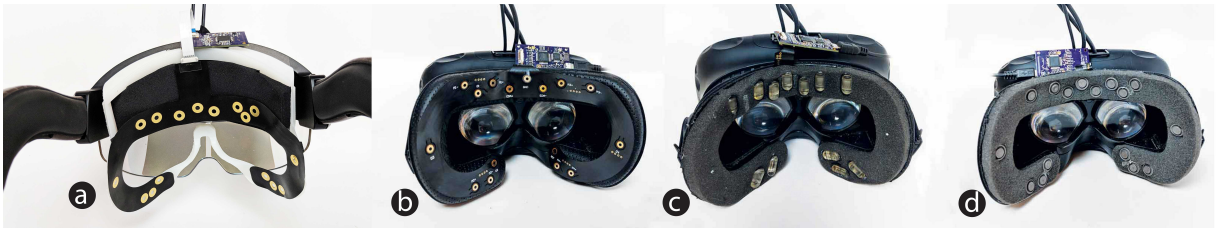

Figure 2-4: The image depicts every headset variation explored during this research. a) AR headset with flexible PCB & gold plated electrodes. b) VR headset with flexible PCB & gold plated electrodes. c) VR headset with hydrogel electrodes. d) VR headset with Ag/AgCI electrodes.

2.2.2 Software

The software side is similarly composed of two main components. First, a signal processing component with normative data for signal preprocessing and feature extraction. This component also features a multi-

variate visualization method for data interpretation by end-users. The second element within the software is a game engine package that can be dropped into any virtual scene.

Machine Learning for Pattern Recognition

A LeNet-5 [56] five-layer CNN architecture is used to classify the collected data as shown in Figure 2-2. There are two convolution layers and two pooling layers, with one full-connection layer. Convolution layers are used to extract the main feature, while pooling layers will sub-sample the feature maps. The multichannel data is reshaped into a matrix and a 3*3 size convolution kernel is used in the first layer and third layer. In the second and fourth layers, the sub-sample window size is 2*2, and max-pooling is used. In the full-connection layer, rectified linear units[57] are used to improve the nonlinear performance of the network.

To train the network, data was collected from 6 users (three females and three males ages 19-30) for 12 different expressions. As part of the data collection procedure, the users were asked to put on the PhysioHMD prototype and repeat an expression 12 times for 5 seconds each with intervals of 3 seconds. The captured data is then pre-processed before feeding it into the network. Notch filters are used to remove the power line interference at 60Hz and 120Hz, and a high-pass filter is applied to cut off the low frequencies below 30Hz. The time sequence sEMG data for each expression is then labeled.

A 0.5 second time window is used to segment the multichannel time series data into sub-sequences. Every sub-sequence is a training or testing sample. The label for a sample is decided by choosing the principal type, which takes the maximum percentage in marker vector. One-hot encoding [58] is then followed to re-encode the labels.

The data augmentation paradigm [59] is utilized to reduce the effects of over-fitting. The augmentation generates sEMG signal translations and horizontal reflections increasing the size of the dataset. Whenever different expression samples are collected, neutral expression samples are obtained in addition to the specific expression being measured.This results in a dataset that is mostly comprised of neutral samples.

A 0.5 dropout rate is used to avoid over-fitting [60] in the training process. From this, a learning rate of 0.001 is established which tells the optimizer how far to move the weights in the direction of the gradient for a mini-batch. In 30 minutes and 800 iterations, the optimized network sees

a classification accuracy of 99.8% in the training set and 92.3% in the testing dataset.

Skin conductance response (SCR) is considered useful as it signifies a response to internal/external stimuli. The Kim's et al.[61] method for SCR extraction from EDA signals was followed by reducing the sampling rate to 20 samples per second, differentiation and subsequent convolution with a 20-point Bartlett window. This procedure yielded the output waveform shown in Figure 2-5b for the input signal shown in Figure 2-5a. The occurrence of the SCR was detected by finding two consecutive zero-crossings, from negative to positive and positive to negative. From this, the SCR was determined in addition to the peak, which does not show exponential decay depending on the context (e.g., if two SCRs occur close together in time, the first response may not decay before the second begins, yet this is not considered an artifact).

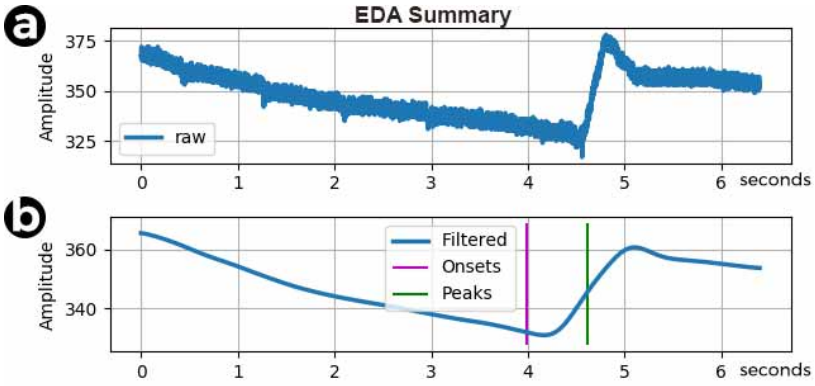

Figure 2-5: Six seconds of EDA signal recording showing a signal peak due to abrupt arousal. a) Typical waveform of EDA under emotional stimulation. b) Output signal from detection module from signal in a).

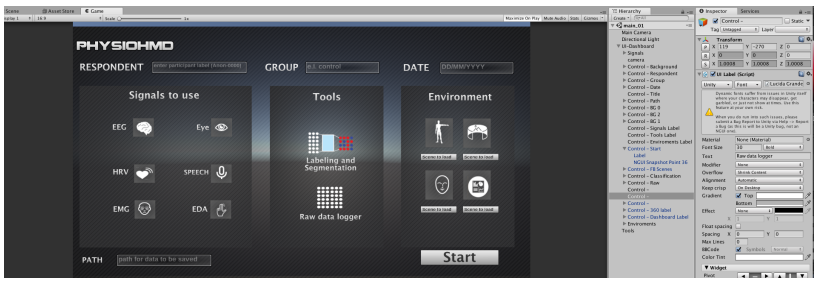

Figure 2-6: Unity package main dashboard, where users can select signals to measure, methods in which to segment data, and environments to test within.

2.2.3 Game Engine Integration

To facilitate integration, the PhysioHMD platform has been encapsulated into a Unity3D package. By encapsulating the platform, less experienced users can drop the package into an empty or already built environment to access the tools. The sample scenes included within the package are set with default configurations that can easily be customized with the

exposed parameters in the editor. The main scene is a dashboard (Figure 2-6) for the person running the study, and here the user can select the signals of interest, choose the data segmentation tool, or merely record raw data. Once those parameters are selected, the user can choose to use one of the demo scenes. Lastly, the user can also choose to take information from external API or SDKs. Those utilities are shown by integrating aGlass SDK[62] to provide point of regard (POR) data and Beyond Verbal affective speech recognition. The following demo scenes were created with the intention to meet most user cases in XR behavioral research.

1. A full body inverse kinematic (IK) scene, where the user can have a room scale experience while embodying a full-size avatar.
2. A mimicry scene where a 3D avatar replicates the facial expressions made by the user wearing the HMD.
3. A 360° scene where 360° video is played.
4. A scene with a particle system that can instantiate animals or objects that the user may have an aversion to or a phobia.

2.3 Evaluation

A set of tests were conducted to evaluate the accuracy of the system and the signal quality vs. ergonomic comfort levels once worn by the user. The primary focus was testing the robustness and usability of the prototype for long periods of time in multiple scenarios. Eight participants (four females and four males), 18-32 years old were asked to put on the PhysioHMD prototype and repeat an expression 12 times for 5 seconds each with intervals of 3 seconds. Each electrode was also evaluated on the following parameters: level of comfort, signal quality, and shelf life. After wearing the headset for 15 minutes for each face pad, we asked the user to self-report on the level of comfort.

2.3.1 Qualitative Analysis

The training and identification processes noted above were conducted for each individual that participated in the study. The recognition accuracy values of the facial expressions are shown in Figure 2-7. This figure shows the testing confusion matrix, which shows the different performance of each expression. Due to obvious signal patterns and high-intensity signal amplitude, Happy, Excited, Angry, Rage, Snarl, and Wink have the

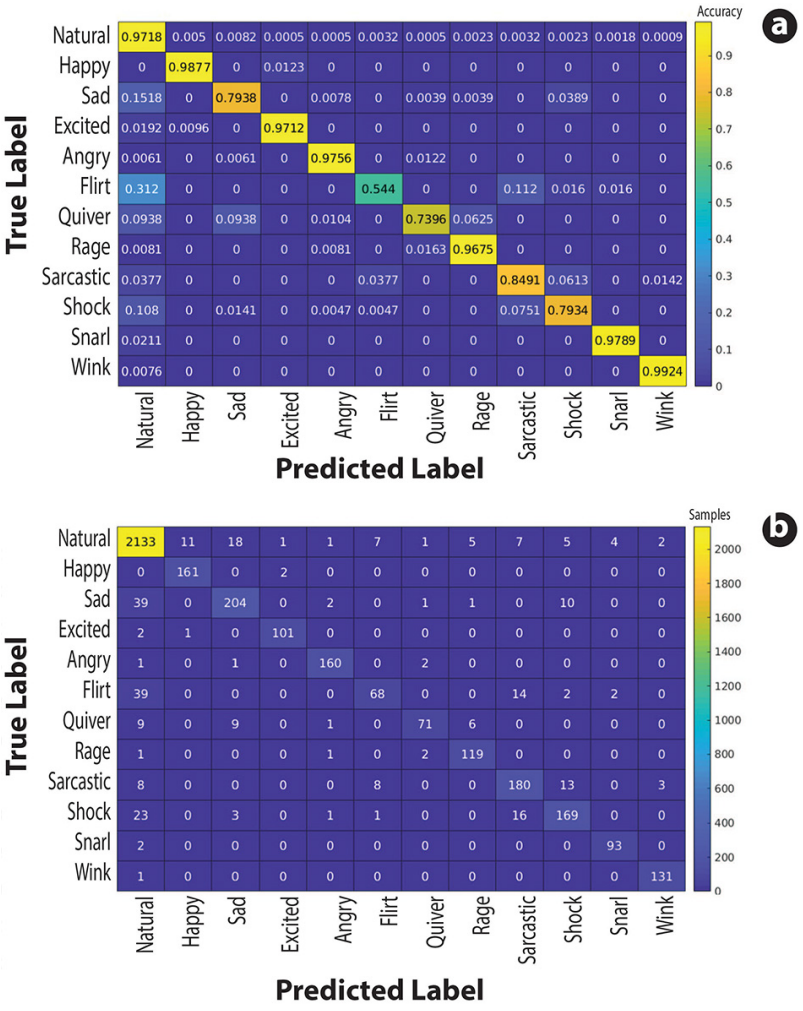

Figure 2-7: Confusion matrix. a) Confusion matrix of prediction accuracy. b) Confusion matrix of prediction amount.

highest recognition accuracy. For Sad, Flirt, Quiver, Sarcastic and Shock, because of the similar signal pattern with other expressions and weak signal amplitude, lower accuracy levels were obtained. Compared with the state-of-the-art results, the PhysioHMD platform can deal with more complex expressions and shows better performance in recognizing basic expressions which Katsuhiro et al. also showed in their paper[63].
Table 2.1 compares the facial recognition model's accuracy of Katsuhiro's et al. research in comparison to the PhysioHMD facial recognition model.

2.3.2 Ergo-Electronics Evaluation

During prototype testing, the three different face pad electrodes were compared: gold-plated pads, standard Ag/AgCl electrodes, and hydrogel-based electrodes. Each electrode was evaluated on the following parameters: level of comfort, signal quality, and shelf life. In this experiment,

Table 2.1: A comparison of facial expression recognition accuracy between Katsuhiro's method and our method

Method	Natural	Happy	Sad	Excited	Angry	Flirt	Quiver	Rage	Sarcastic	Shock	Snarl	Wink
Kats.	95.7%	98.9%	76.2%	—	80.0%	—	—	—	—	92.1%	—	—
Ours	97.2%	98.8%	79.4%	97.1%	97.6%	54.4%	74.0%	96.8%	84.9%	79.3%	97.9%	99.2%

participants were asked how comfortable each type of electrode was on the face while creating different facial expressions while wearing the HMD. A scale of 1-5 was used, where 1 is uncomfortable and 5 is maximum comfort. A standard face pad was also used as a the neutral reference. Hydrogels matched closely to the standard face pad in terms of comfort, whereas gold plated electrodes were the least comfortable for the participants.

Faceplate	Comfort	Signal Gain(dB)	Shelf Life(months)
Facepad	4.5	NA	NA
Gold Plated	3.1	0	>12
Ag/AgCl	4.1	-1	<6
Hydrogel	4.4	+7	<1

Table 2.2: Comparison of comfort, signal quality and shelf life of different electrodes

Table 2.2 gives a summary of the average comfort felt by the participants, the average signal gain, and the shelf life of each electrode.
Further, the signal-to-noise ratio of the signals acquired by each different electrode were compared and evaluated. This evaluation concluded that the Ag/AgCl electrodes had -1dB signal gain and hydrogels had +7dB signal gain on average with the same expression. The shelf life of gold plated electrodes is estimated to be >1 year whereas the shelf life of Ag/AgCl and hydrogels is <6 months and <1 month respectively. The hydrogels also require frequent treatment with saline solution for keeping the signal quality high. Also, based on observations during signal analysis from all three different electrodes, it was found that hydrogels and Ag/AgCl had better mechanical contact compared to gold-plated electrodes because they protrude from the face pad. Given this information, it was concluded that hydrogels will be suitable for physiological data acquisition where high signal quality and comfort are both desirable. Ag/AgCl electrodes will be desirable where both contact requirement and cost are constraints. Gold plated electrodes will be desirable where longevity and minimum cost are required.

2.4 Applications

Four demonstrations were created that demonstrate the capabilities of the PhysioHMD system. First, a demo that uses the system to create more expressive avatars in a social VR setting. Second, a demo that maps user's real-time expression and emotion into the user's VR avatar. Third, a 360 video scene was presented that monitors the user's reactions towards the VE content and modulates the scene based on the user's response. Last, a demostration that presents stimuli for users in VR exposure therapy settings that offers gradual hierarchies of fearful stimuli.

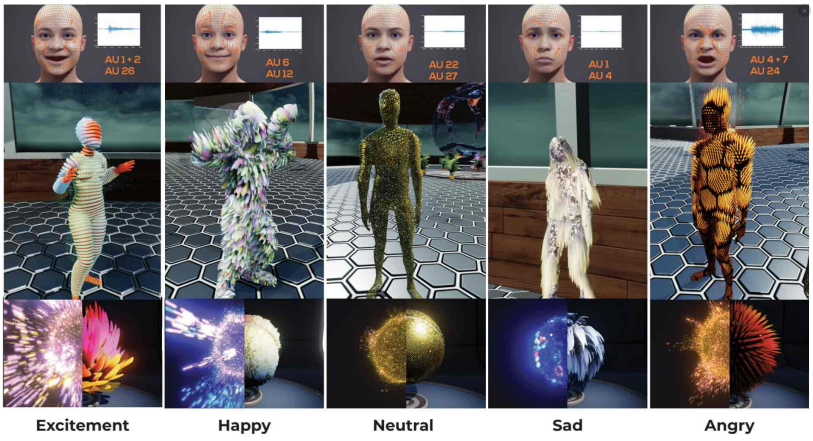

Figure 2-8: The depiction of the range of possible transformations and qualities for an avatar's emotional expressions with a particle system. The figure shows the particle system's variations in particle size, density, brightness, and color which can all adjust to express the emotions of the user visually.

Figure 2-9: The user's real-time expression and emotion are mapped into the user's VR avatar. Natural, Happy, Sad, Excited, Angry, Flirt, Irritated, Rage, Sarcastic, Shock, Snarl, Wink.

2.4.1 Affective Avatars

The first of the two affective avatar demonstrations shows how the system can allow users to express emotions in abstract ways using full-size avatars in a virtual environment while embodying a full-size avatar using an inverse kinematics (IK) system with the PhysioHMD headset (Figure 2-8). The affect of the user is represented visually in two different ways: (1) the fur of the avatar can grow when arousal is high and (2) the color of

the avatar can intensify in brightness or change color to highlight when the user is in a high arousal situation. More detailed information can be found in the publication Emotional Beasts [30]. Within this application area, the goal is to provide agency and express affect in VR through avatars to produce the compelling human-to-human connection.

The second scene expresses affect through facial expressions (Figure 2-9), which is done by mapping the facial expression of the user wearing PhysioHMD into a 3D rigged model avatar. Mimicry was investigated due to its relevance in areas such as autism spectrum disorder research [64]. Participants played an imitation game with both a socially engaged avatar and socially disengaged avatar. This application presents a direct mapping of the user's facial expressions and affect state onto the VR avatar.

2.4.2 Dynamic Occlusion

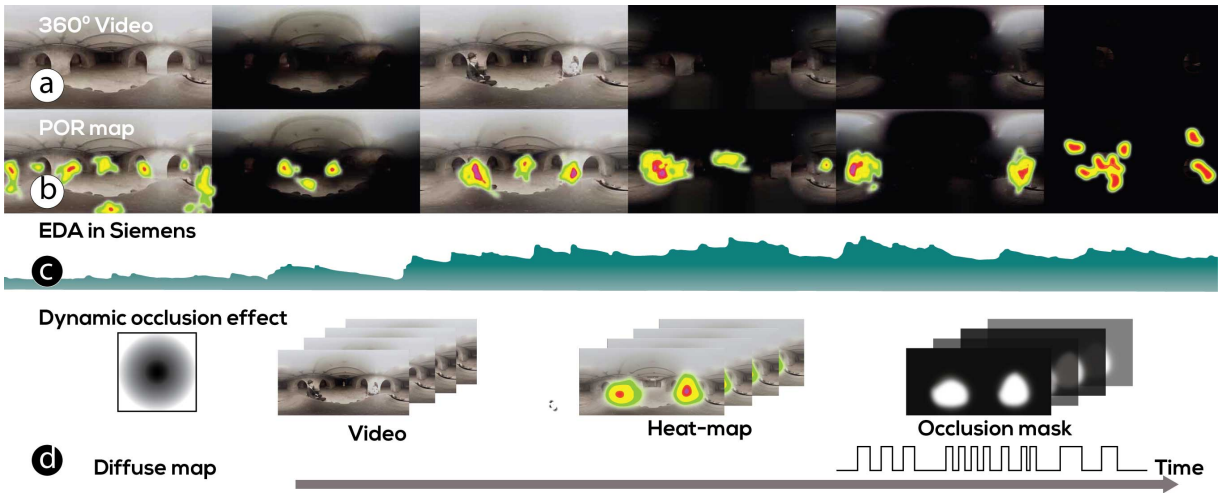

Figure 2-10: a) Frames from the 360 experience. b) Heatmap from point-of-regard (POR) from user's gaze. c) Electrodermal activity in Siemens. d) Diagram showing how the occlusion shader works.

Monitoring user's reactions towards VE content has been a hot topic [65], as it enables the generation of personalized VR experiences. The demo scene presented here uses arousal levels to provides real-time, reliable information about the user's reception of the content and can help the system adapt the content seamlessly. In the 360 video demo player scene, gaze data and SCR data are used to increase the levels of arousal in the user. Figure 2-10 shows how the demo takes standard footage from people in a basement and makes a darker flashing more dramatic 360 captured video, similar to those seen in horror movies.

To direct the user's focus to the people within the video, a surfaces shader is dynamically modulated to occlude locations informed by the Point of Regard (POR) data; the gaze tracking system has the ability to identify areas that are not of interest to the user. The detected Skin Conductance Response (SCR) and peak values are then used to pulse the occlusion shader with modulation.

$$D = \frac{kA - Ymin}{Ymax - Ymin} \tag{2.1}$$

Formula 2.1 shows the simple equation that drives the visibility guided by the user's affective state. D is Duty Ratio of the PWM signal. A is the amplitude of EDA signal. k is the constant coefficient, Ymin and Ymax are the minimal and maximum value about the PWM signal. The POR data is collected by dividing the HTC vive HMD screen into two halves, and each half screen is used for one eye. So, for monocular eye aGlass module, the coordinate is mapping to the half of the screen which size is half of the HTC HMD screen (1080 pixel * 1200 pixel). The coordinate system is normalized, the coordinate of top left is (0, 0) and the coordinate of the right bottom corner is (1, 1). For example, the pixel coordinate of HTC Vive screen where aGlass [62] coordinate (0.5, 0.5) map to is (540, 600). Then this coordinates (POR) are mapped onto a plane at a specific location within the eye tracker coordinate system.

2.4.3 Adaptable Exposure

The PhysioHMD system was also explored in a phobia treatment scenario where a subject is presented stimuli of a feared object using a particle system. The images (sprites) spawned through the particle system can be modified (speed, size, the rate of spawn, movement) in the Unity inspector to increase or decrease the arousal level of the user. This demo shows in Figure 2-11 a participant with entomophobia and her response to the stimulus of the spawning of more insects. The images (sprites) spawned by the particle system can be modified in the Unity inspector, allowing the organizer of the study to control the virtual animal by choosing different functions (e.g., increase/decrease the number of animals; increase/decrease the size of animals; make the animal move continuously or randomly; make the animal stay still).

Taking data input from the EDA signal, control changes were sent to the particle system and synchronously relayed to trigger occurrences in

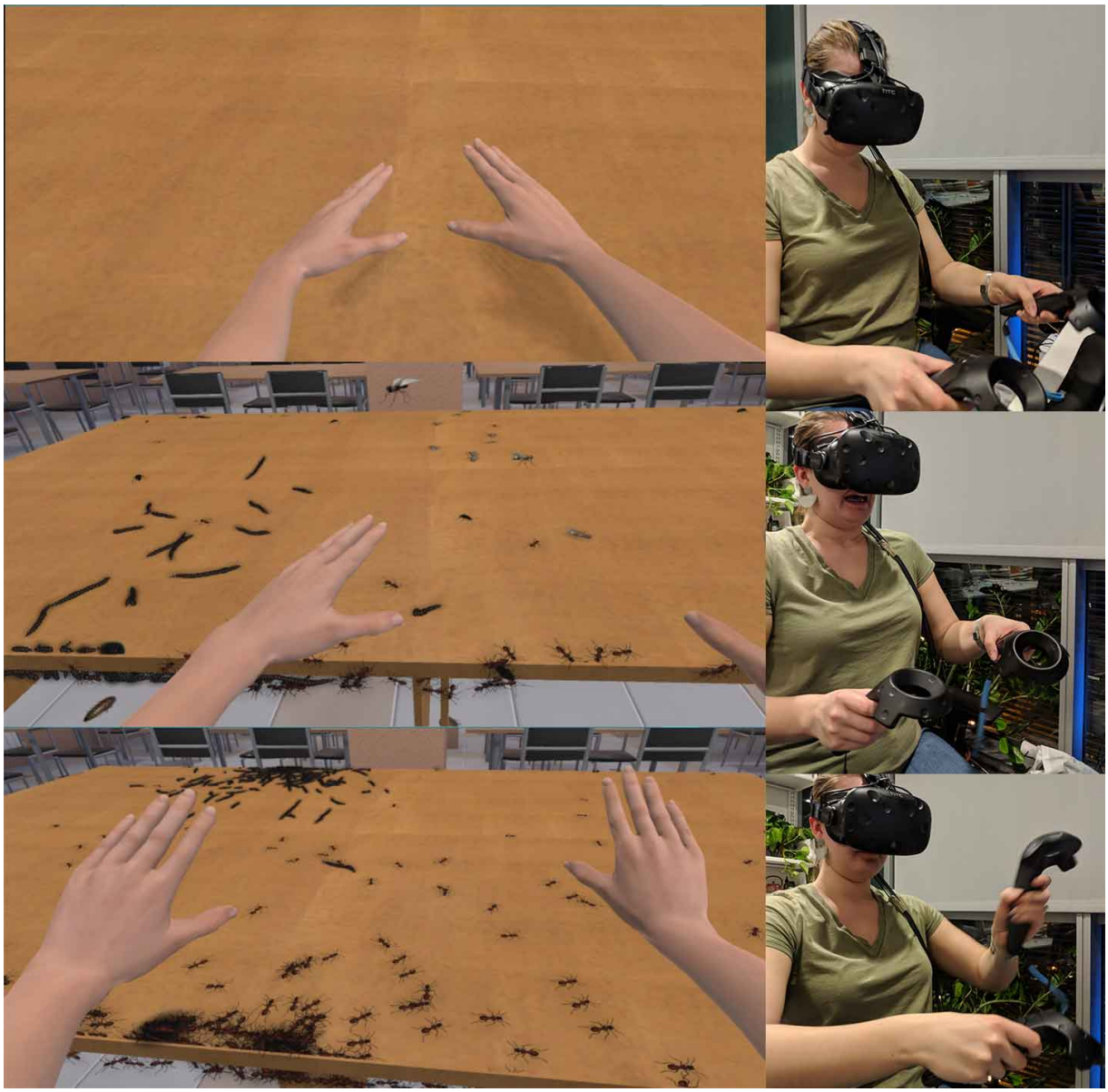

Figure 2-11: Visualization of how users can be exposed to phobias in a therapeutic VR setting. Here, a user with entomophobia is exposed to a virtual setting containing insects. The physiological response recorded by the PhysioHMD modulates the quantity of insects the user is exposed to within the environment.

the behavior of the critters in the scene meant to represent or provoke arousal in the participants. Three levels of participant arousal were determined to range from low to high. Such levels were established based on simple rules regarding how the data from the sensors changed in the short, medium and long-term. Since EDA readings can vary significantly from one participant to another, where possible, the control system was designed to change the criteria by which these rules were based to more accurately reflect the arousal levels of the user group throughout the installation.

2.5 Limitations and Future Work

The applications presented in this research aimed to expose advantages of using physiological computing tools that provide multi-modal sensing for VR psychotherapy, behavioral studies or expression explorations, but there are many features we plan to add in upcoming versions.
For future work, the performance of our CNN on the raw data from more than four channels in the dataset should be investigated. Since the dimensionality of the data is high, an effective channel selection algorithm is necessary. Secondly, the relationship between our CNN structure and its performance is of interest for finding appropriate trade-offs between solution quality and training time. For these reasons, we would like to expand the PhysioHMD platform to a broader community to help grow the quality and quantity of the data.

2.6 Conclusion

In this chapter, we introduced PhysioHMD, a sensor and computing platform designed to analyze multi-modal data related to a user's behavior and responses while utilizing XR technology to enable evaluation and customization of virtual experiences. The toolkit is intended to assist both researchers and non-experts in the arduous task of collecting and processing physiological signals and creating experiences in a game engine. The software provides signal processing methods and data logging for physiological signals in order to provide researchers with accurate, real-time information regarding a user's response to content in a virtual environment. Our intention is to grow a community that contributes to HCI and XR technology research through the pluggable open source platform.

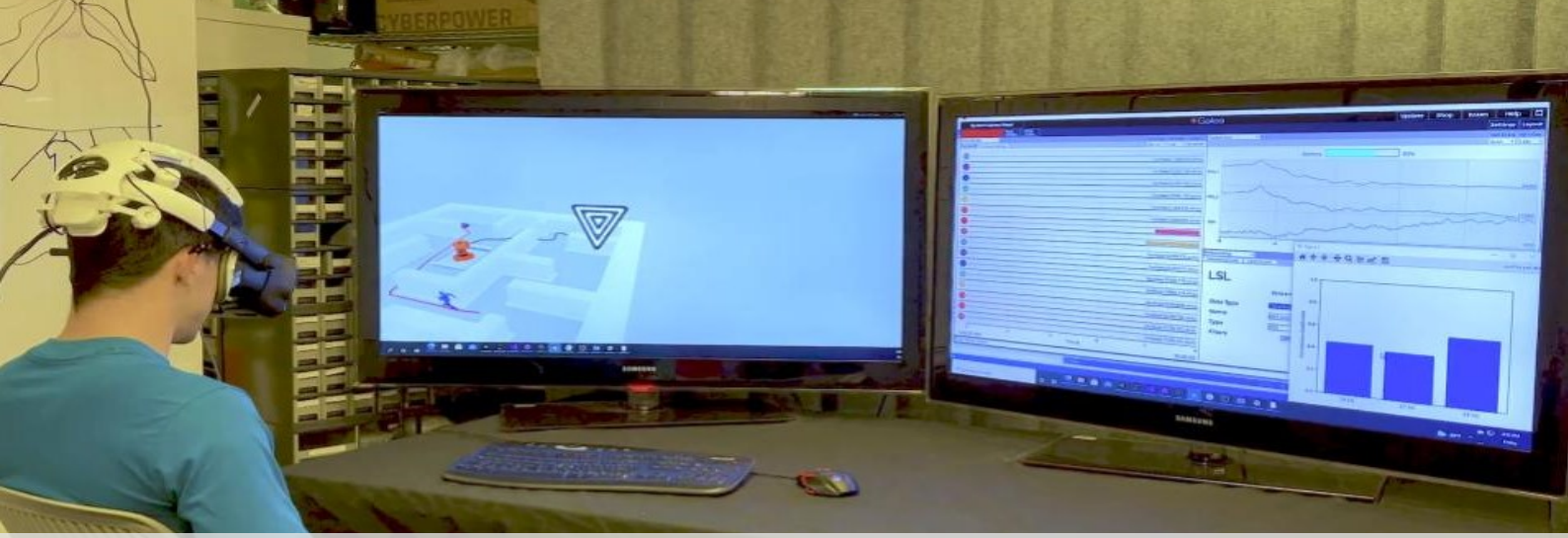

3 Galea

3.1 Introduction

As described earlier, before the development of PhysioHMD, there were no readily available headsets designed to collect the physiological data needed for immersive and adaptive XR experiences. The only approach involved custom integrations using separate sensors and software, which posed significant challenges for potential users. Recognizing the need for a more accessible solution, we set out to create a robust, reliable, and open-source device that could be easily adopted by researchers and practitioners alike.

The journey towards developing a deployable and sustainable solution involved extensive work, from manufacturing and flexible sensor design to collaborating with other researchers and exploring potential partnerships. This chapter will discuss the pivotal collaboration with an Open-Source BCI company dedicated to creating tools for neuroscience and biosensing. Through this collaboration, Galea, a hardware and software platform designed to integrate multi-modal biometrics with mixed reality, was developed. Drawing on the work done with PhysioHMD, Galea expands upon its capabilities and offers a more advanced and accessible solution. Galea's sensors are strategically placed throughout a custom facepad and head strap, designed to be compatible with existing AR and VR headsets, such as the Valve Index. Building on the foundations of PhysioHMD, Galea incorporates sensors for EEG, EMG, EDA, PPG, and EOG. Its software allows for raw data access in various programming languages and supports compatibility with LSL for data merging with other devices.

Galea Publications

The research presented in this chapter has resulted in the following peer-reviewed publications to date.

Bernal, Guillermo, Nelson Hidalgo, Conor Russomanno, and Pattie Maes. ***Galea: A physiological sensing system for behavioral research in Virtual Environments.*** *In 2022 IEEE Conference on Virtual Reality and 3D User Interfaces (VR), pp. 66-76. IEEE, 2022. Bernal, Guillermo, Sean M. Montgomery, and Pattie Maes.* ***Brain-computer interfaces, open-source, and democratizing the future of augmented consciousness.*** *Frontiers in Computer Science 3 (2021): 661300.*

In this chapter, we will delve into the development process and potential applications of Galea, highlighting its role as a powerful tool for researchers, developers, and creators working to better understand and augment human cognition and behavior in the context of extended reality technologies. With its roots in PhysioHMD, Galea represents the next step in the evolution of physiological sensing for XR applications, enabling a new era of research and innovation in this rapidly growing field.

3.2 Related Work

3.2.1 Assessment of Cognitive Responses

Physiological measures are often used to evaluate a user's underlying cognitive process in virtual environments. In the last decade, researchers have employed devices (e.g., head-mounted displays, EEG caps, video capture systems, eye tracking systems, wearable sensing) to improve rehabilitation outcomes of VR-based interventions, such as anxiety therapy [66–68].

The work done by Gupta et al. exploring the measurement of attention or mental workload using physiological sensors to understand trust in virtual agents shows how this approach can provide insights to researchers and designers when developing virtual assistants [69].

Faller et al. in their custom VR closed-loop study have shown that neurofeedback can be used to down-regulate arousal and improve human performance in a demanding sensory-motor task in real time [70].

3.2.2 Commercially Available Devices

The projects mentioned above tackle similar challenges, namely how to utilize insights from the user's physiology in virtual environments. More recently, Looxid Labs, Neurable, and EmteqVR have taken a similar approach as Bernal et. al. and commercialized a sensing add-on for VR headsets. The Looxid Labs product reads brain signals from the prefrontal cortex region in order to assess the user's attention and relaxation [36]. Neurable's proof of concept units collected signals from the occipital region, enabling collection of brain signals related to the visual stimulus presented [37]. The EmteqVR add-on uses facial muscle signals to understand the user's affective state [38]. Each of these products looks at one specific physiological signal, which provides insight into one domain, but does not result in a novel research tool that allows researchers to examine how individual signals may work together or impact each other. In order to understand more complex human behavioral processes, it is important to be able to monitor multiple signals, as is possible with Galea.

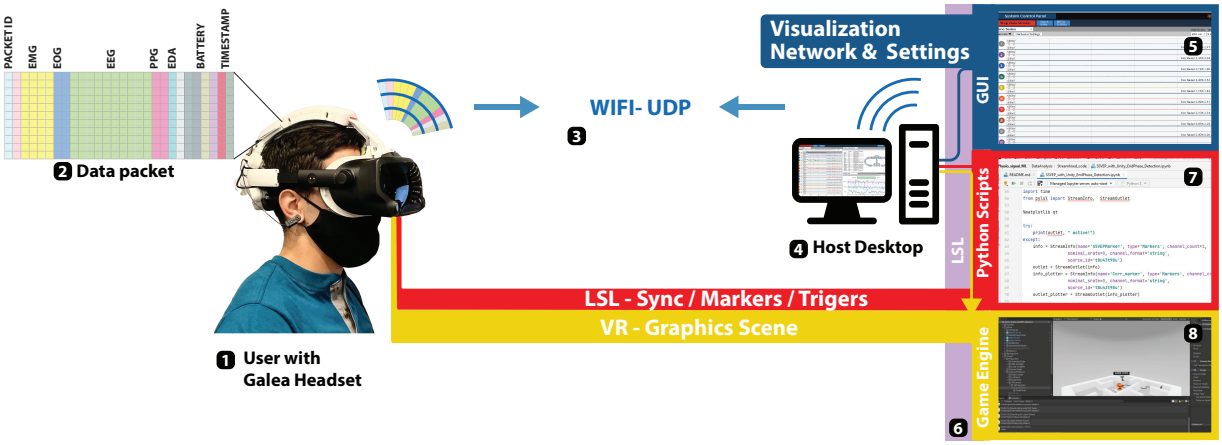

Figure 3-1: System diagram depicting main components: 1) User wearing Galea headset. 2) The device collects indexed data packets from all of the sensors. 3) The packets are sent over WiFi using the UDP protocol. 4) A host computer processes the physiological data, and runs virtual reality experiences. 5) Galea's GUI enables data communication with the headset, hardware settings, and communication with other scripts or software. 6) Lab streaming layer is used to synchronize data received from the headset with events and stimuli generated in the game engine and any middleware scripts. 7) Python scripts are used to do real-time signal processing and classification. 8) Unity3D generated scenes are then presented to the user.

3.3 System Overview

The Galea system simplifies the previously mentioned efforts by providing a solution in the form of open-source hardware and software accessible to the research community. Figure 3-1 shows a flow diagram of

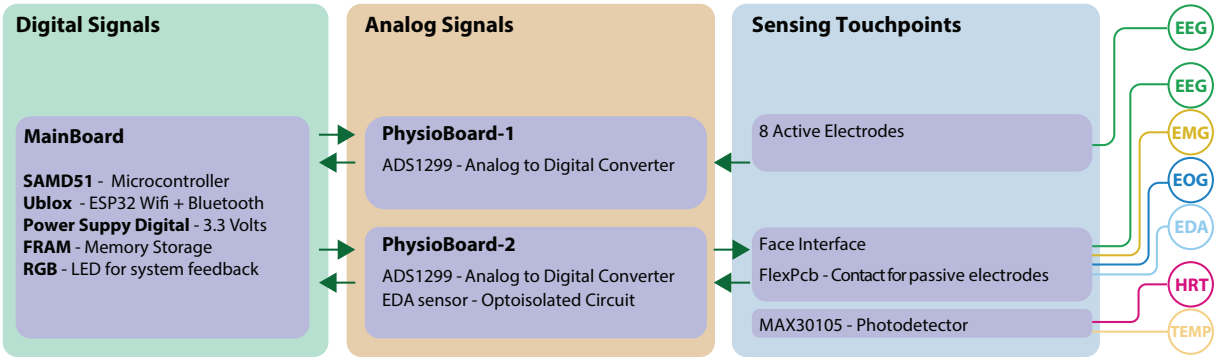

Figure 3-2: Block diagram for Galea's hardware architecture

the system for closed-loop immersive experiences in VR. The sequence of events starts by first connecting the device to a windows machine host over Wifi. Once the communication has been established, the experimenter (or individual using the STEAMVR VR [71] desktop view) uses Galea's Graphical User Interface (GUI), developed by OpenBCI, to check for good conductivity on all channels (below 5uVrms per channel). Next, using the network widget, the LSL stream is initialized. Python scripts are then initialized to process the signal, recognize patterns and do other signal conditioning. Finally, Unity 3D is used to play the VR scenes according to the desired experimental paradigm.

Galea's compact multi-signal hardware architecture can be described in three main blocks: **A** *The digital signals block.* **B** *The analog signals block.* **C** *The sensing touch-points block.* The relationship of these three blocks is shown in Figure 3-2.

The digital signals block manages its own wireless communication in addition to the communication with the other sensing blocks. The analog sensing block is dedicated to collecting data from the brain (Electroencephalogram, EEG), muscles (Electromyogram, EMG) and eyes (Electrooculogram, EOG), and includes an optoisolated section that collects data on the electrical conductance of the skin as a result of sweat secretion (Electro Dermal Activity, or EDA). The third, or sensing touch-points block, utilizes the ergo-electronics face-pad: a flexible Printed Circuit Board (PCB) with gold-plated pickup electrodes that can connect to electrodes like Ag/AgCl (silver/silver chloride), or conductive polymers. This flexible PCB also connects to the optical digital sensing sub-block that detects blood volume changes in the microvascular bed of tissue and skin temperature (Photoplethysmography, PPG).

3.3.1 Signal Characterization

This section, delves into the exploration and analysis of the multi-modal signals captured by Galea. We begin by determining the system's internal noise floor, which is essential for understanding the underlying quality of the data. Next, we present the characteristics for each sensing modality, using both raw and pre-processed in-vivo data. We have made our Python notebooks and anonymized data available at this repository `https://github.com/gbernal/IEEEVR_paper_code`, which includes the code used for generating each of the plots in this section. The data visualizations employed Neurokit2 [72], MNE-Python package [73], and Lab Streaming Layer (LSL) [74].

Input Noise Floor

One of the biggest challenges in building physiological sensing electronics is ensuring that the smallest measurable signal is not drowned in the system amplifier's own noise. At the core of the system is the Texas Instruments ADS1299 [75], a "low-noise, 8-channel, 24-bit analog front-end for biopotential measurements". The device's data sheet states that it has a self-noise of 1 uV over a bandwidth of 0.01 Hz to 70 Hz. When evaluating how the design might introduce other background noise, the desired measurement is the amplitude of the signal that the device measures, even when there is no "real" signal present. Shorting the inputs to ground allows for observing this condition, as anything present is noise.

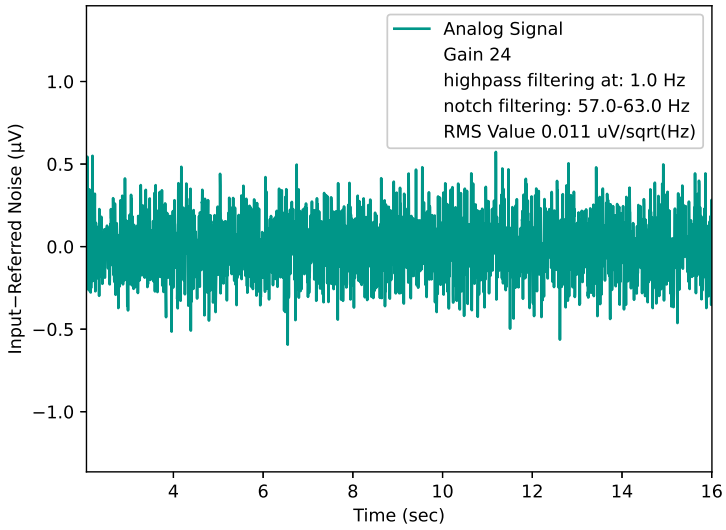

Figure 3-3: Galea physio2 V4, input shorted to AGND, Channel 1.

For the purpose of measuring the input noise floor as shown in Figure 3-3, "input 1" was shorted to "SRB2" with jumper wire, and then "SRB2" was shorted to analog ground with another jumper wire. Figure 3-3 shows 20 seconds of the analog signal recorded by the analog digital converter (ADC) after scaling the raw counts into volts (1 count = 0.022 uV), and after filtering the noise to a bandwidth of 0.1-65 Hz. The root mean square (RMS) value is 0.011 uV/sqrt(Hz). These values are very close to those provided by the manufacturer in the data sheet. The Galea system aims to capture EEG signals which, when measured from the scalp, are typically about 10 µV to 100 µV in amplitude. Having a system with an internal noise of 0.16 uVrms ensures that the device's own noise won't envelop the desired observed signals.

Electrodes

Dry electrodes are becoming popular for both lab-based and consumer-level electro-physiological recordings because they allow for traditional lab-based research to move into the real world. Galea is fitted with two types of dry electrodes: (a) passive-dry electrodes with no on-board amplification, and (b) active-dry electrodes with very high impedance. Conventional sensing areas were utilized using the international 10-20 system, a recognized method to choose the locations of scalp electrodes for brain signal sensing [76]. The face pad electrode placements are based on prior literature reporting of signal activity for each of the signals of interest [**sato_physiological_2020** , 77].

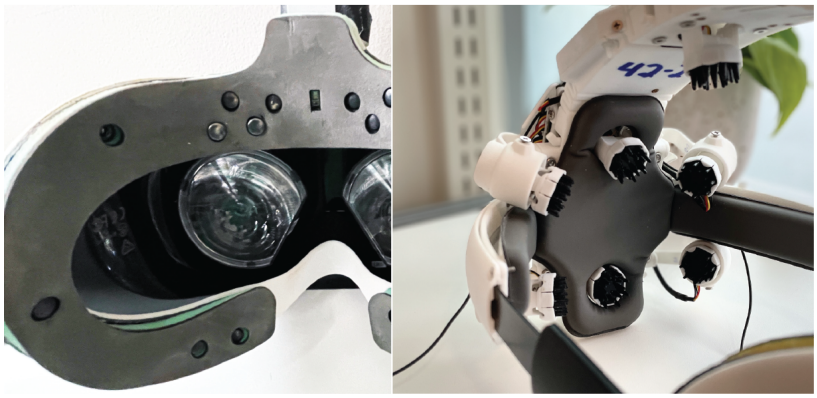

Figure 3-4: Close up view of the electrodes used in Galea. On the left Ag/AgCl passive electrodes are embedded into the face pad. On the right active electrodes with conductive polymer are fit onto the head strap

The face-pad is fitted with Ag/AgCl electrodes and the active electrodes house an op-amp buffer circuit for amplification and a flexible conductive polymer. The signals presented in the following subsections were recorded with both of the electrodes. EEG signals Fp1 and Fp2, EMG from Corrugator Supercilii, EMG from Zygomaticus Major, hEOG Horizontal,

vEOG Vertical and EDA were recorded using the face-pad per Figure 3-4 (Left) and its corresponding mapping in Figure 3-5 (Left).
All of these signals are recorded by the differential circuit module configured for 24-bit resolution, a 500Hz sampling rate, and an amplification gain of 8 for EEG channels, gain of 4 for EMG and EOG, with a 10MΩ input impedance, -110dB CMRR, and a [5-500] Hz passing band.
For the EEG recordings that use the active electrodes, the differential circuit module was used with a 500Hz sampling rate, and an amplification gain of 2 with a [5-50] Hz passing band.

3.3.2 Differential Circuit Module Characterization

Electroencephalogram (EEG)

Electroencephalogram is a technique used to measure the electrical activity of the brain. In EEG, electrodes are most commonly placed on the scalp of a patient to detect the electrical activity of neurons in the cerebral cortex [79]. The electrodes of an EEG device capture electrical activity expressed in various frequencies. Using a Fast Fourier Transform (FFT) algorithm, these raw EEG signals can be identified as distinct waves with different frequencies. Frequency, which refers to the speed of the electrical oscillations, is measured in cycles per second, where one Hertz (Hz) is equal to one cycle per second. These are grouped into frequency bands that are defined by logarithmically increasing center frequencies and frequency widths. Brain rhythm frequency bands include delta (δ) (2 – 4 Hz), theta (θ) (4 – 8 Hz), alpha (α) (8 – 12 Hz), beta (β) (15 – 30 Hz), lower gamma (γ) (30 – 80 Hz), and upper gamma (Γ) (80 – 150 Hz).

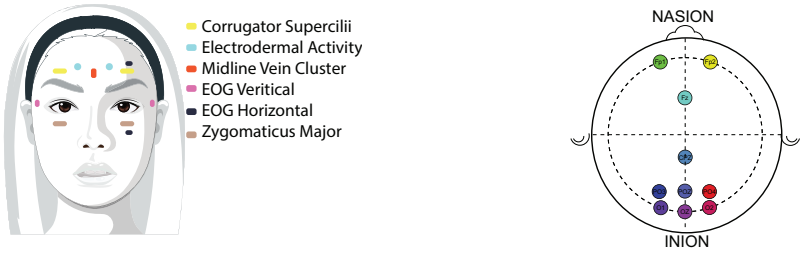

Figure 3-5: (Left) Mapping of sensing touch-points available on the face pad for the Galea system including Fp1 and Fp2, EMG from Corrugator Supercilii, EMG from Zygomaticus Major, hEOG Horizontal, vEOG Vertical, EDA and PPG - **(Right)** Top view of a 10-20 system mapping for the EEG touch-points available in the Galea system including Fp1, Fp2, Fz, Cpz, Poz, Po3, Po4, Oz, O1, and O2.

When validating EEG recording systems, a standard technique is to analyze alpha waves [80]. Following prior research, such signals were recorded in a wakeful human subject during relaxation when the subject's eyes were closed. The EEG detection and recording of alpha waves were tested by measuring the readings from the electrodes shown on the left image of Figure 3-5 and asking the subject to relax, open their eyes for 30

seconds and then stay relaxed with closed eyes for another 30 seconds. First, the Fourier Transform is applied to the input signal,

$$X\left(e^{j\omega}\right) = \sum_{0}^{N-1} x\left(n\right) e^{-j\omega n} \tag{3.1}$$

where $x\left(n\right)$ is the input signal, N is the size of the input signal, $\omega = \frac{2\pi}{N}$, and $X\left(e^{j\omega}\right)$ is the corresponding output after Discrete Fourier Transform. Then, the output of Equation 3.1 is squared and divided by the length of the original signal.

$$\hat{S}_{NX}(\omega) = \frac{1}{N}\left|X(e^{j\omega})\right|^2 \tag{3.2}$$

where $\hat{S}_{NX}(\omega)$ is the Power Spectral Density, Equation 3.2.

Figure 3-6-3 shows the average power spectral density for EEG electrodes Fp1, Fp2, Fz, Cpz, Poz, Po3, Po4, Oz, O1, and O2 for subject 2 in response to the open and closed eyes intervals while wearing the headset in VR. This increased activity in the 7.5–12.5 Hz region in the frequency domain showed a typical alpha wave signal depicted in Figure 3-6.a & b of the brain's occipital lobe area.

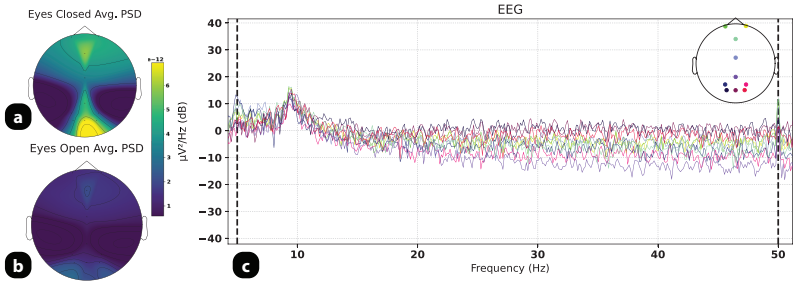

Figure 3-6: Topographical map of average power spectral density in the alpha band across all channels for eyes closed (a) and eyes open (b) states. The power spectral density across all channels in response to the open and closed eyes task while wearing the headset in VR. The increase in power density at the 10Hz mark is generated by the closed eyes condition. (c)

To assess the quality of the alpha power difference detected, it was compared to the existing literature. The average alpha power spectrum difference between the closed eyes state and the open eyes state in the Galea system was 7.86 uV^2, which is comparable to the power difference of 10.67 uV^2 reported in a wet electrode system for a similar task [81]. In addition, Galea's alpha power had a signal to noise ratio (SNR) value of 5.01 dB calculated based on Equation 3.3, where P_{signal} includes the alpha power band of 10-12 Hz and $P_{background}$ includes the power spectrum for less than 10 Hz.

$$SNR = 10 \cdot \log_{10}\left(\frac{P_{signal}}{P_{background}}\right) \tag{3.3}$$

Electromyogram (EMG)

Electromyography is a clinical technique used to study and analyze electrical signals produced by muscles. This section details the EMG signals collected from the facial muscles involved in facial expressions using Galea.

The surface EMG signals are affected by baseline perturbations introduced by undesired movements, which are generated by talking, walking, and contact shifting of the electrodes. A common method to detrend the signal is by using a fourth-order high-pass filter. In Figure 3-7 a high pass filter at 100Hz has been used to detrend the signal.

A standard way of processing an EMG signal is to calculate an activation level of the signal, a process which is called the linear envelope [82, 83]. Based on the square root calculation, the RMS reflects the mean power of the signal and is the preferred recommendation for smoothing.

$$X_{rms} = \sqrt{\frac{1}{T_2 - T_1} \int_{T_1}^{T2} \left[f\,(t)^2 \right] dt} \tag{3.4}$$

The RMS Equation 3.4 represents the square root of the average power of the EMG signal for a given period of time. It is known as a time domain variable because the amplitude of the signal is measured as a function of time.

The recorded EMG signal was compared to Agostini et al. [84] extensive methods for evaluating signal-to-noise ratio (SNR) for EMG signals using Equation 3.5

$$SNR_{emg} = 10 \cdot \log_{10} \frac{P_{Signal} - P_{Noise}}{P_{Noise}} \tag{3.5}$$

Where P_{Nosie} is the estimate of the mean power of the noise, averaging five bins around I_{Noise} and P_{Signal} is the estimate of the mean power of the signal, averaging five bins around I_{Signal}.

An SNR value of 27.6 dB is calculated from the recorded signal from the zygomaticus major muscle, whereas Agostini et al. reported an SNR value of 28.0 dB from the tibialis anterior, a much larger muscle.

The linear envelope consists of two steps: first, the signal is full-wave rectified by computing the absolute value of the signal; then the rectified signal is low-pass filtered with a cutoff frequency typically in the range of 3 to 8 Hz, depending of the contraction muscle characteristics and the specific application for the linear envelope processing. This last step can

also be reproduced with a moving average of the rectified signal with a moving window of 100 to 200 ms of duration.

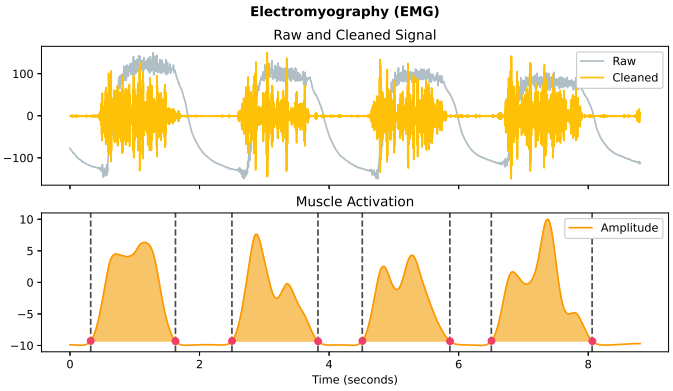

Figure 3-7: Raw and processed EMG signal from Galea

Electrooculogram (EOG)

Electrooculography is the measurement of eye movements based on recording the standing corneal–retinal potential emerging from the hyper-polarization and de-polarization existing between the cornea and the retina. The standing potential in the eye can be evaluated by measuring the voltage induced across the pair of electrodes placed across the vertical and horizontal axes of the eyes as the eye gaze changes. The spatial orientation of the subject's eyes, as they fixate on a particular target point, can then be determined using the identified EOG signal relative to the sphere's origin.

The EOG signal recorded with the Galea system varies from 50 to 350 mV and has a frequency range of about DC-100 Hz. These types of signals are not considered deterministic, and the magnitude varies with time, as shown by the raw signal in Figure 3-8. This means that the variability of the electrooculogram reading depends on many factors that are difficult to limit: perturbations caused by other biopotentials such as EEG or EMG, in turn, brought about by the acquisition system, plus those due to the positioning of the electrodes, skin-electrode contacts, head and facial movements, or blinking. One of the contributions of this research is to mitigate some of these challenges by integrating these electrodes into the face pad.

Figure 3-8 shows the changes in polarity of the signal for hEOG, which was bandpass filtered between 0.01-100Hz and detrended based on an unsupervised signal detrending algorithm [85]. It also shows how blinks, shown in Figure 3-8.B and Figure 3-8.C, can be calculated from the

EOG channels automatically [86, 87]. These artifacts can be used for HCI interaction inputs, or passed along as a feature for eye blink removal to an algorithm processing EEG.

To assess the accuracy of the EOG signal, its SNR was computed based on equation 3.3. In this case, P_{signal} was the EOG frequency of interest from 0 to 10 Hz and $P_{background}$ was the rest of the signal. An SNR value of 13.61 dB was obtained.

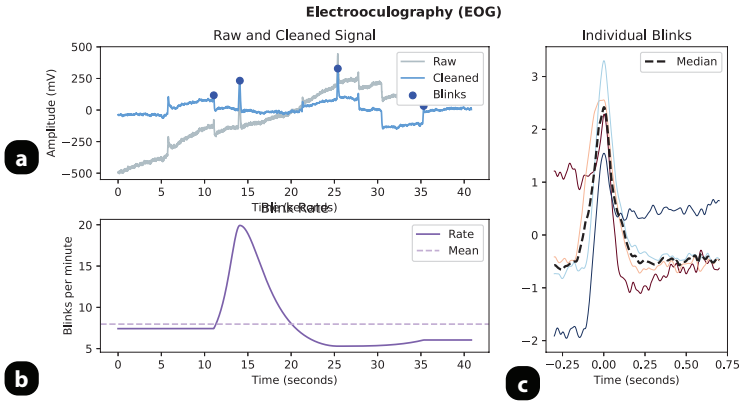

Figure 3-8: Raw and processed vEOG signal from Galea: (A) the detrended and filtered vEOG signal, (B) 1 second window of all blinks detected and their median value, dark dashed line, and (C) the time interval between blinks.

3.3.3 Electrodermal Activity (EDA)

Electrodermal activity measures the variations in conductivity produced in the skin due to accretions in the activity of sweat glands. The preferred sites for EDA measurements are located in the palms of the hands and the soles of the feet. However, it has been shown that the forehead has significantly higher baseline Skin Conductance Levels than any other site, followed by the fingers, which have a considerably higher baseline for Skin Conductance Levels than the wrist and the arch [77].

EDA signals are composed of two different components. The phasic component or Skin Conductance Response (SCR) is seen when the sudomotor nerve is activated. Given this connection, SCR has been broadly used to measure the sympathetic nervous system [88, 89]. SCR is represented by a peak or a burst of peaks with different amplitudes, slopes, and declines depending on the constitution of the person's response to a stimulus [90]. Figure 3-9 shows the SCR components extracted from a 16 second recording wearing the Galea headset and asking the user to sit and stand quickly 3 times. This method is commonly used to elicit EDA response and to collect a baseline from the participant [91, 92].

The other component of EDA is the tonic component, a constant, slowly-changing Skin Conductance Level (SCL). SCL represents the baseline

of skin conductance. SCL varies among people, depending on their physiological states and autonomic regulation [93]. Consequently, the EDA signal is represented by a fast-changing SCR signal modulated by a gradually changing SCL element. This slow response in SCL ranges from 0 to 0.05 Hz, whereas the energy of the SCR component ranges from 0.05 to 1.5 Hz.

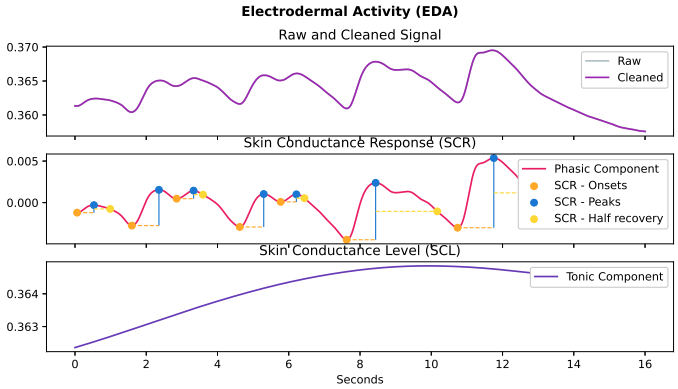

Figure 3-9: Raw and processed EDA signal from Galea

To assess the reliability of the EDA signal collected by Galea, the SNR of the signal was calculated based on Equation 3.3. As proposed by Wan et al. in section 5.3.1 [94], the P_{signal} value is the sum of the power spectrum in the frequency range 0 to 5 Hz, which is the range of useful EDA signals, and it is divided by $P_{background}$, the sum of the power spectrum of the rest of the signal. The Galea EDA signal had an SNR value of 33.09 dB on a physical stress task, whereas a reference EDA sensor by Wan et al. showed 28.52 dB for a similar physical stress task.

A challenge for a configuration like Galea's is that electrodermal activity (EDA) sensors introduce a small DC current applied to the epidermis' outermost layer under the electrodes. When measuring EEG near these electrodes, noise artifacts can be introduced since both sensing circuits share a common ground. These can lead to a ground loop or ripple effect noise generation. To prevent this issue, the EDA signal was optoisolated from the other circuitry on the board.

3.3.4 Optical Digital Sensing

Photoplethysmography Sensor (PPG)

The MAX30105 was used in the Galea headset, which is a particle and proximity sensor with PPG and temperature sensing. This device is placed in its own Printed Circuit Board (PCB). This separation from the main and even secondary PCBs allows the temperature sensor to be

more accurate in representing the temperature of the person wearing the device since any nearby hardware does not skew it. It also enables the PPG sensor to have reduced noise data, as it uses a red LED and infrared sensor to measure the pulses from the blood flow. The forehead region has been reported to be well-perfused by arteries branching from the internal carotid, hence, providing great quality and stable signals [95, 96]. Heart-rate measurements acquired from the forehead have been reported to be less affected by vasoconstriction and to be quicker than fingers in indicating deoxygenations [95, 97]. Figure 3-10 shows a sample recording from the Galea device, where the peaks are calculated to measure heart rate.

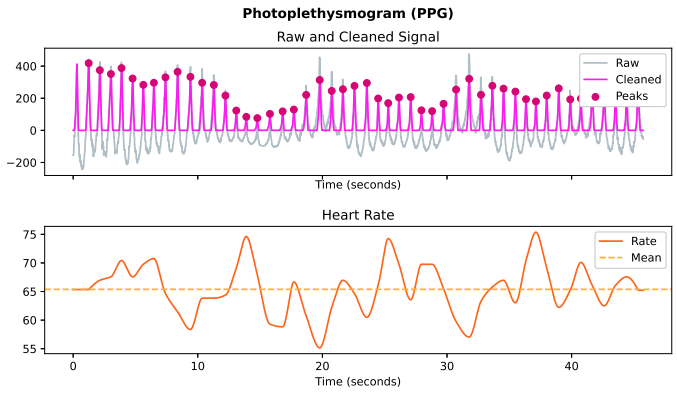

Figure 3-10: Raw and processed PPG signal from Galea

The heart rate typically varies slightly: during a deep breath, it speeds up, and during a deep exhalation, it slows down. An RR tachograph visualizes the recorded values of the RR-interval against time. The RR interval will shorten when the heart speeds up, and lengthen when it slows down.

Several research papers [98, 99] demonstrate the potential of PPG signal-based Poincaré plots in detecting heart-related disorders or irregularities. Figure 3-11 shows a Poincaré plot from a 2 min PPG signal recording from a healthy person at rest. A quantitative examination of the HRV attractor displayed by the Poincaré plot can be made by modifying it to an ellipse. For the performance analysis, the SD1 (Standard Deviation1): 20.699445, SD2 (Standard Deviation 2): 70.189299 and s (area of ellipse described by SD1 and SD2): 4564.355626 are used as evaluation parameters [100].

In addition, The MAX30105 is capable of producing temperature readings from the on-board temperature sensor in both Celsius and Fahrenheit. The temperature sensor is accurate to +/-1 C with the precision of 0.0625 C.

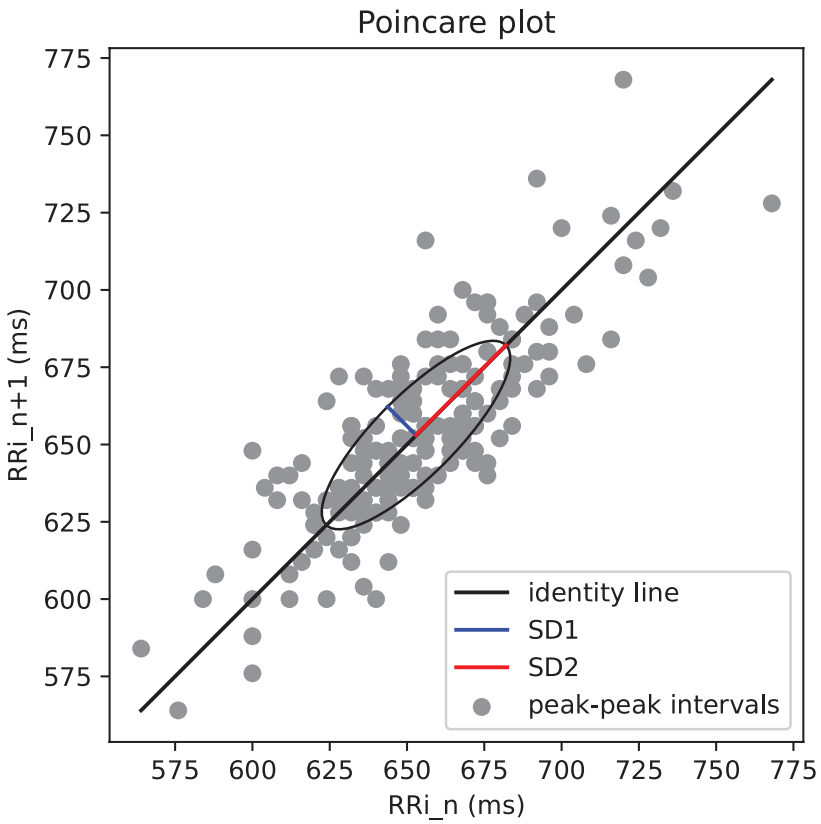

Figure 3-11: Poincaré plot from a 2 min record of PPG signal from a healthy person while at rest

3.4 Validation Use Cases

To help contextualize the signals presented in the previous section, two examples that shows how researchers can use this platform in their research are presented below, thus demonstrating how Physiological Computing can be utilized in VR.

Six healthy subjects with normal or corrected-to-normal vision were recruited to participate in the experiment, ages 18 to 34. Protocols for data collection were approved by MIT COUHES. Before the experiment, subjects were asked to sit in an office chair and wear the Galea headset fitted with Valve Index VR headset. The VR headset was configured for 90Hz FPS which allowed stimulating signals to be generated at frequencies up to 45Hz. The test was run on a desktop fitted with a GeForce GTX 1080 GPU. The experiments were tightly synchronized using LSL due to the small timing errors of less than 1-millisecond [101] between all the physiological signals and the event markers (i.e., Visual stimulus).

3.4.1 SSVEP Accessibility In VR

BCI systems often rely on recognizing specific brain activities such as motor imagery, P300, and steady-state visually evoked potential (SSVEP) [102, 103]. Among them, SSVEP is one of the most broadly used brain responses for developing BCI-based interactions. SSVEP occurs when the user is stimulated by a visual stimulus that has a specific frequency [104]. A VR top-view maze game in which the user controls an avatar using real-time biofeedback was created with SSVEP as the main mechanism for character movement due to the robust nature of the interaction. This game is a great exemplification of how EEG signals can be used in HCI. The SSVEP game mechanic shown in Figure 3-12 works by utilizing the user's voluntary engagement to look at checkerboard stimuli flickering at different frequencies, which are produced using a sampled sinusoidal stimulation method. Equation 3.6 [105] was followed to generate the stimulus, where $L(f_{st}, k)$ is the luminance of the stimulus, $f_s t$ is the target frequency, R_{ref} is the refresh rate of the display, and k is the sample which is drawn iteratively in Unity.

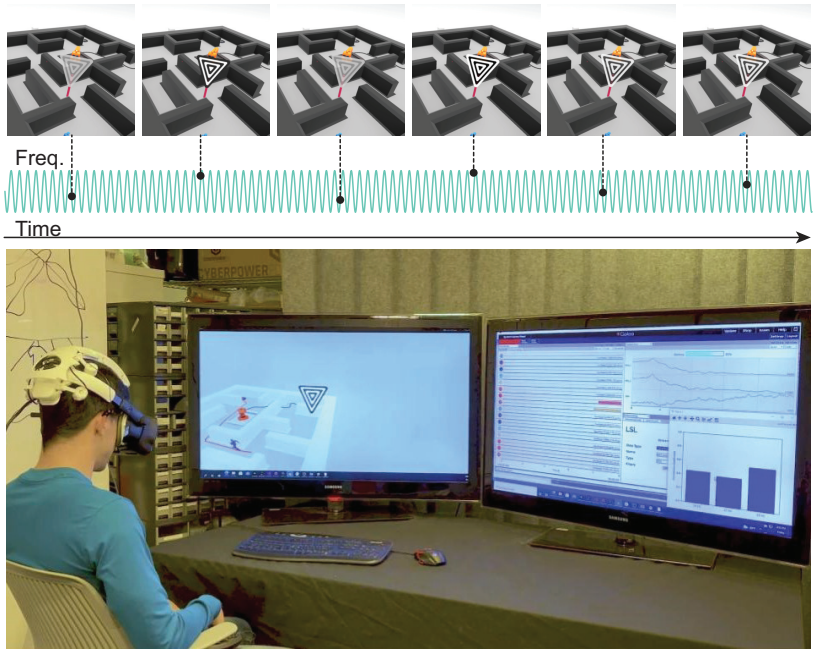

Figure 3-12: The top diagram shows how the stimulus is presented to the user. The triangle changes its visibility at a fixed frequency from fully transparent to fully opaque. On the Bottom is the experiment view, where the left monitor shows the user's perspective view in VR. The maze has checkered patterns flickering at different frequencies used for visual stimulation. On the right monitor is a view of the data being streamed from the GUI to Unity3D via LSL.

$$L(f_{st}, k) = 0.5 \sin\left(\frac{2\pi f_{st} \kappa}{R_{ref}}\right) + 0.5 \tag{3.6}$$

$$X = [X_{POz} X_{Oz} X_{PO3} X_{PO4} X_{O1} X_{O2} \tag{3.7}$$

$$Y_f = \begin{bmatrix} sin(2\pi f) & cos(2\pi f) \\ ... & ... \\ sin(2\pi fN) & cos(2\pi fN) \end{bmatrix} \tag{3.8}$$

$$\max_{W_x, W_y} \rho_f = \frac{E\left[W_x X^T Y_f W_y^T\right]}{\sqrt{E\left[W_x X^T X W_x^T\right] E\left[W_y Y_f^T Y_f W_y^T\right]}} \tag{3.9}$$

The EEG response provoked by these stimuli is analyzed using a Canonical Correlation Analysis (CCA) based algorithm, which is a widely used technique for SSVEP detection [**bin_online_2009** , 106, 107]. CCA computes the correlation between the EEG signal, represented in Equation 3.7 where X is N samples by 6 channels, and the expected stimulus frequency, represented in Equation 3.8 where Y_f is a sinusoid of frequency f and N samples. Then, based on the canonical correlation Equation 3.9, the frequency f which produces maximum correlation ρ_f is picked as the SSVEP prediction. This allows the user to move the avatar to different designated locations in the maze.

To assess the quality and accuracy of SSVEP detection in a more controlled environment, offline experiments were run in VR on 6 users who had normal or minor visual impairment and no history of photosensitive epilepsy. The users looked at 8 stimuli flickering from 16 to 23 Hz for 10 seconds which were presented for a total of 4 trials, each in a randomized order. The results shown in Figure 3-13 exemplify the SSVEP signal obtained from one of the users showing clear peaks at each stimulus frequency in the power spectral density (PSD) plots. In Figure 3-14, the results of the offline CCA analysis across all users is presented. The different window sizes represent the length N of the signal, where 1 second corresponds to 250 samples, used to compute CCA. Shorter time windows mean faster detection time. However, a trade-off between detection time and accuracy was observed: window sizes of 3 and 4 seconds provide a good balance of classification accuracy and time delay.

Comparative Benchmark Results

The SNR of the signal was computed by finding a ratio between the target frequency and adjacent frequencies based on Equation 3.10, where $y(f)$ is the power of the target frequency computed based on the Fast Fourier Transform, Δf is the frequency resolution of 1 Hz, and the denominator

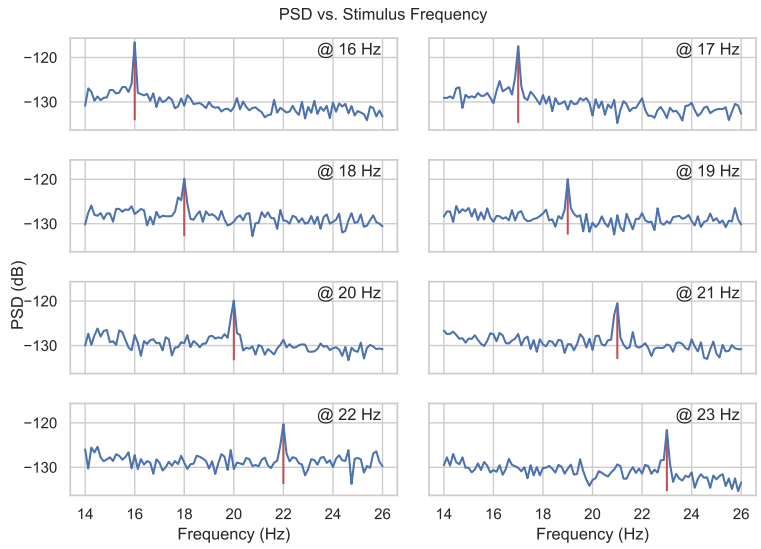

Figure 3-13: PSD of SSVEP response for stimulus frequencies between 16Hz-23Hz. Each PSD is averaged across 4 trials lasting 8 seconds.

performs averaging over adjacent frequencies to f [109, 110].

Table 3.1 is a comparison between the Galea system and other systems that share similarities to the experimental design and methodologies. The Galea system performs similarly to state-of-the-art CCA-based SSVEP experiments using dry-electrode EEG. Galea achieved higher performance (78%) for 3 second time windows, but lower performance for shorter time windows. One possible explanation for the lower performance of the Galea CCA results compared to other systems is that for the shorter time windows, Galea used a sampling rate of 250 Hz while the studies referenced used 1000 Hz.

$$SNR_{ssvep} = \frac{y(f)}{1/8 \sum_{k=1}^{4} (y(f - \Delta f \cdot k) + y(f + \Delta f \cdot k))} \tag{3.10}$$

Literature	Avg. SNR	Avg. SNR (dB values)	Exp. Properties
1 [111]	-	11.0	40 stimuli, 8-14 Hz, Freq. resolution 0.2 Hz
2[107]	4.08	-	45 stimuli, 7-15.8 Hz, Freq. resolution 0.2 Hz
3[110]	4.71	-	1 stimulus, 5Hz-30Hz
4[112]	-	8.17	12 stimuli, 9.25-14.75 Hz, Freq. resolution 0.5 Hz
5 [Ours]	4.29	11.76	8 Stimuli, 16-23 Hz, Freq. resolution 1Hz

Table 3.1: Quality of SSVEPs from dry electrode based BCI in recent years.

The system's information transfer rate (ITR) in bits/min was also calculated based on Equation 3.11, where N is the number of targets, P the average classification accuracy, and T the seconds per stimulus selection. Galea achieved similar or higher ITRs than some of the other systems for the two-second and three-second windows, 32.08 bits/minute and

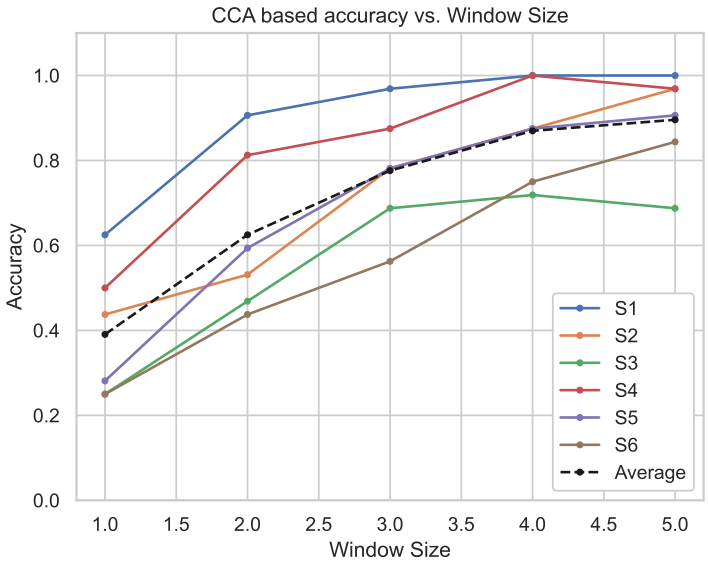

Figure 3-14: Classification accuracy of stimuli 16-23 Hz based on Canonical Correlation Analysis with a maximum correlation coefficient. The plot displays accuracy versus different window sizes, spanning 1 to 5 seconds across 6 users.

29.78 bits/minute respectively. The Galea experimental set-up was not optimized to improve ITR, which is an aim for future work. Improvements in this area may be achieved with the system by using the 360 VR environment to capture more stimuli.

$$ITR = \frac{60}{T}\left[\log_2 N + P\log_2 P + (1-P)\log_2\left(\frac{(1-P)}{(N-1)}\right)\right] \tag{3.11}$$

3.4.2 EOG Visual Attention

A simple VR scene, resembling a museum, was modeled to help developers get started with the use of EOG signals to determine visual attention in VR.

Figure 3-15: Screenshot from participant's point of view in VR when performing the visual attention task.

Figure 3-15 Shows the VR scene that was constructed as a test bed to test and process the signal generated by the EOG. The participant was asked

to look at the different objects starting from the upper left corner and moving their eyes counter-clockwise to each corner every one second. This cycle was repeated six times. This section of the experiment was used to set the threshold value and set an empirical upper bound for the EOG signal corresponding to different saccades. This experiment was performed offline in order to demonstrate a simple use of EOG signals as a tool to assess user attention.

The EOG signals were processed with a bandpass filter in the 1-10 Hz range. This allowed for correction for the offset due to frequencies lower than 1 Hz that are present in the EOG, making the signal more robust to classification based on thresholding. However, this algorithm is not able to separate saccades from blinks, a property that is a goal to be implemented in future work. The EOG signal may be classified with an upper and lower threshold given its characteristic depolarization/repolarization properties [113]. The application first computes a threshold for each EOG channel based on the root mean square value over sliding, 500 ms time windows during the first 1 second of the experiment when the user is instructed to move their eyes between the 4 corners of the gallery.

Based on the threshold, a decision tree tool was manually crafted, Algorithm 1, to classify between right, left, up, down, up left, down left, up right, and down right depending on the activation of the hEOG or vEOG channel. The threshold boundaries showed precise partitions of different saccade directions as shown in Figure 3-16. The location of each section corresponds to saccades moving in that direction, i.e. the magenta region would correspond to looking up and the grey to looking left. These partitions are shown based on the absolute maximum, meaning the positive or negative voltage value which is greatest in magnitude, for each EOG channel across 120 saccades from one user.

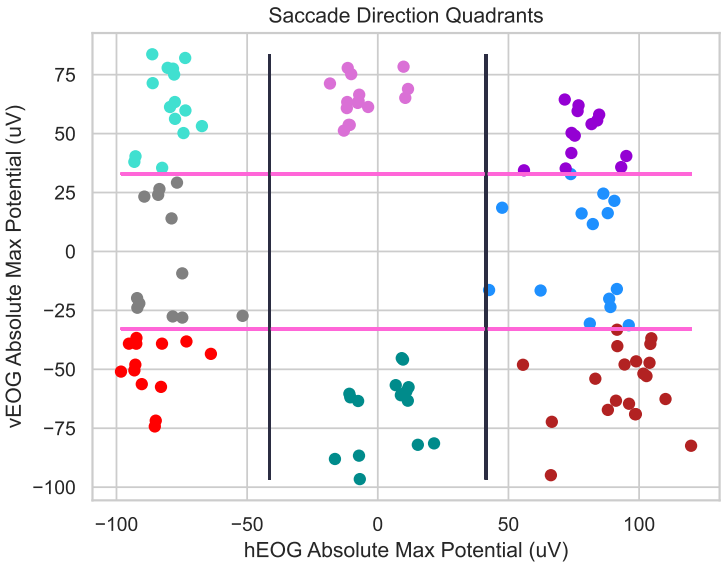

Figure 3-16: Visualization of the threshold partitions when considering the highest magnitude peak of vEOG and vEOG Each partition represents the directions in real space of a saccade.

3.5 Discussion

Some of the most significant challenges that BCI and VR research encounters are the long preparation time to instrument subjects, data synchronization, and comfort levels due to physical constraints that the device's weight puts on the user during long VR experiences. In this work, a novel design has been introduced for collecting physiological data while using a VR headset that helps reduce the setup time and simplifies data wrangling. However, more work still needs to be done for the device to be used during long periods; VR headsets need to become lighter to be comfortable for long-term use. With the current Galea setup, sessions longer than 30 minutes cannot be run without causing strain levels for the participant. As part of the device's ongoing development, these limitations have to be prioritized for successful long-term use. Galea's platform has the potential to enable researchers to develop human testing and training environments in which they can precisely control elaborate stimulus presentations and monitor the resulting physiological responses. As a result, human cognitive and functional performance can be carefully evaluated and rehabilitated.

This writing only touches upon some initial applications and use cases to help readers contextualize the system's advantages. More studies are needed to thoroughly understand the potential of the Galea tool for the target community. Workshops with psychologists, cognitive science departments, and HCI groups will need to be planned to build a community of users and collect valuable feedback informing updates to

the system.

3.6 Conclusion

Galea offers a useful tool for anyone who is interested in collecting and processing physiological signals and creating adaptive experiences in VR by improving the access and ease of use for researchers and practitioners and decreasing the delay between data collection and obtaining results. This section presented a system consisting of hardware and Python notebooks that makes working with physiological sensors in VR straightforward, and can offer a standard for inter and intra experiment comparisons. A primer on detectable human physiology from the signals available through the device was presented and the primary design considerations and circuit characterization results of in-vivo recordings from the wearer's brain, eyes, heart, skin, and facial muscles were discussed. An example to help illustrate how these signals can be used in a virtual reality setting has been presented in detail. Galea is intended to encourage users to become part of a supportive, open-science community with diverse areas of expertise rather than relying on closed-source and proprietary tools, thus shaping the future of physiological computing and its related fields.

With the introduction of PhysioHMD and Galea, researchers now have the tools to measure and analyze multi-modal signals related to a user's behavior and responses in virtual environments. The aim is to provide a platform for evaluation and customization of virtual experiences and to advance the field of Physiological Computing and Human-Computer Interaction through the collection of real-time, accurate physiological data. The next section explores the application of these tools in virtual reality, showcasing how the detected signals can be used to enhance the user's experience and create a more immersive environment.

Part II: Environments for Creating Behavioral Experiments that Utilize Virtual Reality

4 Entwine

4.1 Introduction

With the growing need for virtual interactions and the increasing demand for physiological computing, the development of a toolkit that can streamline the process of setting up virtual reality experiments becomes essential. That is where Entwine comes into the picture. Designed specifically for use with the Galea headset, the Entwine Toolkit was created to reduce the amount of time required to setup experiments and make it easier for researchers and practitioners to collect and process physiological signals and create adaptive experiences in virtual reality. The constantly growing set of tools and VR experiments stored in a central repository allow for easy access and collaboration, further facilitating the virtual reality experiment process.

Entwine was developed as a toolkit where evaluating focus and attention in user response scenarios is especially relevant given today's increased need for virtual interactions to help support the aforementioned claim. The Entwine Toolkit is meant to be a constantly growing set of tools that empower behavioral researchers to create virtual reality experiments. All of the code and VR experiments are kept in a git repository, which is a space where all repositories are kept for ease of access. This space can be found at the GitHub repository.

Entwine is a set of useful modules built in Unity that are meant to help with the necessary features of creating a VR behavioral experiment. These modules are designed so that they can easily be built on or modified however the user sees fit; in fact, the intention is not that they will act as a replacement for Unity development, but rather an aid in lowering the barrier to entry. Entwine can also be thought of as a group of VR experiences that can be used as is, expended, or modified. This chapter introduces Entwine at a high level; a proposed solution that serves to provide both tools and fully featured experiments to researchers that allow for quick development and collaboration in the behavioral VR research space. Chapter 5 and Chapter 6 are focused on studies made using the Entwine experiments available.

4.2 Motivation

As VR becomes more mainstream in both the entertainment and enterprise industries, the interest in VR-focused behavioral research continues to grow. Although many tools help researchers design and build their experiments, there is no existing toolkit or space that allows researchers to collaborate and replicate behavioral VR experiments.

In recent years, virtual reality has continued to grow and gain attention in the consumer space [114]. Low-cost VR headsets such as the Oculus Quest 2 or the recently announced PlayStation VR 2 have continued to bring more users into the industry and appeal to a wide variety of customers and developers. Even the more expensive headsets like the Valve Index have generated a strong hobbyist VR community. VR is making its way into more homes than ever before and will most likely continue to do so in the future, but what's interesting is that these same low-cost headsets are assisting VR in making its way into behavioral lab environments that may not have previously considered VR in their research [115]. Just as consumers have become more aware and more interested in the growing VR industry, researchers from various scientific backgrounds have taken to VR as both an exciting focus of study [116, 117] and a tool to help answer their own questions [115, 118]. Specifically for behavioral researchers, virtual reality is a valuable platform for studying participants' behaviors as it's easy to create any number of environments. These environments can be designed to be safe, controllable, replicable, and accessible to participants from a variety of backgrounds and with a variety of needs [119, 120]. A key concept of behavioral research is analyzing the participant's response to an environment, so VR's capability to efficiently create and share new environments makes it a powerful tool for researchers [121, 122].

As interest in VR continues to grow among behavioral researchers, more and more tools to help researchers in the development of VR experiments are being created. It can be difficult for researchers to keep up with the growing technical requirements for experiment development as the field continues to grow and shift focus.

As described in the previous section, Galea's combination of this multimodal sensor technology with immersive augmented and virtual reality gives researchers, developers, and artists a powerful new way to study and improve the human mind and body.

Using a multi-signal method, researchers may be able to set up training

and testing environments for people that allow for the precise management of complex stimulus presentations. This would allow the cognitive and functional performance of people to be carefully tested.

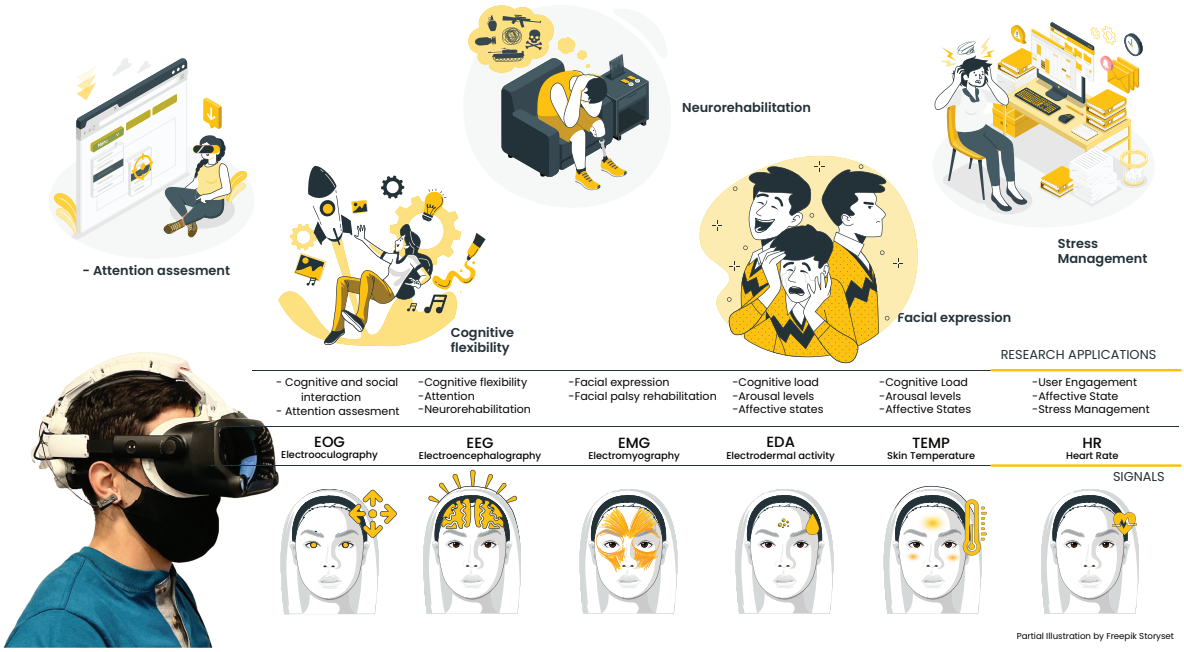

Figure 4-1: Entwines potential impact area based on the sensing capabilities from the Galea headset.

4.3 Entwine Unity Toolkit prefabs

The Unity plugin for creating VR behavioral experiments make up the first half of this chapter. These modules (or prefabs as they are called in Unity) are meant to lower the barrier to entry to Unity development by allowing users to build on top of or modify them. This section will go through some of the modules available in this toolkit. First, we will examine the modules that directly connect to the experiment participant's experience. This consists of user interface, user interaction, and surveys. A more detailed information on the classes and the code available, please look at my collaborator Yodahe Alemu Master of Engineering thesis document

4.3.1 User Interfaces

The User Interface is perhaps one of the most crucial components of developing a VR project. Using the user interface, researchers can provide participants with crucial information throughout an experiment. This includes offering directions on what to do next, explaining the context of

what is occurring, and allowing participants to provide feedback. This is extremely important for trials that require the researcher to be remote from the experiment, as the UI will be the only means of communication. Despite the fact that user interfaces represent a fairly general field, we've designed a few templates, building blocks, and classes that should facilitate the creation of UIs for the majority of purposes. These classes also provide certain programmatic interactions with the user interface, such as the fading in and out of panels and the activation and deactivation of interactive components.

UIComponent

Adding a *UIComponent* to any UI game object in Unity is all it takes to take advantage of the *UIComponent* class and begin using the programmable interactions. The class has four primary methods that function as both setters and getters for the UI element's visibility. Adding this component to a gameobject won't do much on its own, but you may utilize its functions and trigger state changes from any other Unity component or C# script that references it.

```
public virtual void Show ( float duration = 0, float delay = 0);
public virtual void Hide ( float duration = 0, float delay = 0);
public bool IsShowing ();
public bool IsHiding ();
```

Listing 4.1: UIComponent method signatures

The *Show* and *Hide* methods leverage the custom built *OpacityHandler* class to change the visibility of the UI element. Visual UI elements in Unity, such as text or images, can have their opacity animated with fade-ins and fade-outs with the help of the *OpacityHandler*.

```
public void FadeIn ( float duration , float delay = 0) =>
    StartCoroutine ( FadingIn ( duration , delay ));
private IEnumerator FadingIn ( float duration , float delay )
{
    SetOpacity (0);
    if ( delay > 0) yield return new WaitForSeconds ( delay );
    float fadingStartTime = Time . time ;
    while ( Time . time - fadingStartTime <= duration )
{
    float interpolant = ( Time . time - fadingStartTime ) / duration
;
    SetOpacity ( interpolant );
    yield return null ;
  }
SetOpacity (1);
```

```
}
```

The *OpacityHandler* component can be used by simply adding it to a Unity game object that already contains or is a child of a game object that already contains a UI visual element of some kind. Unity's Image and *TextMeshPro* components are two examples of UI visual elements that have been used extensively in our illustrative experiments. After the component is added, all that remains to be configured is the initial opacity and whether or not the visual element should be faded in at the beginning of Unity's playback. Unity's *OpacityHandler* is most useful when referenced from another component, when its public functions can be called to do an on-demand fade-in or fade-out. Additionally, the *UIComponent* class can act as a base class which other classes extend upon to add additional features for specific UI components that need it. As an example and usable component, we've implemented the *ButtonComponent* class which extends the base *OpacityHandler* class with the following two methods which control the component's interactivity state. These methods can be used to make sure a button won't be interacted with when it's not shown to the participant.

Listing 4.2: OpacityHandler fade-in implementation

```
public void EnablePress ( float delay );
public void DisablePress ( float delay );
```

Listing 4.3: ButtonComponent extension

VRInteractables

Although we can decide when a UI component is interactive, the UIComponent class lacks the essential features for adding interactions. The VRInteractable is another component that may be applied to interactive Unity game objects. The class employs an event system to manage its interaction state changes. Other functions or classes can subscribe to the event system of VRInteractable, and when the state changes, the listeners will be invoked. The class exposes public methods for triggering state transitions.

```
private UnityEvent onEnter ;
private UnityEvent onPressUp ;
private UnityEvent onPressDown ;
private UnityEvent onExit ;
private UnityEvent onCancel ;

public void OnEnter () {
onEnter . Invoke ();
```

```
}
```

Listing 4.4: VRInteractable implementation

To use the *VRInteractable* component, the user only needs to add the component to any UI gameobject that they wish to make interactive. The *VRLaserPointer* will manage all interactions between the user and the *VRInteractable* component. The toolkit presently includes two interactive components: the button and the slider. Each of these relies on the *VRInteractable* component in order to function, with the slider utilizing a unique extension class to handle its specific instances. The *VRSliderController* class responds to any event triggers from the *VRInteractable* component by manipulating the slider accordingly. For instance, if a user clicks the trigger button on their controller while hovering over the slider's handle, the *VRSliderController* will begin to track the controller's movements, allowing the user to effectively drag the slider's handle.

4.3.2 Behavioral Questionnaires

In behavioral research, questionnaires are an effective method for measuring the behaviors and opinions of experiment participants. However, the use of questionnaires in VR-based behavioral investigations might result in complexities and undesirable compromises. Considering preparation of the participant, physical setup of the headset, and signal calibration, the setup time for a virtual reality (VR) experiment can be rather lengthy. In some behavioral experiments, such as an assessment of participant reactions to different videos, it is advantageous to administer questionnaires intermittently; however, doing so in a virtual reality (VR) experiment - where the participant taking off their headset requires repeating the setup process - can unnecessarily prolong the experiment and irritate the participant.

Recognizing the significance of surveys, we've integrated the option to construct questionnaires directly into the Unity VR experiment. Implemented as a sequencer that can be activated programmatically, the Questionnaire component will loop over your questions one at a time, showing them to the participant and preserving their response. This component can be applied to any Unity gameobject and then used by other Unity scripts in order to allow the user to control the questionnaire.

Usage

To utilize this questionnaire, you must construct your own Unity component - a C# script - that accepts a reference to the questionnaire as an input and then executes the questionnaire's start and end functions. As an illustration, this is accomplished in our Affective World experiment[1] in both the *VideoManager* and *UIManager* helper components. The UI portion of the questionnaire is constructed using the UI components we've already covered and consists of four main parts: the instructions, a UI panel that explains to the participant what they can expect and what they will need to do; the questions, a series of UI panels and UI inputs; a next question button, which participants will use to navigate through the questionnaire; and the end card, which serves as the questionnaire's off-boarding. In fact, these UI components will exist as different Unity game objects, and references to them should be passed to the Questionnaire component.

1: Only available in github repo

While these questionnaires can be modified by the researcher for a variety of purposes, they are primarily utilized in our example experiments to measure a participant's Likert scale response to an experience. A Likert scale is a visual analog scale that is often used in behavioral research to measure qualitative information, such as participant's opinions and behaviors in reaction to an experience [123]. In the post-video questionnaires for the affective world experiment Affective Worlds, we employ the Likert scale to ask participants to assess the intensity with which they experienced specific emotions as a result of viewing the movie. The Likert scale employs the UI slider component Section 4.3.1 (User Interfaces), and participants are prompted to drag the slider handle to the response option that they believe best represents their opinion.

The questionnaire replies are then saved in a JSON file for examination after the experiment. This procedure is detailed in further depth in the following section.

4.3.3 Data Management

Saving experiment data, such as questionnaire replies, can be handled on a case-by-case basis; however, the more access points to our data we build in the code, the more susceptible our studies become to user error, such as entering the incorrect user id or data location for the experiment. To mitigate this issue and facilitate data manipulation, we've developed

the *DataManager* class, which provides a centralized access point for all data saving.

Usage

To utilize the *DataManager* component, you must first perform a fast setup in the Unity editor. Upon adding the component to any game object, you may change the *DataPath* variable6 to specify where the data is kept. Once this has been established, you may configure the *UserID* and *SessionID* variables to be unique to the participant and experiment trial you will conduct. By doing so, whatever data you save using the class's public methods will be automatically stored in the participant's organized data folder. The data is organized according to the path structure DataPath/UserID/SessionID. When our Questionnaire script calls DataManager::WriteToJSON with the filename example-questionnaire, the new file is saved as [DataPath]/[UserID]/[SessionID]/example-questionnaire.json.

4.3.4 Data Pipeline

Several softwares have become standard across the behavioral research space for inter-device communication and post-experiment data analysis, among other things; therefore, integrating as many of these as possible into the Entwine Toolkit will help researchers overcome the remaining barriers to VR experimentation.

Lab Streaming Layer

Lab Streaming Layer (LSL) is a system for the unified collection of measurement time series in research experiments that handles both the networking, time-synchronization, (near-) real-time access as well as optionally the centralized collection, viewing and disk recording of the data [124].

To facilitate Unity integration, LSL provides a C# library with an API for making connections (inlets and outputs), reading data (streams), and more. As an extension to LSL's library, I developed two utility classes: *LSLOutput* and *LSLInput*. Through the use of these auxiliary classes, LSL may be loaded into Unity and managed like any other component, with full access to the Unity editor for property editing and modification. *LSLOutput* With the *LSLOutput* class, users can quickly make new output streams and add new outputs.

LSLOutput The *LSLOutput* class allows the user to easily create output streams as well as write to the stream.

```
public class LSLOutput : MonoBehaviour
{
// Variables serialized to be set by users in the Unity editor
[ SerializeField ] private string streamName ; // The name of the created
    output stream which can be used to find the stream from an external
    program
[ SerializeField ] private string streamType ; // The content - type of
    the created output stream which can be used to find the stream from
    an external program
[ SerializeField ] private string streamSourceID ; // The source ID of the
     created output stream which can be used to find the stream from an
    external program
[ SerializeField ] private bool initializeOnAwake = true ; // Determines
    whether or not the stream is started when Unity enters play mode

/**
Attempts to initialize the output stream using the input
variables .
If 'initializeOnAwake' variable is set to false , then this
function must be called before the user is able to send any
messages over the stream .
**/
public void TryInitStream ();

/**
Sends a string message over the output stream , if one has
been initialized .
Should be called from external scripts .
**/
public void Write ( string message );
/**
Overloaded function for writing multiple messages
**/
public void Write ( string [] messages );
/**
Automatically called when Unity stops playing .
Closes the LSL stream and frees up any resources .
**/
private void OnApplicationQuit ();
}
```

Listing 4.5: LSLOutput implementation

LSLInput The LSLInput class enables the user to quickly search for input streams making use of a variety of search strategies. Additionally, the user is able to transmit information received via the stream to other

classes and functions.

```
1
2  public class LSLInput : MonoBehaviour {
3  // Stream search settings
4  public string streamName ;
5  public enum SearchMethod
6  {
7  SearchAtStart ,
8  SearchContinuously
9  }
10 public SearchMethod streamSearchMethod ;
11 public double streamSearchTimeout ;
12
13 public UnityEvent <string > onReceived ;
14
15 /**
16 Automatically called when Unity starts playing .
17 Starts the stream search by calling the appropriate function
18 based on the selected stream search method .
19 **/
20 private void Start ();
21 /**
22 Asks LSL to search for the specified stream name , and will
23 search for up to [ streamSearchTimeout ] seconds before giving up.
24 Runs on a separate thread so as to not block the main Unity
25 thread .
26 **/
27 private void SearchForInputStream ();
28
29 /**
30 Continuously polls LSL for the specified stream name until
31 finds the stream . Runs on a separate thread so as to not block
32 the main Unity thread .
33 **/
34 private void ContinuouslySearchForInputStream ();
35
36 /**
37 Automatically called once every frame by Unity while Unity is running .
38 If the input stream has been found and any new data is
39 received , the onReceived event will be triggered in order to
40 notify and share the new data with any listeners .
41 **/
42 private void Update ();
43 /**
44 Automatically called when Unity stops playing .
45 Closes the LSL stream and frees up any resources .
46 **/
47 private void OnApplicationQuit ();
```

```
48 }
```

Listing 4.6: LSLInput implementation

Usage

Both of these classes, *LSLOutput* and *LSLInput*, operate in the same manner. Add the relevant component to a Unity game object for each input or output stream you want to create (this means these steps must be repeated for each stream). The only required input for both components is the name of the stream. One thing to consider for the *LSLOutput* component is if you want the stream to be initialized immediately when Unity starts playing, in which case you must set the toggle *initializeOnAwake* to true. Another factor to consider, this time for the *LSLInput* class, is the search mechanism for your input stream. If you do not select Continuous Search, the component will only look for the input stream once when Unity starts, which means that if the stream is not found right away, there will be no input stream into Unity for the rest of the play session; if you select Continuous Search, this will not be an issue because the component will continue to search for the duration of the Unity session. The *LSLOutput* class is used in all of the supplied Entwine Toolkit experiments. The class is primarily used to generate an LSL output stream for transferring *BrainFlow* [125] data from Unity to *NeuroPype*[126].
This pipeline is explained further in Chapter 5 Section 5.2.6 (Preprocessing Data). The *LSLInput* class is utilized in our experiments where we want data to be delivered to Unity from an external program. In Chapter 5, for the Tetris game, we build an LSL input stream and expect NeuroPype to feed us the processed alpha levels of the participant, which we then utilize to trigger changes to the participant's environment and the game in Unity. Another example is the Maze VR project's use of an LSL input stream Chapter 3 Section 3.4.1 (SSVEP Accessibility In VR). When an SSVEP is triggered in a subject, NeuroPype retrieves the frequency of the stimuli that elicited the reaction; this frequency is then set to Unity over an LSL input.

Neuropype

Neuropype, unlike LSL, does not provide C# libraries or tools for Unity engine integration. It does, however, offer a Python API that allows you to initiate a pipeline without utilizing its graphical user interface. Even though Python is no longer directly supported by Unity, we can still use

C#'s.NET Process API to initiate the pipeline from within Unity. In order to accomplish this, we've developed a new script called *ShellIntegration* that allows you to execute.bat files that you provide during the play mode of Unity. We chose to use.bat files instead of directly using the *Neuropype* python function because *Neuropype* required that it be called from a certain Python environment, which can be ensured via a batch script.

```
public enum ShellTiming {
OnStart ,
BeforeStart ,
AfterDelay
}

public class ShellRoutine {
public string FilePath ;
public bool RunScript ;
public ShellTiming Timing ;
public float TimingDelay ;
}
public class ShellIntegration : MonoBehaviour {
// All the shell commands that will be run
public List < ShellRoutine > routines ;

// The process IDs for each of the running shell instances
private List <int > processIDs ;

/**
Start () is automatically called by the Unity Engine when the engine
     starts playing . In this function , all shell routines are passed to
     one of the running functions based on what timing is selected . e.g.
     routines that have selected ShellTiming . AfterDelay will be passed
     to the RunShellFileAfter () function .
**/
private void Start ();

/**
OnApplicationQuit () is automatically called by the Unity
Engine when the engine stops playing . In this function , all still -
     running shell routines are shutdown using their process IDs.
**/
private void OnApplicationQuit ();

/**
RunShellFile () takes in a shell file and its arguments , and uses .NET's
     Process api in order to run it on the command line .
**/
```

```
34 private RunShellFile ( string filename , string args = "");
35 /**
36 This function creates a new separate thread before calling the
       RunShellFile () command . This keeps the shell file from being on the
        same main thread that the Unity Engine is running on.
37 **/
38 private RunShellFileThreaded ( string filename , string args = "");
39
40 /**
41 This function uses Unity's Coroutine API in order to run the RunShellFile
       () function after [ delay ] amount of time in seconds has passed .
42 **/
43 private RunShellFileAfter ( float delay , string filename , string, args
44 }
```

Listing 4.7: ShellIntegration implementation

Usage

To utilize the ShellIntegration component, just add its script to any Unity gameobject - though it's recommended to build a new, separate gameobject for organizational purposes - and then add the path to your.bat file and specify the component's desired routine. You can add as many.bat files as you wish, each of which will execute its own procedure.

In each of our experiments, we use this ShellIntegration component to launch our NeuroPype pipelines; however, the component can execute any.bat files or shell commands, even those unrelated to Neuropype. We developed a custom property inspector so that whenever a user adds a new routine - a.bat file to execute - they can additionally choose when they want the script to run: before Unity starts, when Unity starts, or after Unity starts with a delay. Additionally, these operations execute on a separate thread to ensure that they do not impede Unity. Whenever the Unity play session ends, the thread and any spawned processes are automatically terminated using the Windows Task Kill utility. This can be a very helpful feature, but it can also have unintended consequences, such as if the generated process is unable to save its data. There is an option to disable this feature, allowing users to manually terminate foreign processes.

4.4 Brain-Computer Interfaces — Paradigm Models

A BCI paradigm use a particular signal source to investigate many phenomena. These occurrences can be divided into two classes: Endogenous and Exogenous

4.4.1 Endogenous

A subject produces aware brain signals when executing mental tasks such as imagining a movement or a word sequence. It does not require external inputs to function, but completing a specific mental job is not easy because the subject must be trained for proper execution and it is notoriously difficult and time-consuming. Fortunately, training makes it easier as it progresses. There are now two primary examples of an endogenous paradigm:

Motor Imagery

Mental simulation involves mental rehearsal of moves without actual movement. The individual must visualize himself/herself performing a bodily action, such as moving the arm from left to right or closing the hand. It investigates the observation that visualizing and doing a movement elicit comparable brain wave patterns. This phenomena has been implemented in a variety of contexts, including robotic prostheses, rehabilitative therapy, and video games.

Non-motor Imagery

Imagining sounds, phrases, pictures, or even completing mental calculations leads to brain wave patterns that can be identified. This is true whether you are imagining sounds, words, or pictures.
Chapter 5 shows an example of a endogenous paradigm. Mental and spatial workloads are among the key drivers when studying cognitive processes. When studying cognitive processes, large portions of research focus on the central nervous system, more specifically the prefrontal cortex and the parietal region. However, the activity of the autonomic nervous system and the interaction between it's two parts, the sympathetic and parasympathetic systems, are involved in both directions in these cognitive processes and the balance in the functioning of these systems

is deeply connected with mental health and wellbeing. Maintaining optimum levels of mental workload during a task is essential for maximizing performance and having balanced autonomic nervous system activity, as further explained by previous studies. In this exploratory study, our aim is to unravel the interconnected nature of the aforementioned domains—specifically, areas of interest such as cognition, affective responses, and physiological reactions—by employing the Galea headset as a key research tool.

4.4.2 Exogenous

Subjects generate brain signals involuntarily in response to external stimuli, which can be auditory, visual, or tactile. This method requires the subject to concentrate on the stimuli, a technique known as selective attention, and typically requires little or no training prior to BCI application. These are the most well-known exogenous approaches:

Auditory Continuous Response (ASSR)

The user is presented with an auditory stimulus, such as a beep-like sound at a constant frequency, in this method. The structures of the inner ear encode auditory information such that the electrical current to be processed by the auditory cortex synchronizes with the source frequency. It is known that an ASSR functions satisfactorily at a bandwidth between 40 and 80 Hz.

Potential Is Visually Evoked by Steady State (SSVEP)

Similar to ASSR, SSVEP investigates the synchronization between the frequency of the external stimulus, now visual, and the frequency of the evoked potential in the visual cortex.
The bandwidth between 5 and 30 Hz is enough for working with SSVEP in terms of accuracy, and although an SSVEP-based BCI would be less unpleasant above 30 Hz, the evoked potential power diminishes dramatically and provides a challenge for SSVEP identification.
For an SSVEP-BCI to function, the user's gaze must be narrowly focused on the visual stimulus of interest; hence, any distracting peripheral stimulus may interfere with the recordings. This paridigm was shown in Chapter 3 Section 3.4.1 (SSVEP Accessibility In VR).

The effects of different stimulus configurations on the Visual Evoked Potentials (VEP)

VEP offer information on the visual pathways from the retina to the occipital cortex. VEPs provide a more accurate measurement of optic circuit functional integrity than MRIs because VEP is used to examine the retina, optic nerves, and visual cortex in the brain.
VEPs are generated from an electroencephalogram by averaging transitory visual stimuli recorded from the visual cortex.
Due to the constraints of a 2D screen, little research has been done on the variations and ramifications of these stimuli being displayed in a 3D space. This study described in chapter Chapter 6 investigates VEP and Event-related Potentials (ERP) BCI paradigms, stimulus onset asynchrony in VR, and characteristics that correlate strongly with these potentials.
Rare disorders limit the amount of data available for vision research studies. Using the Galea headset, it is possible to simulate visual impairments for normally-sighted people so that a person with normal vision can feel low-acuity, color-blindness, or tunnel vision. Then, EEG data can be captured to analyze occipital brain responses.

4.5 Discussion

This chapter discussed components that enable users to develop behavioral studies with the Entwine toolkit and how to integrate these with other software such as NeuroPype pipelines; however, it can also be used to execute any.bat or.sh files. The custom property inspector enables the user to select when the script will execute: before Unity starts, when Unity starts, or with a delay after Unity starts. To prevent them from interfering with Unity, these operations execute on a separate thread. When the Unity play session ends, Windows Task Kill terminates the thread and any spawned processes. This feature can be advantageous, but it may have unintended results if the generated process cannot save its data. There is an option to disable this feature so that foreign processes can be terminated manually.
In our investigation of brain-computer interfaces and paradigm models, we investigated two distinct types of phenomena: endogenous and exogenous. Endogenous processes involve conscious brain signals produced by the subject when performing mental tasks, such as imagining a movement or a sequence of words. Exogenous processes, on the other

hand, involve brain signals generated involuntary in response to external stimuli, such as auditory, visual, or tactile inputs.

Motor imagery and non-motor imagery are two primary examples of endogenous paradigms that have been described. Non-motor imagery includes imagining sounds, phrases, and images, as well as performing mental calculations. Our study in Chapter 5 aims to explore the spatiotemporal dynamics between the autonomic nervous system and the central nervous system during a high cognitive demand task. This study utilized the Galea headset to shed light on the entwined nature of mental workload and the functioning of the autonomic nervous system. Two well-known exogenous approaches are also discussed Auditory Continuous Response (ASSR) and Potential Visually Evoked by Steady State (SSVEP). In ASSR, the subject is presented with an auditory stimulus, such as a constant-frequency beep, and the electrical current processed by the auditory cortex synchronizes with the source frequency. On the other hand, SSVEP investigates the synchronization between the frequency of the external visual stimulus and the frequency of the evoked potential in the visual cortex. For SSVEP-based BCIs to function effectively, the user's gaze must be narrowly focused on the visual stimulus, and any distracting peripheral stimulus may interfere with the accuracy of the results.

5 Cognitive Demands and Neural Interplay

This chapter shifts the focus to the examination of the potential for virtual reality technology to study cognitive function. This study investigates the relationship between working memory, spatial attention, physiological arousal, and performance during a high-demand task in a virtual reality (VR) environment. We utilized a modified version of the popular computer game TETRIS as the task, involving 34 participants, and employed a physiological computing VR headset that simultaneously records physiological data. Our findings indicate a broadband increase in brain power just prior to a helper event, followed by a spike of spatial attention (parietal beta 1-3 seconds) occurring concurrently with a decrease in cognitive load (frontal theta 2-4 seconds), and a subsequent decrease in spatial attention (parietal theta at 14s) and physiological arousal (HRV at 20 seconds). The subjective relief and helpfulness of the helper event were found to be more driven by physiological arousal and the spatial attention response. These findings highlight the importance of multi-modal physiological recording in rich environments, such as real world scenarios and VR, to understand the interplay between the various physiological responses involved in mental workload and attention.

5.1 Background

The interconnected systems of working memory and spatial attention are critical for human interaction with rich stimulus environments. These

systems are mediated by the frontoparietal network, though the degree to which they are dissociable is debated, with both working memory and spatial attention associated with activity in both the prefrontal cortex and the posterior parietal [127]. Mental and spatial workload are among the key drivers in human cognitive processes [128–131]. Studies in this field have particularly focused on the prefrontal and parietal cortex. The prefrontal cortex plays important roles in executive functions, such as the capacity for self-control and long-term planning, which are widely regarded as among the most crucial aspects of a human mind [132, 133]. The parietal cortex, on the other hand, is regarded to be critically important in spatial information processing and in the control of behavioral responses. [134–136] In addition, the autonomic nervous system and the interaction between its two parts, the sympathetic and parasympathetic systems, are involved in top-down and bottom-up directions of mental workload [137, 138]. Maintaining a healthy equilibrium in the operation of these systems can help people achieve optimal performance, better mental health, and improved well-being [139–141].

Studies focused on detecting and quantifying mental workload have increasingly used physiological measures, which have various advantages over using only self-reported measures, as the latter are not optimal in continuous assessment and prone to retrospective reconstruction of the perceived mental workload [142]. Common physiological metrics include electroencephalography (EEG) recordings from parietal and prefrontal regions of the brain [143, 144] and measures of cardiac activity such as heart rate and heart rate variability [145, 146]. These indices of mental workload [147] are among the most studied in this domain. As discussed in previous research, while these measures provide valuable insights on their own, using a multimodal approach can provide more robust representations of mental workload, as each individual multimodal signal represent different facets of mental workload [148, 149].

While measuring physiological markers is critical in mental workload studies, the experimental environment and behavioral response elicited in participants are equally important. In behavioural sciences, researches have studied virtual reality (VR) experiment environments as both an exciting focus of study [116, 117] and a tool for designing realistic experiments [115, 118]. VR is a valuable platform for studying participants' behaviors as it is easy to create any number of environments. These

environments can be designed to be safe, controllable, replicable, and accessible to participants from a variety of backgrounds and with a variety of needs [119, 120]. Most importantly, VR is capable of efficiently generating realistic new environments that are a powerful tool for psychological researchers [121, 122, 150]. There have been important advancements in using VR as an experimental platform to study mental workload. Gupta et al. [151] tracked multiple signal modalities (EEG, Heart-Rate Variability (HRV) and Electrodermal Activity (EDA)) and subjective questionnaires to investigate the trust level towards an auditory virtual agent under different mental workload levels. In another study, Zhang et al. [152] used multimodal physiological data (EEG, EDA, Electromyography (EMG) and skin temperature) in a VR-based driving system to track the mental workload of users with Autism Spectrum Disorder, aiming to build a system that facilitates learning by adjusting task difficulty. Utilizing real-time EEG data in a VR environment, Dey et al. [153] presented an adaptive training system that can adjust task difficulty to an optimal challenging level to facilitate learning. While these recent studies provide valuable insights in terms of mental workload corresponding to the prefrontal cortex activity, little attention has been given to spatial cognitive load in the literature. Furthermore, the temporal dynamics of the central and autonomic nervous system activity in the context of mental workload in VR environments requires further research.

The study presented here aims to explore the relationship between spatial cognitive demands, prefrontal cognitive workload, and the autonomic nervous system during a high-demand task in virtual reality. The popular computer game TETRIS was modified and used as the task in the experiment, which involved 34 participants. We used Galea, a physiological computing VR headset that simultaneously records physiological data (EEG, EDA, EMG, and PPG) [154]. We study the dynamics of the autonomic and central nervous systems, with a focus on the activity of spatial workload in the parietal region and the balance between the sympathetic and parasympathetic responses. The findings of the study highlight the importance of cognitive load and spatial attention in subjective experience and tension relief, as well as the significance of maintaining optimum mental workload for maximizing performance and balanced autonomic nervous system activity. This exploratory study contributes to the growing understanding of the relationship between working memory, spatial attention, the autonomic nervous system, and performance.

The study hypothesizes a decrease in cognitive load, spatial attention, and physiological arousal following the helper clear event, which suddenly makes the game easier.

Our "helper event" is a new feature we've added to the classic game of Tetris. Once the stack of pieces reaches 60% of the height of the playing field, a ball-shaped helper piece appears. It can be played like any other tetromino piece and when placed, it clears the four rows of squares underneath it and sets the game level to 5, slowing down the speed at which the pieces fall.

The study also hypothesizes that the physiological signals examined would be correlated with subjective questionnaire responses about the impact of the helper clear event.

Overall, the study aims to explore the relationship between the central and autonomic nervous system phenomena and cognitive state, particularly in the context of the helper clear event in a highly demanding scenario.

5.2 Methods

5.2.1 Experiment Task

To establish a group of participants for the experiment, 34 individuals were recruited via emails sent to student organizations across the university and dormitories. Six participants were excluded because of a technical failure with the headset and failure to follow the experiment instructions. Participants were compensated 15 dollars per session for their participation, with a bonus of 30 dollars for the person to reach the highest line clear score.

All procedures were approved by MIT's institutional review board, and every participant provided informed consent. In total, there were 34 participants, ages 18 to 44, 15 males, 16 females, three non-binary, 15 Asian or Pacific Islander, 10 Caucasian, 5 Hispanic, 4 African American. Participants reported having normal to corrected-to-normal vision, no known history of epileptic seizures, migraines, or vestibular dysfunction. The individuals also had no known history of claustrophobic events when using VR headsets, and had the ability to sit and follow instructions for 30 minutes.

5.2.2 Test Environment

Physiological measures and instruments Physiological signals were recorded with a Galea headset, and signals were visually inspected after setup at the start of each session. Participants were asked to stay still for calibration and close their eyes for alpha baseline collection. A complete system review can be found in this publication [redacted for anonymity]

5.2.3 Experimental Protocol

The experiment involved playing a modified version of the well-known computer game TETRIS. The game implementation followed the original source code and was implemented in Unity3D. In this game, tetrominoes, which are geometric shapes made of four squares linked edge to edge in various arrangements, descend one at a time vertically from the top of the computer screen. While a tetromino piece falls, the player can move it sideways and rotate it, using the joystick and A and B buttons in the game controller. The object is to arrange the pieces so that complete horizontal rows of squares are formed. When this is done, the squares vanish, giving the player points. The pace of the falling pieces could be changed in the game's current iteration in 13 distinct increments, each of which equated to a different degree of difficulty.
To ensure a variation in mental workload during the experiment, participants played TETRIS in two sessions, which differed in only one condition. Session one has a helper condition that appears in the form of a sphere when the number of tetromino pieces has reached 60% of the height of the TETRIS playing field. Session two is the control condition and no variation from the standard TETRIS rules is made during this session. To reduce any confusion that the helper condition could create for the participant, the researchers explained that there would be a new piece that would appear at some point during the game and that the piece could be used like any other tetromino with the difference that this piece will clear three rows.

Experimental Procedure

The study design follows the structure shown in Figure 5-1 where the experiment started with participants filling out two pre-experiment questionnaires (5 min). Immediately following the questionnaire, the

participant is met with a headset fitting and signal impedance check (5min), and following that, the participant experiences a calibration phase to remove motion artifacts and eyes closed baseline (1 min). During this calibration phase, participants were asked to reduce the number of blinks for 50 seconds and to relax. The next phase in the calibration section was to collect signals for baseline alpha signals. This was done by asking the user to close their eyes for 30 seconds and to open their eyes when they heard a beep sound.

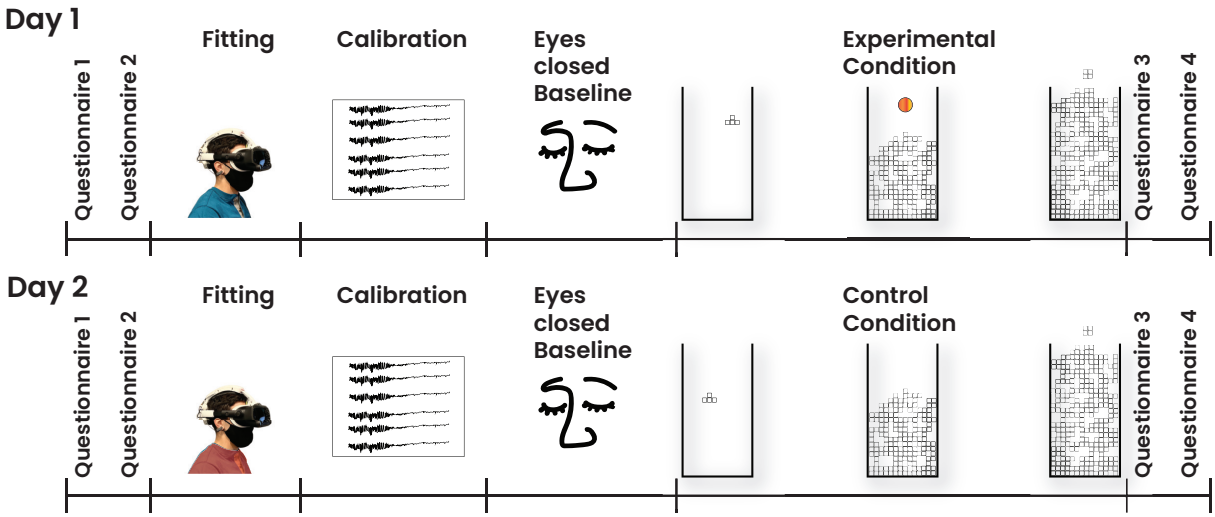

Figure 5-1: Experiment design for the Cognitive load study

After the calibration phase, the participants were asked to play TETRIS for 30 seconds to familiarize themselves with the game controllers. This was done to help reduce the increase of cognitive load that the new controllers might introduce to participants with fewer familiarities with the joystick, or with the game of TETRIS.

Before the participant's first session, participants were randomly assigned to session 1 (experimental) or session 2 (control), each lasting about 7 minutes. Once the user had finished playing the game, they were prompted to fill out a post-experiment questionnaire (5min). At last, the participants were given a debriefing, explaining what the researchers were looking to see during the experiment and the opportunity to provide feedback.

5.2.4 Modifications to the Tetris Game

The game's construction was quite straightforward, as its core is merely a copy of the original Tetris game. The Group class, the Grid class, and the TetrisSpawner class are the most crucial classes in our implementation

of Tetris. The game's construction was quite straightforward, as its core is merely a copy of the original Tetris game. The Group class, the Grid class, and the TetrisSpawner class are the most crucial classes in our implementation of Tetris.

The Group class represents the groupings of blocks that make up tetrominos and contains the majority of their falling and moving logic. The class listens for user input from the controllers and moves itself accordingly; for example, moving the controller's joystick to the left moves the tetromino to the left if possible. It also handles the game over state when it detects that the grid is full and the piece has nowhere to go. The Group class is a Unity component on the tetromino gameobject, therefore there are multiple instances of this class in use at any given moment, each of which is concerned only with its own pieces' placements on the game grid. The component is utilized on each of the tetromino piece prefabs - the game objects that are instantiated during game play - and an example of one of these prefab pieces can be seen in the image file Figure 5-2.

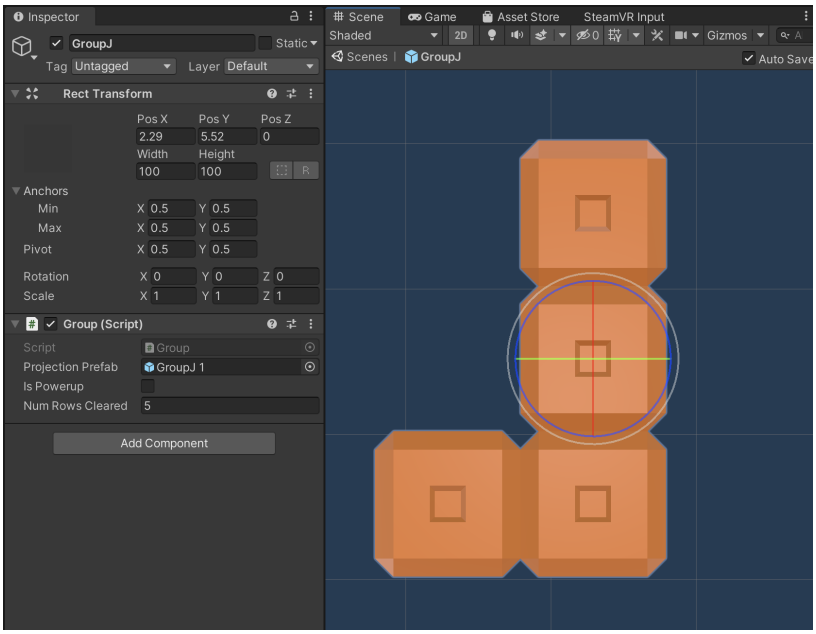

Figure 5-2: The Unity inspector view of the Group component (on the left) and the associated tetromino piece for the prefab (on the right)

Since the core of the game has been established at this point, we are ready to move on to the experiment itself. The objective of this Tetris experiment is to establish a feedback loop centered on changes in the participant's brain signals and the autonomic nervous system during the experiment. The following order of events is what is ideally desired:

- Unity collects EEG data from the Galea headset using BrainFlow.
- Unity shares received data through an LSL output stream to the Neuropype pipeline.

- Neuropype takes in this data, processes it, and analyzes the participant's alpha.
- Neuropype then sends a value ranging from 0 to 1 indicating the strength of the alpha to Unity.
- Based on this value, Unity will infer how easy or difficult the current experience is for the participant and change the difficulty to compensate.
- This cycle continues.

5.2.5 Data Analysis Methodology

The results represent data from 28 subjects, although data was collected from 34 subjects. one subject was excluded based on signal quality, five subjects were excluded based on performance criteria, and one subject was excluded based on outlier timing.

5.2.6 Pre-processing Data

Neuropype is used to pre-process the data collected. Figure 5-3 shows the pipeline used for cleaning the data. The stream data node is used with deterministic timing mode and a chunk length of 2 seconds. The select range node is used to grab EEG data from a specific range (7-17 Hz).

A 1-35 Hz FIR bandpass filter is applied, and certain channels are protected in the remove unlocalized channels and bad channel removal nodes.

In the artifact removal node, specific settings are used, such as a removal threshold of 4.0, sliding window length of 1.0, and a maximum simultaneous artifact fraction of 0.6, with a calibration data gathering time of 50 seconds.

The Jupyter notebook is used to analyze the data and generate plots, with the option to also use an Artifact Regression node to remove heart rate artifacts.

The sampling frequency of the data is 250 Hz, and markers are used to indicate specific events in the data. The baseline data used is 30s of calibration data, 30s of tutorial data, and 10s of eyes closed data. The used frequency bands are the following: 1. Alpha = 8-13 Hz, Beta = 15-30 Hz, Theta = 4-8 Hz and Welch parameters for power spectral density calculations are the following nperseg (window size): 250 and noverlap

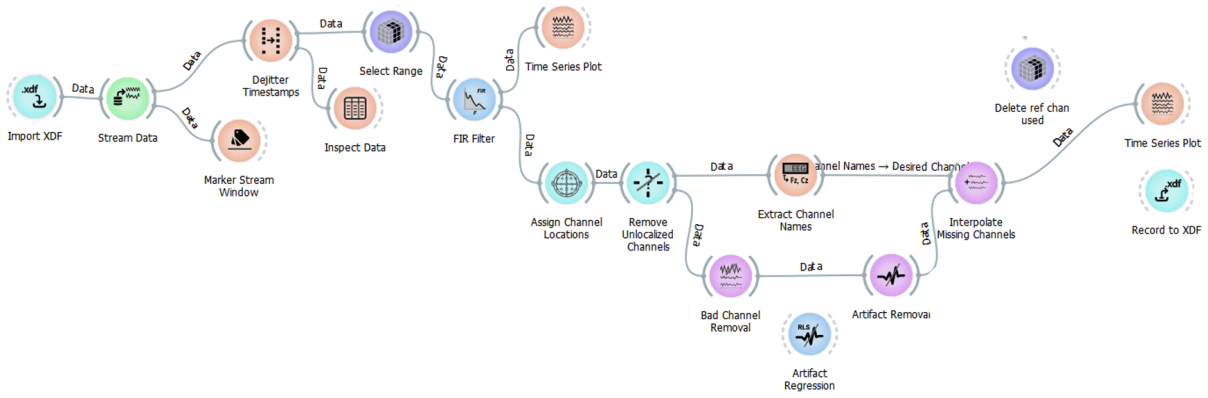

Figure 5-3: Pipeline used for removing artifact and filtering raw data

(overlap): 0. The data is also analyzed using 10s and 2s time bins to examine different time dynamics of the EEG signal.

5.2.7 Power Data

For each subject, for each of the target electrodes, power measures were calculated at each second using a 4 second window on the processed channel data (processing done prior to the work highlighted in this report is not described here). The matlab 'bandpower' function was used to calculate the average power in the target frequency range. This function uses a modified periodogram to determine the average alpha power in each window. While the experimental sampling rate was 250Hz, a single alpha measure was obtained for each second.

The timestamps, obtained at the experimental sampling rate, were rounded to the nearest second for subsequent analysis. The power bands of interest were Alpha and Beta power bands. The frequency band considered here as the "Alpha" frequency band was between [8-12] Hz and for "Beta" the frequency band was between [12.5-30] Hz.

5.2.8 PPG Data

In addition to channel power, PPG data was gathered and analyzed. The PPG data was preprocessed to remove artifacts. Two measures were taken from the processed PPG data:

1. BPM (beats per minute)
2. HRV (heart rate variability)

BPM and HRV were calculated each second using a 10 second sliding window. BPM were obtained via a simple average. HRV can be calculated

many ways, the methodology used here is RMSSD (Root Mean Square of Successive Differences). To obtain this measure, first the time difference between each heartbeat s_{dif} is obtained. Those differences are then squared, the mean is taken, and finally a square root is applied.

5.2.9 Time Series Analysis

Power and PPG data were examined over time at the group level. After the power and PPG measures were calculated, they were centered over time for each subject on the helper clear event. There were three available helper clear labels: the first corresponding to a notification the helper was coming, the second corresponding to the helper appearing, and the third corresponding to the helper clearing the game tiles. The latter is what the data was centered on. The data was then normalized and standardized, and then group level deviations were identified from baseline power within a time window affected by the helper clear event.

Normalization

Given that power values are bounded (at 0), the alpha power data at any given second was highly non-normal, with a rightward skew. As such, a log transform was performed to normalize the data. For each data point for each subject, the log of the alpha power was taken; this allowed for the use of statistics that assume normally distributed data for subsequent analysis. (!graphical example below on the way!).

$$x_{norm} = log(x)$$

Baseline

Baseline measures of the means and standard deviations of the power and PPG data for each subject/electrode were taken from the time period after the start of the experiment until the first helper event label (the helper notification). The helper was presented at different times for different subjects, so for each subject a different amount of time was avaialble from which to calculate the baseline measures. Two methodologies were used:

1. All available time for each subject
2. The last s seconds, where s is the smallest number of available seconds for any subject

The first method takes more data into account, but that data is more varied in its temporal distance to the event in question. As such, the second, while taking less overall data into account, is less likely to be affected by changes in power measures that may occur over time as a result of gameplay. Because many subjects showed significant overall changes in power and PPG data correlating with time played (see section 4.2), the second baseline measure is the primary baseline this report focuses on. For results using the first baseline methodology, see supplementary materials (see section 4.3).

Standardization

Given that the channel signal for each electrode/subject, as well as the corresponding power signals, vary based on factors beyond differences in underlying neural activity (e.g. signal impedance), the power signal was standardized for each electrode for each subject.

$$x_{stand} = \frac{(x - \overline{x}_{base})}{s_{base}}$$

The standardized data was used for subsequent analysis. This effectively weights the contribution of each electrode for each subject's power signal equally, preventing large variations due to signal quality across subjects or electrodes from distorting the group level data.

Analysis Window

Group level second by second analysis was done during the approximate period after the first helper clear label until the end of the recording. The number of seconds between the first helper clear label and the target helper clear label is different for each subject (see results). Analysis was done for any second in which *any* subjects had recieved the helper notification.

Statistics

Once the standardized and normalized data was obtained and centered on the helper clear label, the data was collapsed across electrodes. Subsequent analysis was done for each second within the analysis window. For each second, a group level one sample t-test was done to detect deviations from the baseline. A p-value cutoff of 0.05 was used to

determine a significant event.

5.3 Results

5.3.1 Time Series Analysis

Below are the results for the time series analysis, both of the power and PPG data. Alpha and Beta power results are shown in a collection of frontal [Fp1 Fp2 Fz] and parietal [PO3 PO4 Pz] electrodes. As described above, power data is collapsed across electrodes in the corresponding region of interest. Time series analysis for the PPG data is shown below for both heart rate as well as heart rate variability. This section highlights the significant events identified for each data stream. For all data streams, the time series analysis are graphically depicted with the x-axis representing time and the y-axis representing normalized and standardized group data. Positive values mean increases in the corresponding measure relative to baseline and negative values indicate decreases relative to the baseline measurement. The dark blue line represents the estimated mean value, flanked by the the upper (yellow) and lower (light blue) bounds of a 95% confidence interval of the estimated mean. Significant events, as measured by single sample t-tests, are shown as vertical dotted lines and reported in the corresponding Table 5.1.

Table 5.1: Significant events across multi-channels

	p-value	Estimated Mean	Time of Event (sec.)
FAP-CAE	0.0332	0.4499	-4
	0.0314	-0.2924	4
	0.0422	-0.2932	51
	0.0031	-0.3696	52
PAP-CAE	0.0157	-0.3995	0
	0.0162	-0.3977	1
	0.0198	0.3977	36
	0.0496	0.4674	46
FBP-CAE	0.0181	0.5170	-4
	0.0065	0.4408	-3
	0.0440	0.3164	0
PBP-CAE	0.0146	0.4917	-3
	0.0487	0.4533	-2
	0.0203	0.2963	1
	0.0317	0.4025	2
	0.0191	0.4699	3
PPG-BPM	0.0221	-0.3912	-5
	0.0276	-0.5192	-1
	0.0235	-0.5427	0
	0.0232	-0.4698	7
PPG-RMSSD	0.0250	0.5353	-2
	0.0411	0.4936	12
	0.0402	0.5047	13
	0.0476	0.5202	14
	0.0447	0.5547	20

Frontal Alpha Significant deviations in frontal alpha power from baseline were observed at -4, 4, 51 and 52 seconds. The first event, an increase of alpha power from baseline at -4 seconds, occurs prior to the moment the helper clears the tiles, but after the helper notification for most subjects (see supplementary section 0.4.1). Shortly after the helper clears the game tiles at 4 seconds, there is a significant decrease of alpha power from baseline. At 51-52 seconds, after the helper clears the game tiles, there is a two second sustained significant negativity in the frontal alpha power when compared to the baseline.

Parietal Alpha Significant deviations in parietal alpha power were observed at 0, 1, 36, and 46 seconds. The first event was a significant sustained decrease from baseline parietal alpha from 0 - 1 seconds, corresponding to the time during and immediately following the helper clear event. At 36 and 46 seconds, following the helper clear event, significant increases from baseline parietal alpha power were also observed.

Frontal Beta Significant deviations in frontal beta power were observed at -4, -3, and 0 seconds. The first event was a sustained significant increase from frontal beta power from -4 - -3 seconds, corresponding to the time period after the helper had appeared for the majority (16/25) of subjects (see section 0.4.1 for more info on helper clear event distributions). There was additionally a significant increase from frontal beta baseline power at 0 seconds, when the helper clear event occurred itself.

Parietal Beta Significant deviations in parietal beta power were observed at -3, -2, 1, 2, and 3 seconds. The first event was a sustained significant increase from baseline parietal beta power from -3 - -2 seconds, corresponding to the time period after the helper appeared but before the helper cleared the game tiles for most subjects, and the second event was a sustained significant increase from 1 - 3 seconds, the period immediately following the clear event.

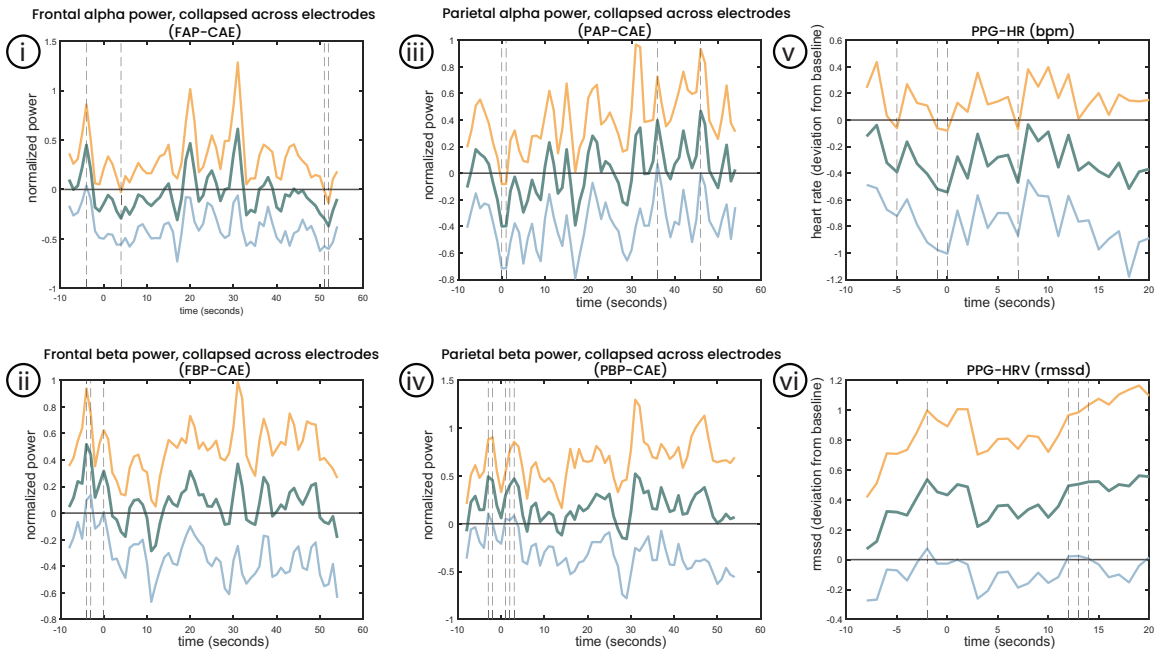

Figure 5-4: The array of figures show the significant deviations from baseline for EEG signal and PPG signal before and after the clear event.**i**) Shows the Frontal alpha power collapsed for electrodes Fp1, Fp2, FpZ.**ii**) Shows the Frontal beta power collapsed for electrodes Fp1, Fp2, FpZ.**iii**) Shows the Parietal alpha power collapsed for electrodes Poz, Po3, Po4,**iv**) Shows the Parietal beta power collapsed for electrodes Poz, Po3, Po4.**v**) Shows the heart rate in beats per minutes deviation form baseline**vi**) Shows the RMSSD, a measure of HRV, deviation from baseline.

Heart Rate - BPM Significant deviations from baseline heart rate were observed at -5, -1, 0, and 7 seconds. The first significant event was a decrease from baseline at -5 seconds, after the helper notification but before the appearance of the helper clear for most subjects. The second

significant event was a decrease from baseline at -1 second, corresponding to the period where the helper had appeared but had not yet cleared the tile for all subjects. There were also significant decreases from baseline at 0 and 7 seconds.

Heart Rate Variability - RMSSD Significant deviations from baseline heart rate variability were observed at -2, 12, 13, 14, and 20 seconds. The first significant event was an increase from baseline HRV at -2 seconds. There was also a sustained significant increase from baseline HRV from 12-14 seconds, as well as a significant increase from baseline at 20 seconds.

5.3.2 Correlations Between Events

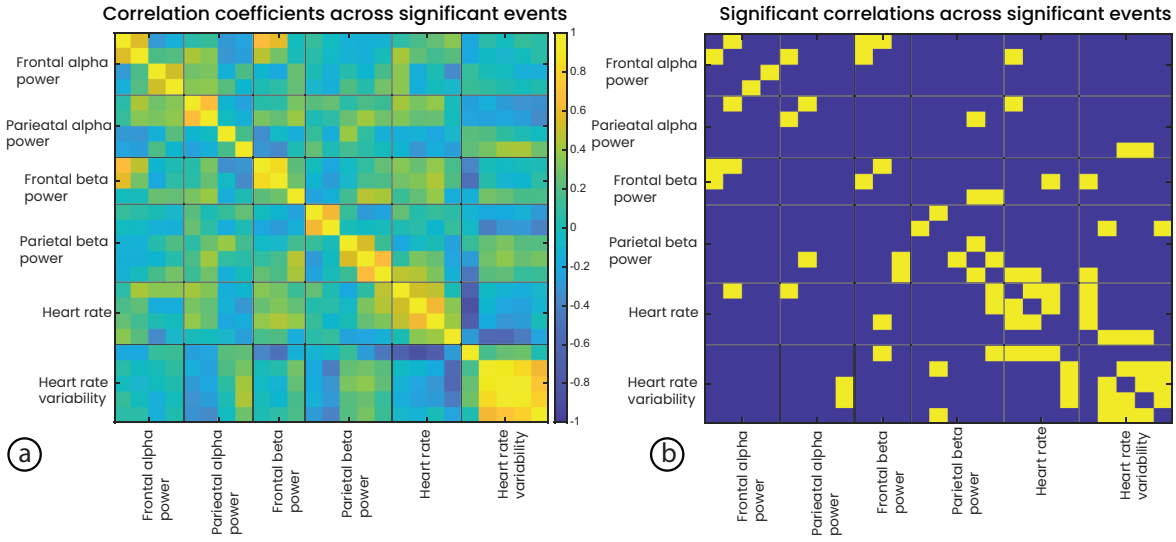

Figure 5-5: Figure (a) shows correlation-coefficient across significant events. Figure (b) shows significant Correlation across significant events

Once significant deviations from baseline were identified, the correlations between significant events were examined. Figure 5-5 (A) shows the correlations coefficients across significant events. Horizontal and vertical lines delineate data streams. Within each resultant box, the correlations between the data streams labeled on the x and y axis can be seen. Correlations within data source overall were larger than correlations between data sources.

Figure 5-5 (B) highlights the significant correlations between data streams (considered as those with a $p<0.05$). Each location on the significance figure corresponds to the same location on the correlation coefficient above.

5.3.3 Linear Regression

This section shows the results of a linear regression analysis predicting questionnaire responses by deviations from baseline EEG & PPG activity. Given the large number of significant deviations from baseline observed across data streams we subselected based on the significance of the correlation between the data at a given deviation from baseline and the target questionnaire response.

For each investigated question, linear models were iteratively created and tested. Of the group level deviations from baseline activity the deviation with the most significant (lowest p-value) correlation between the subject's EEG/PPG data and the target questionnaire response was used as the first predictor variable for a linear model. Then the next most significant correlation between subject EEG/PPG data and the questionnaire was added to the model, provided it wasn't correlated with the previous predictor. This iteratively continued until the p-value of the corresponding linear model began to *increase* as additional predictors were added. This iterative approach, rather than an exploratory approach searching a broad combination of predictor variables, both provides a simple means of model comparison as well as helps control type II statistical error.

Questions were subselected from the post experiment questionnaires on the basis of their relevance to the helper and the helper clear event.

The selected questions were:

Question 5.3.1. *Was the ball shaped piece helpful in the game? If yes, how helpful was it?*

Question 5.3.2. *"Was the effects of ball shaped piece relieving? If yes, how relieving was it?"*

Question 5.3.3. *"Did you notice that the game became slower immediately after the ball cleared some rows? If not, how much longer did it take for you to realize that the game was now slower?"*

Question 5.3.4. *"After [the] ball cleared some rows and slowed down the game, did you feel a tension relief in your body? If yes, to what degree did you feel this?"*

Questionnaire responses were scored

For questions 1, 2, & 4 responses were scored as:

"Very" = 4
"Moderately" = 3
"Fairly" = 2
"Slightly" = 1
"Not at all" = 0

Question 3 was scored as:

"I did not realize" = 4
"Within a couple moves" = 3
"Within one move" = 2
"Almost immediately" = 1
"Immediately" = 0

The results of the most statistically significant of the observed models are reported here for each of the four investigated questions. Questions 1,2, & 4 each had significant models, as measured both by the significance of the F-statistic corresponding to the linear model as well as the significance of the correlation coefficient between the estimated values using the linear model and the observed values. As a note, in the cases where the selected linear model used only a single predictor, the statistical significance of both the linear model and the correlation coefficient are equivalent. In the cases where multiple predictors are used the linear regression statistical results indicate the degree to which one or more of the predictors has a significant linear relationship with the questionnaire response. The correlation results are a more direct measure of the predictive validity of the model, indicating the extent and significance of the relationship between the predicted and observed values. The R^2 value indicates the percentage of variance in the observed data explained by the linear model of the predictor variables.

Question 1: Was the ball shaped piece helpful in the game? If yes, how helpful was it?

$$\hat{y}_{Q1} = \beta_0 + \beta_1 x_1 + \beta_2 x_2$$

$$x_1 \equiv \text{PPG HRV at 20 seconds}$$
$$x_2 \equiv \text{Parietal Beta at 3 seconds}$$

The table below shows the individual contributions of the estimated components.

Table 5.2: Individual contributions of the estimated components for question 1

	Coefficient estimate	SE	tstat	pValue
β_0	2.8113	0.2444	11.503	8.9201e-11
β_1	0.30002	0. 16285	1.8423	0.078946
β_2	0.388	0.22799	1.7019	0.10287

The results of the linear model as a whole, as determined by the F-statistic vs. constant model (3.65) was significant with a p-value(df = 22) = 0.0426. There was furthermore a significant correlation ($p = 0.011; R^2 = 0.2494$) between the predicted and observed questionnaire response values.

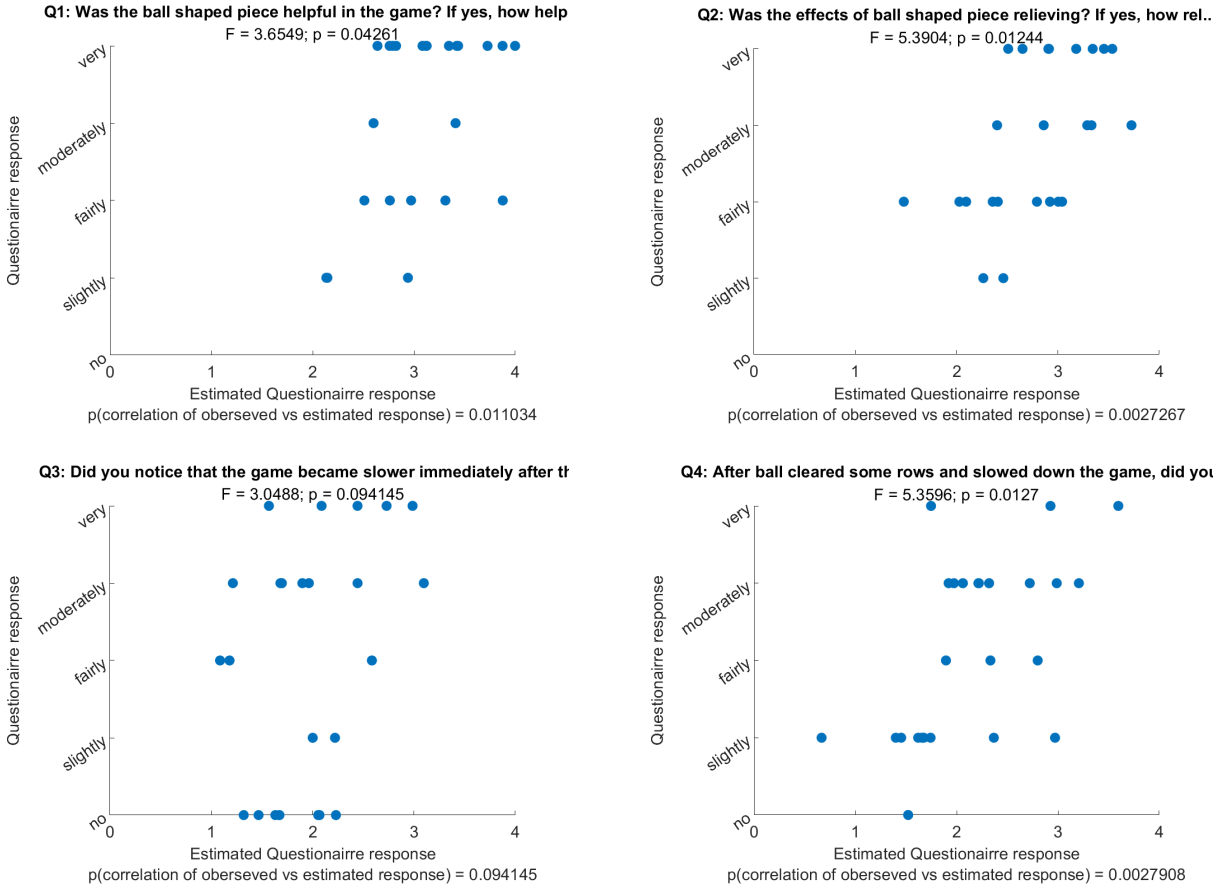

Figure 5-6: Estimated questionnaire response from the linear model for each question

Our findings indicate that the parietal beta activity just following the helper clear event and the heart rate variability 20 seconds following the helper clear event are significantly related to subjective reports of how helpful the helper was. The correlation results indicate that 25% of the variance in subject questionnaire responses to question 1 is explained by a linear combination of the PPG HRV data 20 seconds after the helper clear event and parietal beta activity 3 seconds after the helper clear event. While the individual predictor variables were not significant when individually tested (see table), the significance of the overall model indicates a significant effect. This may indicate a degree of correlation between the predictor variables, though a statistically significant correlation was not observed ($p > 0.05$). Given that this model's performance exceeded the performance of a model with only a single predictor variable, both terms likely contribute. The significant intercept term indicates, as expected, that the mean questionnaire responses differ from 0.

Question 2: "Was the effects of ball shaped piece relieving? If yes, how relieving was it?"

$$\hat{y}_{Q2} = \beta_0 + \beta_1 x_1 + \beta_1 x_2$$

$x_1 \equiv$ Parietal Theta at 14 seconds $x_2 \equiv$ Parietal Beta at 2 seconds

The table below shows the individual contributions of the estimated components.

Table 5.3: Individual contributions of the estimated components for question 2

	Coefficient estimate	SE	tstat	pValue
β_0	2.5109	0.20266	12.389	2.1483e-11
β_1	-0.48211	0.22578	-2.1353	0.044115
β_2	0.40724	0.20894	1.9491	0.06415

The results of the linear model as a whole, as determined by the F-statistic vs. constant model (5.39) was significant with a p-value(df = 22) = 0.0124. There was furthermore a significant correlation ($p = 0.0027; R^2 = 0.329$).

Our findings indicate that the parietal beta activity just following the helper, and parietal theta 14 seconds following the helper, is significantly related to subjective reports of the relief experienced following the helper clear event. The correlation results indicate that 33% of the variance in the subject questionnaire responses can be explained by this linear model.

Question 3: Did you notice that the game became slower immediately after the ball cleared some rows? If not, how much longer did it take for you to realize that the game was now slower?

$$\hat{y}_{Q3} = \beta_0 + \beta_1 x_1$$

$x_1 \equiv$Parietal Theta at 9 seconds

The table below shows the individual contributions of the estimated components.

Table 5.4: Individual contributions of the estimated components for question 3

	Coefficient estimate	SE	tstat	pValue
β_0	1.6421	0.35602	4.6124	0.00012231
β_1	-0.76436	0.43776	-1.7461	0.094145

The results of the linear model as a whole, as determined by the F-statistic vs. constant model (3.05) was *not* significant with a p-value (df = 22) = 0.0941. There was furthermore no significant correlation (p = 0.0953)

between the predicted and observed questionnaire response values.

The intercept term, as expected, was significant. This indicates that the average questionnaire responses were greater than zero, though the insignificant finding of the linear model as a whole indicates there is no linear relationship between the investigated predictor variables and this particular questionnaire response.

Question 4: After the ball cleared some rows and slowed down the game, did you feel a tension relief in your body? If yes, to what degree did you feel this?

$$\hat{y}_{Q4} = \beta_0 + \beta_1 x_1 + \beta_2 x_2$$

x_1 ≡Frontal Beta at -3 seconds

x_2 ≡ Parietal Beta at 3 seconds

The table below shows the individual contributions of the estimated components.

	Coefficient estimate	SE	tstat	pValue
β_0	1.6765	0.25031	6.6977	9.8599e-07
β_1	0.62915	0.28374	2.2173	0.037241
β_2	0.43876	0.22425	1.9566	0.063211

Table 5.5: Individual contributions of the estimated components for question 4

The results of the linear model as a whole, as determined by the F-statistic vs. constant model (5.36) was significant with a p-value(df = 22) = 0.0127. There was furthermore a significant correlation ($p = 0.0028; R^2 = 0.3276$) between the predicted and observed questionnaire response values.

Our findings indicate that the frontal beta activity just prior to the helper clear and parietal beta activity just following are significantly related to subjective reports regarding the degree of tension relief subjects report following the helper clear event. The correlation results indicate that 33% of the variance in the subject questionnaire responses is explained by a linear combination of the Frontal Beta activity just prior and Parietal Beta just following the helper clear event.

5.4 Discussion

The differences from baseline across data streams were largely focused on here in terms of those that contributed to substantial linear models of

subjective questionnaire responses regarding the helper event, as well as those that provide specific insight in relation to our stated hypotheses.

The first event of note is an increase of both frontal and parietal beta power from baseline 3 seconds prior to the helper clear event, corresponding for most subjects to the time after the helper notification but before the clear event itself. This corresponds to an elevation across power signals. While significant deviations were observed in Frontal Alpha and Beta as well as Parietal Beta, there was a positive trend among all other power signals.This broadband increase in power from baseline may indicate a generalized increase in engagement, mental load, and fatigue, corresponding to an increase in both cognitive load (frontal beta) and spatial attention (parietal beta). This may reflect either the impact of the expectation of the helper, or the high degree of task difficulty that subjects faced prior to the helper event occurring. The frontal beta at -3 seconds was a selected predictor variable with a positive coefficient in the linear model of questionnaire responses related to the subjective sensation of tension relief from the body, indicating the larger the positive deviation from baseline the more tension relief subjects reported. The tension relief may actually reflect the *return to baseline* rather than the elevated cognitive load itself. While this result differs from our hypothesis of a decrease in beta power *following* the helper clear event, the general pattern of a return to baseline from an elevated cognitive load *preceding* the helper clear event is consistent with the model underlying the hypothesis. In particular that the helper clear event itself reduces cognitive load.

The second event of note is a sustained increase in parietal beta from baseline 1-3 seconds following the helper clear. At 1 second there is additionally a significant decrease from parietal alpha. This is consistent with a spike in spatial attention following the helper clear. This increase in spatial attention may reflect the subject's re-evaluation of the game state. Subject's parietal beta power in this period is one of the selected predictive variables for linear models for *all three* of significant linear models reported, regarding how helpful and relieving the helper was, as well as the degree to which subjects reported tension leaving their body. The subjective reporting of how helpful/relieving the helper was is significantly and robustly (across question wording) related to degree to which spatial attention was devoted to re-evaluating the game state post helper clear event. At the same time, as predicted, was a large decrease in theta power indicating a decrease in cognitive load. While

the decrease in cognitive load was significant, subjective reports of how helpful/relieving the helper tile was were more driven by the broadband increase in power in anticipation of the helper clear, as well as spatial attention and physiological arousal after the helper event occurred. While the directionality of the cognitive load finding is in line with our hypothesized result, that subjective reports of the helpfulness was driven more by parietal activity was a deviation from our hypothesis.

The third event of note is a decrease in parietal theta power at 14 seconds and a subsequent increase in heart rate variability 20 seconds following the helper clear event. There were additional significant increases from baseline in heart rate variability 12-14 seconds following the helper clear and a significant decrease in heart rate 7 seconds following the helper clear. The decrease in parietal theta (a selected predictor in the linear model of how relieving the ball was) may indicate a corresponding decrease in sustained spatial attention in return reflecting a more relaxed approach to game-play. This is consistent with the hypothesized and observed decrease in physiological arousal following the helper clear event as evidenced by the heart rate data.. Furthermore the heart rate variability at 20 seconds was a selected predictor variable with a positive coefficient in the linear model of the question relating to the helpfulness of the helper clear.

An additional set of events, though not significant with our primary baseline measurement, may be of note. With an alternate baseline (see supplementary materials) several positive deviations from baseline alpha power were observed (19-20s, 24-25s, 30-31s). The sustained positivity, overlapping with a significant increase in heart rate variability, may indicate a sustained increase in frontal alpha power that our current statistical power may not be capturing. This would be consistent with our hypothesis of a decreased cognitive load following the helper clear, and consistent with a more reflective and relaxed game-play post tile clears and the difficulty level decreasing.

The effects of the helper clear event observed here spans multiple data streams across a time interval of over 20 seconds. The data streams include frontal and parietal EEG data as well as PPG heart rate variability data that in turn predict 25-33% of the variance observed in subjective questionnaire responses about how helpful or relieving the helper event was. In this study we observed a broadband increase in brain power just prior to the helper event followed by a spike of spatial attention (parietal

beta 1-3 seconds) that occurred concurrently with decrease in cognitive load (frontal theta 2-4 seconds), in turn followed by a subsequent decrease in spatial attention (parietal theta at 14s) and decrease in physiological arousal (hrv at 20 seconds). While as expected there was a decrease in cognitive load in response the helper clear event, subjective relief and the subjective reports about how helpful the event was were more driven by physiological arousal and the spatial attention response to the helper.

5.5 Conclusion

In conclusion, this study investigated the spatio-temporal dynamics of the autonomic and central nervous systems during a high cognitive demand task. The data streams were analyzed to identify differences from baseline that contributed to linear models of subjective questionnaire responses related to the helper event. Three main events of note were identified. The first event was an increase of both frontal and parietal beta power from baseline 3 seconds prior to the helper clear event, indicating a generalized increase in engagement, mental load, and fatigue. This was found to be a predictor of subjective tension relief reported by the subjects. The second event was a sustained increase in parietal beta from baseline 1-3 seconds following the helper clear, which corresponded to a spike in spatial attention and was found to be a significant predictor of how helpful and relieving the helper was, as well as tension relief reported by the subjects. The third event was a decrease in parietal theta power and a subsequent increase in heart rate variability following the helper clear event, which may indicate a corresponding decrease in sustained spatial attention and return to a more relaxed state.

Overall, the findings suggest that both cognitive load and spatial attention play important roles in subjective experience of the helper event and the level of tension relief felt by the subjects. Deviating from the hypothesis, subjects found the helper helpful, due to the anticipation of the helper clear event. Additionally, the helper event caused an spike in spatial attention after it occurs, which helped individuals to re-evaluate the game state. This exploratory study found that the results indicate that it is possible to detect and intervene with the mental and spatial workload if multimodal physiological activity is tracked during a task. Changing the mental workload enables the researcher to alter the activity of the autonomic nervous system, which ultimately results in prolonged

performance and improved mental wellbeing. This is made possible by the well-explained coupling that exists between these domains. In light of these findings, it can be presumed that by applying the same principles in a closed loop setting, it might be possible to further guide the activity of the central and autonomic nervous systems while performing a mentally taxing task. This would open the door for applications in a wide variety of fields, including gaming, education, and medicine.

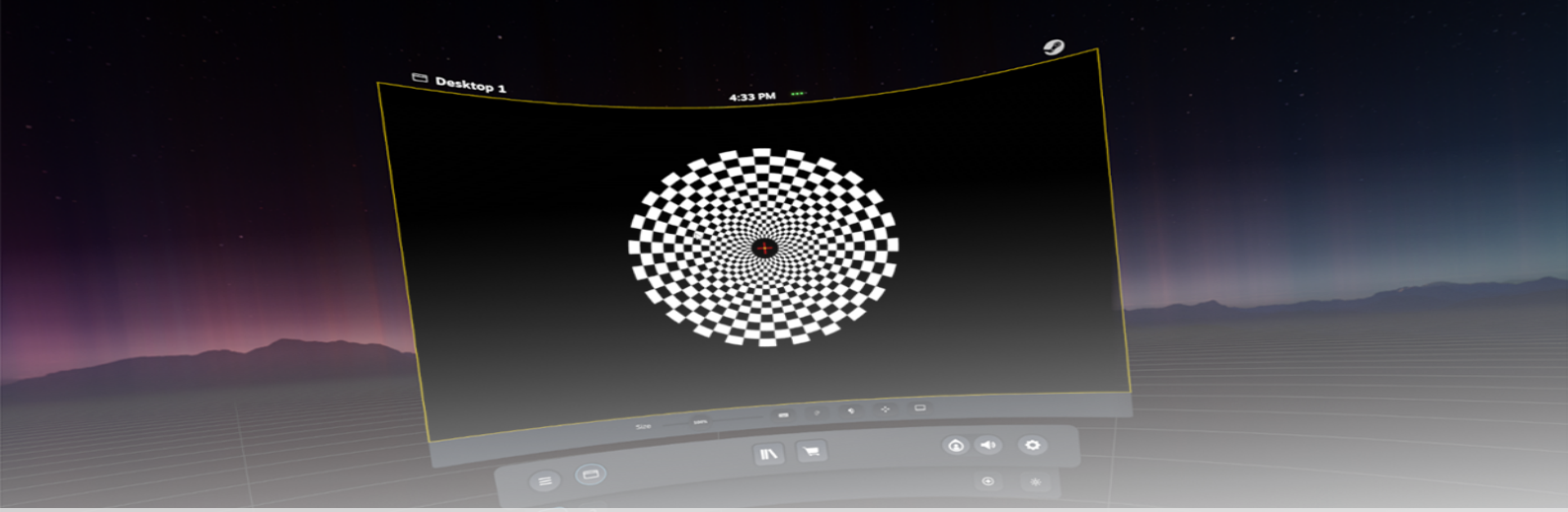

6 Effect of Different Stimulus Configurations on the Visual Evoked Potential in VR

Visual evoked potentials (VEPs) are a commonly used method to study the functional integrity of the visual pathways that extend from the retina to the occipital cortex. These potentials are generated using electroencephalograms (EEGs) by averaging the transitory visual stimuli captured from the visual cortex. Due to the limitations of 2D screens, not much research has been done on how these stimuli change and affect us in a 3D space, even though they are important. The purpose of this study is to look into the VEP-BCI paradigms, as well as stimulus onset asynchrony in VR and variables that are closely related to these potentials. Furthermore, this study intends to investigate the feasibility of using the Galea headset for early stage diagnostics by analyzing EEG data from the occipital brain response of individuals with simulated visual impairments. The results of this study may provide insights into the potential utility of such a system for early detection and diagnosis of visual impairments.

6.1 Light, Eye and Vision

Some theoretical groundwork for understanding human's vision physiology is laid out in this section. The section begins with a definition of light and concludes with a presentation of a BCI application for neurophysiological measurements of the visual field and visual pathways. Figure 6-1 depicts the "path of the light" that a visual stimulus takes from its origin to the human eye. The visual cortex of the brain receives the data, and from there the object's impact on the brain's electrical activity can

be evaluated. A brain-computer interface (BCI) converts the measurable signal into an analog signal. This section presents a quick introduction to the fundamentals of how the human eye and brain perceive and process light. A description of how the visual cortex responds to an image is followed by a discussion of image formation, the visual pathway, the topographic representation of the image, and the visual cortex itself. After that, EEG and VEP will be discussed.

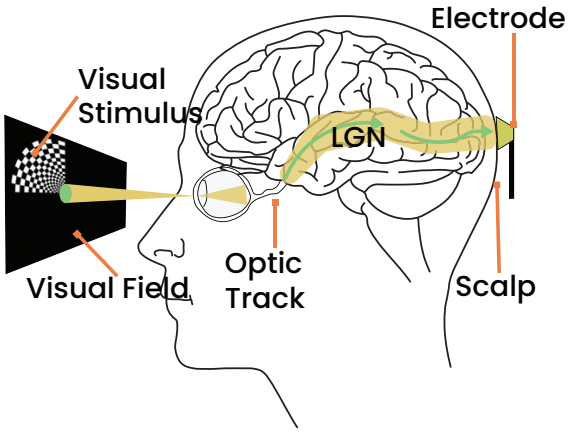

Figure 6-1: Representation of the visual system, together with a stimulus, visual field and single cell electrode

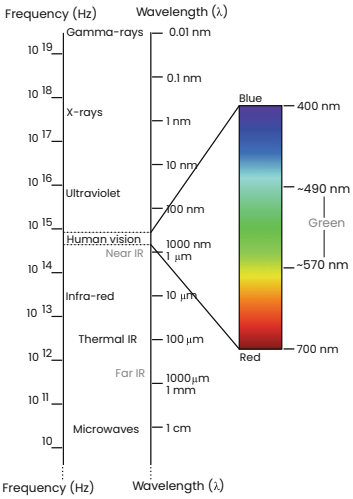

Figure 6-2: The electromagnetic spectrum. The numbers indicate wavelength in nanometers (1 nm = 1 × 10-9 m). The band between 400 and 700nm of visible light is highlighted. It was consider green color has primarily wavelength in the 500-570 nm range

Light is an electromagnetic radiation form emitted by electrically charged materials during their oscillation. The only time the direction of light's motion changes is when it encounters an object that causes it to be reflected or refracted, sending it back along its original path at an angle. In the electromagnetic spectrum, the wavelength corresponds to the color perceived by the human eye. The electromagnetic spectrum is depicted in Figure 6-2. Electromagnetic waves with approximate wavelengths between 450 and 750 nm make up visible light [3, 7]. There is a direct relationship between the brightness of an object and the degree to which it is reflected light. Color contrast allows complex organisms to distinguish surfaces that reflect different parts of the visual spectrum, which is the primary basis for vision. Around 125 million neurons, called photoreceptors, are specialized to convert light into electrical signals in the human eye's complex optic system [2].

Vision occurs when light enters the human eye through the cornea and travels to the pupil. The retinal surface, which functions like the movie screen of the eye, receives a projection of whatever is being looked at. When the lens is properly focused on the object, the image projected is crisp. Retinal images should trigger nerves to send a signal to the brain via the optic nerve. Phototransduction, or the conversion of light energy into electrical energy, takes place in the retina, the innermost layer of the

eye. The photoreceptor cells that detect light waves are located in neural tissue on the retinal surface. Rods and cones are the names given to photoreceptors that respond to low and high levels of light, respectively. The axons of retinal neurons make up the optic nerve, which carries visual data to the brain. Light coming from the visual center is focused in the fovea, located in the center of the retina. It's the sharpest spot on your retina. The optic disk is the area of the retina through which the optic nerve travels.

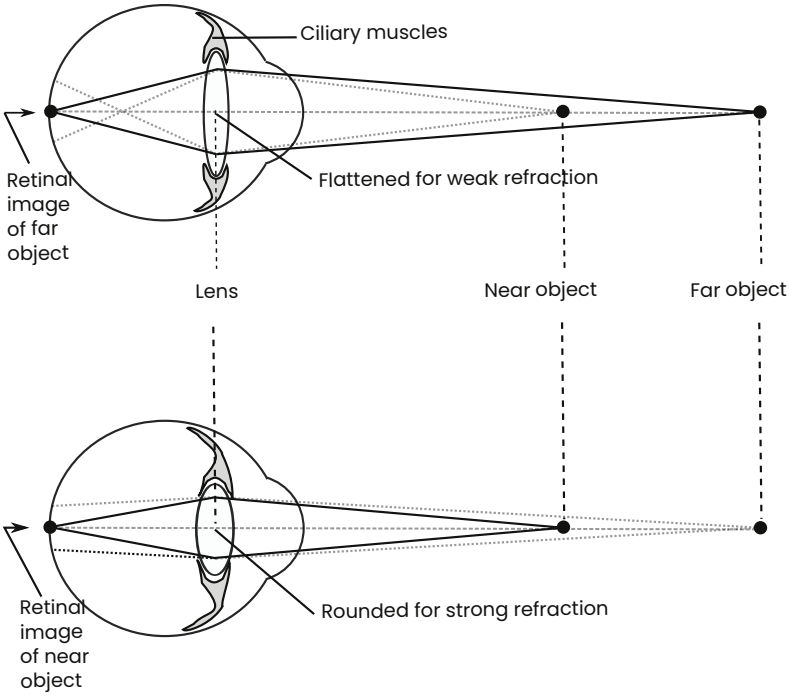

Figure 6-3: Focusing both far-off and nearby sources of light. A The light waves reflected from a distant object on the retina can be brought closer together with a relatively flat (weak) lens. B To converge the light waves reflected from a close object on the retina, a stronger, rounder lens is required.

All visible objects emit light in all directions, which can be thought of as a series of diverging waves. Light must first be focused by the human optical system before it can reach light-sensitive receptor cells of the retina and then send signals to the brain via the visual pathway. A topographic relationship between retinal and cortical fields is related to responses measured in the visual cortex [1].

Focusing the Light To adapt to different viewing distances, the lens is the primary structural component. Humans are able to focus their vision on a particular object thanks to a mechanism called accommodation, which involves a change in the lens's shape. Tiny muscles attached to the lens contract or relax to alter its curvature as needed based on the object's distance, as shown in Figure 6-3. The ciliary muscle is the name given to these skeletal muscle filaments. The iris and the pupil regulate

how much light enters the eye. Stimulation of sympathetic nerves to the iris causes these involuntary contractions, which then enlarges the pupil, whilst the stimulation of the parasympathetic nerves induces the diameter of the iris to get smaller [4].

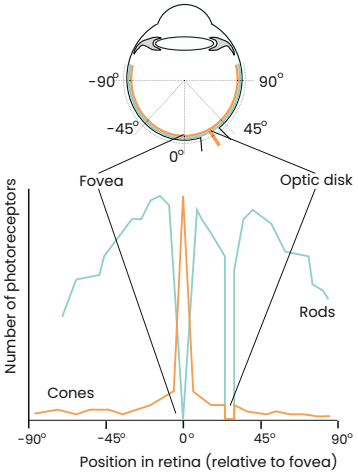

Figure 6-4: Relative distribution of the cones and rods on the retina. The y-axis is the receptor density and the x-axis is the relative distance from the fovea. Note that the highest density of cone receptors is located in the fovea and there are no receptors where the optic nerve leaves the eyeball, thus creating a blind spot. The peripheral vision is primarily due to rods, hence we have minimal abilities to detect colors in those areas

Seeing the object Cone photoreceptor cells perform transduction, transforming photons of light into the electrochemical energy that drives patterns of action potentials in the optic nerve. Rods and cones are both types of photoreceptors found in human eyes. The fovea is a small, central area of the retina that is densely packed with cones, which have a wide field of view and a high sensitivity to light. For this reason, the fovea is crucial for normal daytime vision. This is also where the image of a subject of primary attention is projected onto the retina. When exposed to a certain spectrum of light, cones release molecules that are sensitive to that color. The fovea is devoid of the rods that allow for some vision in low light, but the rods are present elsewhere in the eye. A wide spectrum of wavelengths excites light molecules in rods. Figure 6-4 shows the ratio of cones to rods in a given area. The fovea, a 1.2-millimeter-wide spot in the retina known for its dense concentration of photoreceptors, is essential for sharp central vision. The fovea can be located in the middle of the inner ring of the insets on the left and right sides of Figure 6-4. The density of cones here is nearly 200 times higher than in the rest of the retina [8], reaching a maximum in the very center of this area (Figure 6-7). Thus, foveal cones achieve their high density by having thinner outer segments, making them look like rods.

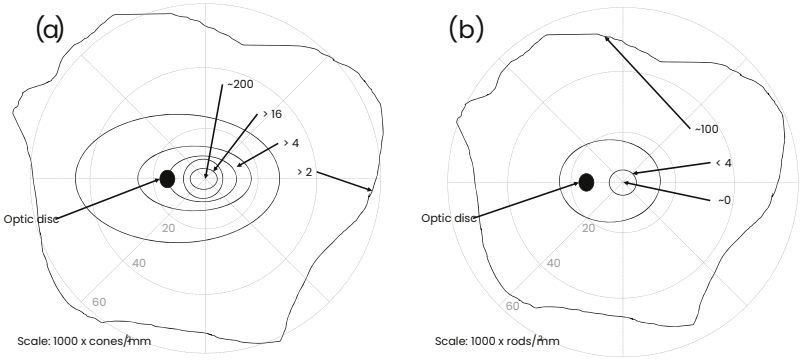

Figure 6-5: Contour curves of topographic maps of cones (Left) and rods (Right) density on the retinal surface. The density of cones on the inner circle of high (exceeds 16000 photoreceptors/mm2). The density of rods is very low on the inner circle. The rings are spaced at intervals of about 20o. The fovea is at the center of the inner ring

The contour lines in Figure 6-5 show that as the density of cones increases in the fovea, the density of rods decreases dramatically [1, 8]. Cones are defined as photoreceptors throughout the text.

Vision Fields Both the left eye's visual field and its periphery are shown in Figure 6-6 [2]. The visual area perceived by the eye at any given time is known as the "field of vision". Calculations are made with the eyes focused on a point in front of the nose. The eccentricity angle measures how far away from the fovea a target is. Around 15 degrees to the side of the optical nerve is a blind spot where rods and cones do not exist due to the optic disc being in the center of the retina.

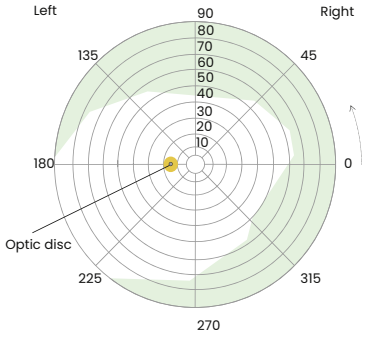

Figure 6-6: Perimeter chart showing the field of vision for the left eye. White and Green regions indicate where the light or object can be seen or it cannot, respectively

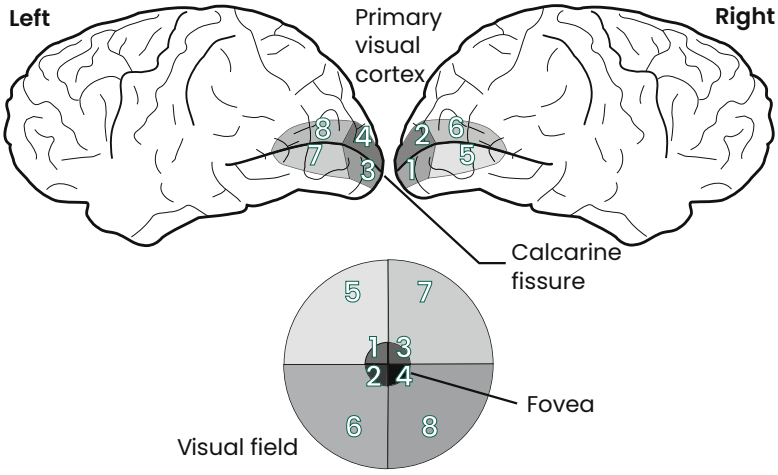

Figure 6-7: Representation of the visual field in the fovea and in the primary visual cortex. This representation is not proportional, for the neural information obtained by the receptors within the fovea projects onto a large portion of the visual cortex

Topography A topographical map is used to describe the representation of various points in the visual field by a group of neurons in the cortex. Numbers in Figure 6-7 represent regions of the primary visual cortex that are responsible for processing information from specific locations in the visual field. In order to maintain the integrity of the retina's map of visual space, the visual system's lower levels (beginning with the ganglion cells) project to the higher levels in a systematic fashion. The fovea-corresponding central visual field area (areas 1-4) is enlarged in the cortex to occupy roughly half of the total cortical representation.

6.1.1 Visual Pathway

The visual pathway consist of the nerve fibers and synapses that carry visual information from the eyes to the brain [1]. This pathway can be recorded in a single cortical cell [9], as shown in Figure 6-1. Retina, optic nerve, Lateral Geniculate Nucleus (LGN), and visual cortex make up what is known as the visual pathway; The optic nerve is formed by the axons of ganglion cells, which are the output neurons from the retina, and the LGN, which acts as a sensory relay transmitting information captured by the retina to the visual cortex, is composed of six layers.

The first two layers of the cerebral cortex are called the magnocellular layers, while the third, fourth, fifth, and sixth layers are called the parvocellular layers; the striated cortex or cortex V1 is the first stage of cortical processing of visual information. The visual field covered by the eyes is completely mapped in cortical area V1. The LGN is the primary source of visual information for this region, and it is also the primary target of visual information sent to other cortical areas. It is commonly accepted that Cortex V1 consists of six horizontal layers, each with its own set of inputs and outputs. On layer 4, we receive inputs from the LGN. This layer, for instance, is broken up into 4A, 4B, 4Cα, and 4Cβ sublayers. Important contributions from the LGN are received in 4C, with magnocellular cells entering 4Cα and parvocellular cells entering 4Cβ.

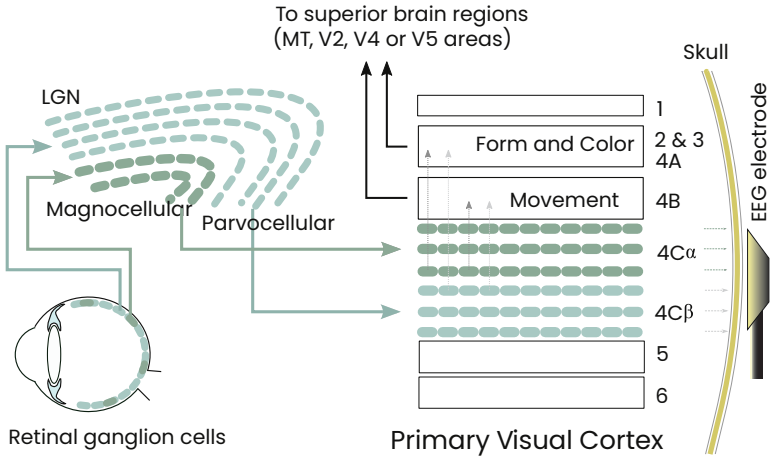

Figure 6-8: Functional representation of visual pathways. The magnocellular (dark green) pathway starts at the ganglion cells, and arrives at the layer 4C α of cortex V1 after passing through the layers 1 and 2 of LGN. The parvocellular (light green) pathway starts at the ganglion cells, passes through the layers 3–6 of LGN and arrives at the layer 4C β of cortex V1. Then, the visual information flows to superior brain regions such as V2, V4 or V5; also called MT

The Parvocellular (or P-pathway) and the Magnocellular (or M-pathway) are depicted in Figure 6-8. In contrast to the S-pathway, the M-pathway is unable to detect or process color. The P-pathway is sensitive to hue but not to subtle contrasts. The large ganglion cells (dark green) trigger the M-pathway, which then projects into the LGN's magnocellular layers and, finally, layer 4C of the primary visual cortex. The P-pathway (light green) originates in the ganglion cells of the retina, travels through the parvocellular layers of the LGN, and finally terminates in layer 4C of the primary visual cortex [1, 2, 9].

In general, the visual system uses distinct brain pathways to interpret and transmit information about visual properties like motion, color, form, and depth [1]. Non-invasive EEG electrodes can be used to measure activity in Cortex V1 even though information is projected to higher visual, temporal, and parietal areas. Figure 6-8 shows a simplified flowchart of parallel

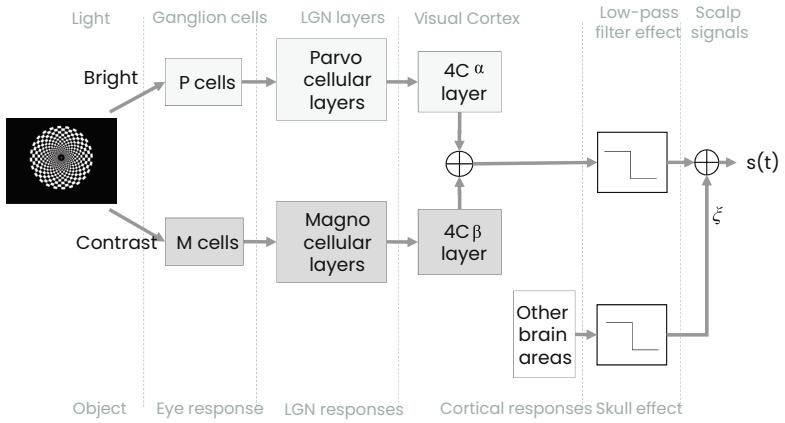

Figure 6-9: Diagrammatic simplification of parallel visual pathways. LGN, lateral geniculate nucleus; M, magnocellular; P, parvocellular. P-cell, Parvocellular layers of LGN, and 4Cα layer of visual cortex make up the Parvo route. Magno pathway consists of M-cells, the PMagnocellular layers of the LGN, and the 4Cβ layer of the visual cortex. LPF and ξ represent, respectively, the effect of the skull and the spontaneous EEG.

processing for contrast and luminance information, in which the skull effect, represented by a low-pass filter (LPF) [10], acts over responses of both layers (4C and 4C). The visual cortex EEG signal, denoted by s(t), can be thought of as the total of the response owing to parallel pathways, with spontaneous EEG designated by ξ.

6.1.2 Brain Signals and Evoked Potentials

The VEP waveforms for pattern reversal, pattern onset/offset, and flash stimulation are depicted in Figure 6-10. The pattern-reversal stimulus consists of sudden, recurrent transitions from black and white to white and black checks. There is little to no fluctuation in brightness since the stimulus is presented as a checkerboard with roughly the same numbers of black and white squares. There is a sudden transition in the pattern's onset/offset, as the checkerboard is replaced with a muted gray background. The ambient light level is identical to that of the stimulus. The stimulus's average brightness, pattern contrast, and field size can be modified, as can the frequency of stimulation (in reversals per second) and the number of reversals [16]. Strobe lights, flashing screens, and other portable light sources are all useful tools for flash stimulation. They can also be used to create the illusion of motion in digital graphics. As such, the VEP can be induced by presenting a short flash in an otherwise well-lit area.

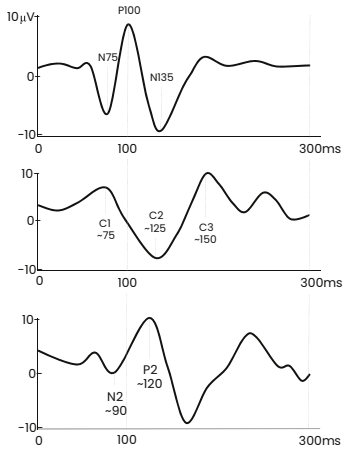

Figure 6-10: Three examples of typical VEP waveforms: pattern reversal (top), pattern onset/offset (middle), and flash stimulation (bottom). Two positive peaks (P50 and P100) and a negative peak (N75) can be seen in pattern-reversal responses. There is minimal to no difference in responses across subjects. There are three peaks in the on/off pattern response, located at 75, 125, and 150 milliseconds (C1, C5, and C3, respectively). There is more variation between study participants. Peaks (N1, N2, and P2) in flash reactions occur at 30, 90, and 120 ms. The comments here are more dispersed than in the past.

Repeating the visual stimulus and averaging the resulting responses allows one to plot a smooth curve. Transient visual responses are waveforms that can be used to determine response latency and peak amplitude. When stimulation is provided at regular intervals, the sensory system needs time to reset before the next stimulus emerges, hence a low repeti-

tion rate is necessary (less than two stimuli per second). The usual VEP response and the brief response generated by a 2 Hz pattern reversal stimulus are shown in the upper inset of Figure 6-11. The repeated stimulation interval (500 ms) is depicted with a gray background to emphasize the fact that it is longer than the average reaction time (300 ms).

Visual Evoked Potential and Refractive Error The amplitude of the pattern of an evoked potential is extremely sensitive to optical blurring, so technical and physiological factors like pupil diameter or refractive errors can affect the VEP [19]. Measuring the amplitude of the VEP with changes in power of trial lenses is one method of determining refractive error in ophthalmology [20]. As the subject's visual acuity will play a role in how the VEP results are interpreted, correcting for refractive errors is essential. Since the 1970s, it has been established that the pattern's amplitude is affected by optical blurring [17].

The sharpness of the checkerboard's edges is diminished due to defocus. One example of eliciting VEPs in a single subject with and without lenses is depicted in Figure 6-12 [21]. To modify the level of defocus, it made use of lenses with varying dioptric powers. As can be seen, refraction errors and differences in visual acuity between the two eyes have a negligible effect on the amplitude of the VEP.

With the increased availability of mixed reality headsets and the ability to record high fidelity physiological recordings with devices like the ones presented in this thesis, it is possible to imagine what it would be like to have more insight into the health of an individual, and potentially diagnose diseases early. When waiting too long for treatment, the treatment efficacy diminishes dramatically, so I ask:

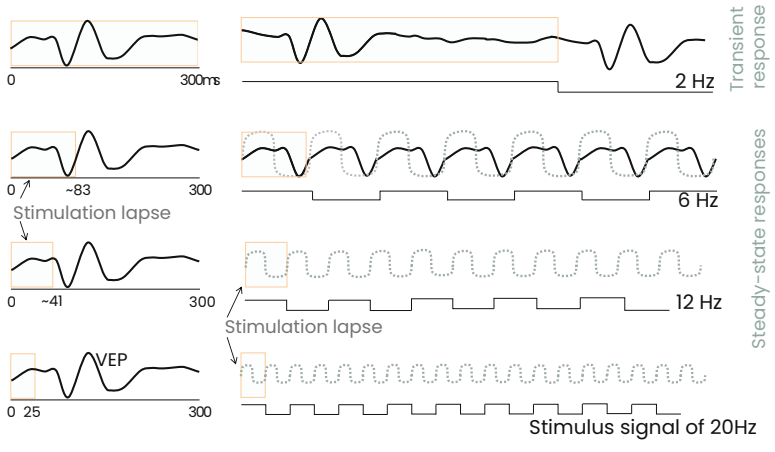

Figure 6-11: Changes in the waveform of the visual evoked potential (VEP) in response to varying frequencies of stimulation. Consider the fact that the wave form is essentially being modulated at the second harmonic of the stimulus frequency. The components of the transient VEP become visible at the slowest frequency (2 Hz).

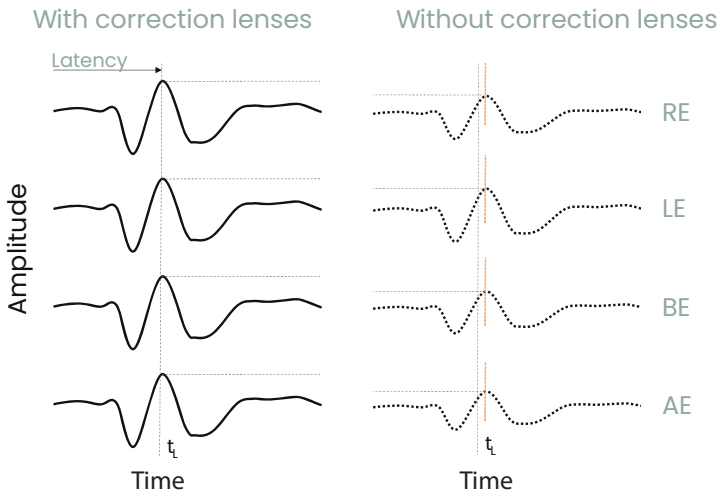

Figure 6-12: VEP waveforms of a subject with a refraction deficit are compared with (left curves) and without the use of corrective lenses (right curves). Right eye (RE) and left eye (LE) traces come first and second, respectively; both eyes (BE) come third; and the grand average (AE) of the potentials comes last. With corrective lenses, the delay is denoted by tL.

Hypothesis 6.1.1 *Can a binocular virtual reality headset be used to improve early detection of vision and/or neuro-degenerative disease?*

Hypothesis 6.1.2 *Can the design of the system pave the way for the evaluation and monitoring of a wide range of other neuro-visual functions?*

Prior studies or methods for evaluating the health of visual fields are replicated in order to provide an objective evaluation of human visual metrics. EEG data is used to analyze the evoked brain potentials produced by the system as a result of periodic visual stimuli shown to the patient's field of view. The occipital lobe is thought to be the source of these potentials. Matlab's EEGlab toolbox [155] is used throughout the signal validation analysis performed on the continuously monitored EEG data. Because this system operates in a closed loop, it is possible to make real-time adjustments to following stimuli, allowing the researcher to conduct more in-depth inspections of potentially damaged regions, or increase the granularity of the investigations.

6.2 Method

6.2.1 Experiment Task

This study investigates Visual Evoked Potentials (VEP) that arise when a flashing visual stimulus is presented. The goal is to explore a novel paradigm for recording VEPs where the stimulus is presented in virtual reality (VR). The investigation aims to differentiate time delays and VEP

properties associated with stimulation of different parts of the visual field.

Eight individuals were recruited through an email list and each of the subjects were asked if they had neurological conditions like epilepsy, as well as whether they have ever had any eye or visual pathway infections. Recordings only proceeded when it was confirmed that there was no risk involved. The participants were told that they could leave at any time without having to give a reason.

All procedures were approved by the Massachusetts Institute of Technology institutional review board, and every participant provided informed consent. Participants (N = 8, ages 18 to 44, 5 males, 3 females, 5 Glasses, 3 No Glasses) reported no known history of epileptic seizures, migraines, or vestibular dysfunction, and had no known history of claustrophobic events when using VR headsets. The participants also had to have the ability to sit and follow instructions for 30 minutes.

6.2.2 Test Environment

Physiological signals were recorded with a Galea headset, and signals were visually inspected after setup at the start of each session. Participants were asked to stay still for calibration, and were asked to close their eyes for alpha baseline collection. A complete system review can be found in this publication [redacted for anonymity].

The VR headset used during the experiment is a Valve index as described in Chapter 3 on page 59. The VR headset was configured for a 90Hz FPS refresh rate which allowed stimulating signals to be generated at frequencies up to 45Hz. Display brightness was set to 130%, motion smoothing to ON and Dashboard position to NEAR in Steam VR settings.

This setup configures the steamVR Desktop about 37 inches away from the participants, and 27 inches tall. This results in the stimulus circle taking up about 36 degrees of the participant's visual field, a digramatic representation can be seen in Figure 6-13.

Stimulus was presented through Neurobehavioral System's Presentation [1] Pattern reversal frequency: 2Hz, one reversal every 0.5 seconds

The brightness of the stimulus was also measured from inside of the VR headset at a similar distance to where the eye would normally be located.

1: The experiment was performed using Presentation® software (Version 18.0, Neurobehavioral Systems, Inc., Berkeley, CA, www.neurobs.com)."

Stimuli	Luminescence (FC)	Luminescence (LUX)
No-stimuli	0.07	0.6
Full	2.04	21.9
Half	1.15	12.2
Quadrant	0.49	5.3

Table 6.1: Luminescence (LUX) measurement for each of the stimuli.

6.2.3 Experimental Protocol

Participants were told first to fill out a short questionnaire. The purpose of the questionnaire was to collect demographic information and to learn about any eye condition, prescription or eye dominance.

Once the questionnaire was filled out, participants received information about the interactions that they would experience during the experiment in VR.

The majority of subjects were unfamiliar with EEG/VEP, therefore they were asked to minimize body movements, eye closures, and talking during the recording. They were told that the goal of the task was to remain focused on the center red cross, specifically the yellow dot in the middle of the red cross, while the checkerboard flashes around it. No medicines for pupil dilatation were administered, and no artificially restricted pupils were employed for any of the reported tests.

Shortly after receiving this information, the participants were asked to put on the headset. During this step, the experimenters adjusted the headset so the noise level in every channel was under 10 uVRMS, prioritizing good signals for channels Fz, Poz, Po3, Po4, Oz, O1, and O2. The electrode locations were as described in Figure 6-14, which have been previously identified as adequate for high-quality Galea headset measurements. On the scalp, neither abrasive preparation agents nor conductive pastes or gels were utilized. Any bulky jewelry or headwear that could interfere with electrodes or the mounting hardware was removed prior to experimentation.

After affixing the Galea headset to the subject, the test required subject alertness for an extended period of time (approximately 15 minutes) in the presence of repetitive visual displays at low light levels. Subject boredom and microsleeps were a concern, so participants were encouraged to count the number of flashes during testing.

One session routine, from start to finish, has a duration of about 30 minutes. Seven routines in total were divided into three, two, and two

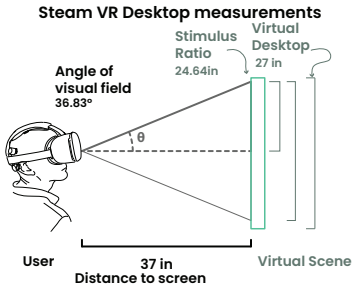

Figure 6-13: Distances and dimensions between the subject and virtual desktop where stimuli are presented

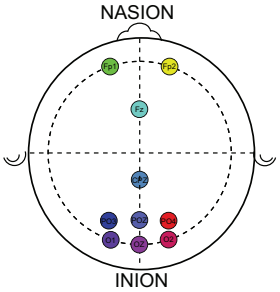

Figure 6-14: Top view of a 10-20 system mapping for the EEG touch-points available in the Galea system including Fp1, Fp2, Fz, Cpz, Poz, Po3, Po4, Oz, O1, and O2.

sessions of measurements for the binocular recording for each subject. The experiment structure was as follows: 1 block = 5 second rest (small white cross in the middle of a black screen), followed by 30 pattern reversals (total of 20 seconds). The entire experiment has 6 blocks -> 20 second rest -> 6 blocks for a total 12x30 = 360 pattern reversals.
This sequence is also shown in the diagram found in Figure 6-15.

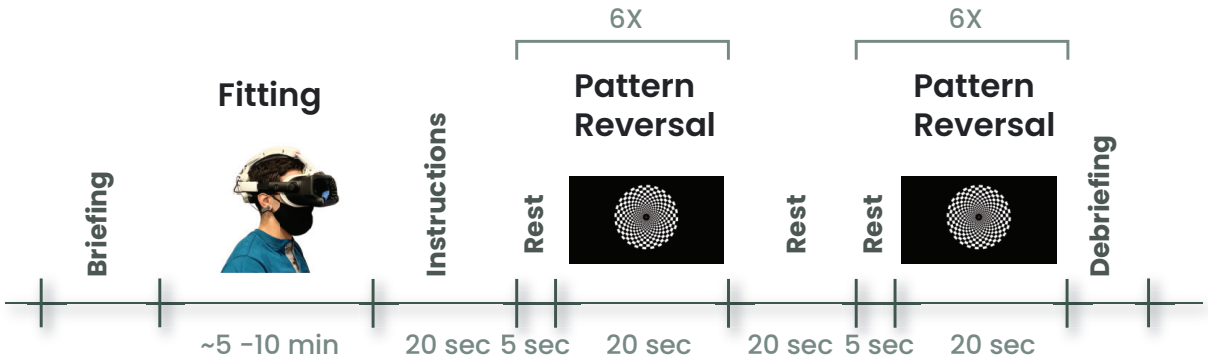

Figure 6-15: Representative normal pattern reversal VEP recorded from mid-occipital scalp using 50′ checkerboard pattern stimuli.

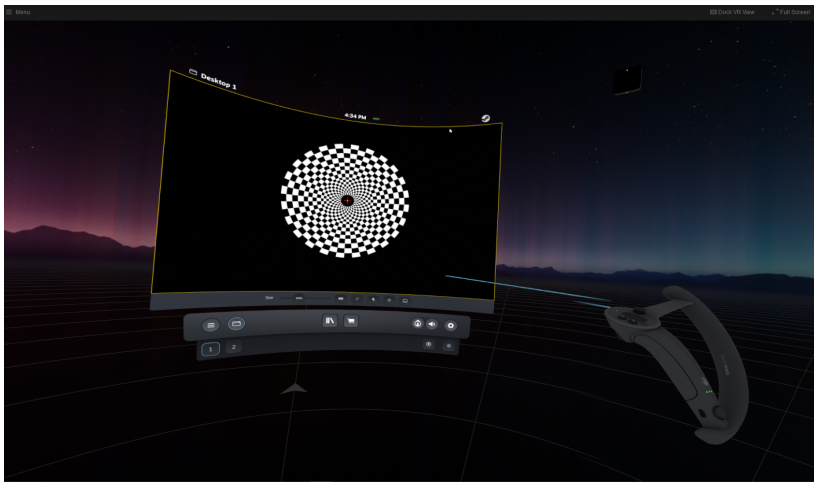

Figure 6-16: Inside view of the VR scene used for the experiment

6.2.4 Data Collection

The data collection follows the same principles mentioned in Chapter 3 on page 59. 3.3

6.2.5 Data Processing

The collected data was processed for further analysis in EEGLAB [155]. 10 channels (Fp1, Fp2, Fz, Cz, Pz, Oz, PO3, PO4, O1, O2) were selected from the full 16-channel recording. A band-stop filter of 48Hz-62Hz was applied to remove line noise. Then, a band-pass filter with a low cut-off

frequency of 0.1Hz to 1Hz and a high cut-off frequency of 30Hz to 35Hz was applied to extract the VEP response. The exact cut-off frequencies were determined by the amount of low frequency and/or high frequency noise in each recording. In one extreme case, we applied a band-stop filter of 8Hz-13Hz to remove strong alpha oscillations from the signal.
Once the raw signal was filtered, it was epoched from 0 seconds to 0.5 seconds after each pattern reversal. For each epoch, its average over the duration of the epoch was removed via baseline removal. Of the 360 total epochs, the first 2 epochs after each rest were rejected to remove the effects of the stimulus appearing on screen from the aggregated VEP. The remaining 336 epochs underwent another round of rejection using a simple voltage threshold. We included all 10 channels. The minimum rejection threshold was -40uV, and the maximum rejection threshold was 40uV. These values were selected based on preliminary recordings, which showed that these settings do not excessively reject epochs while effectively removing epochs containing large noises, such as blinks. We ignored certain channels when applying the voltage threshold, depending on the amount of noise in that channel. Additionally, we increased the rejection thresholds to ±50uV or to ±60uV if the ±40uV threshold flagged too many epochs (100+ out of 336) for rejection. In extreme cases, epochs had to be manually rejected to remove oscillations that were not getting caught by the voltage threshold but influencing the VEP we were getting.
After rejecting epochs, the data was re-referenced to the Fz channel, and channels Pz, Oz, PO3, PO4, O1, O2 were selected. The average value over all epochs was calculated and plotted for each channel.
At this point, we noticed that our system produced a mean P100 latency of 178.428 ms for full visual field stimulus across 7 users. In order to align our P100 latency with the normal range of P100 latency reported in the literature, we shifted the data points by an offset of 78.428ms so that our P100 latency would be within the normal range.

6.3 Results

The VEP amplitude and latency were assessed for the seven visual fields stimuli.

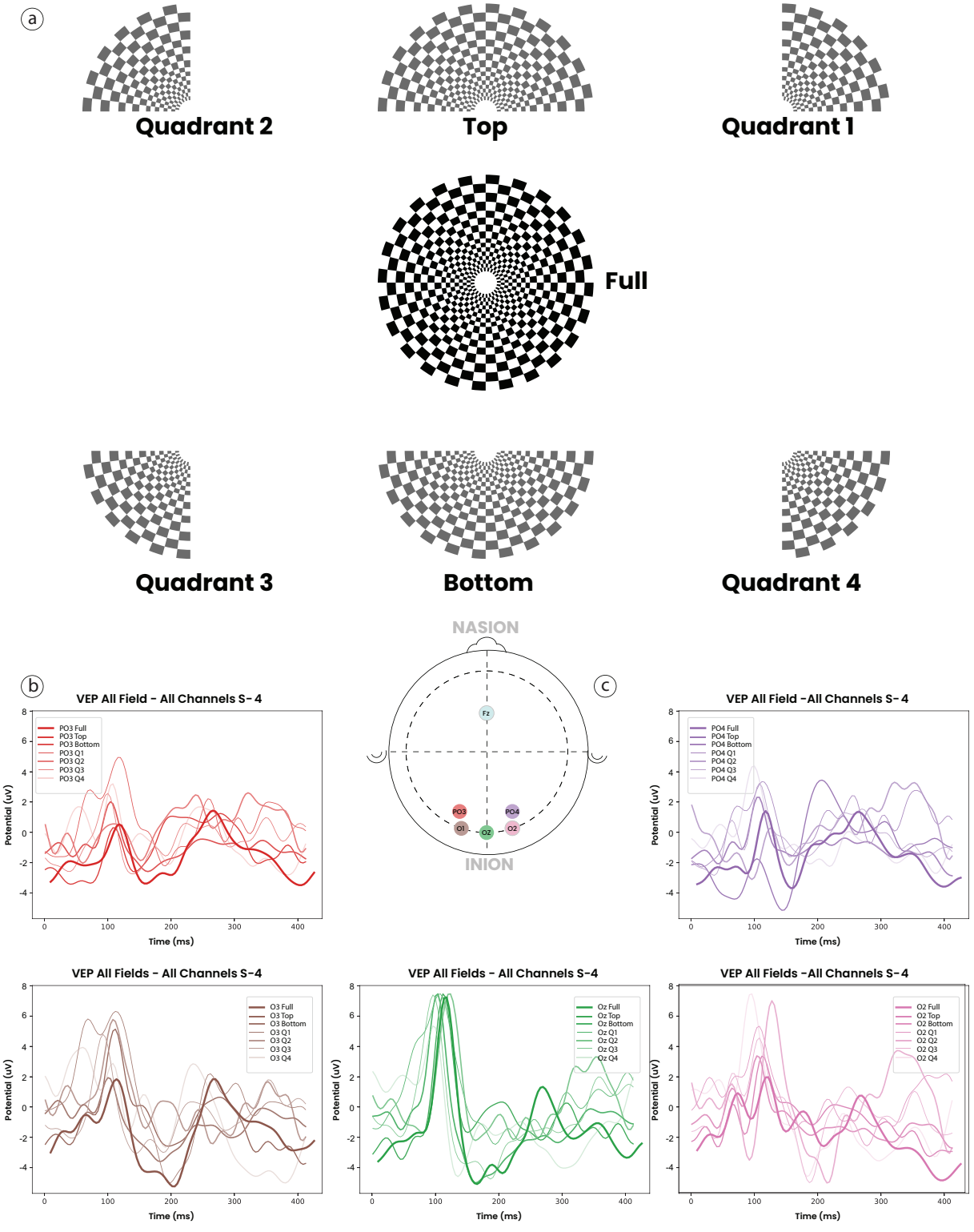

Figure 6-17: Section a) shows the seven stimuli used for the data collection. Each stimulus tries to elicit a response from the visual field. Section b) is a series of VEP plots from subject 4. Each plot shows the signal collected at that specific electrode when presented with one of the seven stimuli. Section c) is a top-down view of the channels following the 10-20 system used for these VEP recordings.

6.3.1 Inverse Visual Evoked Potentials Morphology

At first glance, we noticed that the recorded potentials did not correspond to those depicted in the ISCEV guidelines [156]. The temporal resolution appeared accurate, but the amplitude appeared to be inverted from what we had observed previously for a VEP type in which the P100 is a positive deflection. Through further investigation, we learned that this morphology has previously been described. Two factors appear to account for the positive or negative orientation of the VEP. The configuration of the amplifier can determine the polarity of the waveform. Amplifiers can be configured uni-polar or bi-polar; the polarity will change if the lead is connected to the negative side instead of the positive side when configured with uni-polar leads.

Since the 1970s, when Michael and Halliday [157] explained these inversion effects in terms of changes in the form and polarity of the surface distribution of constant latency components, the second factor has been the subject of research. These changes are the result of the vastly different topography and orientation of the visual cortex regions that represent the upper and lower regions of the visual field, which produce inverted effects [158] Di Russo et al [159] hypothesize that (N75) changes polarity depending on upper or lower field stimulus because "stimulation above and below the horizontal meridian of the visual field should activate neural populations with geometrically opposite orientations" and that (P100) does not change polarity depending on upper or lower field stimulus because it is primarily generated in extratriate visual areas that lack the retinotopic organization of the calcarine cortex.

With these understandings and in order to help the readability of the findings here, from this section forward the signals are mirrored 180 degrees for ease of comparisons.

6.3.2 Visual Evoked Potentials Analysis

For the seven stimulus patterns that were shown to all eight subjects, the VEP waveforms (i.e., the polarity and latency of the individual peaks) were similar, but variations were observed in the actual peak amplitudes for each subject. Subject 4's stimulus and evoked potentials are depicted in Figure 6-17. Section a) shows the seven stimuli used for the data collection. Each stimulus tries to elicit a response from the visual field. Section b) shows a series of VEP waveforms for each channel. The traces

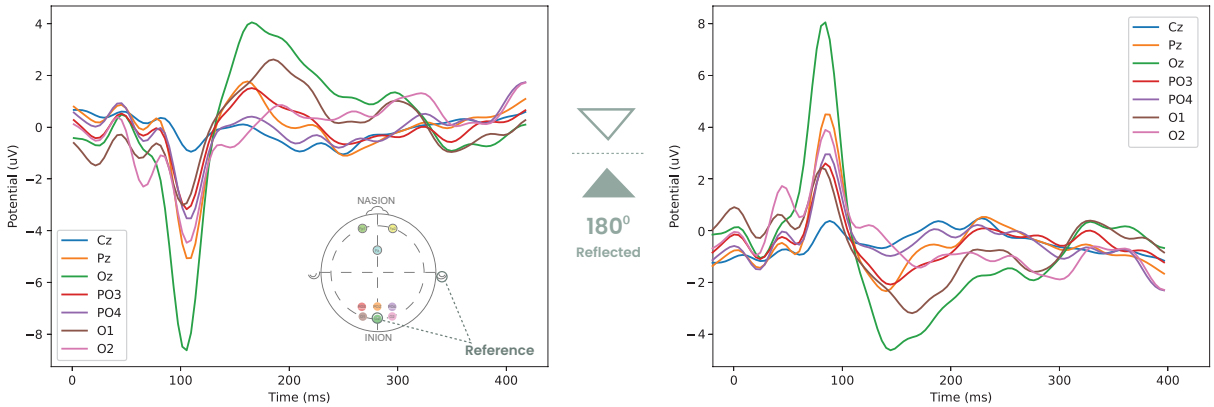

Figure 6-18: On the left, wave-forms from visual evoked potentials generated by the full field of view stimulation recorded using A2 reference electrode. On the right is the signal collected from our system flipped 180 degrees to match standards

in each graph correspond to the stimulus from which they were elicited. The center plot is for the Oz channels, with the largest potential of 8 uV. This observation compares to what has been previously reported by Sharma et al. [160] and the ISCEV standard for clinical visual evoked potentials report for clinical use [156].

6.3.3 VEP Amplitude

Table 6.2 reveal the primary components average amplitudes for all users when presented each of the visual fields stimuli. On average the two largest responses potentials (P100) were recorded for the full and bottom visual field with an amplitude of 5.6 uV and 5.8uV. A comparison between subjects who need prescription lenses and subjects with perfect vision was also calculated. Figure 6-19 shows the difference in amplitude for both groups for each of the stimuli presented. Across the different fields we observed an increase in amplitude for the group with perfect vision and smaller amplitude for those that need prescription glasses.

Table 6.2: Amplitude across visual fields for all users

	Full	Top	Bottom	Q1	Q2	Q3	Q4
P100	5.615143333	4.086039429	5.899372789	2.380506667	3.130152952	3.104096735	3.209792789
N75	0.25727875	0.743542	0.196309286	0.276114	0.17821	0.954635714	0.339243571
N135	3.50224125	1.896242	3.470952143	1.785654	1.906593333	1.264121429	1.751672143

Since the amount of light flashed to the visual field increases based on the visual field stimulus pattern as described in Table 6.1, we decided

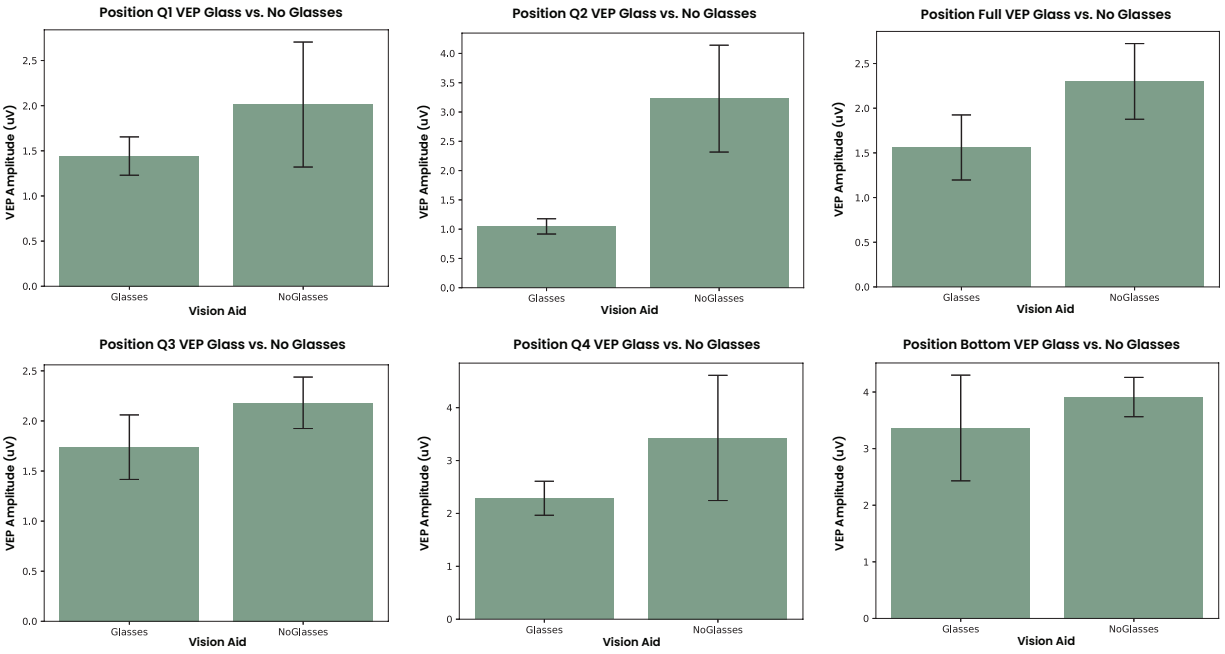

Figure 6-19: Comparison between subjects who need prescription lenses and subjects with perfect vision for each of the stimuli presented. Across all stimuli, the data shows that users with perfect vision have a stronger response in mV than the subjects that need prescription glasses.

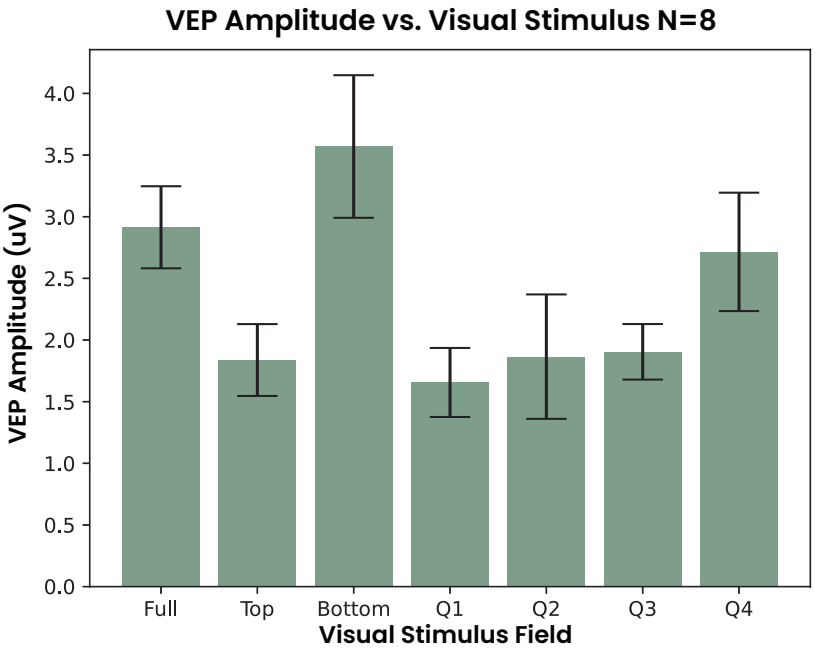

Figure 6-20: Average response for a visual field region in micro-volts to the location and size of the stimulating region.

to measure the amplitude size for each one of the patterns. Figure 6-20 shows the

6.3.4 VEP Latency

Figure 6-21 *i* shows in green the average signal for Channel Oz for all subjects, and the standard deviation is shown in peach when a full-field stimulus is presented. The most relevant event-related potentials

for N75, P100, and N135 are also shown. The latency of these events matches the ISCEV standard as shown in Figure 6-10. The P100 latency response across all users for each stimulus is shown in Figure 6-22. Figure 6-21 *ii* is an example of each channel's response to a full-field stimulus for Subject 4. Figure 6-21 *iii* shows the average signal for the Channel Oz in green, and the standard deviation in peach when a bottom-field stimulus is shown. Figure 6-21 *iv* shows the response to the full-field stimulus for each channel averaged across all subjects. Figure 6-22 presents the average across all users' latency values at P100 for all visual field stimuli. It is shown that the full, bottom, and lower quadrants have a 100 ms or closer stimulus than the upper or top stimulus. The latency for upper visual-fields seems to be consistent across users. Table 6.3 reveals the average latency across all users' temporal changes for each one of the VEP components. P100 and N75 show similar latency as those previously reported. We do observe a larger than usual latency for the N135 components. The reasons for these findings might have to do with the refraction from the VR headset lenses and the noise levels that are averaged across all users.

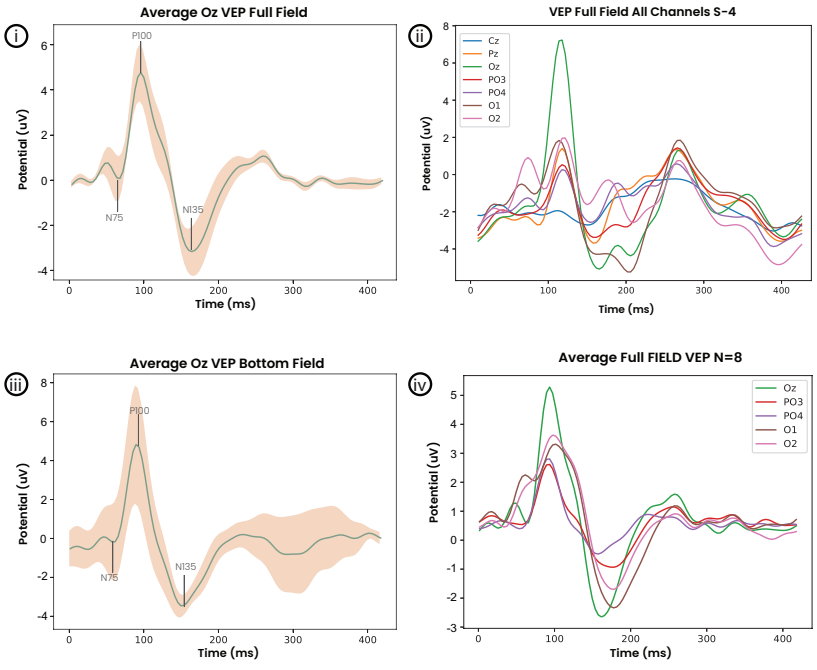

Figure 6-21: In section i), the average signal for the channel Oz is shown in green, and the standard deviation is shown in peach when a full-field stimulus is shown. Section ii) is an example of each channel's response to a full-field stimulus for Subject 4. Section iii) shows the average signal for the channel Oz in green, and the standard deviation is shown in peach when a bottom-field stimulus is shown. Section iv) shows the response to the full-field stimulus for each channel averaged across all subjects.

Table 6.3: Latency

	Full	Top	Bottom	Q1	Q2	Q3	Q4
P100	97.572	114.572	90.572	111.072	108.072	90.572	97.072
N75	65.572	73.572	57.572	69.572	65.572	57.572	57.572
N135	161.572	193.572	149.572	201.572	233.572	145.572	149.572

6.4 Limitations

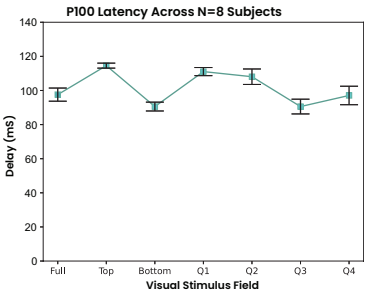

Figure 6-22: P100 latency response across all users for each stimulus.

One of the limitations of this study is the limited adjustability of the Galea headset, which may create challenges when placing electrodes in precise locations of the scalp. This can potentially affect the accuracy of the EEG recordings and the resulting VEP waveform. For example, the limited adjustability of the headset may make it difficult to achieve a consistent and comfortable fit for participants, which can lead to variations in the EEG recordings. Additionally, the limited adjustability of the headset may also make it more challenging to accurately place electrodes in the specific locations on the scalp required to capture the desired EEG signals.

Another limitation of this study is the potential for lens refraction of the VR goggles to create distortions in the VEP waveform. VR goggles are known to create distortions due to the curvature of the lens. These distortions can affect the perception of visual stimuli and create artifacts in the EEG recordings that can affect the accuracy of the VEP waveform.

Another limitation is the weight of the headset, which may prevent studies from being conducted for longer than 20 minutes. Participants may begin to experience discomfort and this may compromise the experimental results. The weight of the headset may lead to discomfort and fatigue for participants, which can affect the accuracy and consistency of the EEG recordings. This can lead to variations in the VEP waveform and potentially limit the conclusions that can be drawn from the study. Additionally, if the headset is too heavy, it may not be comfortable for participants to wear for long periods of time, which can also affect the data collected.

These limitations may affect the accuracy and generalizability of the results and must be taken into account when interpreting the findings of the study.

6.5 Conclusion

In conclusion, this study aimed to investigate the potential of using visual evoked potentials (VEPs) and the Galea headset to study the functional integrity of the visual pathways and to improve early detection and

diagnosis of visual impairments. By using the Galea headset, we were able to simulate visual impairments for normally-sighted individuals and analyze the EEG data from the occipital brain response to gain insights into the potential utility of such a system. The results of this study, as presented in Table 6.3, Table 6.2, Figure 6-21 and Figure 6-22, demonstrate the potential of the Galea headset and VEP-BCI paradigms to provide objective evaluations of human visual metrics, and the potential of this system to pave the way for the evaluation and monitoring of a wide range of other neuro-visual functions.

The study also explored the limitations of the system, such as the limited adjustability of the Galea headset, the potential for lens refraction to create distortions in the VEP waveform, and the weight of the headset, which prevents studies from being conducted for longer than 20 minutes. Despite these limitations, the study was able to provide insights into the potential utility of using the Galea headset for early detection and diagnosis of visual impairments.

The above mentioned limitations should be considered when interpreting the findings of this study and when designing further research in this field. The hypothesis evaluated in this study, namely that a binocular virtual reality headset can be used to improve early detection of vision and/or neuro-degenerative disease, and that the design of the system can pave the way for the evaluation and monitoring of a wide range of other neuro-visual functions, are yet to be proven. However, this study provides a strong foundation for future research to explore the potential of this system in more detail.

This is the final chapter of the awake state investigations. The previous chapter demonstrated that the usage of this sort of system can provide useful insights into researching cognitive processes as well as in the diagnostic aspect by evaluating visual evoked potentials. Such research is critical in order to build more effective, human-centered technology and solutions. The findings provided here have substantial implications for future study on cognitive processes, diagnostics, and tailored treatment development.

Part III: Tools For Sleep Studies In The Wild

Fascia Ecosystem | 7

7.1 Into The Night

In the previous chapters of this thesis, we focused on investigating the relationship between the awake state and various physiological and psychological factors such as cognitive demands, mental workload, and autonomic nervous system activity. In contrast, in this chapter, we will shift our focus from the awake state to the realm of sleep. As highlighted in previous studies, sleep plays a crucial role in various mental and physical processes, making it an important area for research and investigation.

Fascia Publications

The research presented in this chapter has resulted in the following peer-reviewed publications to date.

Bernal, Guillermo, Malika Chhibber, Mradul Bhatnagar, Urvil Jivani, Nelson Hidalgo, Anthony Levasseur, and Pattie Maes. ***Pioneering Remote Sleep Research: A Comparative Study of Sleep Stage Parameters in Diverse Datasets for Enhanced Interventions.****SLEEP 2023, the 37th Annual Meeting of the Associated Professional Sleep Societies, LLC (APSS), June 6, 2023.*

Bernal, Guillermo, Malika Chhibber, Mradul Bhatnagar, Urvil Jivani, Nelson Hidalgo, Anthony Levasseur, and Pattie Maes. 2023. ***Fascia Ecosystem: A Step Forward in Sleep Engineering and Research.*** *45th Annual International Conference of the IEEE Engineering in Medicine and Biology Society (EMBC'23), no. Sydney Australia, (July).*

Carr, Michelle, Adam Haar, Judith Amores, Pedro Lopes, Guillermo Bernal, Tomás Vega, Oscar Rosello, Abhinandan Jain, and Pattie Maes. ***Dream engineering: Simulating worlds through sensory stimulation.*** *Consciousness and cognition 83 (2020).*

In order to fully understand the impact of sleep on the human body, it is necessary to delve into the methods and techniques used to study sleep, specifically the use of polysomnography in sleep studies and diagnosis of sleep disorders. This shift in focus will allow us to gain a comprehensive

understanding of the interplay between sleep, physiological processes, and disorders affecting sleep.

We know that it is essential for humankind to get sufficient and regular sleep, not just for good rest, but also for a collection of critical cognitive developments in the brain [161]. Although very little is still understood about sleep, we know that some of the most important mental and physical processes in the human body happen during sleep, such as memory consolidation [162] and immune system fortification [163]. Sleep studies are imperative because they help sleep experts diagnose patients with sleep disorders that would otherwise be very difficult to find conclusive symptoms. Sleep studies require patients to sleep in "sleep centers" which are equipped for people to sleep while the brain and body of the subjects are monitored. The data typically collected involves EEG sensing, eye movement, oxygen levels in the blood, heart rate and breathing rate, snoring, and body movements [164]. The 'gold standard' diagnostic approach for sleep disorders is Polysomnography (PSG); this is a facility-based overnight recording of several channels of biosignals known as sleep data. This sleep data is then visually analyzed by both sleep physicians and sleep technologists to arrive at a diagnosis of the illness after correlating with various other clinical characteristics.

The Rise of Chronic Sleep Disorders and the Need for New Solutions

According to the American Sleep Association, between 50 and 70 million Americans have chronic sleep disorders, underpinning revenue growth for the Sleep Disorder Clinics industry. Over the next five years, industry revenue is expected to grow at an annualized rate of 2.6% to $9.3 billion. Sleep clinics have gained demand due to the rising number of sleep disorders brought on by electronic stimuli in the form of laptops and smartphones. Research findings show that the light emitted from these gadgets limits the release of melatonin, a hormone that regulates sleep. As the usage of devices increases, so do sleep issues that require attention from industry clinics. [a]

[a] From IBISWorld report September 2021.

Sleep studies have largely been viewed as a nuisance for the subjects being studied. This is due to the major discomfort caused when the subject must come into the research center or hospital to sleep while their vitals and different physiological signals are constantly monitored by

bulky equipment. In order to detect these signals, a variety of electrodes and sensors are distributed across the head and the rest of the body, and secured using tape or glue, therefore causing significant discomfort. Centers assure patients that they'll "still have plenty of room to move and get comfortable" and that they are being monitored by sleep study technologists who "can help if they need to use the bathroom" [1]. Still, according to the National Sleep Foundation, many people wonder how they will be able to sleep under such conditions. Researchers believe this setup and procedure results in inaccurate or at least inconsistent data as the subjects are not sleeping as they normally would in the comfort of their home, free from unfamiliar wires and electrodes probing their bodies. Home-based portable devices may provide a solution to these problems; nevertheless, these devices are, at best, insufficient because of the limited number of biophysical channels that they are able to capture. In this chapter, the levels of sleep studies are introduced, in addition to the instrumentation used and the current state-of-art technology.

7.1.1 Motivation

One of the biggest challenges for patients and sleep researchers alike is the so-called First-Night Effect [1]. In a sleep lab, the structure of sleep is disrupted, especially during the first night. The uncomfortable and incongruous nature of sleep studies requires the patient to sleep with many electrodes attached to the legs, chest, arms, face, and head in a clinical setting which leads to a great deal of discomfort, therefore making it hard for patients to fall asleep and have a full night of restful sleep.
Commercially available sleep devices, such as Muse Sleep, Zmax Hypnodyne, Phillips' SmartSleep Deep Sleep Headband, and Dreem, offer three to five EEG channels and, in some cases, a heart-rate monitor that is placed on the forehead. The number of channels and signals provided by these systems is insufficient for conducting level 1 and 2 sleep studies as discussed in Section 7.2.1 below. The gold standard of sleep study systems, polysomnography (PSG), is bulky and uncomfortable, which disrupts the very thing it aims to measure [165].
The Fascia device introduced in this section meets the requirements of the PSG in a small, affordable and more comfortable form factor that can be deployed in a home setting, thereby also providing more typical data. Its hardware is mounted into an opaque fabric sleep mask and its electrodes are made of a conductive polymer, whose softness is comparable to

silicon. It is also completely wireless, battery powered, and weighs as little as 228 grams (a little lighter than a common grapefruit).
The Fascia ecosystem makes use of three leading technologies that allow for the reinvention of how sleep studies are conducted. First, the Fascia Sleep Mask collects similar data to that of a full polysomnogram in the small, familiar, and comfortable form of a soft sleep mask using the latest technologies in fabric-based sensing. Second, the Fascia Hub allows a researcher or scientist to provide stimulation and feedback in the form of audio and visual stimuli to the patient, expanding the opportunities to understand sleep and dreams by also issuing interventions. Finally, the Fascia Portal is where sleep researchers can inspect the patient's signals in real-time and store experiment information, analyzed by the machine learning API that provides sleep staging, spindles, and k-complex identification information in real-time. The portal also works as a data collection and labeling platform for developing new and more robust datasets to train machine learning models for sleep diagnostics.

7.2 Background

Because sleep affects so many different physiological systems, both central and peripheral, it can have a profound impact on overall health. Yet sleep exists in a social-environmental context: Neuroscientists would be better able to translate sleep health into clinical practice if they considered sleep health in the context of its determinants, which include factors at both the individual and societal levels. Recognition and investigation of sleep's functional roles; clarification of causal mechanisms in relation to important outcomes; development of richer model systems; linking of models to known contextual factors; and exploitation of advances in multisensory technology represent key challenges and opportunities. As a result of addressing these issues, social-environmental factors related to sleep will have a more prominent presence in clinical settings.

7.2.1 Types of Sleep Studies

Depending on the number of channels that record various physiological parameters and the availability of a trained sleep technician during the recording, sleep studies can be categorized into the following four major categories.

Level IV This is the most basic sleep study and involves equipment, that has one or two channels for recording at least one or two respiratory parameters throughout the night. Consequently, while the subject is sleeping, it can record either the oxygen saturation or the respiratory flow, or both of these signals simultaneously. After placing the channel in the correct location where it will remain for the duration of the night, the following morning, the tracing can be derived from the data that was collected by the device. Screening for obstructive sleep apnea can be performed with the use of this type of device. On the other hand, the AASM* does not recommend it for use in the diagnosis of obstructive sleep apnea.

Level III These devices contain a minimum of four channels, some of which include ventilation (at least two channels of respiratory movement or respiratory movement airflow), oxygen saturation (respiratory effort, oxygen movement, and airflow), heart rate or ECG, and oxygen saturation (Figure 7-1). Consequently, they have the following channels:

- Pulse oximeter
- Nasal airflow
- Movements in the chest or the abdomen
- Electrocardiogram

Figure 7-1: Level 3 sleep study singular sleep device

Level II Another name used for this kind of polysomnography is complete portable polysomnography. With the exception of video, it has the ability to record all of the channels recorded during Level I sleep research. A sleep study with a Level II device does not require the presence of a sleep technologist and can even be performed in the patient's own home. In addition to the electrocardiogram and respiratory monitoring channels, these devices also contain channels for electroencephalogram, electrooculogram, and chin electromyogram. As a result, the total number of channels must be at least seven, and they may include the following:

- Pulse oximeter
- Nasal airflow
- Movements in the chest or the abdomen
- Electrocardiogram
- Electromyogram
- Electroencephalogram with a minimum of two channels present

Figure 7-2: Level 2 sleep study Alice device

* The American Academy of Sleep Medicine

- Electro-occulogram
- Body position
- During these studies, Auto-PAP may be used for the titration of PAP pressure in patients with sleep apnea

On either the right or the left side of the patient's head, active electrodes may be positioned in the frontal, central, or occipital regions of the scalp. One electrode is placed on the right mastoid and the other electrode is placed on the left mastoid since they are typically referred to as being in the opposite location of the mastoid. The information provided by these channels is adequate for determining the stages of sleep and arousal. On the other hand, the majority of the monitoring devices that are currently on the market include an option for recording from other regions of the brain, such as the prefrontal and temporal regions. Due to the fact that these devices actually offer capacity for 24–32 channels of EEG, it is possible to use them for monitoring sleep-related seizures and parasomnia.

Figure 7-3: Level 1 sleep study full PSG setup

Level I This study makes use of the same equipment utilized in type II studies with the significant distinction that a level I sleep study must be conducted in a sleep laboratory, and a sleep technologist must be present for the entirety of the investigation. In order to collect more data than what a type II study can offer, the following channels are added:

- Audio and video recordings that are synchronized with the recording of other data.

This type of study can not only diagnose sleep abnormalities, but it can also manually titrate positive airway pressure therapy for patients who have sleep-related breathing issues. Therefore, it possesses a channel for CPAP machines that is utilized during manual titration of CPAP in individuals who suffer from sleep apnea.

The following are some of the channels that, depending on the circumstances, may be added as an option:

- Capnograph: measuring end-tidal carbon dioxide levels or taking readings from the finger capnograph.
- Pharyngeal pH monitoring channel, which aids in the diagnosis of nocturnal gastroesophageal reflux disease (GERD).
- Esophageal pressure monitor: Research is the only use for which it can be used. It is able to distinguish between central and obstructive sleep apnea in an accurate manner.

7.2.2 Sleep Stages and Cycles

Sleep is not uniform and is characterized into stages based on Electromyography (EMG) or muscle electrical activity, EOG or electrical eye movement activity, and Electroencephalography (EEG) or electrical brain wave activity [166]. There are two types of sleep: NREM and REM. Stages N1, N2, and N3 N4 of NREM sleep are further separated. Stages N1, N2, N3 and N4 are referred to as light sleep, deep sleep, and slow-wave sleep, respectively. Each of the four or five cycles of sleep consists of an NREM sleep period and a subsequent REM sleep section. Also during the night, periods of wakefulness are possible. Each cycle's length of REM sleep often lengthens as the night goes on.

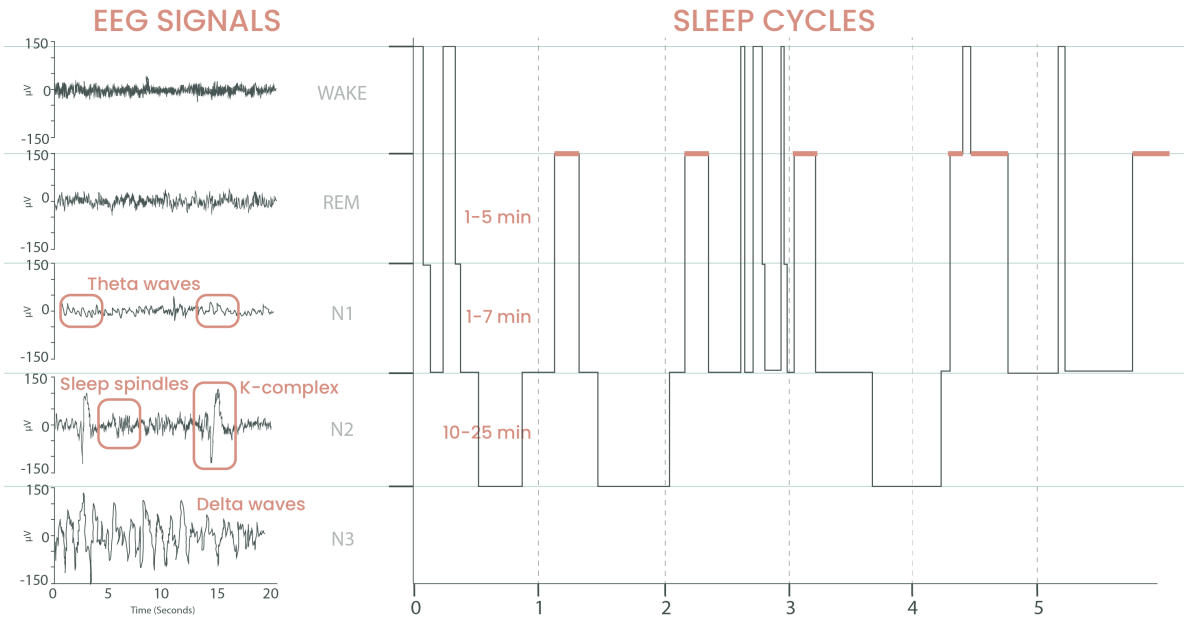

Figure 7-4: Sleep architecture

This nomenclature was modified in 2007 by the American Academy of Sleep Medicine (AASM) and sleep stage 3 and 4 have been merged into stage N3. In humans, a normal night of sleep consists of a repetition of four or five cycles in which sleep stages tend to follow each other in a particular order. Sleep staging is generally done visually by inspecting consecutive PSG segments of 30s. It results in a hypnogram which represents the succession of sleep stages across time.

The hypnogram is an easy way to graphically show how sleep is organized during the night. A level on the graph's vertical axis and the time of night on the horizontal axis represent each stage of sleep, respectively. Often a dark bar is used to indicate REM sleep. In the past, polygraph recordings

Table 7.1: Sleep architecture table.

Sleep stages	Types of sleep	Other names	Normal length
Stage 1	NREM	N1	1-5 min
Stage 2	NREM	N2	10-60 min
Stage 3	NREM	N3,	20-40 min
Stage 4	REM	REM sleep	10-60 min

were used to track sleep by leaving traces on paper that could be read afterwards. It was easy to split the night into periods of time equal to the width of each paper page. The standard paper speed for tracking sleep is 10 mm per second; a 30-cm sheet equals 30 seconds. Sleep is staged in epochs, which are each represented by a single page of time. The habit of grading sleep in 30-second epochs or windows is still the norm even though most sleep recordings are now done digitally. The sleep stage that dominates the majority of a specific epoch is used to identify the stage if there is a transition in sleep stage throughout that time. When the sleep tracings are occluded by an artifact for longer than a half-epoch, it is scored as movement time (MT). The epoch is additionally rated as wake when it is surrounded by epochs that would otherwise be deemed MT. Some sleep facilities do not tabulate MT separately and instead treat it as waking.

7.2.3 The Physiology of a Sleep Study

Complex sleep monitoring calls for specialized expertise in areas such as EEG, respirometry (RM), and electrocardiography (ECG). Being an expert in just one of these fields does not provide an individual with effective polysomnogram interpretation.

The functioning of nearly all systems of the body, including the brain, heart, respiratory system, gastrointestinal system, genitourinary system, endocrine system, and musculoskeletal tone, shifts between two states of consciousness, namely wakefulness and sleep. Even during sleep, the functioning is dynamic, and it gives rise to various sleep stages. During NREM sleep, for instance, breathing becomes steady, heart rate slows, and peripheral muscletone decreases. During rapid eye movement REM sleep, breathing and heart activity become irregular, peripheral muscular tone is decreased, and periodic muscle spasms develop. There is also a notable alteration in the EEG. As the individual falls sleep, EEG activity begins to slow and typical waveforms such as vertex waves, sleep spindles, K complexes, delta waves, and low-amplitude, mixed-frequency EEG begin to appear. In addition to information from muscle tone and

eyechannels, these EEG waves assist in distinguishing sleep stages.

The Electroencephalography Of Sleep

EEG is an electrophysiological detection mechanism used to monitor electrical activity of the brain and record brain wave patterns. Usually this sensor takes the form of noninvasive electrodes (small metal surface connected with thin wire) contacting the scalp, although versions of it which pierce the skin also exist. EEG wave patterns are well-studied and there are known patterns that healthy brains emit, so doctors can observe abnormal patterns and study whether they are a cause for concern and what they might entail. For the purpose of the Fascia platform, EEG can be used to monitor sleep stages and cycles whether the patient is experiencing NREM or NREM sleep.

The frequency in cycles per second or hertz (Hz), amplitude (voltage), and primary deflection direction (polarity) characterize EEG activity. Delta (4 Hz), theta (4 to 7 Hz), alpha (8 to 13 Hz), and beta (>13 Hz) are the conventionally recognized frequency ranges. When the eyes are closed and the patient is awake but relaxed, alpha waves (8 to 13 Hz) are often detected. Conversely, when the eyes are open, they are attenuated and are best documented on the occiput. During sleepy, eyes-closed wakefulness, alpha activity is prominent, but alpha waves can also be detected during brief awakenings from sleep, known as arousals, and during REM sleep. This activity reduces as stage N1 sleep begins. Near the transition from stage N1 to stage N2 sleep, vertex sharp waves—high-amplitude negative waves with a brief duration (upward deflection on EEG tracings)—occur; these are more apparent in central EEG tracings than occipital ones. A sharp wave is characterized by a deflection lasting between 70 and 200 milliseconds.

Sleep spindles are oscillations of 12 to 14 Hz and 0.5 to 1.5 seconds in duration and are representative of the N2 sleep state. They may continue into stage N3, but are typically absent from REM. The K complex is a high-amplitude, biphasic wave with a minimum duration of 0.5 seconds. Traditionally, a K complex consists of an initial abrupt negative voltage (by convention, an upward deflection) followed by a positive deflection (down) slow wave. K complexes are typically overlaid with spindles. Sharp waves are smaller, monophasic, and often have a lower amplitude than K complexes.

As sleep deepens, broad, high-amplitude delta waves occur. For sleep

staging purposes, delta slow-wave activity is defined as waves slower than 2 Hz (longer than 0.5-second length) with a peak-to-peak amplitude of larger than 75 μV. If stage N3 is present, the amount of slow-wave activity as determined by central EEG derivations (see below). Because a K complex resembles slow-wave activity, it might be difficult to distinguish between the two. Nevertheless, a K complex should distinguish itself from the low-amplitude, background EEG activity and therefore, a continuous series of high-voltage slow (HVS) waves is not a succession of K complexes. During REM sleep, sawtooth waves that have a frequency in the theta range (3 to 7 Hz), may be present. Although they are not included in the scoring criteria for REM sleep, their presence is indicative of its presence.

Eye Movement During Sleep

EOG is a physiological signal that detects and measures eye movements (through the eyelid) by measuring the corneo-retinal distance between the front and back of the eye. This is done by placing two electrodes on both sides of the eye, either the right and left, or front and back, and measuring the potential difference between them, which would vary as the eye moves. For Fascia, this is used to detect what stage of sleep the patient is in. REM is an acronym for rapid eye movement, so it is possible to determine that the patient is in REM by detecting random and rapid eye movement. Eye movement tracking serves mostly to identify REM sleep. In order to detect both vertical and horizontal eye movements, an electrode is positioned slightly above and below the eyes [164]. Electrodes for EOG (eye movement) are commonly positioned at the outside corners of the eyes, at the right outer canthus (ROC) and the left outer canthus (LOC). Commonly, two eye channels are recorded, with eye electrodes referred to the opposing mastoid (ROC-A1 and LOC-A2), however some sleep centers utilize the same mastoid reference electrode (ROC-A1 and LOC-A1). Eye movements can be recorded due to a potential difference across the eyeball: front positive (+), back negative (-). Voltage fluctuations are discovered through EOG recordings of eye movements: when the eyeballs travel toward an electrode, a voltage is recorded as positive. By convention, polygraphs are calibrated so that a negative voltage results in a pen deflection to the right (negative polarity up). Consequently, eye movement toward an electrode causes a downward deflection. Note that eye movement is typically conjugate, with both eyes moving toward one

eye electrode while moving away from the other. Eye movements cause out-of-phase deflections in the two eye tracings if the eye channels are calibrated with the same polarity settings (e.g., one up and one down). As ROC is above the eyes and LOC is below, upward eye movements are directed toward ROC and away from LOC. Consequently, an upward eye movement causes a downward deflection in the ROC trace and an upward deflection in the LOC trace.

Muscle Movement During Sleep

EMG is performed to evaluate the healthiness of muscles and the associated motor neurons (nerves that control those muscles). The motor neurons transmit signals to the muscles that cause muscles to either contract or relax. The electrical measurement of such a signal is called EMG. Monitoring and studying the EMG signal can allow doctors to detect muscle and nerve disorders. For this application, EMG variance can be used to assess sleep behaviors in terms of muscle movements around the body. The Fascia device specifically focuses on the cheek, forehead, and chin EMG signals.

Common locations for EMG recordings include the submental muscles and the anterior tibialis muscles of both legs. When a movement disturbance is suspected, however, an EMG may be recorded from the affected area; for instance, the masseter muscles in bruxism or the arms in REM sleep behavior disorder. This thesis began with a discussion of electromyography (EMG), which is a method for recording the collective electrical activity of the body's underlying muscles. There is always some level of muscle tone present, even when the body is at rest. Myocytes, then, continue to exist in a state where they are only half contracted. Myocyte contraction is induced by an alteration in the electrical potential, thus, the EMG channels show activity even when the body is at rest. During a muscular contraction, the motor units (a group of myocytes innervated by a single nerve fiber) are recruited and the firing rate of the nerve fibers supplying the myocytes increases. However, because of the unpredictability of the recruitment process, the signal is not synchronized. The amplitude of the EMG signal drops as sleep begins because of a decrease in basal tone. Because of the substantial physiological atonia that occurs during REM sleep, EMG signals weaken significantly. Muscle signals are most effective when they go the shortest distance possible to the surface from whence they originated. Subcutaneous fat, however,

extends the separations, reducing the strength of the signals.

Heart Rate During Sleep

Unlike the previous signal, the measuring of this signal of interest is not different than your standard heart rate monitor.
PSG uses a type of sensor which is an optically detected plethysmogram, used to measure the volume of blood going through the veins under the skin. This is often done by shining a light on the skin and measuring variations in light absorption. Because the volume of blood changes as the heart pumps it to the periphery, this enables the measurement of the measure heart rate.
The PSG sensor has been found to provide reliable readings of resting heart rate, as measured over standard time intervals of a few seconds [167]. Furthermore, the PPG signal can be analyzed to determine the intervals between heartbeats, allowing for the potential measurement of Heart Rate Variability (HRV) overnight. HRV, an expression of the ANS and its sympathetic and parasympathetic branches, has been extensively linked to different stages of sleep.
An ECG represents the sum of the heart's electrical activity during the pumping process. The heart contains its own conduction system beneath the endocardium: impulses generated in the sino-atrial (SA) node travel to the atrioventricular (AV) node and subsequently to the ventricles via the heart's specialized conduction system. When the conduction system is activated, changes similar to those that occur in skeletal muscles result in contraction and relaxation. There are two atriums and two ventricles in the heart which do not jointly contract. First, the conduction system depolarizes the atria (while the ventricles maintain their resting membrane potential), and a few seconds later, a depolarization wave travels to the ventricles (at which point the atria have reached their resting membrane potential). When the atria depolarize, their outer surface becomes positively charged compared to that of the ventricles. As a result, a dipole is formed and current flows from the right side to the left side (because ventricles are on the left side relative to atria) and also from the back of the chest to the front (because atria are close to the back while ventricles are closer to the anterior chest wall). During an ECG, surface electrodes can detect a dipole caused by a localized shift in the membrane potential of one half of the heart relative to the other. This dipole is constantly changing in time. The orientation of ECG waveforms

is determined by the lead used. For instance, a bipolar lead connects to the right arm and the left arm, with the negative pole of the channel on the right and the positive pole on the left. Since the heart's current flows from right to left, it will produce a positive deflection in this lead, which will be noticed as the first part of the P wave on the ECG. The second half of the P wave indicates that action potentials are returning to the resting membrane potential in the atrial muscles. QRS complex and T waves are formed in this manner due to the shifting dipoles in the heart.

Respiration During Sleep

Typically, a pressure transducer and a thermocouple or thermistor are used to record airflow data. Two metals (in the case of a thermocouple or thermistor) expand and contract in response to changes in temperature Figure 7-1. For those who breathe through their noses and mouths, incoming air is cooler than outgoing air. These metals' signal-generating properties shift as their temperature does. Apnea, in which airflow is blocked in the oro-nasal route, can be detected by these monitors because of their sensitivity to temperature changes. Some airflow persists even during hypopnea and airflow limitation, as seen in upper airway resistance syndrome, resulting in temperature changes and a signal that is typically of the same magnitude as a normal breath. In a nutshell, thermistors and thermocouples cannot detect hypopneas and flow limitations Figure 7-1. A piezoelectric detector receives information about changes in air column pressure via a pressure transducer and converts that data into an electrical signal. The principle of piezoelectricity is the foundation of piezoelectric sensors. There are some substances (like quartz) that can generate an electric charge when subjected to pressure. Piezoelectric sensors generate an electrical signal that is directly proportional to the pressure applied, therefore its output waveform is in tune with the intensity of breathing. It is because of this that pressure transducers are the best devices for monitoring airflow restrictions.

Plethysmography is another technique used to monitor the expansion and contraction of the lungs when a person breathes in and out. Chest and abdominal movement recordings help to distinguish between obstructive and central sleep apnea. Given the differences in their etiology and treatment, this is crucial information to have. Belts are connected across the chest and the abdomen to track the torso's movement; the chest and the abdominal area both enlarge with inspiration and contract

with exhalation. As with the lungs, belts encircling the chest and belly tighten with each inhale and loosen with each exhale. Nylon elastic belts are equipped with a tiny sensor at each end and keep track of this data. A piezoelectric strain gauge, the simplest sort of sensor, generates electricity whenever there is a change in strain in the belts due to the breathing movement. Although useful, strain gauge sensors do have some significant drawbacks. Sometimes the belt's range of motion is constrained by the user's body, and this might result in inaccurate readings from the sensor due to improper pressure being applied to the belt. Furthermore, due to the non-linear nature of the piezo technology's output signal, it is unable to be employed for hypopnea evaluation. Also, if the patient moves about while wearing the belt, the tension on the piezo technology can provide a false paradoxical breathing signal. To get over this problem, an alternative technology based on inductance was developed and implemented. According to Faraday's law, a magnetic field is generated whenever a current flows through a closed loop of wire. Any change in the circumference of this loop causes an equal and opposite current to flow in the opposite direction (Lenz's law).

Non-physiological Signals Used During Sleep Tests

Body Movement Due to the sleep-dependent nature of Sleep-Disordered Breathing (SDB), it is crucial to keep track of the patient's body posture throughout the PSG. Changes in SDB in supine, lateral, and prone positions can be captured by monitoring body position, allowing the technician to precisely assess the genuine severity and appropriate PAP dosage. A gyroscope inside the body position sensor can pinpoint the user's exact location. It has separate signals for the right side, the left side, supine, prone, and upside down positions of the body. It is crucial to ensure that the body position sensor is oriented properly on the patient because the sensor records its own position rather than the patient's.

Audio Data Signals captured by the microphone are transmitted to the computer, where they are displayed as waveforms. These waves change in amplitude and period in response to the loudness and duration of snoring (or any other sound produced in close proximity to the probe). This means that any vocalizations or teeth grinding that occur during sleep will also be recorded. Some labs use a microphone near the head of the bed in addition to the sensor put on the larynx to record a wide variety

of audible signals. This is useful for interacting with the patient during the study if necessary and also adds to the visual data collected while the patient was sleeping. Due to their importance in situations of sleep seizures and parasomnias, microphone signals are synchronized with video recording and other data. If the signal from the cannula airflow sensor is unfiltered, the snoring signal can be seen superimposed on the airflow waveform signal, which is recorded when snoring is captured through nasal pressure cannula.

Video Data The majority of sleep centers that handle suspected sleep-related seizure and parasomnia patients also collect video footage that is time-stamped alongside other channels. As darkness is necessary for sleep, the camera emits infrared light, and its sensors pick up the reflected infrared signals. Through the use of specialized software, the camera's focus and orientation can be adjusted from the control room. By making these adjustments, a sleep technologist can capture even the smallest of sleep-related movements.

7.3 Related Work

The main challenges with conventional sleep studies are twofold: the patient's comfort, and the accuracy of the collected data, given the context in which the patient sleep. At the time of this research, there are two existing products in the market that tackle those issues.
First is a product called Neuroon Open, which is marketed as a sleep enhancing wearable device. This is an IoT product whose selling point is helping customers improve the quality of their sleep through EEG monitoring and lucid dreaming induction, as well as smart meditation sessions. This is achieved by allowing the IoT device control of the lighting, music, and temperature in the bedroom of the customer, which the device adjusts in accordance with what the customer needs are based on the sleep stage they are in. This device is mainly aimed at helping an individual sleep better by monitoring brain waves, and less at helping researchers study sleep in order to diagnose patients with potential sleep disorders or to better understand sleep in general. Therefore, the use-case for this product is limited to helping the customer sleep more soundly, and is thus much narrower than the goal of the Fascia project.
Second is a product called the Muse Headband. Muse monitors mental

activity and uses it to produce "guiding" nature sounds to help the user reach a mental state of what they call a "focused calm." Muse selects different sounds to represent different states of mind: if the subject is calm, it plays peaceful weather sounds, and as the customer starts to get more distracted or busy-minded, it starts to play more stormy and loud weather sounds to cue the user to focus their attention back to their meditation routine. Muse is also mostly limited to the use of EEG sensing to help guide users through immersive meditation sessions. Some iterations of the product include PPG sensors, as well as a gyroscope and accelerometers, although all of these added sensors are used to optimize the same functionality: helping the user to calm their mind.

Both of these products roughly satisfy the form factor for this project, but they lack the ability to sense many of the signals that the Fascia ecosystem aims to encompass with a design that supports medical and scientific sleep research.

7.4 Fascia Ecosystem

The Fascia Ecosystem provides a comprehensive solution for at-home sleep monitoring and analysis, allowing researchers to collect and analyze high-quality sleep data remotely. The Fascia Sleep Mask, with its advanced fabric-based sensors, enables the collection of polysomnogram-like data during sleep, providing accurate measurements of various physiological signals. The Fascia Hub offers real-time treatments and feedback, thereby enhancing the overall understanding of sleep patterns and improving the quality of sleep research.

The Fascia Portal is an integral component of the Fascia Ecosystem, enabling researchers to manage, store, and analyze data collected using the Fascia Sleep Mask. Researchers can monitor patient signals in real-time and utilize a machine learning API for accurate identification of sleep stages, spindles, and slow-waves. This platform provides a robust mechanism for the analysis of sleep patterns, leading to improved diagnosis and treatment of sleep disorders.

The upcoming sections of this chapter aim to provide a comprehensive understanding of the interdependence and collaboration among the various components of the Fascia ecosystem. This exploration will highlight how the Fascia Sleep Mask, Fascia Hub, Fascia Portal, and machine learning API are integrated to enable effective collection, analysis, and

interpretation of sleep data. By examining the intricate functioning of these components, researchers and clinicians can enhance their understanding of sleep patterns and improve the diagnosis and treatment of sleep disorders.

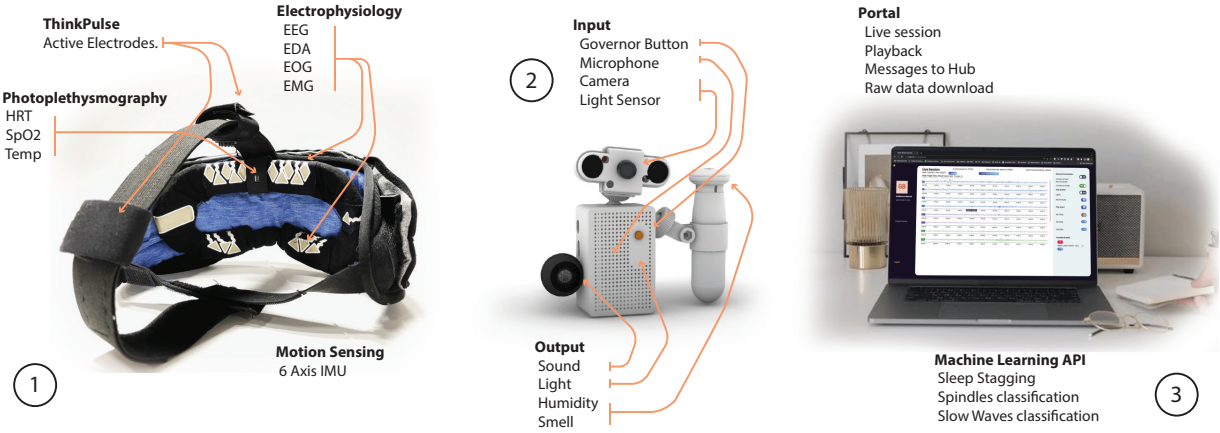

Figure 7-5: Components of the Fascia Ecosystem. **1** One of the Fascia sleep mask prototypes with legends for the different sensing modalities. **2** The Fascia Hub with legends for the different sensing modalities. **3** Image of the user's laptop using the Fascia portal web interface

7.5 System Design

MQTT Protocol

MQTT is an Internet of Things/machine-to-machine (M2M) connection protocol. It was created as a lightweight publish/subscribe messaging transport. It is beneficial for connections with faraway places that require a minimal code footprint and/or have limited network bandwidth. MQTT was created by Dr. Andy Stanford-Clark of IBM and Arlen Nipper of Arcom (now Eurotech) in 1999 [168]. The primary functional basis of MQTT is the existence of topics in a broker-like entity. When a client subscribes to or publishes on a particular topic, the broker registers that topic. A single client can subscribe several times to different topics, and multiple clients can subscribe to the same topic. The same holds true for publishers. Therefore, clients who subscribe to topic X will receive all messages published under that subject [169]. As stated on the website of one of the various brokers, Mosquitto, the broker and MQTT provide a simple, universal interface to which everything can connect[170].

Patients at St. Jude Medical Center who are carrying pacemakers or cardioverter defibrillators can now be monitored continuously from the comfort of their own homes thanks to a device that was developed by IBM. In order to accomplish this goal, a specialized device known as

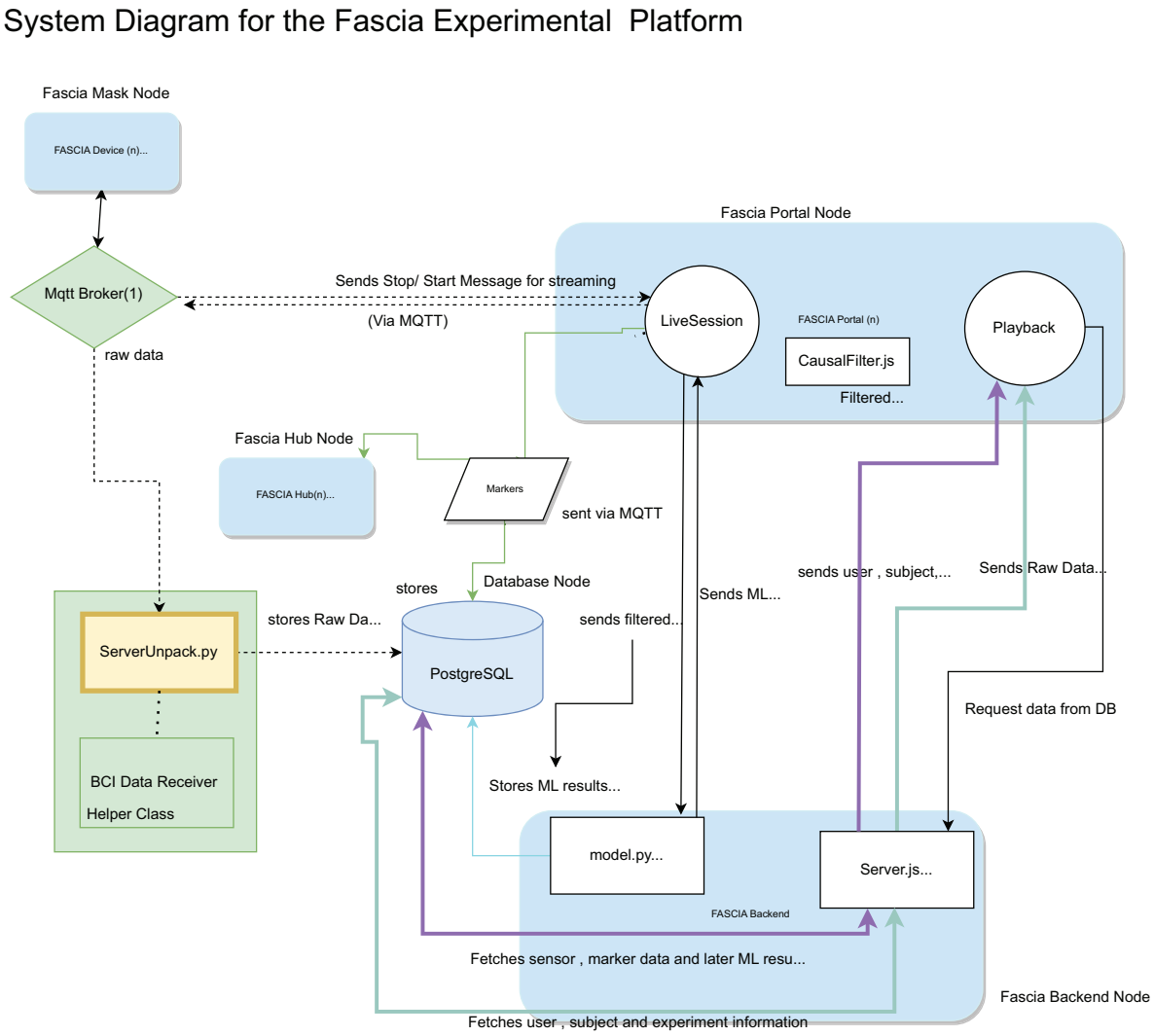

Figure 7-6: System diagram depicting major nodes and data flow for the Fascia ecosystem.

Merlin@home is attached to the various healthcare devices that are being discussed. When an unusual event occurs, this device sends a signal and the relevant data to the medical center [10]. This enables not only a higher level of patient care and early detection of problems, but also enhanced administrative efficiency and maintenance, assistance in conforming to standards, and simple integration of data [171]. Additionally, this enables a higher degree of administrative efficiency. There are around 100,000 heart pacemakers being monitored through MQTT at St. Jude, according to the Software part of the official MQTT website [172]. Although our project's structure can be compared to the one described in IBM's Red Book Building Smarter Planet Solutions with MQTT and IBM WebSphere MQ Telemetry [173], the fact that there were not discovered to be more actual uses of MQTT in health made it innovative and demanding.

7.5.1 Fascia Mask Node

The firmware, after gathering and processing all the sensor data from the Fascia Mask, packs the collected data and sends it to an MQTT broker running on a server over WiFi. On the server, there is a Python script that unpacks data and timestamps the data before inserting it into the PostgreSQL database.

Data Unpack

All the aforementioned data and signals need to be combined into the WiFi packet to be sent over to the software. A full data packet has four EEG data points, three EMG data points, one EOG data point, three acceleration data points, three gyroscope data points, one EDA data point, one heart data point, one temperature data point, one serial number, one valid array, and one time stamp, for a total of 20 data points in the order shown in the table below. The number and sizes of all the elements total to 68 bytes for the whole packet.
It is worth noting here that the IMU data, all six data points, are currently only two bytes each because the conversion has not been deemed as necessary. However, if the conversion is to be performed and the converted data is to be packed into the data packet instead, each of the IMU data points would be four bytes instead of two, which would increase the total size of the packet by 12 bytes, making it 80 bytes in total instead of 68.

Table 7.2: Package structure for the sleep mask

Sequential order	Signal	Size(Bytes)	starting byte
1	Serial packet number	4	0
2	Valid array	4	4
3	EEG	4	8
4	EEG	4	12
5	EEG	4	16
6	EEG	4	20
7	EMG	4	24
8	EMG	4	28
9	EOG	4	32
10	EOG	4	36
11	Acceleration x	4	40
12	Acceleration y	4	42
13	Acceleration z	4	44
14	Gyroscope x	4	46
15	Gyroscope y	4	48
16	Gyroscope z	4	50
17	EDA	4	52
18	Skin temperature	4	56
19	Heart rate	4	60
20	Time stamp	4	64

Due to the fact that not all data is collected at the same (highest) rate, there are some packets for which the only legitimate data is the ADS1299 data, together with the serial packet number and time stamps. Some data is transmitted less frequently and is consequently usually invalid because it was not captured. Some data is actually invalid due to a system error, such as an ADS1299 detecting a lead-off, or a MAX30101 indicating a lack of secure patient connection. For these reasons, a component of the packet known as the valid array, which can be seen as an array of bits, was introduced. One bit is assigned to each item in the packet: if the bit that corresponds to a particular element is set to one, then that data point is invalid. If the element is set to zero, it is determined to be valid.

Calling it a valid array might be a misnomer then, since it could be an invalid array if a data element is returned as 1. When naming this array, the decision was made not to call it an "invalid array" in order to combat the potential confusion of the data that the element contains being invalid (it is the array which is invalid itself). As described, this array can be used to figure out which data points were collected in this packet and should be kept, processed, stored, graphed, filtered, etc., and which ones were not.

Every time a new packet is created, the field for the valid array is initialized to zero. Whether the signals are received and inserted into the packet or not, this array is updated. If a certain signal is not to be collected at this time and this packet will not be updated with it, then the valid array is updated with a one-set in the index corresponding to that data point, marking that signal invalid in this packet. Also, if a sensor reports that the probe for one or more of its inputs no longer has a good connection to the patient's body, the signal from that device for that data point is thrown away, and the valid array is changed to reflect this by setting the bit for that device's specific channel to one.

WiFi Packet Send Rate

In order to increase the system's efficiency, multiple packets of data are collected and grouped together into one WiFi packet to send over to the software. This method allows for the cost of preparing, sending, and receiving a WiFi packet through the network to be amortized over the number of data packets it contains. This aggregate WiFi packet, in the current system, contains 20 data packets. This was a number that is maximized, given the number of data points in the data packet, and

therefore a data packet's size in bytes, to the size limit of the WiFi packet library appears to be able to support. This number was bigger when the data packet size was smaller and has needed adjustment as the data packet size grew.

7.5.2 Fascia Portal Node

The Fascia Portal node is where most of the signal streams come together for the user to interact with the signals. The Fascia Portal has multiple functions, and Chapter 10 goes into more detail. The portal provides three primary functionalities to the Fascia Ecosystem. First, it serves as a front-facing website for people to learn about the project. The second function is registration and authentication for the portal users. This allows for the data to be kept private and management of who has access to the system. The last function is the portal dashboard where the user can create experiments, add users, record data, observe data in real-time, and view the playback, where the data can be replayed once the recording session has concluded.

The live session segment of the portal at the system level can be described as a dashboard to send commands to the Fascia Mask and Hub via MQTT topics. It can also be described as a visualization tool for the incoming data stream sent by the Fascia Mask. The live session is responsible for unpacking the data packets received and restructuring the data so it can be filtered and ready to be visualized. The live session also communicates to the sleep staging API.

The playback segment as mentioned before allows sleep researchers to explore and replay the sleep recordings. The Portal Node requests data from the Fascia Server, the server then goes and fetches the data from the database storage for the desired recorded session.

7.5.3 Fascia Hub Node

The Fascia Hub enables a researcher or scientist to provide stimulation and feedback to a patient in the form of audio and visual stimuli, expanding the possibilities for understanding sleep and dreams, and the ability to issue interventions.

The Hub operates a Python-based client that monitors the portal for MQTT messages. After the portal has established a connection, the Hub applies a decision tree to the incoming message. When a video or audio

recording is created, a file is generated locally and then sent to the database.

7.5.4 Database Node

In cloud-based sensor data applications, the number of data points is frequently in the trillions. How should such enormous data be processed? How can we perform streaming data processing in real time while at the same time having a service that can store records and allow data playback? Fascia's goal of enabling researchers to store physiological data, perform experiments with demographic records and consent forms, review any triggers, analyze, and store data creates a challenging backend design.

Since physiological data has a well-defined structure, follows a data model, and stays in the same order, it was clear that a SQL-based storage system was appropriate, which provides consistent and low-latency read and write performance. PostgreSQL was chosen for the database because it has been utilized for stream processing in IoT applications to process trillions of data records per day in real-time. PostgreSQL is a good product for stream-based data processing, with the potential to process up to 100,000 records per second in real time on a single standard X86 server.

The Fascia database is primarily utilized for cold storage; when the Fascia mask receives a run command from the Fascia Portal, new data is injected into the system. When events are sent to the hub through the portal, markers are added. When the user uses the playback option or decides to download their data, stored data is retrieved from the database. All the physiological data is stored in one table as they were almost always recorded and used together, making it easy to deploy them in one logical table. A primary key index was introduced because while information from the board like packet number and timestamp might be unique to the board, it is not the case globally as there might be more than one board streaming information at the same time.

To further optimize the read times, the table was indexed based on its unique session ID and packet number. This was done because most of the queries query information for a particular session, and to process the data in batches, the data is divided into smaller batches that are identifiable using packet numbers. Thus, the indices improve the performance.

7.6 Discussion

In conclusion, the Fascia Ecosystem represents a major step forward in the field of sleep studies. The combination of the Sleep Mask, Hub, and Portal allow for a more comprehensive and convenient approach to understanding sleep and diagnosing sleep disorders. With the ability to collect data similar to a traditional polysomnogram, offer patient stimulation and feedback, and analyze sleep signals in real-time, the Fascia Ecosystem opens up new avenues for research and advances in sleep medicine. Additionally, the machine learning API and data collection platform provide a powerful tool for further developing our understanding of sleep and improving sleep diagnostics. This innovative approach to sleep studies holds great promise for improving the diagnosis and treatment of sleep disorders and improving overall sleep health.
The next sections of this thesis will focus on a more detail exploration for each one of the main components of the Fascia Ecosystem. The next focused on the Fascia Sleep Mask in more detail and discuss its potential as a home-based polysomnogram device for sleep studies.

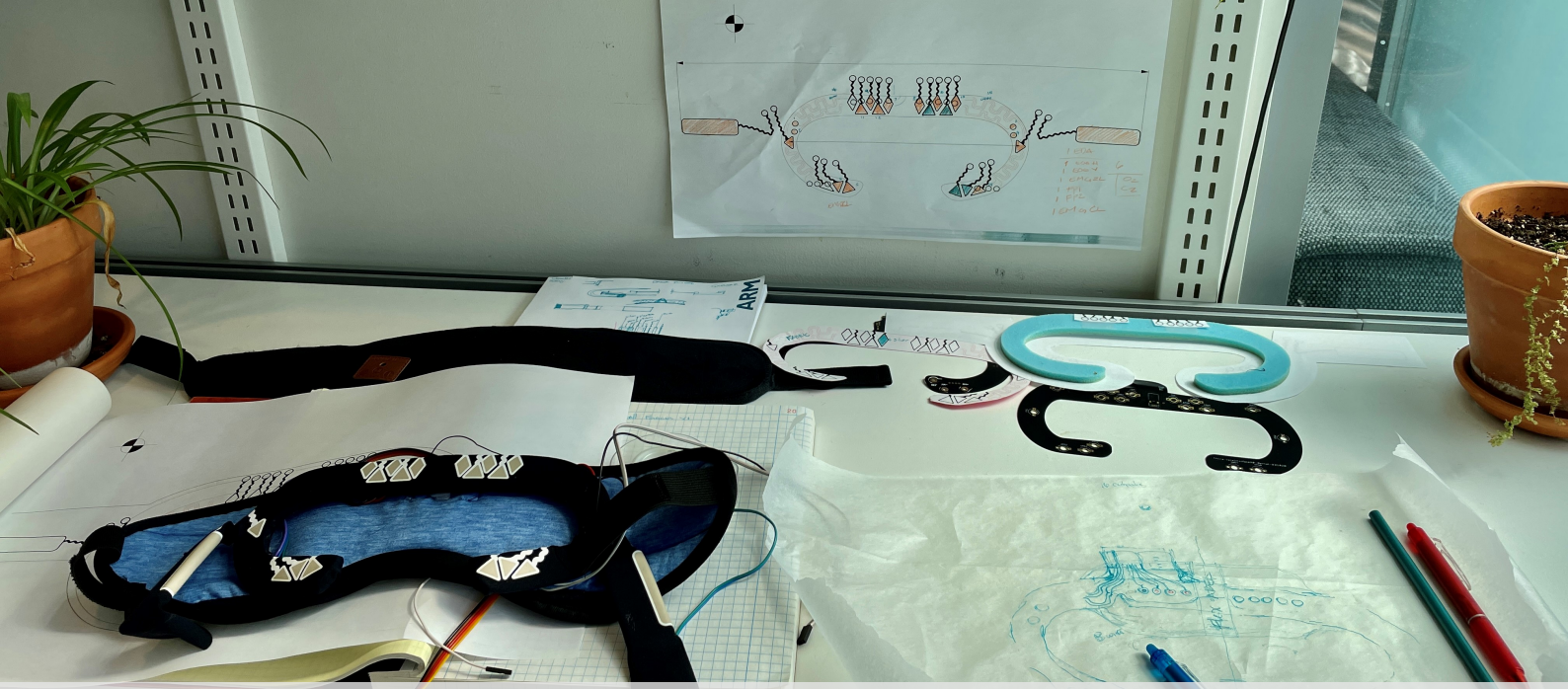

8 Fascia Mask

8.1 Introduction

Sleep studies have largely been viewed as a nuisance for the subjects being studied. This is due to the major discomfort caused when the subject must go into a research center or hospital and sleep there while their vitals and different physiological signals are constantly monitored by bulky equipment. In order to detect these signals, a variety of electrodes and sensors are distributed across the head and the rest of the body, and secured using tape or glue, and therefore cause significant discomfort. Centers assure patients that they'll "still have plenty of room to move and get comfortable" and that they are being monitored by sleep study technologists who "can help if they need to use the bathroom". Still, according to the National Sleep Foundation, many people wonder how they will be able to sleep under such conditions. Researchers believe this setup and procedure result in inaccurate or at least inconsistent data as the subjects are not sleeping as they normally would in the comfort of their home, free of unfamiliar wires and electrodes probing their bodies. Home-based portable devices may provide a solution to these problems; nevertheless, these devices are, at best, insufficient because of the limited number of biophysical channels that they are able to capture.

That is where the Fascia Mask comes in. With the previous insights in mind, this project aims to tackle the challenges noted above by creating a comfortable and minimal device which houses all the required sensors

and electrodes to record the vitals and signals needed for sleep studies. The device takes the form of a sleep mask, which consists of a flexible printed circuit board with integrated electrodes and sensors that are close to the skin, and two conventional PCBs to house the components that perform the signal processing, data analysis, signal forwarding and storage farther away from the skin. The resulting mask can be taken home, enabling sleep studies to be conducted “in the wild".

8.2 Background

Conventional sleep studies have two primary obstacles: the patient’s comfort and the accuracy of the obtained data, given the environment in which the patient sleeps. We are aware of three products that are comparable to the Fascia Mask on the market that address these concerns.
First, a product called Neuroon Open, which is touted as a wearable device that improves sleep. The selling point of this IoT device is its ability to assist clients enhance the quality of their sleep through EEG monitoring, lucid dream induction, and intelligent meditation sessions. This is accomplished by allowing the IoT device to manage the lighting, music, and temperature in the customer’s bedroom, which the device adjusts according to the customer’s demands based on their current sleep stage [174]. This gadget is primarily intended to help an individual sleep better by monitoring brain waves, as opposed to assisting sleep researchers in diagnosing people with suspected sleep disorders and gaining a better understanding of sleep in general. Consequently, the use-case for this product is limited to assisting the consumer in sleeping more soundly, which is far narrower than the project’s objective.
The second product is the Muse Headband. Muse detects mental activity and uses it to generate "guiding" nature sounds in order to help the user achieve a mental state described as "focused calm." Muse selects different sounds to reflect different states of mind: if the subject is tranquil, it plays peaceful weather sounds; if the user becomes more distracted or busy-minded, it plays increasingly stormy and loud weather sounds to remind them to return to their meditation practice. Muse’s use of EEG sensing to guide consumers through immersive meditation sessions is similarly mostly restricted. Some variants of the product feature PPG sensors, as well as a gyroscope and accelerometers, although all of these additional sensors are utilized to maximize the same functionality: assisting the

user to relax [175].

Thirdly, the DREEM headband is a further consumer product for sleep recording and the one that most closely resembles the signals supplied by the Fascia Mask. The gadget incorporates five dry EEG electrodes, a 3-D accelerometer, and a pulse oximeter. Despite the fact that DREEM is designed for sleep research, it has been stated that it is not very comfortable for sleep [176].

All of these devices approximate the form factor for the Fascia project, but they lack the ability to detect a large number of the signals that this project intends to include in a design that supports medical and scientific sleep research. Few of these device manufacturers have released their performance relative to PSG, and those who have often only report aggregated metrics as opposed to raw data, and do not allow open access to the data set so that results can be independently checked.

8.3 Fascia Mask Design

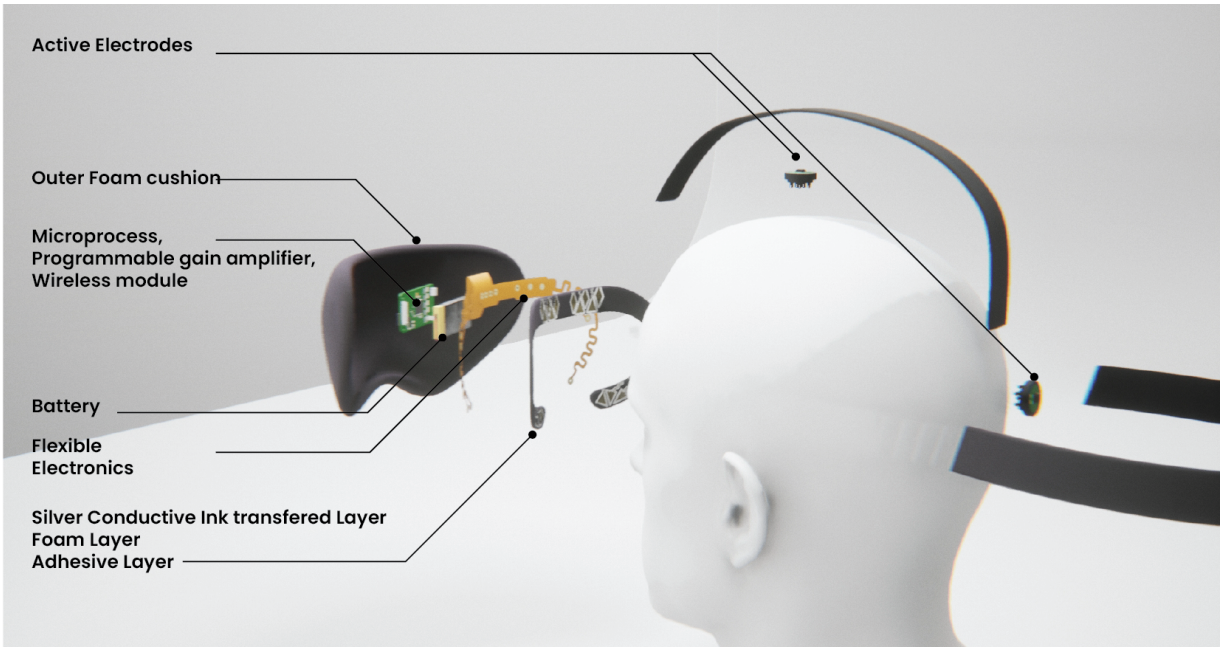

Figure 8-1: Exploded view, showing the main components on the Fascia sleep mask

The physical form of the device was designed with a minimal footprint so as to be the least intrusive as possible, to enable the user to be as comfortable as possible, and the data to be as accurate and error-free as possible. This resulted in the selection of the sleep mask as the form of the device. This form factor would allow for the collection of all the data points that a full PSG system collects, while meeting the minimal

footprint requirement.
A flexible PCB design was used to maximize user comfort while meeting the flexibility needs of the sensors and electrodes. Other considerations included placement of the electrodes on the face region and electrodes on the strap. The main purpose of the flexible PCB is to be a conductor between the conductive transfer layer and the sensor PCB board. The sensor PCB is the module in charge of wirelessly transmitting the signal collected by the programmable amplifier. By screen-printing silver ink onto a fabric, the outer layer of the fabric acts as a grid of electrodes that pick up signals like EOG, EMG, EEG, and EDA. According to the American Academy of Sleep Medicine, the recommended EEG electrode positioning involves three measurements covering the frontal, central, and occipital regions. Using the 10-20 international system, the electrodes on the midline strap are put on the Cz and Pz areas.

8.4 Hardware Design

There are two main components to the Fascia Mask hardware: a main sensor PCB, and an ergo-electronics face pad. The main sensor PCB is an analog front end that collects bio-potential signals from the brain, muscle signas, eye movements, skin response, heart rate, skin temperature, and respiration. These signals are then processed and wirelessly streamed using the MQTT protocol to a remote broker. The ergo-electronics face-pad is a flexible PCB with gold-plated pickup electrodes that connects to an electrode array that is screen-printed onto a breathable fabric. This fabric is then wrapped around a cushion to create the comfortable face pad and connected to the flexible PCB mechanically using grommets. Figure 8-2

8.4.1 Hardware Description

With the goal of making the user as comfortable as possible and the data as accurate, noise-free, and error-free as feasible, the device's physical form was settled upon with the smallest possible footprint. As a result, a sleep mask, a special garment worn solely when sleeping, was chosen as the shape of the device. A flexible PCB layout was used for the electrode-based sensors for improved user comfort.
Protection for the main PCBs comes in the form of a 3D-printed case, foam padding, and cloth, and it rests on the temple region of the forehead

whether you sleep on your side or back. Each printed circuit board (PCB) had its footprint shrunk so it would fit within a sleep mask, improving the wearer's convenience.

8.4.2 Signals of Interest

Polysomnography records brain waves, the oxygen level in the blood, heart rate and breathing, and eye and leg movements during the sleep study.

In order to conduct polysomnography (sleep studies), technologists typically place sensors on the patient's scalp, temples, chest, and legs, as well as a clip on the finger, all of which are connected by wires to a computer. These are used in preparation to monitor the following signals: brain waves, eye movements, heart rate, breathing pattern, blood oxygen level, body position, chest and abdominal movement, limb movement, and snoring.

In the sections that follow, the role of each of the aforementioned "signals of interest" in the construction and placement of the Fascia sleep mask will be detailed.

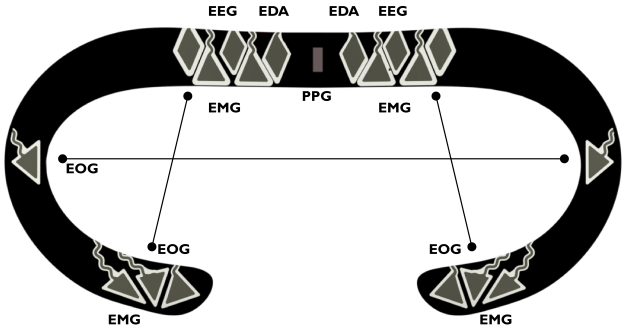

Figure 8-2: System diagram depicting the electrode array for the sleep mask

EEG/EMG/EOG Sensing

The ADS1299, a device from Texas Instruments designed for collecting and measuring biological signals, was used to record all three signals (EEG, EMG, and EOG) in a single hardware unit. This is the most expensive part of our setup, but it's also the most powerful, allowing us to measure eight distinct biopotential signal channels at once with separate gains (1, 2, 4, 6, 8, 12, 24) and operating modes. Each channel can be connected to a positive (P) and a negative (N) lead, and a single

"bias" probe can be used as a signal reference for an unlimited number of channels. It also employs a Right-Leg-Drive (RLD or DRL, for Driven-Right-Leg) circuit that detects "common-mode interference," or noise in the body that could interfere with the signals of interest, and then uses an operational amplifier (op-amp) to subtract the noisy signals from the bio-signals of interest. Connecting the SRB2 for the desired channel enables the capability. The chip's internal circuit is highly configurable, making it possible to determine whether or not the probes and leads are loose or otherwise incorrectly attached to the human body in the face of erroneous biosignals. This function is known as "lead-off detection." This device supports both the I2C and SPI bus types, however we're only using SPI for this application. The device offers both a "continuous conversion" mode, in which it pulls an interrupt pin low when the data is ready, and a "single shot" mode, in which you poll the device for data. Fascia is currently using the continuous conversion mode to ensure the data sampling is done consistently.

Two EOG channels, two EMG channels, and four EEG channels are being used from the ADS1299. In order to measure the potential across a muscle, each EOG and EMG channel makes use of two leads, the positive and negative probes of a channel, which are linked to opposite sides of a muscle. The ADS1299 uses this configuration, known as a sequential montage, to assess the potential difference between the two electrodes that should be positioned across a muscle. Due to their rather large magnitudes, we utilize a gain of 2 or 4 for each of these channels.

For EEG, we just use one channel probe (either positive or negative) and attach the other to the bias probe, measuring the EEG signal relative to a single reference electrode. Due to their significantly lower magnitude compared to other biopotential signals, EEGs benefit greatly from the use of a reference montage to remove noise and clean up. Since the EEG signals are so small, we also employ higher gains of 12 or 24 for these electrodes. We additionally link these channels to SRB2 to make use of the RLD circuit's noise-cancelling capabilities for particularly delicate and weak communications. We employ both passive (like those used for EMG and EOG) and active electrodes to detect EEG, with the latter having in-built electronics to actively amplify the signal as it is sensed for increased precision. It is possible to utilize a gain of 1 for the channels formed by the active electrodes. To begin validating this setup, we first made use of a feature already present in the ADS1299: the

ability to internally generate test signals. This is another feature of the device in which it generates square waves internally at a configurable frequency and amplitude and feeds that signal to the test channels. This is a fantastic way to ensure that the chip's wiring, power levels, register settings, and data out package reception are all functioning properly during the initialization process.

EDA Sensing

The data for Electrodermal Activity (EDA) is collected through a built-in Analog-to-Digital Converter (ADC) on the Arduino platform, which allows for the value at the analog pin corresponding to the EDA data to be sampled and read at any time. The Arduino bootloader reads the analog signal at that pin, converts it to a digital value through the ADC, and returns it to the firmware code that called the analog-pin-reading function.

Given that EDA signals often have lower frequencies (ranging from 1 to 10 Hz) [177] and the data is fairly irregular and noisy, it is recommended to smooth the data by averaging a predetermined number of samples. In this case, it was determined that averaging every 10 EDA data samples to obtain one mean value, which was then used and sent in the data packet, was appropriate. This technique, known as oversampling and averaging [178], also increases the effective resolution of the ADC by allowing for non-integer averages.

However, the EDA measurement was slower than the firmware code for the ADS1299. To address this issue, it was decided to only sample the EDA signal at certain intervals. Sampling the EDA signal every 10 ADS1299 samples was found to be suitable. Additionally, the EDA signal would be sampled at fEDA = fADS1299/10/10 = fADS1299/100 with this methodology, assuming a minor conversion delay after adjusting the prescaler to 16.

The 12-bit ADC count value must then be translated into a practical unit. The most common method for assessing EDA is skin conductance (G) in micro-Siemens (S). The relationship between resistance (Rskin) in Ohms (W), the most direct value obtained by using the voltage level detected and stored by the ADC, and skin conductance (Gskin) is reciprocal. Therefore, the conversion is: Gskin = 1/Rskin [177]. To convert ADC counts to resistance, Rskin is the skin's resistance as measured between the two EDA probes placed on the human body. The voltage across Rskin

is calculated by translating the ADC counts to voltage, and then the current across Rskin is calculated by determining the voltage across the reference resistor Rref. Using these two pieces of information, Rskin is calculated as Vskin/I and skin conductance is calculated as the reciprocal of Rskin.

PPG

The MAX30101 sensor resides on its own rigid PCB that is attached to the flexible PCB in order to improve the quality of the data it transmits. This sensor is supplied with an interrupt pin that we do not utilize at this time (due to the choice that the ADS1299 will lead the data rate and set the frequency of signal collection), as well as two I2C lines that we use to communicate with the device.
The firmware utilizes the SparkFun Arduino library for the MAX30101 to access the data from the device. The library permits us to configure the sampling rate, the data averaging rate, and the power consumption level. Using the library's API, we can initialize the device with the following method call:
`particleSensor_name.setup(powerLevel, sampleAverage, ledMode,sampleRate, pulseWidth, adcRange).`
Then, using the `particleSensor name.getIR()` and `particleSensor-name.readTemperature()` functions, we can extract both PPG and temperature data from the device.
The MAX30101 was configured to have a high data rate, however, an obvious and significant decrease in the device's data collection rate was observed. As a result, an investigation was undertaken to determine the cause of this decrease. Upon further examination of the library's code used to communicate with the device, it was discovered that both the temperature retrieval and IR retrieval routines included a lengthy wait or delay. Specifically, the procedure for `readTemperature()` involved a register-write to request data, followed by a 100-millisecond delay while the device awaited a response to its request. Additionally, the `getIR()` function waited up to 250 milliseconds for fresh data to become available at the IR sensor output FIFO, and regularly checked for the presence of new data.
Consequently, the library was updated by removing the delays from both functions and examining the data they returned. It was observed that over fifty percent of the time, both of the functions returned that no data

was available. In light of this, the wait time was modified to a compromise value, and it was found that the majority of the data points were indeed accessible. The function signatures were also updated in order to improve efficiency based on the use case of the consumer code. For the `\readTemperature()` method, a new function, `\requestTemperature()`, was introduced, which makes the temperature reading request without waiting. Additionally, the `\readTemperature()` function was updated to simply check for the availability of a temperature reading without waiting. The `\getIR(wait ms)` function is a modified version of the `\getIR()` function that accepts as input the number of milliseconds the consumer wishes to wait for data to become available. In the firmware code, the sequence of calling functions was updated as well, first calling `\requestTemperature()`, then `\getIR(1)` (which was determined to be a suitable number, while still allowing for high precision in heart beats and waveform detection), and then calling `\readTemperature()`, indirectly introducing a wait in the temperature collection function. Additionally, the Sparkfun library collects PPG data and returns it as a 32-bit integer, despite the fact that the ADC range cannot be configured to values larger than a 16-bit integer. Since the PPG data units are not relevant to the current application, no further action was taken in this regard.

From this signal's structure, it is possible to detect heartbeats and calculate heart rates, so revealing any anomalies in the patient's cardiovascular system. In order to obtain correct data during PPG measurements, it is crucial to maintain excellent contact with the equipment. Fortunately, the MAX30101 is also a particle and proximity sensor, and once the finger (or palm, or, in our case, forehead) loses excellent contact with the sensor, it immediately changes to proximity sensing, which returns values that are orders of magnitude less than the PPG data. Thus, we can determine if the patient is in proper touch with the sensor and, consequently, if our data are reliable. The Temperature returned by the library method getTemperature() has the correct units, degrees Celsius, and is of type Float (four Bytes). Therefore, no processing is necessary for these data, as the library handles all conversions. Temperature change is a very slow process, and heart beat signals (ranging from 60 to 100 BPM for average resting heart rate in humans [179]) are relatively slow signals compared to the other vitals and biological signals being sensed by our system; therefore, we do not need to sample these signals as frequently as we sample the others. For this reason, we only sample this

data once for every ten times we sample the ADS1299 data, resulting in an effective data rate that is a tenth of the ADS1299's frequency for both the PPG and the temperature sensor. In actuality, the data rate for these signals is significantly less regular, and frequently slower. This is due to the decreased wait times in API services and the frequency of data availability (or lack thereof). This does not impact the quality of our data, since we are able to check the availability of the data and delete it when it is unavailable, but it does impact the practical sampling rate for certain signals.

Temperature

By measuring the temperature of the body, it is possible to deduce the stage and depth of sleep that the patient is in. Sleep stages are associated with temperature ranges, so drops and changes can be observed depending on the stage in the cycle.
The same device used to measure the heart rate is used to measure the skin temperature. It is placed on its own mini PCB board and connected to the rest of the system via a 4-pin JST connector, which connects the I2C and power lines to the board. This separation from the main and even secondary PCBs allows for the temperature sensor to provide more accurate representation of the patient's temperature, as it is not affected by any nearby hardware. Additionally, this separation enables the PPG sensor to produce data with reduced noise, as it uses a red, green and infrared LED to measure the pulses in blood flow in the veins. Furthermore, this separation ensures a more secure connection between the sensor and the patient's skin, acting as a probe on their forehead.

Motion sensing

Measuring the movements of the patients via gyroscopes, magnetometers, or accelerometers enables detection of muscle spasms, and whether the patient is tossing and turning. This data can be valuable for doctors to be able to diagnose certain sleep disorders.
The motion sensing unit used in this project is the MPU6050, which is a device that comprises a three-axis accelerometer and a three-axis gyroscope, and it communicates through the I2C protocol. It should be noted that this device lacks a magnetometer, which was initially considered as a limitation. However, after conducting research and reviewing relevant literature, it was determined that the accelerometer

and gyroscope would suffice for the types of analyses planned for the device in the context of sleep studies.

8.5 Python Data Receiver Portal

8.5.1 WiFi Packet Anatomy

Table 8.1: Table detailing the components of a data packet

Sequential order	Signal	Size (Bytes)	Byte at which it starts
1	Serial packet number	4	0
2	Valid array	4	4
3	EMG	4	8
4	EMG	4	12
5	EOG	4	16
6	EMG	4	20
7	EEG	4	24
8	EEG	4	28
9	EEG	4	32
10	EEG	4	36
11	Acceleration x	2	40
12	Acceleration y	2	42
13	Acceleration z	2	44
14	Gyroscope x	2	46
15	Gyroscope y	2	48
16	Gyroscope z	2	50
17	EDA	4	52
18	Temperature	4	56
19	PPG	4	60
20	Time stamp	4	64

All the signals needs to be combined into the WiFi packet to be sent over to the software. A full data packet has four EEG data points, two EMG data points, two EOG data point, three acceleration data points, three gyroscope data points, one EDA data point, one heart data point, one temperature data point, one serial number, one valid array, and one time stamp, for a total of 20 data points, in the order shown in the Packet Structure in Table 8.1. The number and sizes of all the elements total to 68 Bytes for the whole packet.

9 Fascia Hub

9.1 Introduction

This chapters provides a background discussion of in stimulation in sleep and describes how the hub operates it also describes the different modalities available to the sleep researcher so she can experiment with issuing interventions at specific moments in the sleep cycle.
Some interventions have have shown to benefit sleep quality, memory consolidation and more. These are just a few of the many areas where scientists are attempting to better understand the complex interactions between sleep and the rest of our lives in the hopes of improving our way of living.

9.2 Background

9.2.1 Sleep Interventions

Despite the fact that consciousness is diminished during sleep, some bodily systems are still responsive to environmental changes. During non-rapid eye movement sleep, for instance, the auditory system continues to assess environmental sounds by altering brain wave patterns, enhancing delta patterns, and enhancing sleep spindles [180]. Slow-wave synchronous acoustic stimulation has been shown to be a desired research area for their promising therapeutic implications [181]. Other senses, like haptics and vibration stimulation methods, have been used to deliver a stimulus to interact with the intrinsic heart rhythm and examine the effects of stimulation on sleep and memory [182].

Studies demonstrate that the human body is sensitive to ambient temperature during sleep; even mild exposure to heat or cold considerably impairs sleep quality. Thermoregulatory responses during sleep vary depending on sleep stage [183]. During REM sleep, the sensitivity to hot or cold stimuli is not fully suppressed, but it is lowered relative to NREM sleep. The rate of perspiration is lower in stages N1 and N2 of NREM than in SWS, and it is lowest in REM sleep [184], with reduced evaporative heat dissipation and heat tolerance [183]. These thermoregulatory properties render REM sleep more susceptible to temperature discomfort than other stages of sleep.

Olfactory interventions during sleep have been researched as strong cues to reactivate memories [185].Recent research findings support the idea that memory consolidation during sleep is crucial for actively preserving the memory bank that individuals carry throughout their lives. It is possible that the information that is ultimately retrievable is that which is reactivated during sleep. The discovery that neurocognitive processing during sleep can improve memory storage when memories are subtly prompted by auditory or olfactory stimulus is an unique source of support for this theory [186]. This combination of auditory and olfactory is also being explored to see if humans can learn new information during sleep. Using partial-reinforcement trace conditioning, Arzi et al. matched pleasant and unpleasant scents with various tones during sleep. They then assessed the sniff response to tones alone during the same night's sleep and subsequent wake. The researchers discovered that sleeping subjects formed unique links between tones and scents, causing them to sniff in response to tones alone. In addition, these newly learnt tone-induced sniffs varied according on the pleasantness of the odor previously connected with the tone during sleep. Without later recognition of the learning process, this learned habit remained throughout the night and upon awakening. Thus demonstrating the possibility for individuals to acquire new information during sleep [187].

Another exciting area that is exploring interventions while asleep is lucid dreaming and dream structure, where interventions are needed to better understand the dreamer's mental condition. Researchers Konkoly et al. show that people in rapid eye movement (REM) sleep can hear and respond to an experimenter's questions, allowing for an instantaneous dialogue about dreams. During rapid-eye, researchers tested out a method of two-way communication based on visual and audio cues. The subjects'

reactions included blinking and twitching of the eyes and tightening of some facial muscles. Horowitz et al. developed a device called Dormio consist of a wrist and finger attachment that measures when the person is about to enter into a hypnagogic state by measuring hand movements as muscle tone is lost. During the hypnagogic state, a phone app was used to prompt the user to think about objects and places in order to guide the person's dream [188].
These are just a few of the many areas where scientists are attempting to better understand the complex interactions between sleep and the rest of our lives in the hopes of making people's lives easier.

9.3 Fascia Hub

The Fascia Hub is a multi-interface, multi-component Human-Machine Interface (HMI) device built with modularity in mind. It's a compact, powerful, all-in-one board based on the Raspberry Pi, and it enables the creation of unique Internet of Things based interactions for the management of auxiliary functions.
At its heart, the Fascia Hub is a Raspberry Pi Compute Module 4 (CM4) module equipped with one sound and dual microphone cards, dual-band 2.4GHz/5GHz Wi-Fi, and Bluetooth 5.0, operating on a Pi-based Linux system, and boasting 4 GB RAM and 32 GB eMMC. The board features a number of easily-accessible components and high-speed connectors, all of which were made possible by its modular architecture. It is easily transferable to AI development programs for use in intervention support and AI assistance systems.

9.3.1 Input and Output Modalities

The hub is equipped with a relay, microphones, lights, a speaker, an infrared camera, and a diffuser atomizer. The power indicator light as well as other system user lights on the board can be used by your definition.
The Fascia Hub allows sleep researchers to conduct studies in the wild. Equipped with a variety of sensors and a powerful data platform, the Fascia Hub provides researchers with a unique opportunity to study sleep and gain insights that would otherwise be unavailable. In this section, we will explore the various modalities of the Fascia Hub, such as microphones, lights, a speaker, an infrared camera, and a diffuser atomizer, and how they can be used for sleep studies. We will also discuss

the benefits of using the Fascia Hub for sleep studies, including how it can be used to explore new research areas and develop new interventions and treatments for sleep disorders.

Figure 9-1: Fascia Hub I/O modalities

Privacy Button

The Fascia Hub includes a privacy button, which is an important safety feature that allows participants to communicate when they are ready to sleep and for data to be recorded. This ensures that the system won't record any data until the participant presses the button, providing participants with the assurance that they are in control of when they system collects data.

The privacy button is a critical aspect of conducting sleep studies, as it ensures that participants are comfortable and willing to have their data recorded. It also helps to mitigate any potential ethical concerns, by giving participants control over when their data is being recorded. This is particularly important when conducting studies with sensitive populations.

The privacy button also provides researchers with an added layer of control over the data collection process. By only recording data when the participant presses the button, researchers can ensure that the data collected is of high quality and relevant to the study. Additionally, the privacy button can be used as a trigger for other systems, such as the atomizer during development stages.

The privacy button on the Fascia Hub is an important safety feature that ensures participant data protection and helps to mitigate ethical concerns. It provides participants with control over when their data is recorded and allows researchers to collect high-quality and relevant data for their study. Additionally, the privacy button can be used as a trigger for sending acknowledgements to the remote researcher, making it a

useful tool for researchers.

Audio

The Fascia Hub is equipped with a speaker that is capable of providing auditory stimulation, with researchers able to control the volume and tones using the Fascia Portal. This feature provides participants with the ability to be stimulated in a controlled environment, which can be beneficial for sleep studies. The speaker also provides a more immersive experience for participants, as they can listen to different types of stimulation during their sleep studies.

As mentioned in the background section, auditory stimulation has been shown to have an impact on sleep, with certain sounds and frequencies promoting relaxation and better sleep. For example, white noise and nature sounds have been found to have a calming effect on the body and can be used to improve sleep quality. The speaker on the Fascia Hub allows researchers to study how different types of auditory stimulation can affect sleep, as well as how they can be used to treat sleep disorders.

In addition to providing auditory stimulation, the speaker on the Fascia Hub can also be used by researchers to communicate with participants during the study. For example, the speaker can be used to let participants know if they need to adjust a sensor or if something needs to be reconnected, which can help to ensure that the data collected is of high quality.

The speaker on the Fascia Hub is a useful tool for researchers, as it allows for auditory stimulation in a controlled environment. The speaker can be used to study how different types of auditory stimulation can affect sleep, and how they can be used to treat sleep disorders. Additionally, the speaker is also used by the researcher to communicate with participants during the study, ensuring the data is of high quality.

Atomizer

The Fascia Hub is equipped with a diffuser atomizer, which allows researchers to explore the effects of olfactory interventions on sleep. The Fascia Hub is also equipped with a relay that controls the atomizer, which can be used to adjust the humidity levels in a room. This allows researchers to study the effects of different humidity levels on sleep quality, in particular, how different levels of humidity can affect sleep duration, quality, and other related factors. Additionally, the atomizer can

be used to diffuse various scents into the study environment, enabling researchers to study how different concentrations of scents can affect sleep duration and memory consolidation.

Studies have shown that certain scents can have a relaxing effect on the body, promoting better sleep. For example, lavender and vanilla have been found to have a calming effect on the body and can be used to improve sleep quality. Researchers can use the atomizer to study how different concentrations of these scents can affect sleep, as well as how they can be used to treat sleep disorders [189, 190].

The atomizer can also be used to explore how humidity levels can affect sleep quality. Humidity levels can have a significant impact on sleep, with high humidity levels causing difficulty sleeping, and low humidity levels causing dehydration and sleep disturbance. Researchers can use the relay controlled atomizer to adjust the humidity levels in a room, allowing them to study the effects of different humidity levels on sleep quality for different age groups, such as the elderly, children, and adults.

In conclusion, the atomizer feature on the Fascia Hub provides researchers with a powerful tool to explore the effects of olfactory interventions on sleep. The atomizer can be used to study the effects of different scents on sleep duration and quality, as well as how these scents can be used to treat sleep disorders. Additionally, the atomizer, controlled by a relay, can be used to adjust the humidity levels in a room, allowing researchers to study the effects of different humidity levels on sleep quality and how different levels of humidity can affect sleep duration, quality, and other related factors.

Microphone

The Fascia Hub is equipped with two microphones, which can be used to capture audio from a wide area. These microphones are ideal for capturing sound levels, recording dreams, and exploring the effects of environmental noise on sleep quality and duration.

The data collected from the microphones can be used to study the effects of environmental noise on sleep quality and duration. For example, researchers can use the microphones to study how different noise levels can affect sleep in different environments, such as urban versus rural areas, or in different populations such as shift workers. Additionally, the microphones can be used to study how different sound frequencies can affect sleep quality and duration, for example, the calming effect of white

noise or the disruptive effect of certain high-frequency sounds.
The microphones can also be used to record dream audio, which can be used to study the relationship between dream content and sleep quality. This can be especially useful in studying disorders such as REM sleep behavior disorder (RBD) where abnormal movements or vocalizations occur during REM sleep.
The microphones on the Fascia Hub provide researchers with a powerful tool to capture environmental noise and audio data, which can be used to study the effects of environmental noise on sleep quality and duration, and how different sound frequencies can affect sleep. Additionally, the microphones can be used to record dream audio, providing researchers with a deeper understanding of the relationship between dream content and sleep quality.

Video

The Fascia Hub is equipped with an infrared camera, which can provide valuable data for sleep researchers. The American Academy of Sleep Medicine (AASM) requires that level 1 sleep studies, which are considered the most comprehensive type of sleep study, include video monitoring for body movements.
The infrared camera provides clear images even in low-light conditions, making it ideal for use in a bedroom setting. One example of a sleep study that would require the use of video recording is a study on sleep-related movements and disorders such as restless leg syndrome (RLS) or periodic limb movement disorder (PLMD). These disorders involve repetitive movements of the limbs during sleep and can greatly impact sleep quality and duration. By using video recording, researchers can observe and document these movements in real-time, providing a more accurate and comprehensive understanding of the disorder. The video recording also allows researchers to identify patterns and triggers of the movements, which can aid in the development of more effective treatment options. Additionally, video recording can be used to monitor the effectiveness of existing treatments, providing valuable insights into how to best manage these disorders.
The night camera is particularly useful for nocturnal seizure studies as it allows researchers to monitor the patient closely if a seizure is suspected and provide data to study the patterns and triggers of nocturnal seizures, as well as the effects of interventions on seizure activity. It is worth

mentioning that for this type of study it is recommended to be done in a clinic where an attendant can be present for assistance. The night camera allows the nurses or sleep registered technicians to closely monitor the patient and quickly respond in case of suspected seizure activity. This is particularly important for patients who are at a higher risk for seizures, or for studies that are investigating new treatments for seizures.
In conclusion, the night camera on the Fascia Hub is an essential tool for researchers studying nocturnal seizures. It provides clear images, even in low-light conditions, and allows for close monitoring of the patient. The data collected can be used to study the patterns and triggers of nocturnal seizures, as well as the effects of interventions on seizure activity. This can be especially useful for studies of patients who are at a higher risk for seizures, or for studies that are investigating new treatments for seizures. The night camera allows the technologist to closely monitor the patient and quickly respond in case of suspected seizure activity while ensuring the patient's safety and following all facility protocols.

9.4 Privacy

Ensuring privacy is an essential consideration for researchers using the Fascia Hub, especially in regards to its microphone and video recording capabilities. These features have the potential to collect sensitive personal data, including conversations and movements during sleep. To address this, the Fascia Hub includes a privacy button that allows users to turn off recording at any time, giving them complete control over their data.
Additionally, the Fascia Hub encrypts all data collected by the microphone and video recording functions, ensuring that the data is protected from unauthorized access. The encrypted data is stored securely on the device and can only be accessed by authorized users with appropriate credentials.
Moreover, researchers using the Fascia Hub should take steps to inform participants about the privacy risks associated with the microphone and video recording capabilities. Participants should be informed of the specific data that will be collected, how it will be used, and who will have access to it. Informed consent should be obtained from participants before any data collection takes place.
Overall, the Fascia Hub prioritizes privacy by including a privacy button, encrypting data, and ensuring that participants are fully informed about

data collection practices. These measures are crucial in maintaining ethical research practices and protecting the privacy of participants in sleep studies.

9.5 Conclusion

In conclusion, the Fascia Hub is a powerful tool for sleep researchers, providing access to a wide variety of sensors and a powerful data platform. The hub's relay, microphones, lights, a speaker, an infrared camera, and a diffuser atomizer provide researchers with a unique opportunity to study sleep in the wild. Researchers can leverage the Fascia Hub to collect data from multiple sources, identify patterns and correlations, and gain insights into how sleep is affected by factors such as stress, diet, and environment. The privacy button ensures participant data protection and helps to mitigate ethical concerns. The speaker and microphone provide auditory stimulation and immersive experience for participants. The power indicator light is a quick and easy way to monitor the connection status of the device and ensure that data is being collected correctly. The Fascia Hub is a powerful tool that can unlock the potential of sleep studies in the wild, helping sleep researchers to explore new research areas and develop new interventions and treatments for sleep disorders.

10 Fascia Portal

10.1 Introduction

The Fascia Portal is where sleep researchers can inspect the patient's signals in real-time and store experiment information, analyzed by the machine learning API that provides sleep staging, spindles, and k-complex identification information in real-time. The portal also works as a data collection and labeling platform for developing new and more robust datasets to train machine learning models for sleep diagnostics.

Identifying different sleep stages and analysing them is very important for diagnosing and treating sleep disorders, as well as understanding the neuroscience of healthy sleep. Polysomnography (PSG) is a recording of the major physiological signals associated with sleep. PSG involves the recording of multiple electrophysiological signals from the body, such as brain activity from Electroencephalography (EEG), heart rate from Electrocardiography (ECG), muscle tone through Electromyography (EMG) and eye-movement through Electrooculography (EOG), along with respiratory and temperature data.

The collection of PSG data involves a tedious process with several electrodes throughout the head and body. This results in an unnatural setting for sleep, and causes the PSG signals to be unfaithful to those present in true sleep.

Further, the process of manual sleep staging requires sleeping in a hospital or laboratory with an expert monitoring and scoring signals in real-time. This results in an unnatural sleep setup for the subject that affects the diagnosis and is a intensely time-consuming process. Because of this, there has been a significant development in research on

automating sleep staging with better devices.

The Fascia mask is designed to combine all of these sensors into a novel sleep mask which promotes sleep in natural settings. The prototype is designed to maximize the quantity and quality of sensor signals, as well as ensuring user comfort so as to produce accurate data and reduce the first night effect typical of clinical sleep studies.

Thus, we are now presented with a unique opportunity to delve into the depths of the neuroscience of natural sleep. Several automatic sleep staging tools currently present in the market don't provide sleep researchers with open access to the data collected. Fascia is the one of first real-time web-based interface to present PSG signals collected, characteristics of the signal, as well as interpretable and automatic sleep staging for sleep researchers.

10.2 Background

In the field of polysomnography, data visualization plays an important role in the analysis and interpretation of sleep study data. The use of visual representations, such as graphs and charts, can help researchers and clinicians identify patterns and trends in the data that may not be immediately apparent from raw numbers. There are several state-of-the-art software packages available for visualizing polysomnography data, such as:

Figure 10-1: Screenshot of the profusion software

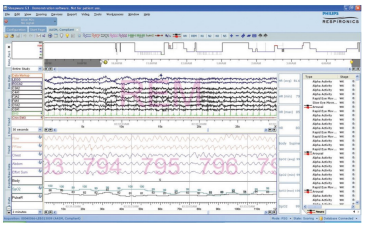

Figure 10-2: Screenshot of the Somnolyzer software integrated into Sleepware

- Profusion: This software is used to analyze data about sleep and breathing. It has a number of tools for showing the data, such as hypnograms, spectral analysis, and event detection*.
- Somnolyzer is a clinically-validated, computer-assisted sleep scoring system designed to help simplify and improve manual scoring productivity, accuracy and consistency. It will score full PSG and portable studies. This software is an add on that companies can add to their excisting software pipeline like Phillis Sleepware†
- Actiware: This software is used for the scoring and analysis of actigraphy data, which is collected using a wrist-worn device that measures movement. Actiware has a number of visualization tools that can be used to look at data from studies ‡.

* https://www.compumedics.com.au/en/products/profusion-sleep-software/
† https://www.philips.ie/healthcare/product/HC1082462/sleepware-g3-sleep-diagnostic-software
‡ https://www.usa.philips.com/healthcare/sites/actigraphy

The software packages that I mentioned earlier, such as Profusion, Somnolyzer, and Matlab, are typically used by researchers and healthcare professionals for the analysis and interpretation of polysomnography data. These types of software are typically designed for specialized use and are not widely available to the general public. So, the end user often pays a license fee to cover the cost of making, maintaining, and distributing the software. Prices for these types of software can vary depending on factors such as the version of the software, the number of licenses, and the length of the license. It is not uncommon for the prices of these software to be in the tens of thousands of dollars' range. One of the reasons for the high cost of these software products is that they are typically developed by specialized companies or research groups who invest a significant amount of resources into the development and maintenance of the software. Additionally, many of these software packages are developed with the specific needs of researchers and healthcare professionals in mind, which can make them more complex and more expensive to develop than more general-purpose software. Another reason for the high cost is that these software packages often come with specialized features and capabilities, such as advanced visualization tools, that are not available in more general-purpose software. These features can be critical for the analysis and interpretation of complex sleep study data, and their inclusion in the software can justify the cost for many users. It's also important to note that some companies may offer educational or academic discounts on the software. Also, cloud-based version of the software may be more affordable as they don't require a large investment in IT infrastructure.

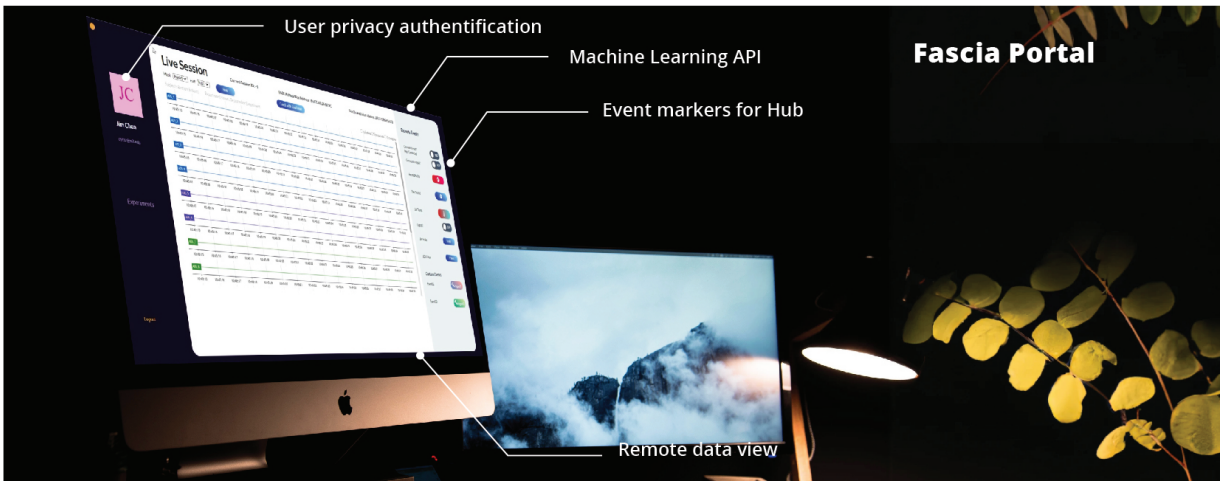

Figure 10-3: Main components for the Fascia Portal

10.3 Fascia Portal

The Fascia Portal described in this section is designed to facilitate remote sleep studies through its advanced features. In this section, a more in-depth description of the three main components of the Fascia Portal will be provided: the live session, the playback, and the backend. Figure 10-3 shows the components of the Fascia Portal.

The live session is the primary feature of the Fascia Portal, which allows researchers to view all sensor data in real-time. The live session also includes a panel to change zoom and panning data, as well as a panel to change filters bandpass and bandstop fillers. Researchers can also use the live session to communicate with the subject and the Fascia Hub, ensuring the accuracy and integrity of the data collected.

The playback feature allows researchers to review and analyze the data collected during the sleep study. The playback feature includes options to adjust the speed and view different data sets, as well as the ability to apply filters and other data analysis tools.

The backend of the Fascia Portal is responsible for storing, processing, and analyzing the data collected during the sleep study. The backend includes a database that stores the collected data, and advanced algorithms that process the data to identify patterns and potential issues. The backend also allows for easy sharing and collaboration among researchers, making it an essential component of the Fascia Portal.

Overall, the Fascia Portal aims to provide a comprehensive and efficient solution for remote sleep studies through its advanced technical capabilities, user-friendly interface, real-time monitoring capabilities, and the three main components - the live session, the playback, and the back-end.

10.3.1 Live Session

The live session is the primary feature of the Fascia Portal, which allows researchers to view all sensor data in real-time. This feature provides a comprehensive view of the data being collected during the sleep study, enabling researchers to effectively monitor the study and make adjustments as needed. One of the key functions of the live session is the ability to view all sensor data in real-time. This includes data from the Fascia Hub and Mask, which is critical for understanding the subject's sleep patterns and identifying any potential issues. The live session

also includes a panel for adjusting zoom and panning of data, allowing researchers to focus on specific areas of interest. This is particularly useful for isolating and analyzing specific data sets.

Figure 10-4: Main components for the live session component. Area 1, shows information about the study and device, Area 2, shows the time series data plotted in real-time. Area 3. Button to connnect to remove devices, Area 4, Buttons to send messages to the Fascia Hub

The live session also provides researchers with the option to apply bandpass and bandstop filters. These filters can help isolate specific data sets for analysis, such as heart rate or movement, making it easier for researchers to identify patterns and potential issues. Another important aspect of the live session is the ability to interact with the Fascia Hub and connect to the mask. The live session includes buttons for these functions, which allows researchers to easily adjust the study and ensure the accuracy of the data being collected. At the top of the live session interface, labels provide important information about the experiment, subject, and devices connected. This is crucial for understanding the context of the data being collected and keeping track of the study.

It also allows the researchers to have a clear picture of the overall progress of the study. All of the components mentioned above are marked in Figure 10-4 Overall, the live session feature of the Fascia Portal is designed to provide researchers with a comprehensive and real-time view of the data being collected, allowing them to effectively monitor the study and make adjustments as needed. The live session is the backbone of the Fascia Portal and ensures that the data collected is accurate and of high quality, making it an essential tool for remote sleep studies.

10.3.2 Playback

The playback feature of the Fascia Portal allows researchers to review and analyze the data collected during the sleep study. This feature is designed to provide researchers with the tools they need to thoroughly review the data offline and identify patterns and potential issues.

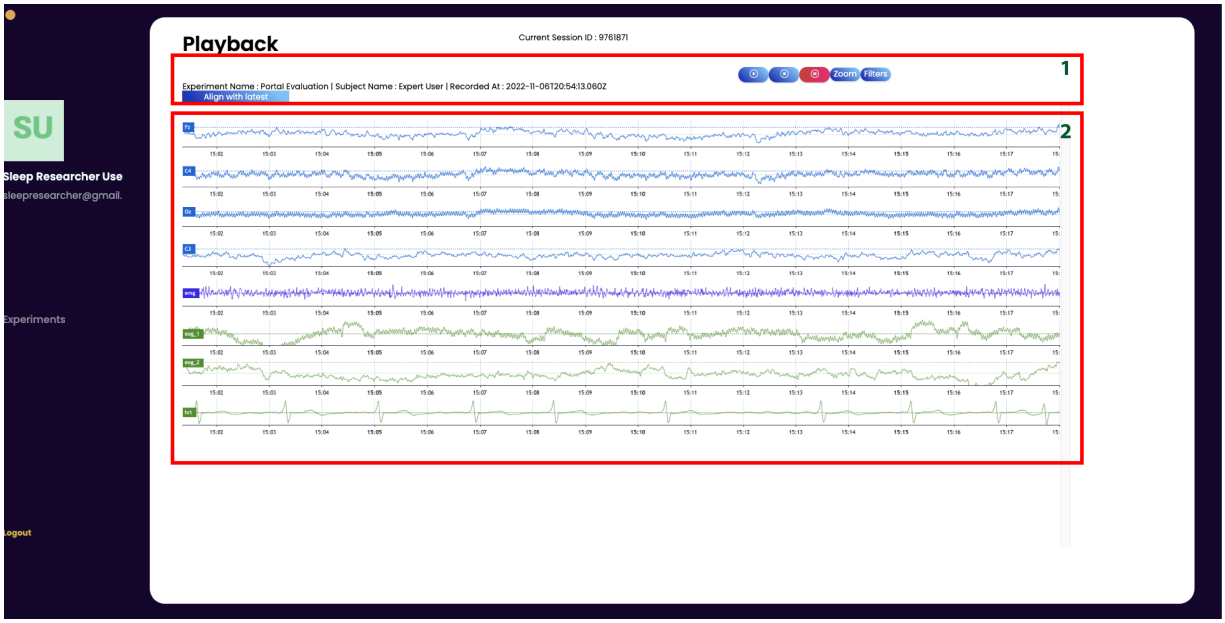

Figure 10-5: Main components for the playback session component. Area 1, shows information about the study and device and controllers, Area 2, shows the time series data plotted in real-time.

The playback feature has many of the same controls as the live session as shown in Figure 10-5, such as the ability to apply filters and view data. This allows researchers to review the data in the same way they would during the live session. One of the key functions of the playback feature is the ability to play the data stream from a desired experimental session as if it were in real-time. Additionally, researchers can also choose to review the data in 30-second increments. This is particularly useful for isolating specific data sets for analysis.

Another important aspect of the playback feature is the ability to use the machine learning pipeline to identify spindles, slow waves, and sleep scoring. These features use advanced algorithms to automatically analyze the data and identify patterns that may be difficult for researchers to spot manually. This helps researchers to speed up the sleep scoring process, allowing them to quickly and accurately score the subject's sleep patterns. This makes it easier for researchers to identify potential issues and make adjustments to the study as needed.

Overall, the playback feature of the Fascia Portal is designed to provide

researchers with a comprehensive and detailed view of the data collected during the sleep study. The playback feature allows researchers to review the data in the same way they would during the live session and use machine learning algorithms to identify patterns and potential issues. This makes the playback feature a valuable tool for remote sleep studies and allows researchers to analyze the data in more depth.

10.3.3 Back-end

The back-end of the Fascia Portal is responsible for storing, processing, and analyzing the data collected during the sleep study. This is a crucial component of the Fascia Portal as it ensures that the data is accurate, reliable, and easily accessible for researchers.

The back-end of the Fascia Portal uses node.js and PostgreSQL as the primary technologies. PostgreSQL is a high-performance, enterprise-class open-source relational database that can be queried using SQL (relational) and JSON (non-relational). This database management system has been developed over more than 20 years, contributing to its high levels of resilience, data integrity, and accuracy. Many online, mobile, geospatial, and analytics applications utilise PostgreSQL as their primary data storage as well as data warehouse.

PostgreSQL has been chosen over Redshift because of its ability to handle streaming data, which is a continuous stream of semi-structured data, usually in JSON or XML format, transferred in real-time or very real-time across the internet. Due to the extra ETL work required to structure streaming data for analysis and the larger cluster sizes required to store volumes of data that frequently reach petabyte-scale, the costs of storing and querying this data in Redshift can be astonishingly high. Redshift's "INSERT" query takes a long time to process, making it unsuitable for real-time applications.

Additionally, the Fascia Portal has a feature that allows researchers to download CSV files containing data from the device for the particular sessions. Data can be analyzed and processed to gather further information about the sleep of the individual. The data consists of Message ID, Session ID, Board Mac Address, Board Nickname, Packet Number, Validity Number, ADS1, ADS2, ADS3, ADS4, ADS5, ADS6, ADS7, ADS8, IMU1, IMU2, IMU3, IMU4, IMU5, IMU6, EDA, TEMP, PPG, Board Timestamp, Created At,Trigger Id,Hub Mac Address, Hub Nickname, Event Type, Event Details, Smallest Time,Epoch Ts.

Overall, the back-end of the Fascia Portal is designed to provide a reliable and efficient solution for storing, processing, and analyzing the data collected during the sleep study. The use of technologies such as node.js and PostgreSQL, as well as the ability to handle streaming data, makes the Fascia Portal a powerful tool for remote sleep studies.

10.4 Machine Learning API

Recent developments in machine learning have prompted research into classifying sleep using different types of automated systems. In recent years, a number of different automatic sleep-staging algorithms have come into existence.

While the Fascia Portal's pipeline is made so it can easily integrate new ML models, two models were explored further as part of this work.

.

A Long Short-Term Memory (LSTM) + Convolutional Neural Network (CNN) approach for sleep staging recognition can be a powerful method for accurately identifying sleep stages.

The LSTM network is well-suited for time series data such as sleep staging, as it can capture long-term dependencies in the data. The LSTM network can be trained on a dataset of sleep staging to learn the patterns of sleep stages over time.

The CNN network is used to extract features from the raw data. CNNs are particularly useful for image and time-series data, as they are able to learn local and global features in the data. In this case, the CNN would be applied to the raw data to extract relevant features that can be used by the LSTM network for sleep staging recognition.

The combination of LSTM and CNN networks can be used to provide confident values for sleep staging. The LSTM network can be trained to predict the sleep stage at each time step in the data, while the CNN network can be used to extract relevant features that can be used to improve the accuracy of the LSTM network.

By training the LSTM network on the extracted features, it can provide confident values for each sleep stage, by providing probability scores for each stage. This can be used to calculate a confidence score for each epoch, providing an additional level of analysis for sleep research.

Overall, an LSTM+CNN approach for sleep staging recognition can provide a powerful and accurate method for identifying sleep stages and

can also provide confident values for each stage. This approach can be useful for sleep research and for building practical applications such as sleep tracking devices.

Although a comprehensive analysis of such sleep-staging algorithms is outside the scope of this section, some of the models explored in this section are based on an in-depth review by Fiorillo et al. [191].

10.4.1 Automated Sleep Staging

As mentioned before, sleep staging is generally done visually by inspecting consecutive PSG segments of 30s. It results in a hypnogram which represents the succession of sleep stages across time. Apart from being time-consuming, visual sleep scoring is subject to both inter and intra-rater variability and is thus far from being optimal. By contrast, automatic sleep scoring has the advantage of being fast, reproducible and with generally good agreement with visual scoring, yet its usage is far from being widespread and most sleep laboratories still rely on visual scoring, using either commercial software or in-house packages.

Nevertheless, as far as we are aware of, none of these systems implement the classification of sleep stages in just 5-second epochs in real-time for PSG data.

The sleep staging classification is done using the YASA model: a model trained and tested using a large and diverse set of polysomnographic recordings from both healthy subjects and those with sleep disorders [192]. In general, the results show that YASA is as accurate as human inter-rater agreement (85%) when compared to expert consensus scoring.

The automated sleep scoring that the playback section provides is meant to supplement human scorers and speed up the sleep staging process. Until the model has been made more general and robust, it is recommended that a trained sleep scorer visually verify the ML model's predictions, paying special attention to low-confidence epochs and/or N1 sleep epochs, which are the most frequently misclassified epochs. Because of this, the YASA model has been modified to include a confidence and salience map for use in sleep studies.

Finally, the predicted hypnogram is available at the bottom of the time series data and can be used by the user. These kinds of graphs are great for spotting obvious mistakes in the hypnogram. Figure 10-6 shows an example of sleep staging output generated using the API for 2.5 hours of sleep.

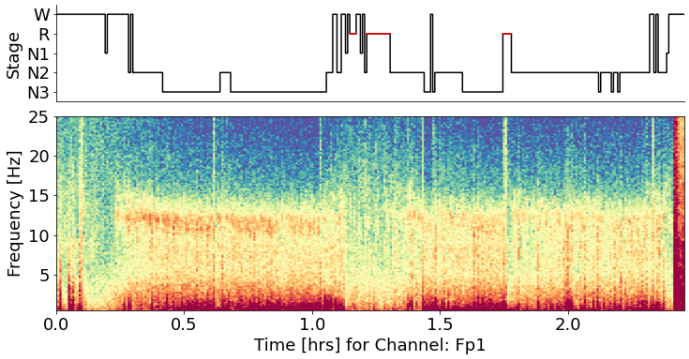

Figure 10-6: On the top a hypnogram generated from the output of the sleep stage API. At the bottom a spectogram for the FP1 channel is shown showing brain activity during the 2.5 hours of sleep

10.4.2 Automated Spindle Detection

The sleep spindle detection algorithm is based on the work of Lacourse et al. [193]. The Lacourse et al. design of the spindle detector incorporates a correlation filter into the connection between the EEG signal that has been filtered in the sigma band and the raw EEG signal itself. Because of this, their approach is biased toward detecting spindles that are apparent on the raw EEG signal. This is accomplished by needing a strong correlation between the raw EEG signal and the filtered sigma burst, which is the pattern that denotes a spindle.

A call to the yasa.spindles detect() function allows for the automatic detection of spindles to be carried out. The detection method utilizes the algorithm that was outlined in Lacourse et al.'s 2018 paper.

10.4.3 Automated Slow Waves Detection

The slow-wave detector from YASA was used, which is based on algorithms made by Massimini, et al., [194] and Carrier et al., [195]. The technique was developed to recognize discrete Slow Waves (SW) with a frequency ranging from 0.5 to 3.5 Hz by employing a linear phase Finite Impulse Response filter that featured a 0.2 Hz transition band. SWs with negative trough amplitudes of more than 40 µV and less than 300 µV and positive peak amplitudes of more than 10 µV and less than 200 µV were found to exist within the bandpass frequencies that were determined. The method then computes peak-to-peak amplitudes and keeps SWs between 75 and 500 µV after sorting recognized negative peaks with succeeding positive peaks. Finally, for the purpose of further study, the SW down-states that last longer than 300 ms and shorter than 1500 ms have been retained, as well as the up-states that last longer than 100 ms and less than 1000 ms. Then, for each participant, session, and

condition, the SW densities (number of SWs per minute), peak-to-peak amplitudes, durations, and slopes of discrete SWs were measured in channel C3-A2.

10.4.4 Salience Maps

While it is convenient to solve complex issues by building vast neural networks, it is difficult to grasp the impact of each weight on the outcome. In actuality, the relationship between a neural network's weights and the function it represents is exceedingly intricate, especially when the network contains billions of weights.

Visualizing the network is useful for diagnosing model faults, interpreting the meaning of models, or just teaching deep learning ideas. Decision boundaries, model weights, activations, gradients, performance metrics, the result of applying a learnt filter to an image, or the filters themselves can all be seen.

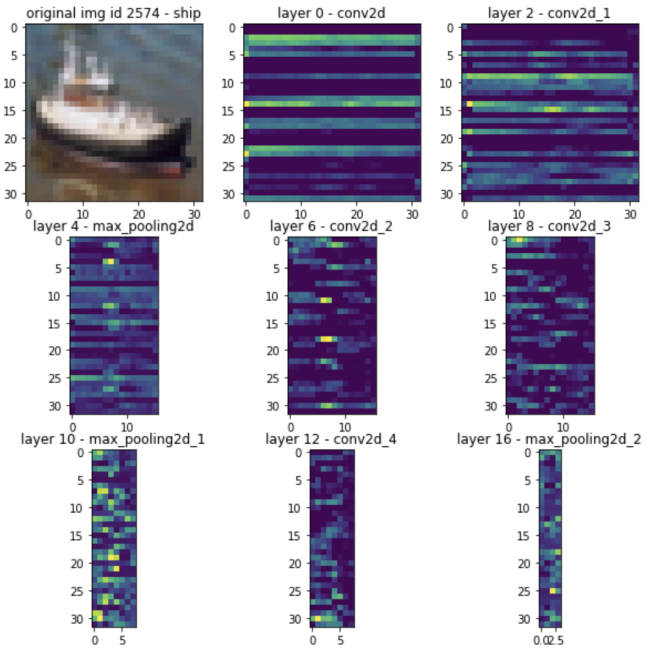

Figure 10-7: Each image shows a heatmap of the features learned by the corresponding layer when recognizing a ship.

Figure 10-7 shows how to extract feature maps from hidden convolutional layers using a heat map plotting technique. Each image depicts a heatmap of the features discovered by the relevant layer when recognizing a ship. Saliency maps go one step further by offering an interpretable method for investigating hidden layers in CNNs. The concept of saliency maps was initially introduced in the paper:

Deep Inside Convolutional Networks: Visualising Image Classification Models and Saliency Maps [196]

The concept is straightforward: the gradient of the output category with respect to the input image is computed. This should inform how the output category value varies as the input image pixels shifts. All of the positive gradient values indicate that a slight adjustment to that pixel will increase the output value. As a result, showing these gradients, which have the same form as the image, should convey some attention intuition.

Backward methods for decision attribution include saliency maps. Grad-CAM [197] and gradient base saliency maps were employed for the Fascia API because they were discovered to be the most consistent techniques for time-series data.

Saliency For sleep data, saliency maps can be used to identify which parts of the sleep signal are most important for the model's predictions of sleep stages. For example, if a saliency map for a sleep stage prediction model shows that the model is paying attention to the high frequency components of the signal, it might suggest that these high frequency components are important for the model's predictions.

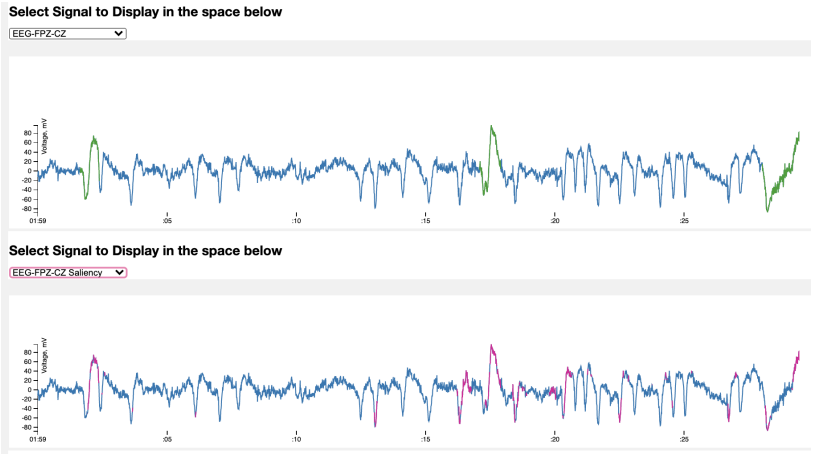

Figure 10-8: On the top extracted k-complex and on the bottom saliency maps generated by the model

Saliency maps can be useful for clinicians and researchers as it can provide insights into how the model is making predictions, and which features of the sleep signal are most important. This information can be used to improve the model's performance, and to provide a better understanding of the underlying sleep physiology.

Additionally, saliency maps can be used to identify which parts of the sleep signal are most important for the model's predictions of sleep stages, and this information can be used to design interventions that target these specific features of the sleep signal.

Overall, saliency maps can be a valuable tool for understanding how models make predictions and identifying important features of the sleep

signal, and they can be beneficial for both researchers and clinicians.

10.5 Conclusion

In conclusion, the Fascia Portal is a comprehensive and efficient solution for remote sleep studies. It is designed to facilitate remote sleep studies by providing advanced technical capabilities, user-friendly interface, real-time monitoring capabilities, and the three main components - the live session, the playback, and the backend.

The live session is the primary feature of the Fascia Portal, which allows researchers to view all sensor data in real-time. It provides a comprehensive view of the data being collected during the sleep study, enabling researchers to effectively monitor the study and make adjustments as needed. The live session also includes a panel for adjusting zoom and panning of data, allowing researchers to focus on specific areas of interest. Additionally, it includes options to apply bandpass and bandstop filters, and to interact with the Fascia Hub and connect to the mask.

The playback feature allows researchers to review and analyze the data collected during the sleep study. It includes options to adjust the speed and view different data sets, as well as the ability to apply filters and other data analysis tools.

The backend of the Fascia Portal is responsible for storing, processing, and analyzing the data collected during the sleep study. It includes a database that stores the collected data, and advanced algorithms that process the data to identify patterns and potential issues. The backend also allows for easy sharing and collaboration among researchers, making it an essential component of the Fascia Portal.

Overall, the Fascia Portal provides a comprehensive and efficient solution for remote sleep studies through its advanced technical capabilities, user-friendly interface, real-time monitoring capabilities, and the three main components - the live session, the playback, and the backend. These features make it a valuable tool for sleep researchers and clinicians, allowing them to effectively monitor and analyze sleep studies, and make data-driven decisions.

In the next chapter, we will thoroughly evaluate the Fascia Portal using both qualitative and quantitative methods. This evaluation will consist of two main parts:

A qualitative analysis of interviews conducted with experts in the field

of sleep research, in order to evaluate the usability of the Fascia Portal in terms of reliability, novelty, and user satisfaction. A quantitative pilot study, where we will analyze the signals collected during 12 nights of sleep studies using the Fascia mask. This will allow us to evaluate the accuracy and performance of the Fascia Portal in collecting and analyzing sleep data.

Overall, the evaluation will provide a comprehensive analysis of the Fascia Portal and its potential impact on the field of sleep research, including the implications of our findings for future developments and applications of the technology.

11 Fascia Evaluation

11.1 Introduction

In this chapter, a comprehensive evaluation of the Fascia Ecosystem is presented, which includes the Fascia Portal and the Fascia Sleep Mask. The Fascia Ecosystem is a remote sleep study solution that provides advanced technical capabilities, user-friendly interface, and real-time monitoring capabilities. The evaluation will be conducted using both qualitative and quantitative methods, including ten interviews with experts in the field of sleep research and a pilot study analyzing the signals collected during 12 nights of sleep studies using the Fascia mask. The evaluation will focus on assessing the usability, reliability, novelty and user satisfaction of the Fascia ecosystem, as well as its accuracy and performance in collecting and analyzing sleep data. The findings of this evaluation will provide a deeper understanding of the Fascia Ecosystem's potential impact on the field of sleep research and its future developments and applications.

11.2 Experts Interviews

To investigate user interaction with the Fascia Ecosystem, we designed a mixed-methods study consisting of an observed portal usage task and a six-part survey. The goal of this study was to gain a deeper understanding of the needs, wants, and aims of sleep researchers when looking for a sleep wearable for conducting future studies, as well as how they perceived the Fascia Ecosystem.

The study was conducted over a period of one month, during which we recruited 10 sleep researchers who were informed about the Fascia Ecosystem. These researchers participated in 1-hour semi-structured interviews, during which they were asked to interact with the Fascia Portal and provide feedback on their experience. Additionally, they anonymously filled out questionnaires to provide more detailed information about their needs, wants, and aims when looking for a sleep wearable, as well as their perception of the Fascia Ecosystem. Figure 11-1 shows the demographic and key take aways.

The observed portal usage task was designed to evaluate the ease of use and navigation of the Fascia Portal. The task consisted of a series of scenarios that simulate real-world usage of the portal, such as setting up a study, connecting to the Fascia mask, and analyzing the collected data. Researchers were asked to complete the task while providing verbal feedback on their experience. This provided valuable insights into the usability of the Fascia Portal and how it can be improved.
The six-part survey consisted of multiple-choice and open-ended questions that aimed to gather information about the researchers' needs, wants, and aims when looking for a sleep wearable, as well as their perception of the Fascia Ecosystem. The survey covered topics such as the features that are most important when choosing a sleep wearable, the challenges that researchers face when conducting sleep studies, and the perceived benefits and drawbacks of the Fascia Ecosystem.

11.2.1 Formative Study

As part of our initial exploration, we conducted a formative study with 10 participants. With all of the participants we conducted open-ended, interpretation-focused interviews, which allowed us to get in-depth understanding on user impressions and feedback on their interactions using the portal.
They were instructed and shown what the Fascia Ecosystem is, how it operates, and its capabilities. (specific protocol information: live session and playback) Then, they independently investigated the Fascia's Web Portal. During this interactive testing session, they were instructed on how to engage with the Portal, and an open-ended conversation was maintained throughout the interview. They were then requested to respond to a questionnaire about their perceptions of the Portal's usability, consistency, and dependability, as well as its capabilities and how it compared to any alternatives they were aware of. They responded to the questions both verbally in conversation with the interviewer and in writing on an anonymous, open-ended questionnaire.

11.2.2 Recruitment

Potential participants were invited through our network of sleep researchers. Some sleep researchers were sleep epidemiologists, while others dealt with animal sleep, clinical research, fundamental research, and dreams. These researchers had a high level of knowledge and ex-

perience: 40% were classified as advanced users, with extensive prior knowledge of sleep research and having worked with multiple sleep signal processing devices, and 50% were classified as intermediate users, with significant prior knowledge of sleep research and having worked with at least one sleep signal processing device in the past.

11.2.3 Interview Results

This section presents the findings of the formative study, which aimed to evaluate the usability of the Fascia Portal for remote sleep studies. The study included interviews with 10 experts and a questionnaire divided into three sections: difficulty, comparison to other solutions, and agreement with statements. The results of the study indicate that the majority of the experts found the Fascia Portal to be easy to access, navigate and use. Additionally, the majority of the experts found the Fascia Portal to be on par or better in comparison to the existing solutions they use and generally agreed that the Fascia Portal is reliable and easy to use. Figure 11-2 shows all the question in a gantt chart format, which allows for a quick visual representation of the results and highlights the areas where the experts had a positive or negative opinion about the Fascia Portal

When asked about difficulty, the results of the first section show that the majority of the experts found the Fascia Portal to be very easy to access and navigate, with 44.4% of the experts saying it was very easy to access and 33.3% saying it was very easy to navigate. Furthermore, 60% of the experts found it extremely simple to become acquainted with the portal's interface, and 43.5% found it simple to understand the names of the buttons and commands employed. However, there were some areas of difficulty, with 20% of experts saying accessing the site was neutral in terms of difficulty and 13% saying navigating the portal in general was neutral in terms of difficulty.

The outcomes of the second portion in comparison to present solutions that they employ. indicate that the majority of professionals thought the Fascia Portal was on par with or better than the existing alternatives they use. When compared to the alternative platform, 40.5% of the experts found it to be extremely easy in terms of capacity, 34.3% found it easy in terms of consistency and dependability, 66.7% found it easy in terms of meeting their expectations, and 55.8% found it easy in terms of user-friendliness. However, 27% of experts said it was difficult in terms

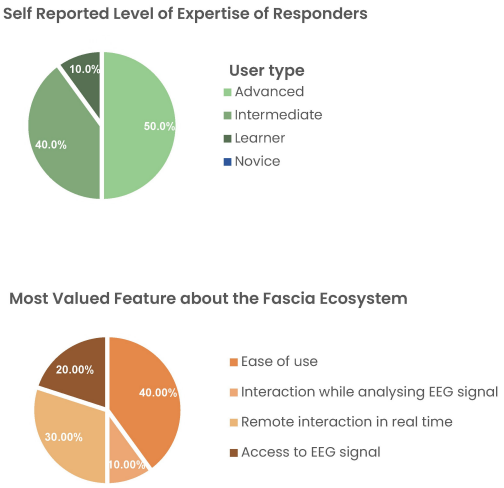

Figure 11-1: Pie graph for demographic and key take away

of capacity, 5.7% thought it was difficult in terms of consistency and reliability, and 20.9% thought it was neutral in terms of user-friendliness. Despite a few areas where experts found it difficult or neutral, the majority of experts regarded the Fascia Portal to be at least as easy as the existing solutions they use.

Figure 11-2: Interview Gantt chart

When asked about agreement to the claims in the third section, the majority of the professionals agreed that the Fascia Portal is reliable and simple to use. 53.3% of experts thought the data was accurate, 51.1% thought the platform ran smoothly on their device, 62.5%thought the prompts for inputs were clear, 48.8% thought the communication functionalities between the portal user and the sleep mask user were adequate, 53.2% thought the information the portal provided was readable, and 62.5% thought the way the portal organizes data was adequate for the needs of studies. Furthermore, 37.5% of experts thought the way the portal organizes downloaded data was adequate for the purposes of studies, and 52.1% thought the use of words throughout the platform was consistent. However, 20% of experts considered the way the portal organizes data difficult, 14.6% found the communication features between the portal user and the sleep mask user difficult, and 10% found the way the portal organizes downloaded data difficult. In general, the majority of specialists thought the Fascia site was usable and found it to be reliable

and simple to use.

11.2.4 Insights from Expert Interviews: Usability and Feedback of the Fascia Portal

The study with the 10 experts provided valuable insights into the usability of the Fascia Portal for remote sleep studies. The majority of experts found the portal to be easy to access, navigate, and use, indicating its user-friendly design. They expressed their enthusiasm for using the portal in future experiments, particularly for home-based studies and interventions. One expert stated, *"The possibility to record sleep at home easily"* showcases the convenience and flexibility offered by the Fascia Portal. Another expert mentioned, *"I would love to use this for lucid dreaming experiments! I'm also interested in the scents and TMR,"* highlighting the potential for innovative research in the field.

The positive feedback and constructive suggestions were encouraging for the Fascia team. However, one expert mentioned, *"A long-range/lower priority thing that might be interesting would be the ability to integrate with other devices besides Fascia."* This comment emphasizes the potential for expanding the portal's capabilities by incorporating data from additional sources.

The positive feedback and excitement expressed by the experts was very encouraging, as it reinforces their commitment to adopt new tools and appreciate a user-friendly platform for sleep research. We will carefully consider the suggestions provided by the experts, including the need for numerical participant identification, improved data export formats, and display enhancements. One of my goals is to continuously improving the portal to meet the evolving needs of sleep researchers and ensure a seamless and valuable user experience.

11.3 At Home Fascia Sleep Mask Signal Validation

We used the Fascia sleep mask for 12 nights in a pilot study with two participants, each of whom used it in their home. And had a video call with the remote researcher before wearing the sleep mask. No interaction over Zoom continued once the participant had put on the mask; instead, all feedback was provided via the Fascia Hub.

Comparing the signals collected with the Fascia Mask to existing datasets can provide insight into the validity of our system. We will compare our results to two gold standard datasets: the Physionet CAP sleep Database [198] and the sleep-EDF Expanded [199] Database Expanded. Both datasets used clinical grade PSG for the data collection, allowing for more accurate and reliable results. By comparing our results to these two datasets, we can better understand the implications of our findings.
This comparison will provide a basis for evaluating the accuracy of our system and will enable us to determine whether the Fascia Mask is suitable for use in sleep studies

11.4 Awake State

11.4.1 Muscle Activity

We will further investigate and discuss the differences between our signals and the existing datasets. To provide a more complete and comprehensive analysis, we will conduct a statistical analysis of the data and compare the results. Additionally, we will discuss any limitations of the existing datasets that may have an impact on our results.
EMG is a commonly used method to measure muscle activity during sleep stages. The electrical activity of muscles is recorded and analyzed to differentiate between different stages of sleep. It has been established that the Awake stage presents the highest muscular activity, in contrast to the REM stage, which has the lowest EMG activity. This is because muscle activity is strongly linked to the epoch energy. EMG epochs containing high muscular activity also have high energy levels, while EMG segments with low levels of energy have low levels of muscular activity.
Figure 11-3 shows the activation shown as measured by electromyography sensor. for the sleep-EDF Expanded dataset(SEDF), CAP dataset and Fascia dataset.
The sleep-EDF Database Expanded was down sampled to 10 Hz, making it difficult to accurately observe muscle activity. We will compare the data from the sleep-EDF Database Expanded to the data from the Physionet CAP sleep Database and the data collected with the Fascia device, to determine if the down sampling had any effect on the accuracy of the measurements. Additionally, we will discuss any limitations of the sleep-EDF Database Expanded that may have an impact on our results.
The raw data and the signal envelope of the EMG signal is taken from the

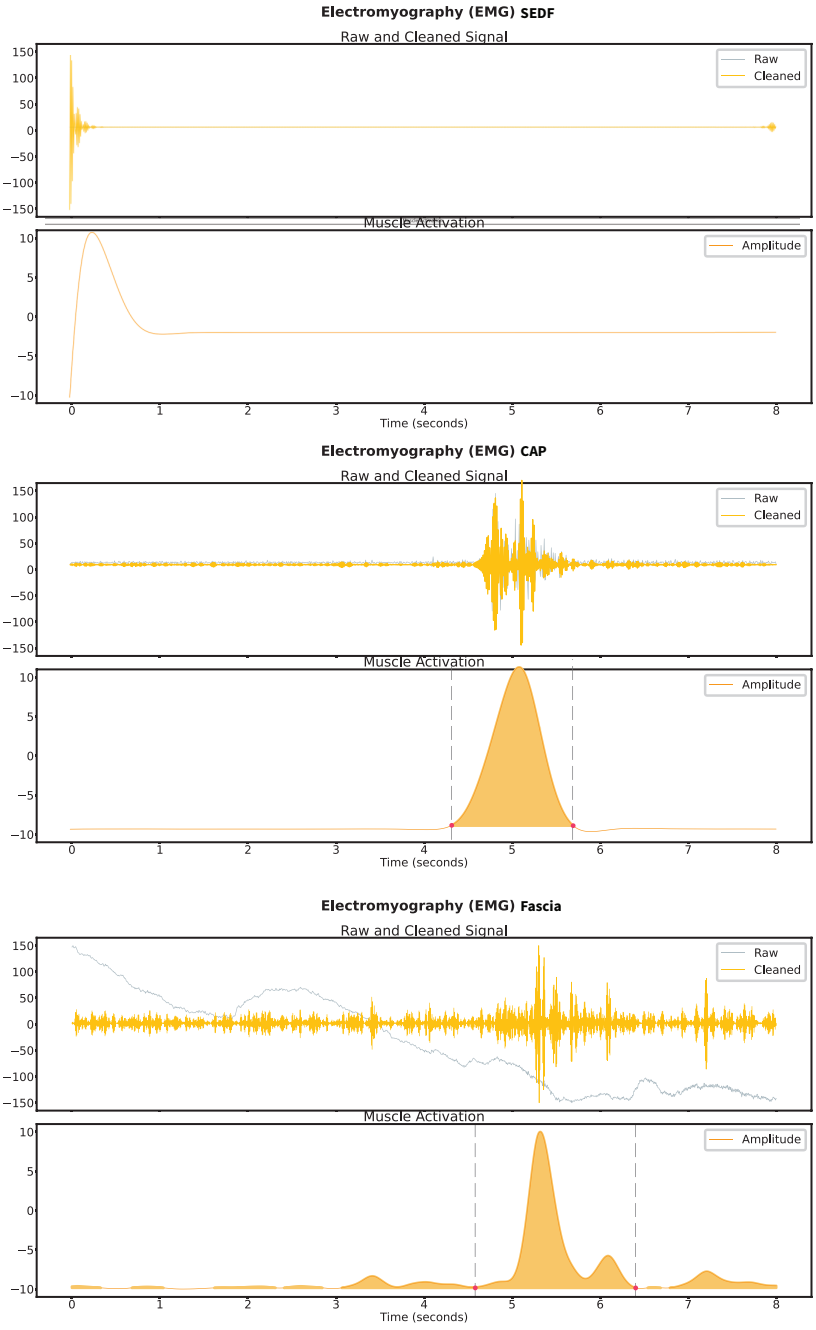

Figure 11-3: EMG comparison across the sleep EDF, CAP and Fascia PSG data

Zygomaticus major (cheeky muscle). This figure provides a comparison between the raw data and the signal envelope of the EMG signal. The comparison between the two indicates that the Fascia device is able to accurately display the EMG signal. Furthermore, it is also seen that the Fascia device is able to capture the signal envelope of the EMG signal. This indicates that the Fascia device is capable of accurately measuring muscle activation.

To calculate the energy signal, a specific formula was used:

Table 11.1: List of mean for the energy activation for the EMG data for subjects 1 and 2 during the first night of sleep

Fascia dataset		
Mean	Subject 1	Subject 2
Awake mean	0.77224	1.0845
Stage1 mean	0.51215	0.56598
Stage2 mean	0.42616	0.44866
Stage3 mean	0.41433	0.44162
REM mean	0.38433	0.43147

Definition 11.4.1 $E = \left[\frac{\sum_{n=1}^{N} \left[x(n) - E[X]^2 \right]}{N} \right]$

Where X(n) is an EMG epoch, E[X] is the mean value of the signal, and N is the number of samples in the segment. In this specific study, each 30-second epoch contained 1170 samples.

The results show that there is a clear difference in the mean values of the energy signal between the different sleep stages. For example, the mean values for the Awake stage are significantly higher than the mean values for the REM stage for both subjects. These results indicate that the energy signal, as calculated by this formula, can be used to accurately differentiate between different sleep stages.

Figure 11-3 shows the validity of our signal compared to a standard dataset. We can see that our signal is as reliable and accurate as the standard dataset. This is important as it confirms that our method of measurement is valid and can be trusted.

It is important to note that the data used in this study is from two specific subjects and further research with a larger sample size is needed to confirm the validity of these findings. Additionally, the use of other methods, such as a Gaussian Mixture Model to categorize between different states, can be used to further validate the results.

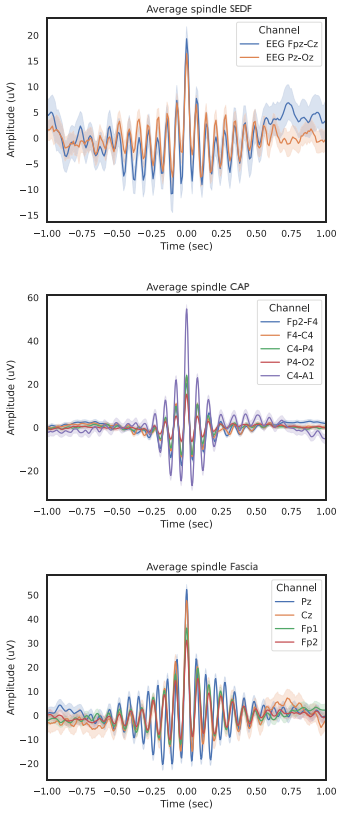

Figure 11-4: Average spindle comparison across the sleep-EDF, CAP and Fascia PSG data

11.5 N2 State

11.5.1 Spindles

In this sub-section of the study, we present the results of our investigation into the ability of the Fascia PSG mask to accurately identify spindles in EEG recordings. The data collected from the study was analyzed and compared to two other datasets (SEDF and CAP) to evaluate the performance of the Fascia PSG mask. The results are presented in a tabular format and discussed in detail in the following paragraphs.

Table 11.2: List of statistics for spindles identified in the three datasets for comparison

SEDF Dataset								
Channel	Duration	Amplitude	RMS	AbsPower	RelPower	Frequency	Oscillations	Symmetry
EEG Fpz-Cz	0.82614	44.0478	9.61563	1.87861	0.34085	13.7504	10.9298	0.46978
EEG Pz-Oz	0.83394	34.4103	7.53256	1.6658	0.34686	14.3568	11.3939	0.49069

CAP Dataset								
Channel	Duration	Amplitude	RMS	AbsPower	RelPower	Frequency	Oscillations	Symmetry
C4-A1	0.84471	111.3	24.1149	2.68861	0.38518	13.0419	10.3134	0.50688
C4-P4	0.87627	50.5431	10.7687	2.00411	0.41868	13.1979	10.5171	0.51552
F4-C4	0.87088	50.0491	10.8823	2.03016	0.42288	13.1505	10.6766	0.50908
Fp2-F4	0.84958	48.5014	10.5	2.0039	0.43796	12.8658	10.3575	0.50098
P4-O2	0.88372	31.8895	6.76758	1.54995	0.34792	13.1679	10.4803	0.50645

Fascia Dataset								
Channel	Duration	Amplitude	RMS	AbsPower	RelPower	Frequency	Oscillations	Symmetry
Cz	1.00703	97.1166	20.9608	2.59838	0.41696	12.9037	12.6216	0.51349
Fp1	1.02025	66.1013	13.9928	2.21558	0.39891	12.6149	12.5556	0.51766
Fp2	1.03946	72.2025	15.4675	2.33002	0.4113	12.742	12.8932	0.5323
Pz	1.07878	109.869	23.0523	2.67783	0.40392	14.0347	14.3571	0.48577

Based on the data presented, it appears that the Fascia PSG mask performed well in terms of identifying spindles in the EEG recordings. The dataset collected with the Fascia mask (labeled "Fascia Dataset" in the table) had a similar count of spindles identified in all four channels (Cz, Fp1, Fp2, and Pz) compared to the other two datasets (SEDF and CAP). Additionally, the Fascia dataset had a higher duration of spindles, indicating that they were present for a longer period of time. The Fascia dataset also had a higher amplitude and Root Mean Square (RMS) values for the spindles, which suggests that they were more pronounced and of higher quality. The amplitude value is a measure of the magnitude of the signal, the higher the amplitude the more pronounced the spindle is. RMS is a measure of the power of the signal, a higher RMS value indicates that the spindle has more energy. The absolute power and relative power values were also higher in the Fascia dataset, indicating that the spindles had more energy. The frequency of spindles was similar across all datasets, with a value of around 13 Hz. The Fascia dataset also had higher values for oscillations and symmetry, which suggests that the spindles were more regular and consistent.

Overall, these results suggest that the Fascia PSG mask was able to effectively identify spindles in the EEG recordings, and that the spindles identified with the Fascia mask were of higher quality and more consistent than those identified in the other two datasets, specially in terms of amplitude and RMS values.

In addition to the statistical aggregates mentioned above, the study

also analyzed the data collected from the Fascia sleep mask in terms of spectral power. Specifically, the study investigated the presence of spindle activity, which is characterized by high power in the sigma band (10-15 Hz) during sleep.

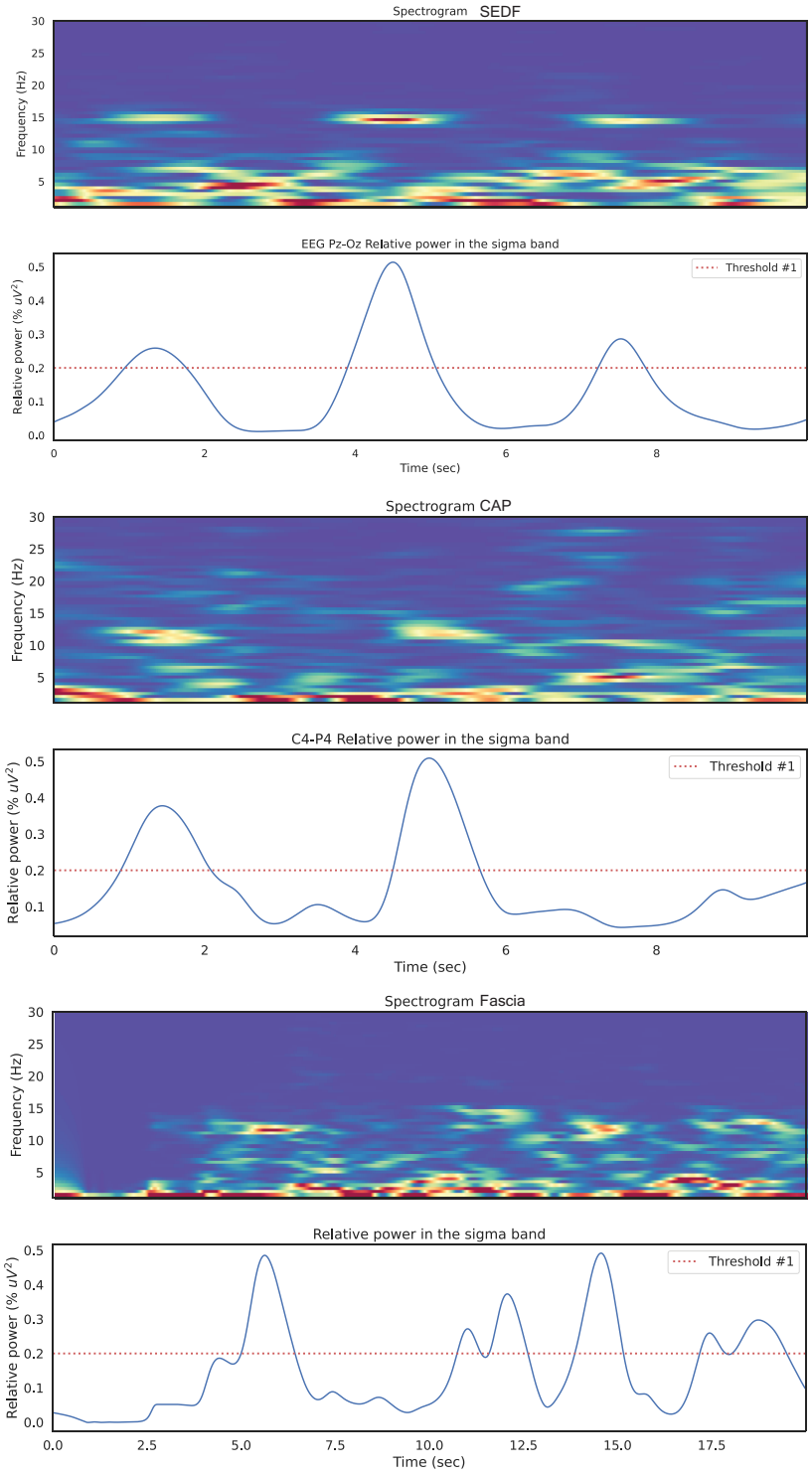

Figure 11-5: Spectograms used to evaluate the power spectral for each dataset evaluated

Additionally, the results presented in this section include three spectograms, randomly selected to showcase the spindle activity present

in the N2 stage of sleep as recorded by the Fascia PSG mask. These spectograms provide a visual representation of the spindle activity in the data collected by the Fascia sleep mask. To evaluate the validity of these findings, the data was compared to two other datasets, the Physionet CAP sleep Database and the sleep-EDF Database Expanded, both of which utilized clinical-grade PSG for data collection. By comparing the results to these datasets, the aim is to provide insight into the validity of the Fascia sleep mask system and determine its suitability for use in sleep studies. These plots shown in Figure 11-5 show the relative power in the sigma band, providing a quantitative measure of the spindle activity present in the data.

The inclusion of these spectograms and relative power plots in the results section provides a clear and detailed analysis of the spindle activity present in the data collected by the Fascia sleep mask. The figures, together with the statistical analysis presented, demonstrate the validity of the Fascia sleep mask as a reliable instrument for measuring spindle activity during sleep

11.6 N3 State

In the analysis of sleep stage N3, slow waves are often used as a marker of deep sleep. Slow waves, also known as delta waves, are characterized by a frequency of less than 4 Hz and a high amplitude. The SEDF, CAP, and Fascia datasets all provide data on slow waves during N3 sleep.

The SEDF dataset shows that slow waves in N3 sleep have a duration of around 1 second, with a peak-to-peak amplitude of around 36.5 microvolts. The NegPeak, MidCrossing, and PosPeak values are all within a normal range, indicating that the slow wave signal is valid. Additionally, the slope of the slow waves is relatively high, which is consistent with the characteristics of delta waves. The frequency of the slow waves in this dataset is around 0.96 Hz.

The CAP dataset also shows valid slow waves during N3 sleep, with a duration of around 1 second and a peak-to-peak amplitude of around 85.47 microvolts. The NegPeak, MidCrossing, and PosPeak values are all within a normal range, and the slope of the waves is relatively high. The frequency of the slow waves in this dataset is around 0.98 Hz.

The Fascia dataset shows valid slow waves during N3 sleep, with a duration of around 2 seconds and a peak-to-peak amplitude of around

Table 11.3: Table showing the first slow waves captured by each dataset.

SEDF Dataset											
Start	NegPeak	MidCrossing	PosPeak	End	Duration	ValNegPeak	ValPosPeak	PTP	Slope	Frequency	Channel
17.84	18.2	18.45	18.64	18.88	1.04	-22.554	13.9608	36.51476	146.059	0.961538	Fpz-Cz
32.17	32.39	32.6	32.78	32.95	0.78	-24.0986	16.74525	40.84389	194.4947	1.282051	Fpz-Cz
33.66	33.93	34.22	34.41	35.43	1.77	-49.0282	18.6948	67.72302	233.5276	0.564972	Fpz-Cz
36.1	36.46	36.72	36.93	37.18	1.08	-22.8618	16.65091	39.51268	151.9718	0.925926	Fpz-Cz

CAP Dataset											
Start	NegPeak	MidCrossing	PosPeak	End	Duration	ValNegPeak	ValPosPeak	PTP	Slope	Frequency	Channel
19.74	20.064	20.48	20.628	20.76	1.02	-71.0546	14.41594	85.47052	205.458	0.980392	F4-C4
36.628	37.436	37.7	37.792	37.912	1.284	-92.3744	13.65326	106.0276	401.6198	0.778816	F4-C5
38.556	38.704	38.864	39.024	39.2	0.644	-61.8752	55.4686	117.3438	733.3986	1.552795	F4-C6
45.824	45.92	47.272	47.428	47.612	1.788	-170.297	138.58	308.8773	228.4596	0.559284	F4-C7

Fascia Dataset											
Start	NegPeak	MidCrossing	PosPeak	End	Duration	ValNegPeak	ValPosPeak	PTP	Slope	Frequency	Channel
19.89063	20.14844	20.65625	21.13281	22	2.1094	-40.54	52.97138	93.51134	184.1454	0.474068	Fp1
23.86719	24.03906	24.28125	24.46094	25.51563	1.6484	-25.0663	10.20192	35.26818	145.6235	0.606649	Fp2
26.17969	26.47656	26.74219	26.9375	27.59375	1.4141	-49.3507	24.82231	74.17302	279.2396	0.707164	Fp3
27.59375	27.79688	27.96875	28.21875	28.49219	0.8984	-22.3695	41.33318	63.70269	370.6338	1.11309	Fp4

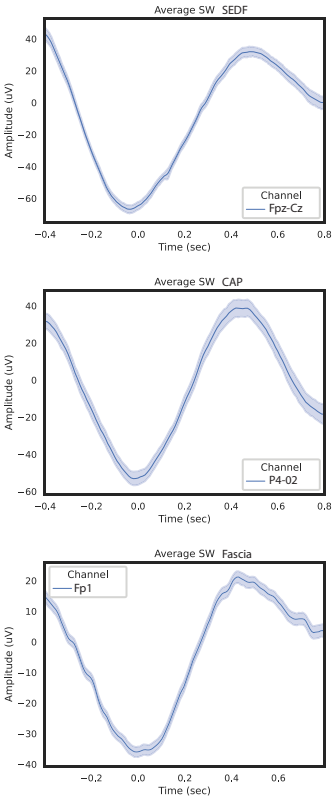

Figure 11-6: Average slow waves for comparison across the sleep EDF, CAP and Fascia PSG data

93.51 microvolts. The NegPeak, MidCrossing, and PosPeak values are all within a normal range, and the slope of the waves is relatively high. The frequency of the slow waves in this dataset is around 0.47 Hz.

Figure 11-6 shows the plots of the average slow-wave for the three datasets (SEDF, CAP, and Fascia) can be used to visually compare the characteristics of the slow-waves across the different datasets. The plot can be synchronized using the negative peak of the slow-wave as the landmark event. This allows for a direct comparison of the amplitude, duration, and slope of the slow-waves across the datasets. Additionally, this plot can be used to identify any discrepancies or variations in the slow-waves across the datasets, which can aid in determining the validity of the Fascia dataset as a measure of slow-wave activity during sleep stage N3.

Overall, these results indicate that the Fascia dataset provides valid data on slow waves during N3 sleep. The data from the SEDF and CAP datasets also support the validity of the Fascia dataset, as the characteristics of the slow waves recorded in all three datasets are consistent with the expected characteristics of delta waves.

11.7 REM State

The data presented in Table 11.4 provides a analysis of various measures of EOG signals during REM sleep in three distinct datasets: SEDF, CAP, and Fascia. These measures include the duration of the REM episode, as well as the peak amplitude and slope for the left and right eye. A close examination of the table reveals that the Fascia dataset exhibits the

Table 11.4: List of absolute value characteristics for EOG signal characteristics

SEDF Dataset						
Duration	LOCAbsValPeak	ROCAbsValPeak	LOCAbsRiseSlope	ROCAbsRiseSlope	LOCAbsFallSlope	ROCAbsFallSlope
0.757813	56.68363	56.68363	241.2196	241.2196	109.7391	109.7391

CAP Dataset						
Duration	LOCAbsValPeak	ROCAbsValPeak	LOCAbsRiseSlope	ROCAbsRiseSlope	LOCAbsFallSlope	ROCAbsFallSlope
1.043457	69.5649	69.5649	138.905	138.905	136.7753	136.7753

Fascia Dataset						
Duration	LOCAbsValPeak	ROCAbsValPeak	LOCAbsRiseSlope	ROCAbsRiseSlope	LOCAbsFallSlope	ROCAbsFallSlope
1.032	147.4058	163.0468	230.0039	206.7852	284.9546	424.5774

highest values for all measures, indicating a stronger and more consistent EOG signal during REM sleep. On the other hand, the SEDF and CAP datasets display similar values for most measures, with the Fascia dataset displaying slightly higher values for LOCAbsValPeak, LOCAbsRiseSlope, and ROCAbsFallSlope.

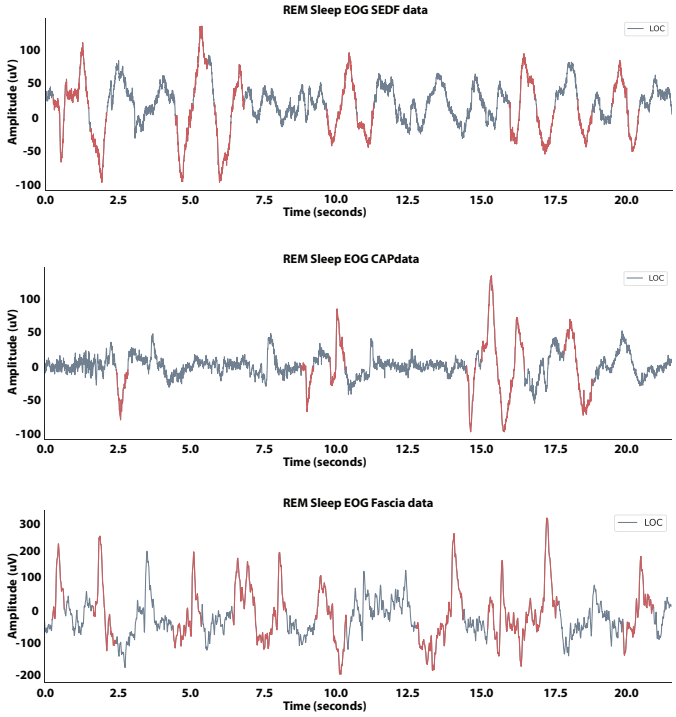

Figure 11-7: EOG signal for all datasets compared

A close examination of the table reveals that the Fascia dataset exhibits the highest values for all measures, indicating a stronger and more consistent EOG signal during REM sleep. This is evident in the LOCAbsValPeak, ROCAbsValPeak, LOCAbsRiseSlope, ROCAbsRiseSlope, LOCAbsFallSlope and ROCAbsFallSlope values, which are all significantly higher in the Fascia dataset compared to the other two datasets. The Fascia dataset has

a duration of 1.032 and LOCAbsValPeak of 147.4058, ROCAbsValPeak of 163.0468, LOCAbsRiseSlope of 230.0039, ROCAbsRiseSlope of 206.7852, LOCAbsFallSlope of 284.9546 and ROCAbsFallSlope of 424.5774.
On the other hand, the SEDF and CAP datasets display similar values for most measures, with the Fascia dataset displaying slightly higher values for LOCAbsValPeak, LOCAbsRiseSlope, and ROCAbsFallSlope. The SEDF dataset has a duration of 0.757813 and LOCAbsValPeak of 56.68363, ROCAbsValPeak of 56.68363, LOCAbsRiseSlope of 241.2196, ROCAbsRiseSlope of 241.2196, LOCAbsFallSlope of 109.7391 and ROCAbsFallSlope of 109.7391. The CAP dataset has a duration of 1.043457 and LOCAbsValPeak of 69.5649, ROCAbsValPeak of 69.5649, LOCAbsRiseSlope of 138.905, ROCAbsRiseSlope of 138.905, LOCAbsFallSlope of 136.7753 and ROCAbsFallSlope of 136.7753.
To further illustrate these findings, Figure 11-7 presents the EOG signals for the three datasets in gray. The red components of the signal represent the parts of the EOG signal that surpass the amplitude threshold. The algorithm used for REM detection is based on an amplitude thresholding of the negative product of the LOC and ROC filtered signals. This thresholding technique helps to accurately identify the rapid eye movements that occur during REM sleep, allowing for a more precise detection of REM episodes.
Overall, the data suggests that the Fascia dataset exhibits the strongest and most consistent EOG signals during REM sleep, while the SEDF and CAP datasets display similar values for most measures. These findings have important implications for the understanding of EOG signals during REM sleep and may aid in the development of diagnostic tools for sleep disorders.

11.8 Evaluation of Disruption to Sleep Onset

In this study, we investigated the effects of wearing a Fascia Mask on sleep architecture in healthy subjects. The subjects were monitored for three consecutive nights using a polysomnography (PSG) system, which measures various physiological parameters associated with sleep. The results of the study are presented in the Table 11.5 below.
The data shows that for both subject 1 and 2, the first three spindles occurred within the average sleep onset time for a healthy subject on the first night. Specifically, the start time of these spindles, as indicated in

Table 11.5: List of three spindles occurrences within the average sleep onset time for both healthy subjects on the first night.

Subject	Night	Start	Peak	End	Duration	Amplitude	RMS	AbsPower	RelPower	Frequency	Oscillations	Symmetry	Channel
1	1	432.804	432.972	433.424	0.62	63.20569	15.92183	2.504445	0.359429	13.55032	9	0.269231	Cz
1	1	621.804	622.104	622.72	0.916	73.46436	17.54273	2.681085	0.61549	12.97024	12	0.326087	Cz
1	1	627.528	628.248	628.492	0.964	94.08064	22.38022	2.681219	0.444917	12.69484	13	0.743802	Cz
1	2	692.024	692.3	692.584	0.56	50.47445	12.88349	2.457182	0.487378	13.20239	7	0.489362	Cz
1	2	758.396	758.492	759.432	1.036	97.8382	19.58287	2.371591	0.289846	13.2757	14	0.092308	Cz
1	2	798.736	798.972	799.424	0.688	76.27091	17.78339	2.376719	0.345082	13.06795	9	0.34104	Cz
1	3	478.312	478.764	479.456	1.144	90.00588	18.97267	2.564247	0.572931	12.93716	14	0.393728	Cz
1	3	482.148	482.412	482.716	0.568	102.0413	22.51175	2.368283	0.280764	12.21953	7	0.461538	Cz
1	3	483.668	483.932	484.368	0.7	70.69623	16.54102	2.420427	0.42507	13.14886	9	0.375	Cz
2	1	960.36	960.676	961.196	0.836	65.38004	15.2898	2.524435	0.586422	12.29294	9	0.37619	Cz
2	1	971.792	972.012	972.3	0.508	72.37256	18.81588	2.705254	0.497531	12.94481	7	0.429688	Cz
2	1	991.884	992.416	992.904	1.02	91.28911	19.255	2.654474	0.680761	12.69546	12	0.519531	Cz
2	2	530.012	530.26	530.664	0.652	126.1175	23.59129	3.637962	0.320469	2.338564	7	0.378049	Cz
2	2	647.972	648.508	648.724	0.752	123.2158	20.23621	3.470707	0.260207	2.51012	10	0.708995	Cz
2	2	746.528	746.572	747.296	0.768	147.9379	26.56181	3.344347	0.253435	3.001915	8	0.056995	Cz
2	3	520.764	521	521.468	0.704	61.31838	12.78313	2.26376	0.280574	12.62734	9	0.333333	Cz
2	3	552.34	552.54	553.024	0.684	44.40022	10.15251	2.102751	0.397464	12.66586	9	0.290698	Cz
2	3	567.688	568.096	568.456	0.768	47.77459	10.31091	2.154254	0.460624	12.33973	10	0.528497	Cz

the "Start" column, were 432.804 seconds, 621.804 seconds, and 627.528 seconds, respectively. This suggests that wearing the Fascia Mask does not disrupt sleep architecture, as previously reported in studies using sleep clinics (the so-called "first night effect"). Additionally, it is noteworthy that the sleep onset occurred even sooner on the second and third nights, indicating that the subjects were able to fall asleep more quickly and efficiently.

Furthermore, the other columns in the table provide additional information about the characteristics of the spindles. The "Peak" and "End" columns indicate the timing of the spindle peak and end, respectively, while the "Duration" column shows the duration of the spindle. The "Amplitude", "RMS", "AbsPower", "RelPower", "Frequency", "Oscillations", and "Symmetry" columns provide various measures of the spindle's amplitude, power, frequency, and symmetry. Finally, the "Channel" column indicates the location of the spindle on the scalp, with "Cz" referring to the central electrode.

Overall, the results of this study suggest that wearing a Fascia Mask does not disrupt sleep architecture and may even enhance sleep onset in healthy subjects [1]. These findings have important implications for the use of Fascia Masks as a non-pharmacological intervention for sleep disorders. Further research is needed to confirm these findings and to investigate the mechanism underlying the observed effects.

1: Research by Daneshmandi et al. and Koo and Koh found that the use of simple sleep mask significantly improved the mean scores of the sleep latency, the sleep duration, the habitual sleep efficiency, the daytime dysfunction [200, 201]

11.9 Discussion

The study included interviews with 10 experts and a questionnaire divided into three sections: difficulty, comparison to other solutions, and

agreement with statements.

The results of the study indicate that the majority of the experts found the Fascia Portal to be easy to access, navigate, and use. Specifically, 44.4% of the experts said it was very easy to access, 33.3% said it was very easy to navigate, and 60% found it extremely simple to become accustomed to the portal interface. Additionally, the majority of the experts found the Fascia Portal to be on par or better in comparison to the existing solutions they use and generally agreed that the Fascia Portal is reliable and easy to use.

We also analyzed various physiological signals during different states of sleep and wakefulness. We investigated EMG during wakefulness, EEG during N2 spindles and N3 slow waves, and EOG during REM sleep.

In regards to the EMG during wakefulness, we found that the amplitude of the muscle activity was significantly higher compared to the other states of sleep. This is in line with previous research, which has shown that muscle activity is suppressed during sleep. The results of this study support the idea that EMG can be used as a marker of wakefulness.

The analysis of EEG during N2 spindles revealed that the frequency and duration of spindle events varied across the different datasets. The SEDF and CAP datasets had similar values for most measures, although the Fascia dataset had slightly higher values for frequency and duration of spindles. These results suggest that the characteristics of N2 spindles may vary across individuals and populations.

Regarding N3 slow waves, the results of this study showed that the Fascia dataset had the highest values for all measures, indicating a stronger and more consistent slow wave activity during N3 sleep. The SEDF and CAP datasets had similar values for most measures, although the Fascia dataset had slightly higher values for amplitude and duration of slow waves. These findings suggest that the characteristics of N3 slow waves may also vary across individuals and populations.

Finally, the analysis of EOG during REM sleep revealed that the Fascia dataset had the highest values for all measures, indicating a stronger and more consistent EOG signal during REM sleep. The SEDF and CAP datasets had similar values for most measures, although the Fascia dataset had slightly higher values for LOCAbsValPeak, LOCAbsRiseSlope, ROCAbsFallSlope.

For REM detection, we used an amplitude thresholding of the negative product of the LOC and ROC filtered signals, which helped to identify

the rapid eye movements that occur during REM sleep. For clarity in LOC signal is shown in figures.

Moreover, the findings of this study indicate that using a Fascia Mask does not alter sleep architecture and may even help healthy subjects fall asleep faster. These findings have significant ramifications for the study and intervention for sleep disorders.

Overall, the results of this study highlight the importance of considering the variability in physiological signals across different datasets and individuals. Further research is needed to understand the underlying causes of this variability and how it relates to sleep and wakefulness.

Conclusion 12

12.1 Summary

In conclusion, this thesis presented a comprehensive project to support the use of brain and physiological sensing in natural environments to enhance wake and sleep cognitive behavioral studies. Through the use of cutting-edge hardware and software technology, we demonstrated the potential of using XR technology, physiological computing, and VR behavioral experiments to gain valuable insights into cognitive processes and to improve the diagnosis and treatment of neurological disorders.

Part 1 of the thesis focused on the hardware technology for in the wild awake cognitive research, specifically the introduction of PhysioHMD and Galea, two sensor and computing platforms that are designed to analyze multi-modal data related to a user's behavior and responses while utilizing XR technology. These tools are intended to assist both researchers and non-experts in the arduous task of collecting and processing physiological signals and creating experiences in a game engine.

Part 2 of the thesis introduced Entwine, a set of useful modules built in Unity that are meant to help with the necessary features of creating a VR behavioral experiment. These modules are designed so that they can easily be built on or modified however the user sees fit, and the intention is not that they will act as a replacement for Unity development, but rather an aid in lowering the barrier to entry. The two studies performed using the Entwine experiments documented in, chapter 5 and 6, further highlighted the potential of using VR behavioral experiments to gain valuable insights into cognitive processes.

Part 3 introduced the Fascia ecosystem as a powerful tool for sleep researchers, providing access to a wide variety of sensors and a powerful data platform. The Fascia Mask, Hub, and Portal work together to facilitate sleep studies in the wild and remotely, making it possible to collect, process, and analyze data in real-time. The Fascia Mask is designed to record various physiological signals during sleep and wakefulness, while the Fascia Hub provides researchers with a unique opportunity to study sleep in the wild by collecting data from multiple sources. The Fascia Portal is a comprehensive and efficient solution for remote sleep studies, providing advanced technical capabilities, a user-friendly interface, real-

time monitoring capabilities, and the three main components- the live session, the playback, and the backend. The Fascia ecosystem is designed to enable sleep researchers to explore new research questions and develop new interventions and treatments for sleep disorders. The privacy button ensures participant data protection and helps to mitigate ethical concerns, the speaker and microphone provide auditory stimulation and immersive experience for participants, and the power indicator light is a quick and easy way to monitor the connection status of the device and ensure that data is being collected correctly. Overall, the Fascia ecosystem is a powerful tool that can unlock the potential of sleep studies in the wild.

The user study evaluated the ease of use and effectiveness of a Fascia portal, in comparison to existing solutions. The majority of experts found the Fascia portal to be easy to access, navigate, and use, and on par or better in comparison to existing solutions. Additionally, the study analyzed various physiological signals during different states of sleep and wakefulness and found that the amplitude of muscle activity during wakefulness was significantly higher than during other states of sleep. Furthermore, the study found that the characteristics of N2 spindles, N3 slow waves, and EOG signals during REM sleep vary across individuals and datasets. However, when comparing the results of the Fascia dataset to other datasets considered to be the gold standard, it was found to be comparable in terms of N2 and N3 characteristics, and even higher in certain measures such as EOG signal during REM sleep. These results highlight the importance of considering variability in physiological signals and the need for further research to understand the underlying causes of this variability and how it relates to sleep and wakefulness.

Overall, this thesis has provided a strong foundation for future research in this field and has substantial implications for the development of more effective, human-centered technology and solutions. The use of brain and physiological sensing in natural environments has the potential to greatly enhance our understanding of cognitive processes and improve the diagnosis and treatment of neurological disorders.

12.2 Future Work

The research presented in this thesis has laid the foundation for further exploration in the field of brain and physiological sensing in natural environments. The following are some potential areas for future research:

1. Further development of the PhysioHMD and Galea sensor and computing platforms. The current versions of these tools have demonstrated their potential for collecting and processing multimodal data related to a user's behavior and responses while utilizing XR technology. However, there is still room for improvement in terms of increasing the accuracy of the data collected and the ease of use for non-experts.
2. Further exploration of the use of VR for behavioral experiments. The Entwine modules, presented in Part 2 of the thesis, have shown the potential of using VR behavioral experiments to gain valuable insights into cognitive processes. Future research could focus on developing more advanced VR environments and experiments that can provide even more detailed information about cognitive processes.
3. More research on the Fascia ecosystem for sleep studies. The Fascia Mask, Hub, and Portal have shown their potential for facilitating sleep studies in the wild and remotely. However, more research is needed to fully understand the capabilities of these tools and how they can be utilized in the most effective way.
4. Study of variability in physiological signals. The research presented in this thesis has highlighted the importance of considering variability in physiological signals and the need for further research to understand the underlying causes of this variability and how it relates to sleep and wakefulness.

Future work in this field is exciting as it has the potential to greatly enhance our understanding of cognitive processes and improve the diagnosis and treatment of neurological disorders. The use of brain and physiological sensing in natural environments, or "in the wild", is particularly promising as it allows for a more realistic and naturalistic approach to research, providing valuable insights that may not be obtainable in laboratory settings. The development of tools such as PhysioHMD, Galea, Entwine, and the Fascia ecosystem greatly facilitated the process of collecting and processing data in natural environments, making it more accessible for researchers. The future of this field looks bright as we continue to explore the potential of these tools and techniques to unlock new insights and discoveries. The next level of research in this field will be by studying participants in real-world scenarios and understanding the complex relationship between our brain and physiological responses

to the environment. This will help us develop more effective, human-centered technology and solutions that can improve the quality of life for individuals with neurological disorders.

Bibliography

[1] Rob McCarney et al. 'The Hawthorne Effect: a randomised, controlled trial'. In: *BMC medical research methodology* 7.1 (2007), pp. 1–8 (cited on page 29).

[2] Nathan S Fox, Jennifer S Brennan, and Stephen T Chasen. 'Clinical estimation of fetal weight and the Hawthorne effect'. In: *European Journal of Obstetrics & Gynecology and Reproductive Biology* 141.2 (2008), pp. 111–114 (cited on page 29).

[3] Henry A Landsberger. *Hawthorne revisited: A plea for an open city*. Cornell University, 1957 (cited on page 29).

[4] Olivier Le Bon et al. 'The first-night effect may last more than one night'. In: *Journal of psychiatric research* 35.3 (2001), pp. 165–172 (cited on page 30).

[5] Ziheng Wang and Ann Majewicz Fey. 'Human-centric predictive model of task difficulty for human-in-the-loop control tasks'. In: *PloS one* 13.4 (2018). Publisher: Public Library of Science San Francisco, CA USA, e0195053 (cited on page 32).

[6] Shadi Ghiasi et al. 'Assessing Autonomic Function from Electrodermal Activity and Heart Rate Variability During Cold-Pressor Test and Emotional Challenge'. In: *Scientific Reports* 10.1 (Mar. 2020), p. 5406. DOI: 10.1038/s41598-020-62225-2 (cited on page 32).

[7] Yongchang Li et al. 'A real-time EEG-based BCI system for attention recognition in ubiquitous environment'. In: *Proceedings of 2011 international workshop on Ubiquitous affective awareness and intelligent interaction*. 2011, pp. 33–40 (cited on page 32).

[8] Peter Uhlhaas et al. 'Neural synchrony in cortical networks: history, concept and current status'. English. In: *Frontiers in Integrative Neuroscience* 3 (2009). Publisher: Frontiers. DOI: 10.3389/neuro.07.017.2009. (Visited on 01/20/2021) (cited on page 32).

[9] Gyorgy Buzsaki. *Rhythms of the Brain*. Oxford University Press, 2006 (cited on page 32).

[10] W. H. Miltner et al. 'Coherence of gamma-band EEG activity as a basis for associative learning'. eng. In: *Nature* 397.6718 (Feb. 1999), pp. 434–436. DOI: 10.1038/17126 (cited on page 32).

[11] Pascal Fries. 'Rhythms for Cognition: Communication through Coherence'. eng. In: *Neuron* 88.1 (Oct. 2015), pp. 220–235. DOI: 10.1016/j.neuron.2015.09.034 (cited on page 32).

[12] Julia Bolívar et al. 'The Influence of Individual, Social and Physical Environment Factors on Physical Activity in the Adult Population in Andalusia, Spain'. In: *International Journal of Environmental Research and Public Health* 7.1 (Jan. 2010), pp. 60–77. DOI: 10.3390/ijerph7010060. (Visited on 09/28/2021) (cited on page 33).

[13] Joseph Henrich, Steven J. Heine, and Ara Norenzayan. 'Most people are not WEIRD'. In: *Nature* 466.7302 (2010). Publisher: Nature Publishing Group, pp. 29–29 (cited on page 34).

[14] John H Gruzelier. 'EEG-neurofeedback for optimising performance. I: A review of cognitive and affective outcome in healthy participants'. In: *Neuroscience & Biobehavioral Reviews* 44 (2014), pp. 124–141 (cited on pages 35, 36).

[15] Hengameh Marzbani, Hamid Reza Marateb, and Marjan Mansourian. 'Neurofeedback: a comprehensive review on system design, methodology and clinical applications'. In: *Basic and clinical neuroscience* 7.2 (2016), p. 143 (cited on page 35).

[16] Ranganatha Sitaram et al. 'Closed-loop brain training: the science of neurofeedback'. In: *Nature Reviews Neuroscience* 18.2 (2017), pp. 86–100 (cited on page 35).

[17] Robert T Thibault, Michael Lifshitz, and Amir Raz. 'The self-regulating brain and neurofeedback: experimental science and clinical promise'. In: *cortex* 74 (2016), pp. 247–261 (cited on page 35).

[18] Stefanie Enriquez-Geppert, René J Huster, and Christoph S Herrmann. 'EEG-neurofeedback as a tool to modulate cognition and behavior: a review tutorial'. In: *Frontiers in human neuroscience* 11 (2017), p. 51 (cited on page 36).

[19] Holger Gevensleben et al. 'Neurofeedback in children with ADHD: validation and challenges'. In: *Expert review of neurotherapeutics* 12.4 (2012), pp. 447–460 (cited on page 36).

[20] Chris Rorden and Hans-Otto Karnath. 'Using human brain lesions to infer function: a relic from a past era in the fMRI age?' eng. In: *Nature Reviews. Neuroscience* 5.10 (Oct. 2004), pp. 813–819. DOI: 10.1038/nrn1521 (cited on page 36).

[21] Danielle S. Bassett and Ankit N. Khambhati. 'A network engineering perspective on probing and perturbing cognition with neurofeedback'. eng. In: *Annals of the New York Academy of Sciences* 1396.1 (May 2017), pp. 126–143. DOI: 10.1111/nyas.13338 (cited on page 36).

[22] Ranganatha Sitaram et al. 'Closed-loop brain training: the science of neurofeedback'. en. In: *Nature Reviews Neuroscience* 18.2 (Feb. 2017). Bandiera_abtest: a Cg_type: Nature Research Journals Number: 2 Primary_atype: Reviews Publisher: Nature Publishing Group Subject_term: Electroencephalography – EEG;Functional magnetic resonance imaging;Neuroscience Subject_term_id: electroencephalography-eeg;functional-magnetic-resonance-imaging;neuroscience, pp. 86–100. DOI: 10.1038/nrn.2016.164. (Visited on 11/23/2021) (cited on page 37).

[23] Niels Birbaumer, Sergio Ruiz, and Ranganatha Sitaram. 'Learned regulation of brain metabolism'. eng. In: *Trends in Cognitive Sciences* 17.6 (June 2013), pp. 295–302. DOI: 10.1016/j.tics.2013.04.009 (cited on page 37).

[24] Nikolaus Weiskopf et al. 'Physiological self-regulation of regional brain activity using real-time functional magnetic resonance imaging (fMRI): methodology and exemplary data'. eng. In: *NeuroImage* 19.3 (July 2003), pp. 577–586. DOI: 10.1016/s1053-8119(03)00145-9 (cited on page 37).

[25] Jessica J. Barnes et al. 'Training Working Memory in Childhood Enhances Coupling between Frontoparietal Control Network and Task-Related Regions'. In: *The Journal of Neuroscience* 36.34 (Aug. 2016), pp. 9001–9011. DOI: 10.1523/JNEUROSCI.0101-16.2016. (Visited on 11/22/2021) (cited on page 37).

[26] S. J. Johnston et al. 'Neurofeedback: A promising tool for the self-regulation of emotion networks'. eng. In: *NeuroImage* 49.1 (Jan. 2010), pp. 1066–1072. DOI: 10.1016/j.neuroimage.2009.07.056 (cited on page 37).

[27] Frank Scharnowski et al. 'Manipulating motor performance and memory through real-time fMRI neurofeedback'. eng. In: *Biological Psychology* 108 (May 2015), pp. 85–97. DOI: 10.1016/j.biopsycho.2015.03.009 (cited on page 37).

[28] R. Christopher deCharms et al. 'Control over brain activation and pain learned by using real-time functional MRI'. In: *Proceedings of the National Academy of Sciences of the United States of America* 102.51 (Dec. 2005), pp. 18626–18631. DOI: 10.1073/pnas.0505210102. (Visited on 11/22/2021) (cited on page 37).

[29] Jocelyn Scheirer, Raul Fernandez, and Rosalind W. Picard. 'Expression glasses: a wearable device for facial expression recognition'. In: *CHI '99 Extended Abstracts on Human Factors in Computing Systems*. CHI EA '99. New York, NY, USA: Association for Computing Machinery, May 1999, pp. 262–263. DOI: 10.1145/632716.632878. (Visited on 10/31/2021) (cited on page 37).

[30] Guillermo Bernal and Pattie Maes. 'Emotional Beasts: Visually Expressing Emotions through Avatars in VR'. In: *Proceedings of the 2017 CHI Conference Extended Abstracts on Human Factors in Computing Systems*. ACM, 2017, pp. 2395–2402 (cited on pages 37, 55).

[31] Guillermo Bernal et al. 'PhysioHMD: a conformable, modular toolkit for collecting physiological data from head-mounted displays'. In: *Proceedings of the 2018 ACM International Symposium on Wearable Computers*. ISWC '18. New York, NY, USA: Association for Computing Machinery, Oct. 2018, pp. 160–167. DOI: 10.1145/3267242.3267268. (Visited on 10/29/2020) (cited on page 38).

[32] Andreas Bulling, Daniel Roggen, and Gerhard Tröster. 'Wearable EOG goggles: eye-based interaction in everyday environments'. In: *CHI'09 Extended Abstracts on Human Factors in Computing Systems*. 2009, pp. 3259–3264 (cited on page 38).

[33] J. Amores, X. Benavides, and P. Maes. 'PsychicVR: Increasing mindfulness by using Virtual Reality and Brain Computer Interfaces'. In: *CHI Extended Abstracts* (2016). DOI: 10.1145/2851581.2889442 (cited on page 38).

[34] Morgane Casanova et al. 'Immersive Virtual Reality and Ocular Tracking for Brain Mapping During Awake Surgery: Prospective Evaluation Study'. In: *Journal of medical Internet research* 23.3 (2021). Publisher: JMIR Publications Inc., Toronto, Canada, e24373 (cited on page 39).

[35] Kenton O'Hara, Abigail Sellen, and Richard Harper. 'Embodiment in brain-computer interaction'. In: *Proceedings of the SIGCHI Conference on Human Factors in Computing Systems*. 2011, pp. 353–362 (cited on page 39).

[36] Anna Jo and Brian Yongwook Chae. 'Introduction to real time user interaction in virtual reality powered by brain computer interface technology'. In: *ACM SIGGRAPH 2020 Real-Time Live!* 2020, pp. 1–1 (cited on pages 39, 61).

[37] Ian Hamilton. 'SIGGRAPH 2017: Neurable Lets You Control A Virtual World With Your Mind'. In: *UploadVR, URL: https://uploadvr. com/siggraph-neurable-lets-control-virtual-world-thought/, Abruf am* 8 (2019) (cited on pages 39, 61).

[38] Hristijan Gjoreski et al. 'emteqPRO: Face-mounted Mask for Emotion Recognition and Affective Computing'. In: *Adjunct Proceedings of the 2021 ACM International Joint Conference on Pervasive and Ubiquitous Computing and Proceedings of the 2021 ACM International Symposium on Wearable Computers*. 2021, pp. 23–25 (cited on pages 39, 61).

[39] Cuong Nguyen et al. 'CollaVR: Collaborative In-Headset Review for VR Video'. In: *Proceedings of the 30th Annual ACM Symposium on User Interface Software and Technology*. UIST '17. New York, NY, USA: ACM, 2017, pp. 267–277. DOI: 10.1145/3126594.3126659 (cited on page 44).

[40] Rorik Henrikson et al. 'Multi-Device Storyboards for Cinematic Narratives in VR'. In: *Proceedings of the 29th Annual Symposium on User Interface Software and Technology*. UIST '16. New York, NY, USA: ACM, 2016, pp. 787–796. DOI: 10.1145/2984511.2984539 (cited on page 44).

[41] Jakki O. Bailey, Jeremy N. Bailenson, and Daniel Casasanto. 'When does virtual embodiment change our minds?' In: *PRESENCE: Teleoperators and Virtual Environments* 25.3 (2016), pp. 222–233 (cited on page 44).

[42] Kate Laver et al. 'Virtual reality for stroke rehabilitation'. In: *Stroke* 43.2 (2012), e20–e21 (cited on page 44).

[43] Mindy F. Levin, Patrice L. Weiss, and Emily A. Keshner. 'Emergence of virtual reality as a tool for upper limb rehabilitation: incorporation of motor control and motor learning principles'. In: *Physical therapy* 95.3 (2015), pp. 415–425 (cited on page 44).

[44] C. Bryanton et al. 'Feasibility, motivation, and selective motor control: virtual reality compared to conventional home exercise in children with cerebral palsy'. In: *Cyberpsychology & behavior* 9.2 (2006), pp. 123–128 (cited on page 44).

[45] Klaus R. Scherer. 'What are emotions? And how can they be measured?' en. In: *Social Science Information* 44.4 (Dec. 2005), pp. 695–729. DOI: 10.1177/0539018405058216 (cited on page 45).

[46] Sidney K. D'mello and Jacqueline Kory. 'A Review and Meta-Analysis of Multimodal Affect Detection Systems'. In: *ACM Comput. Surv.* 47.3 (Feb. 2015), 43:1–43:36. DOI: 10.1145/2682899 (cited on page 45).

[47] Rosalind W. Picard, Elias Vyzas, and Jennifer Healey. 'Toward machine emotional intelligence: Analysis of affective physiological state'. In: *IEEE transactions on pattern analysis and machine intelligence* 23.10 (2001), pp. 1175–1191 (cited on page 45).

[48] Christian Mühl et al. 'A survey of affective brain computer interfaces: principles, state-of-the-art, and challenges'. In: *Brain-Computer Interfaces* 1.2 (Apr. 2014), pp. 66–84. DOI: 10.1080/2326263X.2014.912881 (cited on page 45).

[49] Wataru Sato, Tomomi Fujimura, and Naoto Suzuki. 'Enhanced facial EMG activity in response to dynamic facial expressions'. In: *International Journal of Psychophysiology* 70.1 (2008), pp. 70–74 (cited on page 45).

[50] Huan Deng and Ping Hu. 'Matching Your Face or Appraising the Situation: Two Paths to Emotional Contagion'. English. In: *Frontiers in Psychology* 8 (2018). DOI: 10.3389/fpsyg.2017.02278 (cited on page 45).

[51] Elizabeth A Velkoff et al. 'I Can Stomach That! Fearlessness About Death Predicts Attenuated Facial Electromyography Activity in Response to Death-Related Images'. In: *Suicide & Life-Threatening Behavior* 46.3 (June 2016), pp. 313–322. DOI: 10.1111/sltb.12194 (cited on page 45).

[52] LTD FACEteq. *Emteq*. en-GB. 2017. URL: https://emteq.net/ (visited on 06/24/2018) (cited on page 45).

[53] Mask MindMaze. *MASK: real emotions in virtual reality*. en-US. 2018. URL: https://www.mindmaze.com/mask/ (visited on 06/24/2018) (cited on page 45).

[54] Judith Amores, Xavier Benavides, and Pattie Maes. 'PsychicVR: Increasing Mindfulness by Using Virtual Reality and Brain Computer Interfaces'. In: *Proceedings of the 2016 CHI Conference Extended Abstracts on Human Factors in Computing Systems*. CHI EA '16. New York, NY, USA: ACM, 2016, pp. 2–2. DOI: 10.1145/2851581.2889442 (cited on page 45).

[55] Stephen Gilroy et al. 'PINTER: interactive storytelling with physiological input'. en. In: ACM Press, 2012, p. 333. DOI: 10.1145/2166966.2167039 (cited on page 45).

[56] Song Han et al. 'Learning both weights and connections for efficient neural network'. In: *Advances in neural information processing systems*. 2015, pp. 1135–1143 (cited on page 49).

[57] Vinod Nair and Geoffrey E Hinton. 'Rectified linear units improve restricted boltzmann machines'. In: *Proceedings of the 27th international conference on machine learning (ICML-10)*. 2010, pp. 807–814 (cited on page 49).

[58] Alireza Makhzani et al. 'Adversarial autoencoders'. In: *arXiv preprint arXiv:1511.05644* (2015) (cited on page 49).

[59] Andrej Karpathy et al. 'Large-scale Video Classification with Convolutional Neural Networks'. In: (2014) (cited on page 49).

[60] Nitish Srivastava et al. 'Dropout: A simple way to prevent neural networks from overfitting'. In: *The Journal of Machine Learning Research* 15.1 (2014), pp. 1929–1958 (cited on page 49).

[61] K. H. Kim, S. W. Bang, and S. R. Kim. 'Emotion recognition system using short-term monitoring of physiological signals'. en. In: *Medical and Biological Engineering and Computing* 42.3 (May 2004), pp. 419–427. DOI: 10.1007/BF02344719 (cited on page 50).

[62] System aGlass. *Eye tracking*. Chinese, english. gadget store. 2017. URL: http://www.aglass.com (cited on pages 51, 56).

[63] K. Suzuki et al. 'Recognition and mapping of facial expressions to avatar by embedded photo reflective sensors in head mounted display'. In: *2017 IEEE Virtual Reality (VR)*. Mar. 2017, pp. 177–185. DOI: 10.1109/VR.2017.7892245 (cited on page 52).

[64] Paul A. G. Forbes, Xueni Pan, and Antonia F. de C. Hamilton. 'Reduced Mimicry to Virtual Reality Avatars in Autism Spectrum Disorder'. en. In: *Journal of Autism and Developmental Disorders* 46.12 (Dec. 2016), pp. 3788–3797. DOI: 10.1007/s10803-016-2930-2 (cited on page 55).

[65] Rachel Metz. *Virtual Reality's Missing Element: Other People - MIT Technology Review*. URL: https://www.technologyreview.com/s/607956/virtual-realitys-missing-element-other-people/ (cited on page 55).

[66] Debra Boeldt et al. 'Using Virtual Reality Exposure Therapy to Enhance Treatment of Anxiety Disorders: Identifying Areas of Clinical Adoption and Potential Obstacles'. In: *Frontiers in Psychiatry* 10 (2019), p. 773. DOI: 10.3389/fpsyt.2019.00773. (Visited on 10/25/2021) (cited on page 60).

[67] Meng-Chang Tsai et al. 'An Intelligent Virtual-Reality System With Multi-Model Sensing for Cue-Elicited Craving in Patients With Methamphetamine Use Disorder'. eng. In: *IEEE transactions on bio-medical engineering* 68.7 (July 2021), pp. 2270–2280. DOI: 10.1109/TBME.2021.3058805 (cited on page 60).

[68] Patrice L. Weiss et al. 'Virtual reality in neurorehabilitation'. In: *Textbook of neural repair and rehabilitation* 51.8 (2006). Publisher: Citeseer, pp. 182–97 (cited on page 60).

[69] Kunal Gupta et al. 'In AI We Trust: Investigating the Relationship between Biosignals, Trust and Cognitive Load in VR'. In: *25th ACM Symposium on Virtual Reality Software and Technology*. VRST '19. New York, NY, USA: Association for Computing Machinery, Nov. 2019, pp. 1–10. DOI: 10.1145/3359996.3364276. (Visited on 03/05/2022) (cited on page 60).

[70] Josef Faller et al. 'Regulation of arousal via online neurofeedback improves human performance in a demanding sensory-motor task'. In: *Proceedings of the National Academy of Sciences* 116.13 (Mar. 2019). Publisher: Proceedings of the National Academy of Sciences, pp. 6482–6490. DOI: 10.1073/pnas.1817207116. (Visited on 03/05/2022) (cited on page 60).

[71] *SteamVR, https://store.steampowered.com*. en. 2021. URL: https://store.steampowered.com/app/250820/SteamVR/ (visited on 01/02/2022) (cited on page 62).

[72] Dominique Makowski et al. 'NeuroKit2: A Python toolbox for neurophysiological signal processing'. eng. In: *Behavior Research Methods* 53.4 (Aug. 2021), pp. 1689–1696. DOI: 10.3758/s13428-020-01516-y (cited on page 63).

[73] Lorenz Esch et al. 'MNE Scan: Software for real-time processing of electrophysiological data'. eng. In: *Journal of Neuroscience Methods* 303 (June 2018), pp. 55–67. DOI: 10.1016/j.jneumeth.2018.03.020 (cited on page 63).

[74] C. Kothe, D. Medine, and M. Grivich. 'Lab Streaming Layer (2014)'. In: *URL: https://github. com/sccn/labstreaminglayer (visited on 26/02/2020)* (2018) (cited on page 63).

[75] Texas Instruments. 'Ads1299-x low-noise, 4-, 6-, 8-channel, 24-bit, analog-to-digital converter for eeg and biopotential measurements'. In: *Jul-2012.[Online]. Available: http://www. ti. com/lit/ds/symlink/ads1299. pdf.[Accessed: 12-May-2017]* (2017) (cited on page 63).

[76] Richard W. Homan, John Herman, and Phillip Purdy. 'Cerebral location of international 10–20 system electrode placement'. In: *Electroencephalography and clinical neurophysiology* 66.4 (1987). Publisher: Elsevier, pp. 376–382 (cited on page 64).

[77] Andrew FH Payne, Anne M. Schell, and Michael E. Dawson. 'Lapses in skin conductance responding across anatomical sites: Comparison of fingers, feet, forehead, and wrist'. In: *Psychophysiology* 53.7 (2016). Publisher: Wiley Online Library, pp. 1084–1092 (cited on pages 64, 69).

[78] Wataru Sato, Takanori Kochiyama, and Sakiko Yoshikawa. 'Physiological correlates of subjective emotional valence and arousal dynamics while viewing films'. In: *Biological Psychology* 157 (2020). Publisher: Elsevier, p. 107974.

[79] L Haas. 'Hans Berger (1873–1941), Richard Caton (1842–1926), and electroencephalography'. In: *Journal of Neurology, Neurosurgery, and Psychiatry* 74.1 (Jan. 2003), p. 9. DOI: 10.1136/jnnp.74.1.9. (Visited on 01/07/2022) (cited on page 65).

[80] Michael J. Aminoff. 'Chapter 3 - Electroencephalography: General Principles and Clinical Applications'. en. In: *Aminoff's Electrodiagnosis in Clinical Neurology (Sixth Edition)*. Ed. by Michael J. Aminoff. London: W.B. Saunders, Jan. 2012, pp. 37–84. DOI: 10.1016/B978-1-4557-0308-1.00003-0. (Visited on 10/10/2021) (cited on page 65).

[81] Robert J. Barry et al. 'EEG differences between eyes-closed and eyes-open resting conditions'. eng. In: *Clinical Neurophysiology: Official Journal of the International Federation of Clinical Neurophysiology* 118.12 (Dec. 2007), pp. 2765–2773. DOI: 10.1016/j.clinph.2007.07.028 (cited on page 66).

[82] J.-JJ Chen, Richard G. Shiavi, and Li-Qun Zhang. 'A quantitative and qualitative description of electromyographic linear envelopes for synergy analysis'. In: *IEEE transactions on biomedical engineering* 39.1 (1992). Publisher: IEEE, pp. 9–18 (cited on page 67).

[83] Sandra Márquez-Figueroa, Yuriy S. Shmaliy, and Oscar Ibarra-Manzano. 'Optimal extraction of EMG signal envelope and artifacts removal assuming colored measurement noise'. en. In: *Biomedical Signal Processing and Control* 57 (Mar. 2020), p. 101679. DOI: 10.1016/j.bspc.2019.101679. (Visited on 10/21/2021) (cited on page 67).

[84] Valentina Agostini and Marco Knaflitz. 'An Algorithm for the Estimation of the Signal-To-Noise Ratio in Surface Myoelectric Signals Generated During Cyclic Movements'. In: *IEEE Transactions on Biomedical Engineering* 59.1 (Jan. 2012). Conference Name: IEEE Transactions on Biomedical Engineering, pp. 219–225. DOI: 10.1109/TBME.2011.2170687 (cited on page 67).

[85] M.P. Tarvainen, P.O. Ranta-aho, and P.A. Karjalainen. 'An advanced detrending method with application to HRV analysis'. In: *IEEE Transactions on Biomedical Engineering* 49.2 (Feb. 2002). Conference Name: IEEE Transactions on Biomedical Engineering, pp. 172–175. DOI: 10.1109/10.979357 (cited on page 68).

[86] Mohit Agarwal and Raghupathy Sivakumar. 'Blink: A fully automated unsupervised algorithm for eye-blink detection in eeg signals'. In: *2019 57th Annual Allerton Conference on Communication, Control, and Computing (Allerton)*. IEEE, 2019, pp. 1113–1121 (cited on page 69).

[87] Kelly Kleifges et al. 'BLINKER: Automated extraction of ocular indices from EEG enabling large-scale analysis'. In: *Frontiers in neuroscience* 11 (2017). Publisher: Frontiers, p. 12 (cited on page 69).

[88] Jason J. Braithwaite et al. 'A guide for analysing electrodermal activity (EDA) & skin conductance responses (SCRs) for psychological experiments'. In: *Psychophysiology* 49.1 (2013), pp. 1017–1034 (cited on page 69).

[89] H. Storm et al. 'Skin conductance correlates with perioperative stress'. In: *Acta Anaesthesiologica Scandinavica* 46.7 (2002). Publisher: Wiley Online Library, pp. 887–895 (cited on page 69).

[90] Wolfram Boucsein. *Electrodermal activity*. Springer Science & Business Media, 2012 (cited on page 69).

[91] Robert F. Rushmer. 'Postural Effects on the Baselines of Ventricular Performance'. In: *Circulation* 20.5 (Nov. 1959). Publisher: American Heart Association, pp. 897–905. DOI: 10.1161/01.CIR.20.5.897. (Visited on 10/21/2021) (cited on page 69).

[92] D. J. van der Mee et al. 'Validity of electrodermal activity-based measures of sympathetic nervous system activity from a wrist-worn device'. en. In: *International Journal of Psychophysiology* 168 (Oct. 2021), pp. 52–64. DOI: 10.1016/j.ijpsycho.2021.08.003. (Visited on 10/21/2021) (cited on page 69).

[93] Gaetano Valenza, Antonio Lanata, and Enzo Pasquale Scilingo. 'The role of nonlinear dynamics in affective valence and arousal recognition'. In: *IEEE transactions on affective computing* 3.2 (2011). Publisher: IEEE, pp. 237–249 (cited on page 70).

[94] Chunting Wan et al. 'A Wearable Head Mounted Display Bio-Signals Pad System for Emotion Recognition'. en. In: *Sensors* 22.1 (Jan. 2022). Number: 1 Publisher: Multidisciplinary Digital Publishing Institute, p. 142. DOI: 10.3390/s22010142. (Visited on 01/07/2022) (cited on page 70).

[95] Tomas Ysehak Abay, Kamran Shafqat, and Panayiotis A. Kyriacou. 'Perfusion Changes at the Forehead Measured by Photoplethysmography during a Head-Down Tilt Protocol'. In: *Biosensors* 9.2 (May 2019), p. 71. DOI: 10.3390/bios9020071. (Visited on 10/02/2021) (cited on page 71).

[96] Geeta S. Agashe, Joseph Coakley, and Paul D. Mannheimer. 'Forehead pulse oximetry: headband use helps alleviate false low readings likely related to venous pulsation artifact'. In: *The Journal of the American Society of Anesthesiologists* 105.6 (2006). Publisher: The American Society of Anesthesiologists, pp. 1111–1116 (cited on page 71).

[97] Alrick B. Hertzman and Laurence W. Roth. 'The absence of vasoconstrictor reflexes in the forehead circulation. Effects of cold'. In: *American Journal of Physiology-Legacy Content* 136.4 (1942). Publisher: American Physiological Society, pp. 692–697 (cited on page 71).

[98] Guohua Lu et al. 'A comparison of photoplethysmography and ECG recording to analyse heart rate variability in healthy subjects'. In: *Journal of medical engineering & technology* 33.8 (2009). Publisher: Taylor & Francis, pp. 634–641 (cited on page 71).

[99] Nandakumar Selvaraj et al. 'Assessment of heart rate variability derived from finger-tip photoplethysmography as compared to electrocardiography'. In: *Journal of medical engineering & technology* 32.6 (2008). Publisher: Taylor & Francis, pp. 479–484 (cited on page 71).

[100] Claudia Lerma et al. 'Poincaré plot indexes of heart rate variability capture dynamic adaptations after haemodialysis in chronic renal failure patients'. eng. In: *Clinical Physiology and Functional Imaging* 23.2 (Mar. 2003), pp. 72–80. DOI: 10.1046/j.1475-097x.2003.00466.x (cited on page 71).

[101] Matthew Grivich. *LSL Validation*. UCSD. May 2013. URL: https://sccn.ucsd.edu/~mgrivich/LSL_Validation.html (visited on 10/26/2021) (cited on page 72).

[102] Gernot R. Müller-Putz et al. 'Steady-state visual evoked potential (SSVEP)-based communication: impact of harmonic frequency components'. eng. In: *Journal of Neural Engineering* 2.4 (Dec. 2005), pp. 123–130. DOI: 10.1088/1741-2560/2/4/008 (cited on page 73).

[103] Danhua Zhu et al. 'A Survey of Stimulation Methods Used in SSVEP-Based BCIs'. en. In: *Computational Intelligence and Neuroscience* 2010 (Mar. 2010). Publisher: Hindawi, e702357. DOI: 10.1155/2010/702357. (Visited on 09/13/2021) (cited on page 73).

[104] Hovagim Bakardjian, Toshihisa Tanaka, and Andrzej Cichocki. 'Optimization of SSVEP brain responses with application to eight-command Brain-Computer Interface'. eng. In: *Neuroscience Letters* 469.1 (Jan. 2010), pp. 34–38. DOI: 10.1016/j.neulet.2009.11.039 (cited on page 73).

[105] Nikolay V. Manyakov et al. 'Sampled sinusoidal stimulation profile and multichannel fuzzy logic classification for monitor-based phase-coded SSVEP brain–computer interfacing'. In: *Journal of neural engineering* 10.3 (2013). Publisher: IOP Publishing, p. 036011 (cited on page 73).

[106] Alexandre Armengol-Urpi and Sanjay E. Sarma. 'Sublime: a hands-free virtual reality menu navigation system using a high-frequency SSVEP-based brain-computer interface'. In: *Proceedings of the 24th ACM Symposium on Virtual Reality Software and Technology*. 2018, pp. 1–8 (cited on page 74).

[107] Xiaogang Chen et al. 'A high-itr ssvep-based bci speller'. In: *Brain-Computer Interfaces* 1.3-4 (2014). Publisher: Taylor & Francis, pp. 181–191 (cited on pages 74, 75).

[108] Guangyu Bin et al. 'An online multi-channel SSVEP-based brain–computer interface using a canonical correlation analysis method'. In: *Journal of neural engineering* 6.4 (2009). Publisher: IOP Publishing, p. 046002.

[109] Bingchuan Liu et al. 'BETA: A Large Benchmark Database Toward SSVEP-BCI Application'. In: *Frontiers in Neuroscience* 14 (2020), p. 627. DOI: 10.3389/fnins.2020.00627. (Visited on 01/04/2022) (cited on page 75).

[110] Xavier Duart et al. 'Evaluating the Effect of Stimuli Color and Frequency on SSVEP'. In: *Sensors (Basel, Switzerland)* 21.1 (Dec. 2020), p. 117. DOI: 10.3390/s21010117. (Visited on 01/04/2022) (cited on page 75).

[111] Bingchuan Liu et al. 'Align and pool for EEG headset domain adaptation (ALPHA) to facilitate dry electrode based SSVEP-BCI'. In: *IEEE Transactions on Biomedical Engineering* (2021). Conference Name: IEEE Transactions on Biomedical Engineering, pp. 1–1. DOI: 10.1109/TBME.2021.3105331 (cited on page 75).

[112] Fangkun Zhu et al. 'An Open Dataset for Wearable SSVEP-Based Brain-Computer Interfaces'. en. In: *Sensors* 21.4 (Jan. 2021). Number: 4 Publisher: Multidisciplinary Digital Publishing Institute, p. 1256. DOI: 10.3390/s21041256. (Visited on 01/04/2022) (cited on page 75).

[113] Manuel Merino et al. 'A Method of EOG Signal Processing to Detect the Direction of Eye Movements'. In: *2010 First International Conference on Sensor Device Technologies and Applications*. July 2010, pp. 100–105. DOI: 10.1109/SENSORDEVICES.2010.25 (cited on page 77).

[114] Li Zeng et al. 'Landscapes and emerging trends of virtual reality in recent 30 years: a bibliometric analysis'. In: *2018 IEEE SmartWorld, Ubiquitous Intelligence & Computing, Advanced & Trusted Computing, Scalable Computing & Communications, Cloud & Big Data Computing, Internet of People and Smart City Innovation (SmartWorld/SCALCOM/UIC/ATC/CBDCom/IOP/SCI)* (2018), pp. 1852–1858 (cited on page 84).

[115] Davide Castelvecchi. 'Low-cost headsets boost virtual reality's lab appeal'. In: *Nature* 533.7602 (2016) (cited on pages 84, 102).

[116] Jaziar Radianti et al. 'A systematic review of immersive virtual reality applications for higher education: Design elements, lessons learned, and research agenda'. In: *Computers & Education* 147 (2020), p. 103778 (cited on pages 84, 102).

[117] P Cipresso et al. *The past, present, and future of virtual and augmented reality research: a network and cluster analysis of the literature. Front. Psychol. 9, 1–20 (2018)*. 2018 (cited on pages 84, 102).

[118] Alexandre Armengol-Urpi and Sanjay E Sarma. 'Sublime: a hands-free virtual reality menu navigation system using a high-frequency SSVEP-based brain-computer interface'. In: *Proceedings of the 24th ACM Symposium on Virtual Reality Software and Technology*. 2018, pp. 1–8 (cited on pages 84, 102).

[119] Dorothy Strickland. 'Virtual reality for the treatment of autism'. In: *Virtual reality in neuro-psycho-physiology* (1997), pp. 81–86 (cited on pages 84, 103).

[120] Dorothy Strickland et al. 'Overcoming phobias by virtual exposure'. In: *Communications of the ACM* 40.8 (1997), pp. 34–39 (cited on pages 84, 103).

[121] Wei-Long Zheng and Bao-Liang Lu. 'A multimodal approach to estimating vigilance using EEG and forehead EOG'. In: *Journal of neural engineering* 14.2 (2017), p. 026017 (cited on pages 84, 103).

[122] Catherine RG Jones et al. 'A multimodal approach to emotion recognition ability in autism spectrum disorders'. In: *Journal of Child Psychology and Psychiatry* 52.3 (2011), pp. 275–285 (cited on pages 84, 103).

[123] Todd J Maurer and Heather R Pierce. 'A comparison of Likert scale and traditional measures of self-efficacy.' In: *Journal of applied psychology* 83.2 (1998), p. 324 (cited on page 89).

[124] Christian Kothe et al. *Lab streaming layer (LSL)*. 2014 (cited on page 90).

[125] Andrey Parfenov. *BrainFlow*. en. URL: https://brainflow.org/ (visited on 01/10/2023) (cited on page 93).

[126] *NeuroPype - Home*. URL: https://www.neuropype.io/ (visited on 01/10/2023) (cited on page 93).

[127] Joan Stiles et al. 'Spatial Attention, Working Memory, and Executive Function'. In: *Neural Plasticity and Cognitive Development: Insights from Children with Perinatal Brain Injury*. Ed. by Joan Stiles et al. Oxford University Press, June 2012, p. 0. DOI: 10.1093/acprof:osobl/9780195389944.003.0006. (Visited on 03/22/2023) (cited on page 102).

[128] Sandra G Hart and Lowell E Staveland. 'Development of NASA-TLX (Task Load Index): Results of empirical and theoretical research'. In: *Advances in psychology*. Vol. 52. Elsevier, 1988, pp. 139–183 (cited on page 102).

[129] Mark S Young et al. 'State of science: mental workload in ergonomics'. In: *Ergonomics* 58.1 (2015), pp. 1–17 (cited on page 102).

[130] GM Hancock et al. 'Mental workload'. In: *Handbook of human factors and ergonomics* (2021), pp. 203–226 (cited on page 102).

[131] John Sweller. 'Cognitive load theory: Recent theoretical advances.' In: (2010) (cited on page 102).

[132] Naomi P Friedman and Trevor W Robbins. 'The role of prefrontal cortex in cognitive control and executive function'. In: *Neuropsychopharmacology* 47.1 (2022), pp. 72–89 (cited on page 102).

[133] Earl K Miller. 'The prefontral cortex and cognitive control'. In: *Nature reviews neuroscience* 1.1 (2000), pp. 59–65 (cited on page 102).

[134] Yale E Cohen and Richard A Andersen. 'A common reference frame for movement plans in the posterior parietal cortex'. In: *Nature Reviews Neuroscience* 3.7 (2002), pp. 553–562 (cited on page 102).

[135] Alexander T Sack. 'Parietal cortex and spatial cognition'. In: *Behavioural brain research* 202.2 (2009), pp. 153–161 (cited on page 102).

[136] Jody C Culham and Nancy G Kanwisher. 'Neuroimaging of cognitive functions in human parietal cortex'. In: *Current opinion in neurobiology* 11.2 (2001), pp. 157–163 (cited on page 102).

[137] Julian F Thayer and Richard D Lane. 'Claude Bernard and the heart–brain connection: Further elaboration of a model of neurovisceral integration'. In: *Neuroscience & Biobehavioral Reviews* 33.2 (2009), pp. 81–88 (cited on page 102).

[138] Masaaki Tanaka et al. 'Central nervous system fatigue alters autonomic nerve activity'. In: *Life sciences* 84.7-8 (2009), pp. 235–239 (cited on page 102).

[139] G Robert J Hockey. 'Compensatory control in the regulation of human performance under stress and high workload: A cognitive-energetical framework'. In: *Biological psychology* 45.1-3 (1997), pp. 73–93 (cited on page 102).

[140] Robert Mearns Yerkes, John D Dodson, et al. 'The relation of strength of stimulus to rapidity of habit-formation'. In: (1908) (cited on page 102).

[141] Julian F Thayer et al. 'Heart rate variability, prefrontal neural function, and cognitive performance: the neurovisceral integration perspective on self-regulation, adaptation, and health'. In: *Annals of behavioral medicine* 37.2 (2009), pp. 141–153 (cited on page 102).

[142] Pieter Vanneste et al. 'Towards measuring cognitive load through multimodal physiological data'. In: *Cognition, Technology & Work* 23 (2021), pp. 567–585 (cited on page 102).

[143] Raul Fernandez Rojas et al. 'Electroencephalographic workload indicators during teleoperation of an unmanned aerial vehicle shepherding a swarm of unmanned ground vehicles in contested environments'. In: *Frontiers in neuroscience* 14 (2020), p. 40 (cited on page 102).

[144] Pavlo Antonenko et al. 'Using electroencephalography to measure cognitive load'. In: *Educational psychology review* 22 (2010), pp. 425–438 (cited on page 102).

[145] Rebecca L Charles and Jim Nixon. 'Measuring mental workload using physiological measures: A systematic review'. In: *Applied ergonomics* 74 (2019), pp. 221–232 (cited on page 102).

[146] Soroosh Solhjoo et al. 'Heart rate and heart rate variability correlate with clinical reasoning performance and self-reported measures of cognitive load'. In: *Scientific reports* 9.1 (2019), pp. 1–9 (cited on page 102).

[147] Marek Malik et al. 'Heart rate variability: Standards of measurement, physiological interpretation, and clinical use'. In: *European heart journal* 17.3 (1996), pp. 354–381 (cited on page 102).

[148] Fang Chen et al. *Robust multimodal cognitive load measurement*. Springer, 2016 (cited on page 102).

[149] Arthur F Kramer. 'Physiological metrics of mental workload: A review of recent progress'. In: *Multiple-task performance* (2020), pp. 279–328 (cited on page 102).

[150] Guillermo Bernal et al. 'PhysioHMD: a conformable, modular toolkit for collecting physiological data from head-mounted displays'. In: *Proceedings of the 2018 ACM International Symposium on Wearable Computers*. 2018, pp. 160–167 (cited on page 103).

[151] Kunal Gupta et al. 'Measuring human trust in a virtual assistant using physiological sensing in virtual reality'. In: *2020 IEEE Conference on virtual reality and 3D user interfaces (VR)*. IEEE. 2020, pp. 756–765 (cited on page 103).

[152] Lian Zhang et al. 'Cognitive load measurement in a virtual reality-based driving system for autism intervention'. In: *IEEE transactions on affective computing* 8.2 (2017), pp. 176–189 (cited on page 103).

[153] Arindam Dey, Alex Chatburn, and Mark Billinghurst. 'Exploration of an EEG-based cognitively adaptive training system in virtual reality'. In: *2019 ieee conference on virtual reality and 3d user interfaces (vr)*. IEEE. 2019, pp. 220–226 (cited on page 103).

[154] Guillermo Bernal et al. 'Galea: A physiological sensing system for behavioral research in Virtual Environments'. In: *2022 IEEE Conference on Virtual Reality and 3D User Interfaces (VR)*. IEEE. 2022, pp. 66–76 (cited on page 103).

[155] Arnaud Delorme and Scott Makeig. 'EEGLAB: an open source toolbox for analysis of single-trial EEG dynamics including independent component analysis'. In: *Journal of neuroscience methods* 134.1 (2004), pp. 9–21 (cited on pages 133, 136).

[156] J Vernon Odom et al. 'ISCEV standard for clinical visual evoked potentials:(2016 update)'. In: *Documenta Ophthalmologica* 133.1 (2016), pp. 1–9 (cited on pages 139, 140).

[157] AM Halliday and WF Michael. 'Changes in pattern-evoked responses in man associated with the vertical and horizontal meridians of the visual field'. In: *The Journal of Physiology* 208.2 (1970), pp. 499–513 (cited on page 139).

[158] DA Jeffreys and AT Smith. 'The polarity inversion of scalp potentials evoked by upper and lower half-field stimulus patterns: latency or surface distribution differences?' In: *Electroencephalography and Clinical Neurophysiology* 46.4 (1979), pp. 409–415 (cited on page 139).

[159] Francesco Di Russo et al. 'Cortical sources of the early components of the visual evoked potential'. In: *Human brain mapping* 15.2 (2002), pp. 95–111 (cited on page 139).

[160] Ruby Sharma et al. 'Visual evoked potentials: normative values and gender differences'. In: *Journal of clinical and diagnostic research: JCDR* 9.7 (2015), p. CC12 (cited on page 140).

[161] Daniel Freeman et al. 'The effects of improving sleep on mental health (OASIS): a randomised controlled trial with mediation analysis'. In: *The Lancet Psychiatry* 4.10 (2017), pp. 749–758 (cited on page 148).

[162] Robert Stickgold. 'Sleep-dependent memory consolidation'. In: *Nature* 437.7063 (2005), pp. 1272–1278 (cited on page 148).

[163] Adriano Zager et al. 'Effects of acute and chronic sleep loss on immune modulation of rats'. In: *American Journal of Physiology-Regulatory, Integrative and Comparative Physiology* 293.1 (2007), R504–R509 (cited on page 148).

[164] Jessica Vensel Rundo and Ralph Downey III. 'Polysomnography'. In: *Handbook of clinical neurology* 160 (2019), pp. 381–392 (cited on pages 148, 156).

[165] Lisa J Meltzer et al. 'Use of actigraphy for assessment in pediatric sleep research'. In: *Sleep medicine reviews* 16.5 (2012), pp. 463–475 (cited on page 149).

[166] Patrick M Fuller, Joshua J Gooley, and Clifford B Saper. 'Neurobiology of the sleep-wake cycle: sleep architecture, circadian regulation, and regulatory feedback'. In: *Journal of biological rhythms* 21.6 (2006), pp. 482–493 (cited on page 153).

[167] Brinnae Bent et al. 'Investigating sources of inaccuracy in wearable optical heart rate sensors'. In: *NPJ digital medicine* 3.1 (2020), p. 18 (cited on page 158).

[168] *Meet IBM Master Inventor and IoT evangelist Andy Stanford-Clark*. en-US. Sept. 2016. URL: https://www.ibm.com/blogs/internet-of-things/andy-stanford-clark/ (visited on 11/28/2022) (cited on page 163).

[169] Urs Hunkeler, Hong Linh Truong, and Andy Stanford-Clark. 'MQTT-S—A publish/subscribe protocol for Wireless Sensor Networks'. In: *2008 3rd International Conference on Communication Systems Software and Middleware and Workshops (COMSWARE'08)*. IEEE. 2008, pp. 791–798 (cited on page 163).

[170] Eclipse Mosquitto. 'An open source MQTT broker'. In: *Eclipse Mosquitto™[cit. 2018-04-23]. Dostupné z: Mosquitto. org* (2018) (cited on page 163).

[171] RICHARD MACMANUS of ReadWriteWeb. *MQTT Poised For Big Growth-An RSS For Internet of Things? - NYTimes.com*. Cad: 0. URL: https://archive.nytimes.com/www.nytimes.com/external/readwriteweb/2009/07/23/23readwriteweb-mqtt-poised-for-big-growth---an-rss-for-int-25425.html (visited on 11/28/2022) (cited on page 164).

[172] Daniel Barata et al. 'System of acquisition, transmission, storage and visualization of Pulse Oximeter and ECG data using Android and MQTT'. In: *Procedia Technology* 9 (2013), pp. 1265–1272 (cited on page 164).

[173] Valerie Lampkin et al. *Building smarter planet solutions with mqtt and ibm websphere mq telemetry*. IBM Redbooks, 2012 (cited on page 164).

[174] Kamil Adamczyk. *Neuroon Open - Product Information, Latest Updates, and Reviews 2023*. en. URL: https://www.producthunt.com/products/neuroon-open (visited on 01/12/2023) (cited on page 172).

[175] *Neurofeedback EEG Device - How it Works*. en-US. URL: https://choosemuse.com/how-it-works/ (visited on 01/12/2023) (cited on page 173).

[176] Stanisław Saganowski et al. 'Review of consumer wearables in emotion, stress, meditation, sleep, and activity detection and analysis'. In: *arXiv preprint arXiv:2005.00093* (2020) (cited on page 173).

[177] Wolfram Boucsein. *Electrodermal activity*. Springer Science & Business Media, 2012 (cited on page 177).

[178] *AN118: Improving ADC Resolution by Oversampling and Averaging*. URL: https://docslib.org/doc/1484837/an118-improving-adc-resolution-by-oversampling-and-averaging (visited on 01/12/2023) (cited on page 177).

[179] Robert E Kleiger, Phyllis K Stein, and J Thomas Bigger Jr. 'Heart rate variability: measurement and clinical utility'. In: *Annals of Noninvasive Electrocardiology* 10.1 (2005), pp. 88–101 (cited on page 179).

[180] Caroline Lustenberger et al. 'High-density EEG characterization of brain responses to auditory rhythmic stimuli during wakefulness and NREM sleep'. In: *NeuroImage* 169 (2018), pp. 57–68 (cited on page 183).

[181] Marek Piorecky et al. 'Real-Time Excitation of Slow Oscillations during Deep Sleep Using Acoustic Stimulation'. In: *Sensors* 21.15 (2021), p. 5169 (cited on page 183).

[182] Sang Ho Choi et al. 'Weak closed-loop vibrational stimulation improves the depth of slow-wave sleep and declarative memory consolidation'. In: *Sleep* 44.6 (2021), zsaa285 (cited on page 183).

[183] Kazue Okamoto-Mizuno and Koh Mizuno. 'Effects of thermal environment on sleep and circadian rhythm'. In: *Journal of physiological anthropology* 31.1 (2012), pp. 1–9 (cited on page 184).

[184] JC Sagot et al. 'Sweating responses and body temperatures during nocturnal sleep in humans'. In: *American Journal of Physiology-Regulatory, Integrative and Comparative Physiology* 252.3 (1987), R462–R470 (cited on page 184).

[185] Julia S Rihm et al. 'Reactivating memories during sleep by odors: odor specificity and associated changes in sleep oscillations'. In: *Journal of cognitive neuroscience* 26.8 (2014), pp. 1806–1818 (cited on page 184).

[186] Delphine Oudiette and Ken A Paller. 'Upgrading the sleeping brain with targeted memory reactivation'. In: *Trends in cognitive sciences* 17.3 (2013), pp. 142–149 (cited on page 184).

[187] Anat Arzi et al. 'Humans can learn new information during sleep'. In: *Nature neuroscience* 15.10 (2012), pp. 1460–1465 (cited on page 184).

[188] Adam Haar Horowitz et al. 'Dormio: Interfacing with dreams'. In: *Extended Abstracts of the 2018 CHI Conference on Human Factors in Computing Systems*. 2018, pp. 1–10 (cited on page 185).

[189] Namni Goel, Hyungsoo Kim, and Raymund P Lao. 'An olfactory stimulus modifies nighttime sleep in young men and women'. In: *Chronobiology international* 22.5 (2005), pp. 889–904 (cited on page 188).

[190] Peir Hossein Koulivand, Maryam Khaleghi Ghadiri, and Ali Gorji. 'Lavender and the nervous system'. In: *Evidence-based complementary and alternative medicine* 2013 (2013) (cited on page 188).

[191] Luigi Fiorillo et al. 'Automated sleep scoring: A review of the latest approaches'. In: *Sleep medicine reviews* 48 (2019), p. 101204 (cited on page 201).

[192] Raphael Vallat and Matthew P Walker. 'An open-source, high-performance tool for automated sleep staging'. In: *Elife* 10 (2021), e70092 (cited on page 201).

[193] Karine Lacourse et al. 'A sleep spindle detection algorithm that emulates human expert spindle scoring'. In: *Journal of neuroscience methods* 316 (2019), pp. 3–11 (cited on page 202).

[194] Marcello Massimini et al. 'The sleep slow oscillation as a traveling wave'. In: *Journal of Neuroscience* 24.31 (2004), pp. 6862–6870 (cited on page 202).

[195] Julie Carrier et al. 'Sleep slow wave changes during the middle years of life'. In: *European Journal of Neuroscience* 33.4 (2011), pp. 758–766 (cited on page 202).

[196] Karen Simonyan, Andrea Vedaldi, and Andrew Zisserman. 'Deep inside convolutional networks: Visualising image classification models and saliency maps'. In: *arXiv preprint arXiv:1312.6034* (2013) (cited on page 203).

[197] Julius Adebayo et al. 'Sanity checks for saliency maps'. In: *Advances in neural information processing systems* 31 (2018) (cited on page 204).

[198] M. G. Terzano et al. 'Atlas, rules, and recording techniques for the scoring of cyclic alternating pattern (CAP) in human sleep'. eng. In: *Sleep Medicine* 2.6 (Nov. 2001), pp. 537–553. DOI: 10.1016/s1389-9457(01)00149-6 (cited on page 212).

[199] B. Kemp et al. 'Analysis of a sleep-dependent neuronal feedback loop: the slow-wave microcontinuity of the EEG'. In: *IEEE Transactions on Biomedical Engineering* 47.9 (Sept. 2000). Conference Name: IEEE Transactions on Biomedical Engineering, pp. 1185–1194. DOI: 10.1109/10.867928 (cited on page 212).

[200] Mohammad Daneshmandi et al. 'Effect of eye mask on sleep quality in patients with acute coronary syndrome'. In: *Journal of caring sciences* 1.3 (2012), p. 135 (cited on page 221).

[201] Yoon Jung Koo and Hyo Jung Koh. 'Effects of eye protective device and ear protective device application on sleep disorder with coronary disease patients in CCU'. In: *Journal of Korean Academy of Nursing* 38.4 (2008), pp. 582–592 (cited on page 221).

Special Terms

A

ANS Autonomic Nervous System. 10, 158

B

BCI Brain-Computer Interfaces. 9, 96

C

CNS Central Nervous System. 10

E

EDA Electrodermal Activity. 165

EEG Electroencephalography. 148, 149, 152–156, 161, 162, 165

EMG Electromyography. 153, 157, 165

EOG electrooculographic. 9, 153, 156, 165

ERP Event-related Potentials. 98

F

Fascia Ecosystem The Fascia Ecosystem makes use of three leading technologies that allow for the reinvention of how sleep studies are conducted.. 167, 169

Fascia Hub The Fascia Hub allows a researcher or scientist to provide stimulation and feedback in the form of audio and visual stimuli to the patient, expanding the opportunities to understand sleep and dreams by also issuing interventions.. 150, 167, 185–191, 197, 205, 211

Fascia Mask The Fascia Sleep Mask collects similar data as a full polysomnogram in the small, familiar, and comfortable form of a soft sleep mask using the latest technologies in fabric based sensing.. 165, 171, 173, 174, 212, 220, 221, 223

Fascia Portal The Fascia Portal is where sleep researchers can inspect the patient's signals in real-time and store experiment information, analyzed by our machine learning API that provides sleep staging, spindles, and k-complex identification information in real-time. . 150, 167, 168, 193, 196–200, 205, 206, 209, 210, 222

H

HMD Head-Mounted Display. 38

HRV Heart Rate Variability. 158

L

LGN Lateral Geniculate Nucleus. 129

LSL Lab Streaming Layer. 90

N

NREM Non-Rapid Eye Movement. 153–155

P

POR Point of Regard. 56

PSG Polysomnography. 148, 153, 158, 160

R

REM Rapid Eye Movement. 153–157

RMS Root Mean Square. 215

S

SCR Skin Conductance Response. 56

SSVEP Steady State Visual Evoked Potential. 9, 93

V

VEP Visual Evoked Potentials. 9, 98, 133

Alphabetical Index